Neurobiological mechanisms of hallucinations in schizophrenia

Colleen Peggy Elizabeth Rollins

Department of Psychiatry

University of Cambridge

This dissertation is submitted for the degree of

Doctor of Philosophy

Declaration

I hereby declare that except where specific reference is made to the work of others, the contents of this dissertation are original and have not been submitted in whole or in part for consideration for any other degree or qualification at the University of Cambridge, or any other University. This dissertation is the result of my own work, except analyses done in collaboration with co-authors, students, or colleagues, which I specifically outline below. This dissertation contains less than 60,000 words, excluding figures, tables, equations, and bibliography, and has fewer than 150 figures.

The following people have contributed to my thesis (listed by chapter):

Chapter 2 – John Suckling, Graham K Murray, and Jane R Garrison confirmed the inclusion/exclusion criteria for studies in the systematic review and meta-analyses and discussed with me uncertainties of whether studies met criteria. Emilio Fernandez, James B Rowe, and the clinical teams at Cambridgeshire and Peterborough Foundation NHS Trust Clozapine Clinic, the Cambridge Parkinson's Disease Research Clinic, and Cambridge University Hospitals NHS Trust Memory Clinic recruited participants for *Sound and Vision*.

Chapter 3 – MRI and clinical data for the Shanghai dataset was provided by Raymond CK Chan and Zhi Li. The UK dataset was provided by John Suckling, Bill Deakin, Rachel Upthegrove, and the BeneMin Study Team. The following University of Cambridge undergraduate students manually traced the paracingulate sulcus, following training and supervision by me and Jane R Garrison: Maite Arribas, Aniket Patel, Rory Durham, Charlotte Jones. MA and AP were supervised by CPER, and RD and CJ were supervised by JRG. Their length measurements were used for the interrater reliability calculations. Arnaud Cachia taught me how to use BrainVISA and how to manually label the extracted sulci.

Chapter 4 – Rafael Romero-Garcia shared with me a script for plotting cortical surfaces.

Chapter 5 – Matthew Lemming provided me with the speedyPP resting-state fMRI processing scripts and the guidance on how to use them. Rafael Romero-Garcia provided me with the mapping between the Glasser parcellation and Yeo networks.

Colleen Peggy Elizabeth Rollins

June 2021

Abstract

Neurobiological mechanisms of hallucinations in schizophrenia

Colleen Peggy Elizabeth Rollins

All perception is a construct of the brain. Yet occasionally, sensory constructions emerge without origin in the physical world and are experienced as hallucinations. Hallucinations occur transdiagnostically, cross-culturally, and in all sensory modalities. They are common in people with schizophrenia, presenting in 60-80% of patients. Despite over 20 years of active neuroimaging research on hallucinations, the neural systems supporting these anomalous perceptual experiences remain disputed. This dissertation investigates the neurobiology of hallucinations, integrating research across structural and functional magnetic resonance imaging (MRI) to elucidate how hallucinations, chiefly in the context of schizophrenia, are supported by the brain, drawing on MRI indices of neurodevelopment. I introduce the phenomenon of hallucinations and motivate the utility of MRI for studying hallucinations. Considering their prevalence in other medical conditions, I conduct a meta-analysis and systematic review of the structural brain basis of hallucinations across diagnoses, primarily schizophrenia spectrum disorders and Parkinson's disease. This illustrated distinct neuroanatomical organizations of grey matter associated with hallucinations that occur in neurodevelopmental compared to neurodegenerative disorders, which I hypothesise constitute at least two distinct mechanisms. Focussing on the neurodevelopmental mechanism characterized by fronto-temporal and insular grey matter reductions, I turn to the contribution of cortical sulcation, a product of second and third trimester neurodevelopmental processes, which has been robustly implicated in schizophrenia pathology, and, more recently, in hallucinations. Sulcal patterns derived from structural MRI provide a proxy in adulthood for early brain development. I studied two independent datasets of patients with schizophrenia who underwent clinical assessment and 3T MRI from the United Kingdom and Shanghai, China, stratified into those with and without hallucinations, and healthy controls from Shanghai. I first replicate the finding that left hemisphere paracingulate sulcus (PCS) length is reduced in patients who experience hallucinations, then demonstrate similar associations for superior temporal sulcus depth. Length and depth alterations occurred with focal deviations in sulcal geometry. The interindividual and interhemispheric variability of the PCS

necessitated the development of semi-automated methods to characterize its morphology and validation to a manual protocol. I used structural covariance networks of the local gyrification index to investigate how specific sulcal deviations relate to global neurodevelopmental coordination, demonstrating that hallucinations correspond to increased covariance within and between salience and auditory networks. Hypothesizing structure-function relationships, I analyse resting-state functional MRI data from the same datasets described, finding significant interactions between PCS length and hallucinations status, but no main effects. There were no effects of hallucination status on salience and auditory network connectivity or in graph theoretical measures of connectivity, suggesting that resting-state connectivity is not a trait marker for hallucinations. Together, the discovery of neurodevelopmental alterations contributing to hallucinations provides mechanistic insight into the pathological consequences of prenatal origins. The interaction of sulcal alterations and hallucination status are associated with connectivity, which may have a role in the pathophysiology of hallucinations. I provide clear predictions and recommendations for future research.

In his anthology "Hallucinations", Oliver Sacks entwines personal narrative and clinical accounts to chart the experiential landscape of hallucinations: "the great range, the varieties, of hallucinatory experience, an essential part of the human condition".

He limits the scope to "organic" psychoses, acknowledging that "The hallucinations often experienced by people with schizophrenia also demand a separate consideration, a book of their own, for they cannot be divorced from the often profoundly altered inner life and life circumstances of those with schizophrenia."

I hope that this thesis contributes a very small chapter to that book.

Acknowledgements

Publications associated with this research

Rollins CPE, Garrison JR, Arribas M, Seyedsalehi A, Li Z, Chan RCK, et al. (2020): Evidence in cortical folding patterns for prenatal predispositions to hallucinations in schizophrenia. Transl Psychiatry. 10:387.

Rollins CPE, Garrison JR, Simons JS, Rowe JB, O'Callaghan C, Murray GK, et al. (2019): Meta-analytic Evidence for the Plurality of Mechanisms in Transdiagnostic Structural MRI Studies of Hallucination Status. EClinicalMedicine. 8:57-71.

Yang J, Wang D, Rollins C, Leming M, Liò P, Suckling J, et al. (2019): Volumetric Segmentation and Characterisation of the Paracingulate Sulcus on MRI Scans. bioRxiv.859496.

Conference Posters

Rollins CPE, Garrison JR, Li Zhi, Chan RCK, Simons JS, Murray GK, Suckling J. Sulcal alterations and functional implications associated with hallucinations in schizophrenia. *Organization for Human Brain Mapping 2020*.

Rollins CPE, Garrison JR, Simons JS, Rowe JB, O'Callaghan C, Murray GK, Suckling J. Meta-analytic evidence for the plurality of mechanisms in transdiagnostic structural MRI studies of hallucination status. *International Consortium for Hallucination Research Satellite Meeting 2018*.

Presentations

January 2021: "Alterations in Cingulate and Temporal Lobe Cortical Folding Associated with Hallucinations in Schizophrenia". Douglas Mental Health University Institute, Cerebral Imaging Centre Lecture Series.

September 2019: "Evidence for a structural reality monitoring network involved in hallucinations in schizophrenia". Early Career Hallucination Research Group.

February 2019: "Hearing and seeing things that are not there: Quantifying brain structure related to hallucinations". Darwin College Lunchtime Seminar Series.

Contents

List of Figures

List of Tables

Nomenclature

AD: Alzheimer's disease

AVH: auditory verbal hallucination

BD: bipolar disorder

CT: cortical thickness

DLB: dementia with Lewy bodies

DMN: default mode network

FDR: false discovery rate

GM: grey matter

H+: person with schizophrenia diagnosis currently experiencing hallucinations

H–: person with schizophrenia diagnosis not experiencing hallucinations

HC: healthy control

LGI: local gyrification index

mPFC: medial prefrontal cortex

MRI: magnetic resonance imaging

PANSS: The Positive and Negative Syndrome Scale

PD: Parkinson's disease

PCS: paracingulate sulcus

ROI: region of interest

rsfMRI: resting-state functional magnetic resonance imaging

sMRI: structural magnetic resonance imaging

STS: superior temporal sulcus

VBM: voxel-based morphometry

WM: white matter

Chapter 1   Introduction

All perception is a construction of the brain from sensory input. Yet occasionally, sensory constructions emerge without origin in the physical world and are experienced as hallucinations. Despite over 20 years of active neuroimaging research on hallucinations, the neural systems supporting these anomalous perceptual experiences remain disputed.

Overall, the work in this thesis aims to advance understanding of the neural foundations of hallucinations, chiefly in the context of schizophrenia.

1.1   What is a hallucination?

Before the seventeenth century, the experiences we now call hallucinations were culturally situated, spiritually meaningful, and representative of enlightenment or philosophical insight. They began to acquire a medical quality over the seventeenth and eighteenth century, but it was not until the 1830s that they were fully integrated into clinical and scientific discourse by Jean-Étienne Esquirol, a French psychiatrist (Telles-Correia et al., 2015).

"Hallucinations of sight […] have been denominated visions. Who would dare to say visions of hearing, visions of taste, visions of smell? […] A generic name is needed. I have proposed the word hallucination" (Esquirol and Hunt, 1845, p.110).

Although a word was proposed, "hallucination" remains difficult to demarcate from related concepts like illusion and misperception, and is often colloquially likened to mental imagery and dreams. While most people can willingly conjure an image of a bear riding a bicycle or the sound of their mother's voice, this imagery is held in the mind's eye. In contrast, hallucinations are projected into external space and arise without volition. In this regard, they are more similar to dreams than imagery, although hallucinations occur in the

waking state, whereas most dreaming happens during rapid eye movement (REM) sleep (Waters et al., 2016). Hallucinations that occur while falling asleep ("hypnagogic") or waking up ("hypnopompic") – both sometimes referred to as "pseudo-hallucinations" – suggest a continuum between hallucinations and dreams, but there is insufficient evidence to conclude whether they share a common aetiology (Waters et al., 2016). Illusions and misperceptions differ from hallucinations in that they correspond to transformations or distortions of real perceptions, whereas for hallucinations, there is nothing there to begin with. However, the boundaries between such perceptual distortions and hallucination-like experiences are not always clear to discern. Hallucinations are generally considered to be a distinct category of conscious life, but they may share neurocognitive mechanisms with illusions, misperceptions, dreams, and mental imagery, and these related phenomena may enable useful models for investigating hallucinations.

For this thesis, I consider hallucinations as perception-like experiences without a corresponding stimulus in the external world. This definition entails three components: (1) the sensorial nature of the experience, which can present in any sensory modality, or a combination of senses, and may hold the same qualia as veridical perception; (2) the conviction of its reality: the hallucination often feels real, although some people can have insight into whether they are hallucinating (for instance, by recognizing a hallucinatory voice or image that has appeared before); (3) the absence of a real object – there is no corresponding percept in the physical world that is related to the present perception. Variations in this definition have been proposed by others (Blom, 2010) and many argue for more precise categories or subtypes within this definition (McCarthy-Jones et al., 2014). I echo these concerns and use a broad definition to encompass all these accounts; where appropriate, I will specify types of hallucinations, for instance categorized by a specific sensory modality.

1.1.1 A note on terminology

A consequence of the medicalization of the term "hallucination" was the loss of its profundity. While hallucinations "were in earlier times culturally integrated and semantically pregnant, i.e. their content was believed to carry a message for the individual or the world",

(Berrios, 1996, p.35), their link to the patient rooted them to madness and disease. These connotations prevail today. Especially within Western medical and academic contexts, hallucination is a term that carries stigma, often stirring associations to mental illness or drug use. Although they occur in a range of non-disease contexts, hallucinations, particularly auditory hallucinations, are considered a cardinal symptom of schizophrenia by the Diagnostic and Statistical Manual of Mental Disorders (DSM-V) (American Psychiatric Association, 2013) and are one of Schneider's first rank symptoms (Soares-Weiser et al., 2015). As a symptom of one of the most disputed diagnoses in psychiatry, hallucinations shoulder some of the burden of the "schizophrenia label" (Moncrieff and Middleton, 2015; Geekie and Read, 2009).

In opposition to this diagnostic label, the figure of "the voice-hearer" was introduced in 1987 as part of the international Hearing Voices movement and UK Hearing Voices Network. This lexicon was brought about to challenge psychiatric authority and assert that the experience of hearing voices or utterances is a meaningful experience, key to a person's identity and narrative, and "a non-pathological part of ordinary human experience" (Woods, 2013, p.265). This has allowed many to embody an identity that better describes their lived experience.

While the political and sociocultural complexities of language and diagnoses are not a focus of this thesis, research is conducted within this dialogue. As an example, the International Consortium on Hallucination Research (ICHR) has evolved rapidly since its inaugural meeting in 2011 to integrate these complexities into hallucination research and collaborates with members of the Hearing Voices Movement and other people with lived experience (Waters et al., 2014). The decision to use the word "hallucination" in this thesis to describe sensory experiences that diverge from consensus reality was made to acknowledge the plurality and breadth of hallucinations, which may occur in sensory forms beyond audition, often spanning multiple sensory modalities, and may manifest through different mechanisms. In using the term "hallucination", I aim to reorient its definition to earlier historical times, when such experiences were rich with personal and collective meaning. A different term may be used when referencing prior work or if it is more descriptively

appropriate to use another term, such as "voice-hearer" or "auditory verbal hallucinations (AVH)".

1.1.2 Prevalence, outcomes, and risk factors

Who experiences hallucinations? Hallucinations are a transdiagnostic and transmodal phenomenon. They present in 60–80% of people with a schizophrenia spectrum disorder (Jadri et al., 2011; Lim et al., 2016), in other psychiatric conditions like borderline personality disorder (43%; Niemantsverdriet et al., 2017), bipolar disorder (34%; Shinn et al., 2012), in neurodegenerative diseases like Parkinson's disease (PD) (28%; Eversfield and Orton, 2019), Lewy body dementia (LBD) (62%; Eversfield and Orton, 2019), Alzheimer's disease (AD) (23%; Ballard et al., 2020), and among the general population at a prevalence rate estimated from 5–13%, depending on age (Maijer et al., 2018). Hallucinations may equally be brought about by unfavourable or transient states, such as stress, trauma, bereavement, seizure, drug use, the transition from wakefulness to sleeping (hypnagogia) or sleeping to wakefulness (hypnopompia) (Kamp et al., 2020; Waters et al., 2017). Hallucinations are not always, or even often, associated with distress; in certain cases, they are benign, in others, they may contribute to meaningful experiences (Laroi et al., 2014). While acknowledging the plurality of hallucinations, this thesis will focus primarily on the neural basis of hallucinations in schizophrenia spectrum disorders. For comparison, I will touch upon hallucinations in neurodegenerative illness.

Expanding research recognizes that hallucinations can occur in more than one sensory modality (auditory, visual, olfactory, gustatory, tactile/somatosensory) (Lim et al., 2016), either simultaneously or serially (see Montagnese et al., 2021 for a recent review on multimodal hallucinations (MMH)). Although the research remains scarce, emerging studies indicate that MMH are nearly twice as common as unimodal auditory hallucinations for people diagnosed with a schizophrenia spectrum disorder (Lim et al., 2016), and that the prevalence and clustering of sensory modalities vary between psychotic and neurodegenerative conditions (Dudley et al., 2018). For instance, in a study of hallucinating patients with schizophrenia (n=100) or Parkinson's (n=100), 83% of schizophrenia patients experienced auditory hallucinations compared to 45% of PD patients, while 88% of PD

patients experienced visual hallucinations, compared to 55% of schizophrenia patients (Llorca et al., 2016).

Irrespective of diagnosis, the presence of hallucinations is associated with poor prognosis. This can manifest as increased global severity of illness and reduced likelihood of recovery in schizophrenia (Goghari and Harrow, 2016), more severe cognitive deficits in PD and risk for dementia (FFytche et al., 2017), and increased suicidal behaviour in psychotic and non-clinical adults (Kjelby et al., 2015). Experiencing auditory verbal hallucinations (AVH) may also predict transition to later mental illness in healthy children and young adults (Baumeister et al., 2017; Johns et al., 2014). There is therefore strong incentive to understand why some people develop hallucinations in order to mitigate risk and tailor treatments to those who might benefit. Treatments for distressing hallucinations lie outside the scope of this thesis, but for hallucinations in schizophrenia they include cognitive behavioural therapy and antipsychotic medication, and there is active research assessing the efficacy of new treatment options, including AVATAR therapy and transcranial magnetic brain stimulation (Sommer et al., 2012b; Craig et al., 2018).

Risk factors for schizophrenia and psychotic experiences interact in a complex story of genetic predisposition, social factors, and environmental affordances, such as perinatal factors, childhood trauma, social adversity, or urbanization (Dean and Murray, 2005; Murray et al, 2017; Weinberger, 2017). Although few studies have investigated risk factors for specific symptoms like hallucinations, their aetiology appear similarly rooted in genetic variation (Lizano et al., 2018), in-utero brain development (Garrison et al., 2015; 2018), socioeconomic factors (McGrath et al., 2015), and trauma (Luhrmann et al., 2019).

1.1.3 Phenomenology

I have defined the term "hallucination" to refer to sensory experiences without a corresponding external source. Yet the lived experience of hallucinations entails many more facets.

The first large-scale systematic study on the phenomenology (subjective experience) of hallucinations was led by Nayani and David in 1996. By analysing clinical interview data

from 100 patients with a psychotic disorder (69% with a schizophrenia or schizoaffective diagnosis) who had experienced auditory hallucinations, the authors concluded that auditory hallucinations were repetitive, emotive utterances, that developed over time into a more complex dialogue between hallucination and patient. To reproduce these findings, McCarthy-Jones et al. (2014) performed a cluster analysis of interview data characterizing auditory hallucinations in 199 psychiatric patients (81% with a schizophrenia diagnosis), revealing four clusters: commanding and commenting voices, voices that were more thought-like than external, non-verbal auditory hallucinations, consisting of non-sensical words or non-voice sounds, and hallucinations identical to a memory of heard speech. Taking a transdiagnostic perspective, Woods et al. (2015) developed a survey about voice hearing experiences that was completed by 153 individuals with and without clinical histories (24% with a schizophrenia or schizoaffective diagnosis, 59% with another psychiatric diagnosis; 17% no diagnosis). The survey results illustrated the rich experiential diversity of hallucinations across location, nature, content, emotion, onset, anticipation, and embodiment. For instance, 66% of voice hearers reported an accompanied bodily affect, such as feeling heat, tingling or a dream-like state, and 69% reported characterful voices with distinct personalities. Fear and depression associated with voice-hearing were significantly more common in people with a psychiatric diagnosis, but no select attributes (such as location, number of voices, or commanding nature) were significantly different between participants with a schizophrenia spectrum diagnosis compared to all other participants, suggesting some continuity in experience across the diagnostic spectrum.

Understanding the lived experience of hallucinations is necessary to found neurocognitive models in the experiences they aim to explain. Moreover, insight into the lived experience may indicate the specific brain mechanisms involved. The work in this thesis has been conducted alongside conversations with experts by experience (formally and informally) to help keep neural descriptions of hallucinations grounded in the words of people who experience them. In one such conversation, I spoke with a young artist from Cambridgeshire who has been experiencing florid psychotic symptoms for over two decades. They created an artwork portraying their hallucinations for a journal cover submission (Figure 1.1).

Figure 1.1. Painting depicting the lived experience of hallucinations. Created by sk172 (@sk_oneseventwo), a young artist from Cambridgeshire who has been experiencing florid psychotic symptoms for over two decades, which he treats with clozapine. His artwork is a dialogue between the internal stimuli and the external stressors with a unique style merging urban-street narrative and primitivism. I was invited to submit a cover image along with publication of an article in a peer-reviewed journal, and, following conversation with and permission of sk172, submitted an image of their painting. Their painting (this image) was selected for the cover of EClinicalMedicine Volume 8, February 2019.

1.1.4 Culture

Hallucinations exist across cultures and historical eras. From visionary encounters with spirits in the Middle Ages, to the use of hallucinogenic plants or mushrooms for healing and divinity purposes, to hearing the voices of God in religious context, hallucinations have played, and continue to play, important functions in human life.

Phenomenological interviews have shown that local cultural milieu influences the form and content of AVH, with people in India and Ghana ascribing positive meaning to voices and recognizing them as kin or God, whereas people in the USA are more likely to describe voices as commanding or violent (Lurhmann et al., 2015). Prevalence rates of hallucination modality differ across geographical boundaries, with West African countries showing higher rates of visual hallucinations than European countries (Bauer et al., 2011). The religious content of hallucinations and delusions is culturally specific and follows societal changes, such as a gradual decrease in the diversity of religious themes over the past 80 years, but a relatively stable number of contacts with religious figures (i.e., contact with God or the devil) (Dudek et al., 2019).

This thesis uses data from independent populations of different ethnicities, primarily British white and Han Chinese. Although phenomenological data about the hallucinatory experiences was not available, and ethnicity cannot be conflated with culture, it is important to acknowledge that these experiences occurred within different sociocultural milieus and healthcare systems.

1.2   Theories and models

1.2.1 Neurodevelopmental origins of schizophrenia pathology

Over 30 years ago it was proposed that schizophrenia involves early neurodevelopmental deviations, beginning in foetal life and interacting with subsequent maturation to express the associated pathology – including hallucinations (Weinberger, 2017). Supporting this view, gestational maternal malnutrition, stress, infection and inflammatory response, and obstetric

complications increase risk for schizophrenia, and imaging studies demonstrate deviant trajectories of brain maturation. It is hypothesized that these abnormal processes in utero begin the sequelae for altered maturational wiring of structural and functional brain connections, leading to the grey matter loss and aberrant network connectivity apparent at the onset of illness. The microstructural causes for these macrostructural changes may include interacting cascades of failure in glial cell differentiation and immune activation of microglial cells, which result in alterations in myelination and synaptic pruning, and ultimately in cortical folding (Dietz et al., 2020).

The past decade has seen accumulating evidence that cortical sulcation, a marker of early brain development, confers vulnerability for the experience of hallucinations in people with a diagnosis of schizophrenia. These studies have documented focal deviations in cingulate and temporal lobe folding, including reduced left paracingulate sulcus length (Garrison et al., 2015) and reduced local sulcal index in the bilateral superior temporal sulcus, left middle frontal sulcus and left sylvian fissure (Cachia et al., 2008), suggesting that specific, prenatally determined variants of brain folding might confer later vulnerability to hallucinations. However, these findings require replication, extension, and integration with the global structural and connectomic landscape observed when hallucinations present for the matured individual.

1.2.2 Cognitive and computational theories describing hallucinations

"Other people try to tell me these are just thoughts and images you're having, but I find it very hard to believe. [Mary] has told me in the past that these are just thoughts and images through schizophrenia, but I find it hard to be convinced by it because it feels so real when I'm having them. I'm trying to convince myself that there's no one out there, but it just feels very, very real." (participant from *Sound and Vision*, see Chapter 2, section 2.5.6)

The neurobiology of schizophrenia pathology has been extensively studied in relation to the cognitive functions they support. Hallucinations are often accompanied with a strong sense of reality, and those who experience them sometimes struggle to discriminate between information (i.e., thoughts, percepts, imagery) generated internally versus information

perceived from the outside world. Biases in reality monitoring, the cognitive process of distinguishing internal from external experiences, are robust in schizophrenia patients compared to healthy controls, and show specificity to hallucinations (Simons et al., 2017). Neuroimaging research has long implicated the medial prefrontal cortex (mPFC) in reality monitoring, and more recently, morphological variability of the paracingulate sulcus (PCS), a tertiary fold on the mPFC, has been associated with reality monitoring performance in healthy individuals, such that poorer performance is associated with bilateral PCS absence (Buda et al., 2011). This same structure has been associated with lifetime hallucination history in patients with schizophrenia, such that a 1 cm reduction in the length of the left hemisphere PCS is associated with a 20% increase in the likelihood of experiencing hallucinations (Garrison et al., 2015).

From a computational perspective, perceptual decision processes like reality monitoring can be understood as processes that aim to maximize correct classification of sensory inputs or minimize perceptual classification errors. This perspective extends from two central concepts. The first is that to minimize error, judgements on the origin of information need to reduce the associated uncertainty. For an internal auditory percept, this ambiguity could manifest as variability of the auditory cortex intrinsic neuronal activity (Hunter et al., 2006); for an external auditory percept, this could represent identifying a single percept from background noise. The second is that prior knowledge can be beneficial for reducing the uncertainty of a perceptual judgement. For instance, prior learning about typical patterns of illumination is adaptive for recognizing edges, but can also make us susceptible to visual illusions (King et al., 2017). Similarly, prior experience with language can cause people to hear speech from non-speech sounds, such as sine-wave speech (artificially degraded speech). The influence of prior beliefs applies also for past life experiences: we actively infer the causes of what we sense, and this inference is coloured by past experiences, by how things have previously looked and sounded, by beliefs and emotions. Recent theoretical and empirical work suggests that hallucinations arise from an imbalance between reliance on prior knowledge and reliance on incoming sensory signals, with a bias towards prior knowledge (Powers et al., 2017; Corlett et al., 2019; Horga and Abi-Dargham, 2019).

At a brain systems level, this thesis is motivated by neurodevelopmental brain indices, and at a cognitive level, by computational frameworks and reality monitoring, but will refer to other theories (further described in Chapter 2), where relevant for the appropriate level of evidence.

1.3   Brain basis of hallucinations: Insights from structural and functional MRI

The way in which we perceive and interpret the world is underpinned by the structure and function of the brain, which can be assessed using neuroimaging methods such as structural magnetic resonance imaging (sMRI) and functional MRI (fMRI). Many other neuroimaging methods have shown insights about the brain basis of hallucinations, but this thesis will be limited to T1-weighted sMRI and to resting-state fMRI (rsfMRI), save for where other methods are relevant to discuss (see Braun et al., 2003 and Boes et al., 2015 for studies of focal brain lesions causing hallucinations, Hjelmervik et al., 2019 for evidence of the underlying neurochemistry (glutamate and GABA), Di Biase et al., 2020 and Leroux et al., 2017 for white matter integrity alterations, as assessed by diffusion tensor imaging-based tractography, Arora et al., 2021 for alpha and beta band EEG alterations, and Francis et al., 2020 and Fisher et al., 2014 for mismatch negativity amplitudes associated with hallucinations).

1.3.1 Structural MRI

Structural MRI enables the *in vivo* study of neuroanatomy by manipulating magnetic gradients to measure the radio-frequency signal of hydrogen atoms in brain tissue (Lerch et al., 2017). The difference between grey and white matter (GM, WM) in macromolecule and water content produces a T1-weighted image, which can be used to quantify different morphological indices of neuronal health by applying a wide range of freely available software packages, such as FSL, FreeSurfer, and ANTS. There are three broad approaches to quantifying macrostructure. The first, segmentation, involves either manual tracing or using automated/semi-automated tools to delineate regions of interest (ROI) on an MR image,

typically to measure the volume of GM within an ROI. An example of this is identifying and measuring cortical sulci, which is currently done either manually for anatomically variable sulci, or automatically for a select few sulci that are morphologically stable across individuals (see Chapter 3 for an introduction to these practices and challenges). Sulcal measures from MRI show high agreement with measures from post-mortem data (Mellerio et al., 2016) and are considered to reflect neurodevelopmental processes (Mangin et al., 2004). Second, morphometry algorithms like volume-based morphometry (VBM) or deformation-based morphometry measure alterations in GM across groups of subjects. Third, surface-based analyses computationally extract the inner and outer surfaces of the cortex, thus capturing its complex folding topography. From this deformable model, measures like cortical thickness, surface area, or the degree of folding can be extracted. Cortical thickness (CT) quantifies the distance between the inside surface and outside surface, while local gyrification index (LGI) is the ratio between the amount of cortex within the sulcal folds to the amount along the outer surface in a given region of interest. These different indices (GM, CT, LGI), have different genetic underpinnings, maturational trajectories, and different relationships with disease pathophysiology (Winkler et al., 2010; Storsve et al., 2014; Kong et al., 2015). MRI measures of macrostructure are indirect measures of anatomy and thus depend on the underlying hardware, software and acquisition sequence. 3 Tesla MRI produces an average resolution of 1 mm^3 per voxel, containing an estimation of 100 000 neurons, 0.4 km of dendrites, 4 km of axons, and 0.4 to 1 x 10^9 synapses (Logothetis, 2008). Undoubtedly, there are vast processes occurring within the contents of a voxel (referred to as microstructure), to which MRI is not sensitive. These limitations are important to consider when interpreting results from sMRI analyses. Despite them, sMRI is a powerful method to measure *in vivo* anatomy in a large number of subjects with widely available automated software pipelines.

sMRI studies have shown heterogeneity in macrostructure associated with hallucinations, but findings that have reproduced include: A negative correlation between current auditory hallucination severity and GM in the left temporal gyrus (Nenadic et al., 2010; Gaser et al., 2004), reduced CT in left temporal gyrus in schizophrenia patients with a history of hallucinations compared to those without (Cui et al., 2018; Morch-Johnsen et al., 2017), and reduced LGI in medial prefrontal and paracentral regions (Garrison et al., 2015;

2018). A possible reason for the variability in structural findings is that cortical features like grey matter and cortical thickness are plastic to aging, learning and experience. On the other hand, sulcal length and depth and certain gyrification indices are relatively stable across the first few decades of life (Cachia et al., 2016). As gyral and sulcal architecture reflect neurodevelopment in the late second to third trimester of gestation, these measures may provide unique insight to the contribution of early brain development to risk for hallucinations. Structural correlates of hallucinations will be reviewed and meta-analysed in Chapter 2.

1.3.2 Functional MRI

Functional MRI (fMRI) can be used to measure brain activity during a specific psychological task (task-based fMRI), or when the participant is not engaged in any task (resting-state fMRI (rsfMRI)), by detecting changes in blood flow. This blood oxygenation level-dependent (BOLD) signal provides an indirect measure of neuronal firing and reflects slow-evolving hemodynamic activity (Logothetis, 2003).

There are two lines of functional neuroimaging studies of hallucinations: (1) "state studies" or "symptom capture studies", which ask, "What is happening in the brain while an individual is hallucinating?", and (2) "trait studies", which ask, "What characterizes the brain of individuals who tend to hallucinate?", thus indicating possible brain mechanisms that predispose a person to experience hallucinations. Trait studies include sMRI, since brain structure does not fluctuate during a hallucination. Considering that hallucinations arise in the absence of an external stimulus, some researchers have hypothesized that their origin relates to abnormal resting-state activity (Northoff and Qin, 2011; Hunter et al., 2006). When an individual is idle ("at rest") in the scanner, the spontaneous neural activity (BOLD fluctuations) of specific spatially distinct sets of brain regions correlate to form large-scale resting-state networks ("large-scale networks" and "resting-state networks" will be used interchangeably). These functionally distinct networks are thought to reflect intrinsic organization of the brain and have been reproducibly associated with cognitive processes in health and illness. These networks include the default mode network (DMN; classically associated with self-referential processing and internally-oriental cognition, but also responds

to external information), the salience network (involved in determining the origin and salience of internal and external stimuli and coordinating the transition between functional networks related to self- and task-processing), and the central executive network (supports executive function and cognitive control) (Li et al., 2019; O'Neill et al., 2019). Few studies have explored large-scale network alterations related to hallucinations, but some authors suggest they arise from atypical interaction between sensory, self-monitoring, and subcortical networks (Hare et al., 2018), or more broadly, disrupted communication between the DMN, salience, and central executive networks (Alderson-Day et al., 2016). Functional alterations in hallucinations will be summarized and reported in Chapter 5.

1.4   Thesis objectives

Hallucinations are complex experiences. It is likely that they manifest through different mechanistic pathways for different aetiologies (i.e., epilepsy, drugs, schizophrenia), and from a plurality of risk factors within a given aetiology (i.e., genetic, environmental, sociocultural). The structural and functional architecture of the brain is associated with hallucinations, indicating one biological class of mechanisms. In particular, variation in cortical sulcation, a marker of early brain development, confers vulnerability for schizophrenia pathology, including hallucinations, but it is not clear what role sulcal deviations play in global brain organization. The goal of my thesis has been to identify and characterize the organization of the human brain that predisposes individuals to hallucinate, chiefly in the context of early schizophrenia, drawing on MRI indices of perinatal brain development. This has involved an in-depth meta-analysis and systematic review, developing and validating protocols for quantifying cortical sulcation, and processing and analysing two independent sMRI and rsMRI datasets of schizophrenia patients with and without hallucinations and healthy controls to address the following aims and hypotheses.

1. **What is the evidence for brain structural correlates of hallucinations? Are there common or distinct neuroanatomical correlates across the spectrum of diagnoses that involve hallucinations?**

Chapter 2 adopts a transdiagnostic approach to review brain structural associations of hallucinations and meta-analyse the grey matter correlates of hallucinations, comparing individuals who experience hallucinations to those who do not. I identified distinct grey matter substrates for hallucination presence in neurodevelopmental (primarily schizophrenia) compared to neurodegenerative (primarily Parkinson's) diseases, which I hypothesize constitute at least two distinct mechanisms. Chapters 3 and 4 focus on the neurodevelopmental mechanism.

2. **Cortical sulcation has been associated with hallucinations in schizophrenia. Does reduced left hemisphere paracingulate sulcus length replicate in two independent, ethnically-distinct datasets? Does a similar relationship exist between hallucinations and right hemisphere superior temporal sulcus depth? What is the role of cerebral asymmetries?**

Chapter 3 replicates an earlier finding, the association of reduced left paracingulate sulcus (PCS) length with hallucinations, in two independent samples representing British and Han Chinese ethnicities. I extend this work to the superior temporal sulcus (STS), which has also associated with hallucinations. Each of these sulci show hemispheric asymmetries in the general population that are aberrant in schizophrenia patients with hallucinations.

3. **PCS morphology is highly variable. Is an accessible manual segmentation protocol valid for enabling replicable measurements between different raters? Can this method be implemented with existing software packages to develop a new, semi-automated method to measure the PCS?**

To make the analysis in Chapter 3 tractable, I validate a manual segmentation protocol for measuring the PCS, showing that with sufficient training, consistent measures are produced between raters. I use an existing neuroimaging software package for segmenting cortical folds (BrainVISA) to develop a semi-automated method for identifying the PCS, which is consistent with the manual method, and allows for additional anatomical detail of the PCS.

4. **Sulcal patterns are products of early neurodevelopment. How do deviations in sulcal geometry of the PCS and STS relate to whole-brain neurodevelopmental**

coordination of large-scale networks, specifically the salience and auditory networks, which have been implicated in hallucinations? Do other whole-brain metrics characterize hallucinations?

Chapter 4 investigates how specific sulcal properties relate to global neurodevelopmental coordination. I focus on the salience and auditory networks, considering their involvement in hallucinations, and their respective inclusion of the PCS and STS (the PCS is on the anterior cingulate cortex, which coordinates the salience network, while the STS borders Heschl's gyrus, which is involved in the auditory network). Structural covariance networks of the local gyrification index demonstrate increased gyrification covariance across the auditory and salience networks for patients with hallucinations. I compliment this work with whole brain analyses of cortical thickness, local gyrification, and grey matter volume.

5. **Local sulcal morphology influences functional connectivity and functional networks are associated with hallucinations. Does a structural marker (sulcal morphology) for hallucinations correlate with connectivity? Is resting-state connectivity alone a trait marker for hallucinations in schizophrenia?**

Chapter 5 presents analyses of resting-state data from the same British and Han Chinese samples described in Chapters 3 and 4. Seed-based and graph theoretical approaches were used to test the hypotheses that sulcal and gyral architecture related to hallucinations would correspond to alterations in functional connectivity and large-scale networks. The results show that the interaction between PCS length and hallucination status associates with seed-based connectivity, but suggest that resting-state connectivity alone is not a trait marker for hallucinations.

Defining the brain mechanisms of hallucinations offers empirical opportunities to test aetiological models of hallucinations and opens lines of investigation for mitigating hallucinations in people at risk. If "[studying] the abnormal is the best way of understanding the normal" (William James), then hallucinations offer a fascinating window to understand normal perception and the processes governing how we distinguish thoughts and imagery as coming from ourselves, as opposed to non-self sources, and provide new understanding of the consequences of cortical folding variation to experiencing diverse worlds.

Chapter 2   A systematic review and meta-analysis of transdiagnostic structural MRI studies of hallucination status

2.1   Abstract

Hallucinations are transmodal and transdiagnostic phenomena, occurring across sensory modalities and presenting in psychiatric, neurodegenerative, and non-clinical populations. Despite their cross-category occurrence, little empirical work has directly compared between-group neural correlates of hallucinations. I performed whole-brain voxelwise meta-analyses of hallucination status across diagnoses using anisotropic effect-size seed-based d mapping (AES-SDM) and conducted a comprehensive systematic review in PubMed and Web of Science until May 2018 on other structural correlates of hallucinations, including cortical thickness and gyrification. 3214 abstracts were identified. Patients with psychiatric disorders and hallucinations (eight studies) exhibited reduced grey matter (GM) in the left insula, right inferior frontal gyrus, left anterior cingulate/paracingulate gyrus, left middle temporal gyrus, and increased in the bilateral fusiform gyrus, while patients with neurodegenerative disorders with hallucinations (eight studies) showed GM decreases in the left lingual gyrus, right supramarginal gyrus/parietal operculum, left parahippocampal gyrus, left fusiform gyrus, right thalamus, and right lateral occipital gyrus. Group differences between psychiatric and neurodegenerative hallucination meta-analyses were formally confirmed using Monte Carlo randomizations to determine statistical significance, and a jackknife sensitivity analysis established the reproducibility of results across nearly all study combinations. For other structural measures (28 studies), the most consistent findings associated with hallucination status were reduced cortical thickness in temporal gyri in schizophrenia and altered

hippocampal volume in Parkinson's disease and dementia. Distinct patterns of neuroanatomical alteration characterize hallucination status in patients with psychiatric and neurodegenerative diseases, suggesting a plurality of anatomical signatures. This approach has implications for treatment, theoretical frameworks, and generates refutable predictions for hallucinations in other diseases and their occurrence within the general population. This chapter addresses the questions:

- What is the evidence for brain structural correlates of hallucinations? Are there common or distinct neuroanatomical correlates across the spectrum of diagnoses that involve hallucinations?

2.2   Introduction

Hallucinations are transdiagnostic and transmodal perceptions of stimuli that do not exist in the physical world. The evolution of hallucination research has witnessed an expanding interest in the experiences of people across the diagnostic spectrum, in both psychiatric disorders, such as schizophrenia and bipolar disorder, and neurodegenerative diseases, such as Parkinson's disease (PD), dementia with Lewy Bodies (DLB), and Alzheimer's disease (AD), and of people with no clinical diagnosis. Historically, hallucinations were considered a cardinal symptom of schizophrenia, but they are not pathognomic: one-third of patients do not hallucinate (Lim et al., 2016), and the experience is often heterogeneous among those who do (Woods et al., 2015). Inter-individual differences among hallucinations prompt several conceptual, mechanistic, and clinical questions: Does phenomenological heterogeneity translate into neurobiological plurality? How would this influence theoretical models of hallucinations and inform treatments? Does the epidemiological and experiential diversity of hallucinations reflect a continuum model, in which symptoms like hallucinations are distributed over a spectrum of individuals who do and do not meet criteria for mental illness, and thus arise from a common mechanism instantiated to different degrees of severity (van Os and Reininghaus, 2016)? Establishing the validity of this conceptual framework against alternatives is important for how we understand and treat hallucinations.

Despite the plurality of hallucinations, there is little empirical work comparing between-group neural correlates of hallucinations. Prior meta-analyses on the brain structural and functional correlates of hallucinations have generally limited their scope to a single diagnosis or modality (Jardri et al., 2011; Kuhn et al., 2012). Only two reviews have investigated hallucinations transdiagnostically or in more than one modality: one without quantitative meta-analytic comparison (Allen et al., 2008), the other focussed on acute functional correlates of hallucinations (Zmigrod et al., 2016). Two meta-analyses have explored the structural correlates of hallucinations, but assessed correlates of hallucination severity rather than presence/absence, and limited their scope to auditory verbal hallucinations (AVH) in schizophrenia (Modinos et al., 2013; Palaniyappan et al., 2012). I therefore planned meta-analyses to evaluate MRI-derived volumetric structural grey matter (GM) correlates of hallucination status across populations, complemented with a comprehensive review of other structural measures, including cortical thickness, gyrification, and structure-specific morphometrics.

A significant issue in neuroimaging studies of hallucinations has been the lack of a clinical control group, thus confounding abnormalities specific to hallucination status with those of the broader phenotype (i.e., schizophrenia). Equally challenging has been a tangled conceptual landscape, with numerous models proposed as cognitive or neurobiological accounts of auditory or visual hallucinations (Figure 2.1). Though an influential model of auditory hallucinations is the inner speech model (Alderson-Day and Fernyhough, 2015), which proposes that AVH arise from misattributing inner speech to a non-self source, alternative models posit the causal agent to be memory-related processes (Waters et al., 2006), spontaneous activation in auditory and related memory areas (Northoff and Qin, 2011), inappropriate proximal salience (Palaniyappan and Liddle, 2012), skewed balance of top-down/bottom-up control dynamics between secondary sensory cortices and frontal regions (Allen et al., 2008; Hugdahl, 2009) or of inhibition/excitation at the physiological level (Jardri et al., 2016) or the mismatch between processes comparing predictive representations of the external world to sensory evidence (Corlett et al., 2019; Horga and Abi-Dargham, 2019). While these models attempt to explain auditory hallucinations in schizophrenia and non-clinical populations, a separate array of models have been proposed

for visual hallucinations in neurodegenerative disorders like PD and AD (Muller et al., 2014; Onofrj et al., 2013; Collerton et al., 2005). Auditory and visual hallucination models overlap in alluding to deficits in reality monitoring, memory, salience, inhibition, and excitation. Additionally, hallucinations have been subcategorized by different neurocognitive mechanisms (Jones, 2010) or by differential contribution of a range of neurochemical systems (Rolland et al., 2014). Obtaining differentiating evidence is difficult as these models are not mutually exclusive, each drawing upon a similar repertoire of constituents, making it non-trivial to derive corresponding predictions. However, brain morphological variation can differentiate patients who do and do not hallucinate (Garrison et al., 2015; Morch-Johnsen et al., 2017; Cuit et al., 2018), indicating that structural MRI can provide insights into why individuals hallucinate.
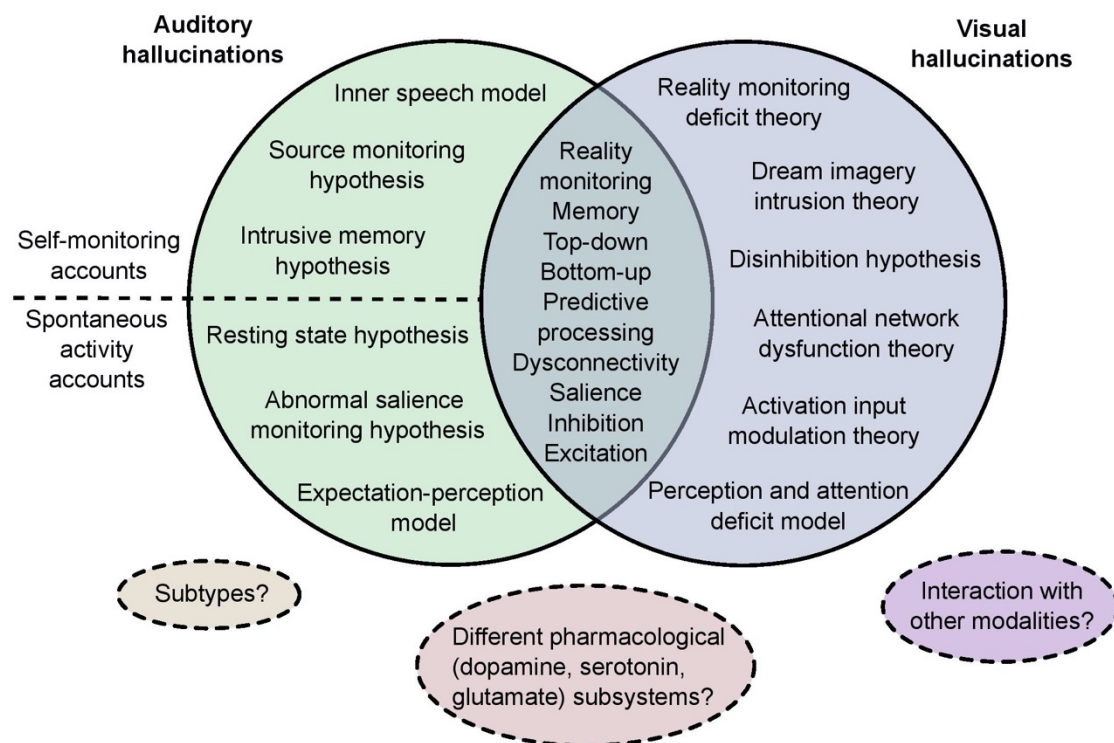
Figure 2.1. Landscape of theoretical models of hallucinations. The major cognitive, psychological, and neurobiological theories for auditory and visual hallucinations are depicted. Separate theories have been proposed to underlie auditory versus visual hallucinations, although they share many common themes. Different

theories within each modality category are not mutually exclusive and may overlap in their predictions. Dotted lines delineate proposals of divisions between, extensions to, or limitations of current theories.

Voxel-based morphometry (VBM) is a common method for unbiased, automated quantification of GM differences between groups. Conducting a meta-analysis of VBM studies is an objective approach to synthesize the extant literature and identify replicable findings (Muller et al., 2018). Knowledge of neuroanatomical signatures of hallucinations present in certain populations and absent in others would clarify the continuum model by identifying whether there exist common neural correlates and contribute towards a clearer neurobiological picture of the origins and mechanisms of hallucinations. Considering the cultural and historical influences on hallucination interpretation (Laroi et al., 2014), an organic model of hallucinations could moreover substantiate accurate diagnostic criteria. This meta-analysis and systematic review quantitatively compared people with and without hallucinations in terms of brain structure to identify the neuroanatomy related to the transdiagnostic presence of hallucinations.

2.3   Methods

2.3.1 Search strategy and selection criteria

A systematic review of the literature for the structural correlates of hallucinations was conducted in October 2017, with update notifications received until May 2018. Following PRISMA guidelines (Moher et al., 2009), articles were identified by searching PubMed and Web of Science using the keyword combination (hallucinat*) AND (MRI OR magnetic resonance imaging OR morphology OR voxel?based OR morphometr* OR neural correlate OR structur*) with no date limit. Reviews and meta-analyses on neuroimaging of hallucinations were cross-referenced to ensure no relevant studies were missed (Carter et al., 2015; Modinos et al., 2013; Palaniyappan et al., 2012; Pezzoli et al., 2017, Allen et al., 2008).

Studies were included in the meta-analyses if they: (a) employed structural MRI in a whole-brain investigation of voxelwise differences in GM reported in standard stereotaxic space; (b) included a direct comparison between groups with and without hallucinations

within the same diagnostic category. Corresponding authors were contacted to request coordinate information if not reported in the original article, or to clarify methodological issues. I evaluated all studies and JS, GM, or JRG confirmed the selection criteria, with uncertainties discussed to consensus. Region of interest (ROI) VBM studies and studies using non-voxelwise structural MRI methods that otherwise matched inclusion criterion (b) were included in the systematic review.

2.3.2 Data analysis

2.3.2.1   Voxel-based morphometry

VBM is a fully automated method for identifying regional changes in grey matter (GM) or white matter (WM) between groups of individuals across the whole brain or within a hypothesized ROI. In broad strokes, the technique entails classifying the brain into GM, WM and cerebrospinal fluid (CSF), smoothing with a Gaussian kernel to estimate the amount of tissue type of interest (i.e., GM) at each voxel, and comparing the amount of GM across subjects after linear or non-linear registration to an average brain template in a mass-univariate analysis (Lerch et al., 2017). The advantages of VBM are that it uses unbiased, standardized methods to quantify brain structure between groups, and it has been used extensively in the investigation of brain structural alterations in psychiatric illness (Glahn et al., 2008). However, as VBM does not provide a direct measure of GM, the outcomes depend on MRI acquisition sequence and hardware, as well as software package (Lerch et al., 2017). These limitations must be considered when interpreting results, though protocols for standardizing sequences across scanning sites show promise in mitigating site differences, as do approaches for modelling site differences in existing neuroimaging datasets (Segall et al., 2009; Lisiecka et al., 2015). A meta-analysis of VBM studies allows for consolidating a disparity of results and quantifying replicable findings.

2.3.2.2   Seed-based d Mapping

Seed-based d Mapping (SDM) is a coordinate-based meta-analysis method used to summarize the findings of voxel-based neuroimaging studies. Such studies often report coordinates and statistics of the peaks of clusters of statistically significant voxels. SDM combines this information to produce summary maps of the structural or functional group differences to synthesize functional and structural neural correlates of neuropsychiatric disorders or symptoms (Zhang et al., 2016; Gharehgzlou et al., 2021; Pezzoli et al., 2018). In contrast to univariate voxel-wise tests of VBM, SDM tests for spatial convergence, that is, whether more studies report findings in the neighbourhood of a given voxel compared to neighbourhoods of other voxels (Albajes-Eizagirre and Radua, 2018). The Anisotropic Effect Size (AES) version of SDM (AES-SDM) refers to the use of anisotropic kernels when creating effect size maps (meaning maps are weighted by the size of the statistical difference). These kernels assign different values to the different neighboring voxels depending on the spatial correlation between them (Radua et al., 2014). In summary, AES-SDM uses peak coordinates and effect sizes from primary studies to create maps of meta-analytic effect size and variance of the signed (positive or negative) GM differences. Similar to other popular coordinate-based meta-analytic methods like Activation Likelihood Estimation (ALE) (Eickhoff et al., 2009), loci from primary studies are estimated as smoothed spheres and meta-analytic maxima calculated by weighting the encompassed voxels. AES-SDM diverges from ALE in that it additionally incorporates the effect sign (indicating increases or decreases in GM) and the t-statistic associated with each peak, increasing both sensitivity and accuracy of the analysis. AES-SDM also allows inclusion of non-significant studies, reducing bias towards positive results. A detailed procedure for using the software is provided in the tutorial (https://www.sdmproject.com/software/tutorial.pdf).

2.3.2.3   Meta-analytic procedure

Voxel-wise meta-analyses were undertaken using (AES-SDM; https://www.sdmproject.com/) (Radua et al., 2012; 2014) following recommended guidelines (Müller et al., 2018). In brief, peak coordinates and t-statistics representing GM differences between patients with and

without hallucinations were extracted from each study. When only z- or p-values were available, they were converted to t-values using the SDM online Statistics Converter. Coordinates reported in Talairach space were converted to MNI space using the Lancaster icbm2tal transform provided by GingerALE software v.2.3.6 (http://brainmap.org/ale/). The effect size signed map of hallucination vs. no-hallucination GM neuroanatomical differences were recreated independently for each study using an anisotropic Gaussian kernel to assign voxel effect sizes weighted by their distance to close peaks. Next, the effect size variance maps were constructed from the effect size maps and the sample size for each study. For studies with non-significant results, voxels within the effect size map are estimated to have a null effect size. Finally, the mean meta-analytic map was calculated with a voxelwise random effects model. The recommended AES-SDM parameters were applied: full width at half-maximum (FWHM) = 20 mm, voxel $P < 0.005$, peak height threshold (SDM Z) ≥ 1, and cluster extent ≥ 10 voxels. These parameters have been empirically validated to optimize between sensitivity and specificity and balance false positives and false negatives. For visualization, I overlaid the study-specific SDM maps on the Colin27 anatomical T1 brain template in Mango Brain viewer.

Anticipating differences in mechanisms of hallucinations between psychiatric illnesses and neurodegenerative diseases based on distinctions in phenomenology, modality, prevalence (Llorca et al., 2016), and the significant participant age separation amongst primary studies ($t(25) = 17.324$, $p<0.001$), I performed two meta-analyses: one meta-analysis of psychiatric diagnoses with neurodevelopmental origins (referred to as the psychiatric or neurodevelopmental meta-analysis), including schizophrenia, first episode schizophrenia (FES), first episode psychosis (FEP), and young adults at clinical risk for psychosis (at-risk mental state long-term, ARMS-LT), and bipolar disorder (BD), and a second meta-analysis of neurodegenerative disorders (referred to as the neurodegenerative meta-analysis), including Parkinson's and Alzheimer's disease (PD and AD). Of the 16 studies included in these two cross-sectional meta-analyses, three (see Table 1) did not make an explicit comparison between a hallucination (H) and no-hallucinations (NH) group, though the majority of patients in each group respectively either did or did not have hallucinations, and were

therefore included (van Swam et al., 2012; Smieskova et al., 2012; Lee et al., 2016). A jackknife sensitivity analysis was performed on the meta-analyses to test reproducibility of significant brain regions by iteratively repeating the statistical analysis systematically excluding one study. Finally, I formally assessed group differences between psychiatric and neurodegenerative hallucination meta-analyses using Monte Carlo randomizations to determine statistical significance and performed a conjunction analysis of the simple overlap between meta-analyses to detect whether there were GM differences common to both psychiatric and neurodegenerative hallucinations (Radua et al., 2013).

2.4 Results

2.4.1 Included studies

The literature search identified 2259 articles from PubMed and 1785 from Web of Science, for a merged total of 3214 after duplicates were excluded (Figure 2.2). 99 articles were selected for whole text retrieval after title/abstract screening. 16 studies met criteria for the meta-analyses (see Table 2.1 for sample characteristics; Table 2.2 for imaging details and results summary) and 28 papers (18 psychiatric; 10 neurodegenerative) for the systematic review of other structural metrics comparing groups with and without hallucinations.

Three of the included studies considered proxy comparisons between hallucinating and non-hallucinating groups. Van Swam et al. (2012) used voxel-wise cortical thickness (VWCT), as opposed to VBM. Though a different analysis, VWCT and VBM are considered complementary methods (*a in Table 2.1). Smieskova et al. (2012) compared FEP to ARMS-LT participants, though the groups differed significantly (p<0.0001) in their hallucination score, with the FEP group having a mean (S.D.) score of 3.5 (2.0) on the Brief Psychiatric Rating Scale hallucination item 10, rated as moderate to moderately severe, and the ARMS-LT group having a mean score of 1.4 (1.0), with a score of 1 being the lowest possible score (*b in Table 2.1). Lee et al. (2016) compared AD patients with misidentification subtype to AD patients without psychosis, though they classified AD patients with hallucinations into the misidentification subtype (*c in Table 2.1).
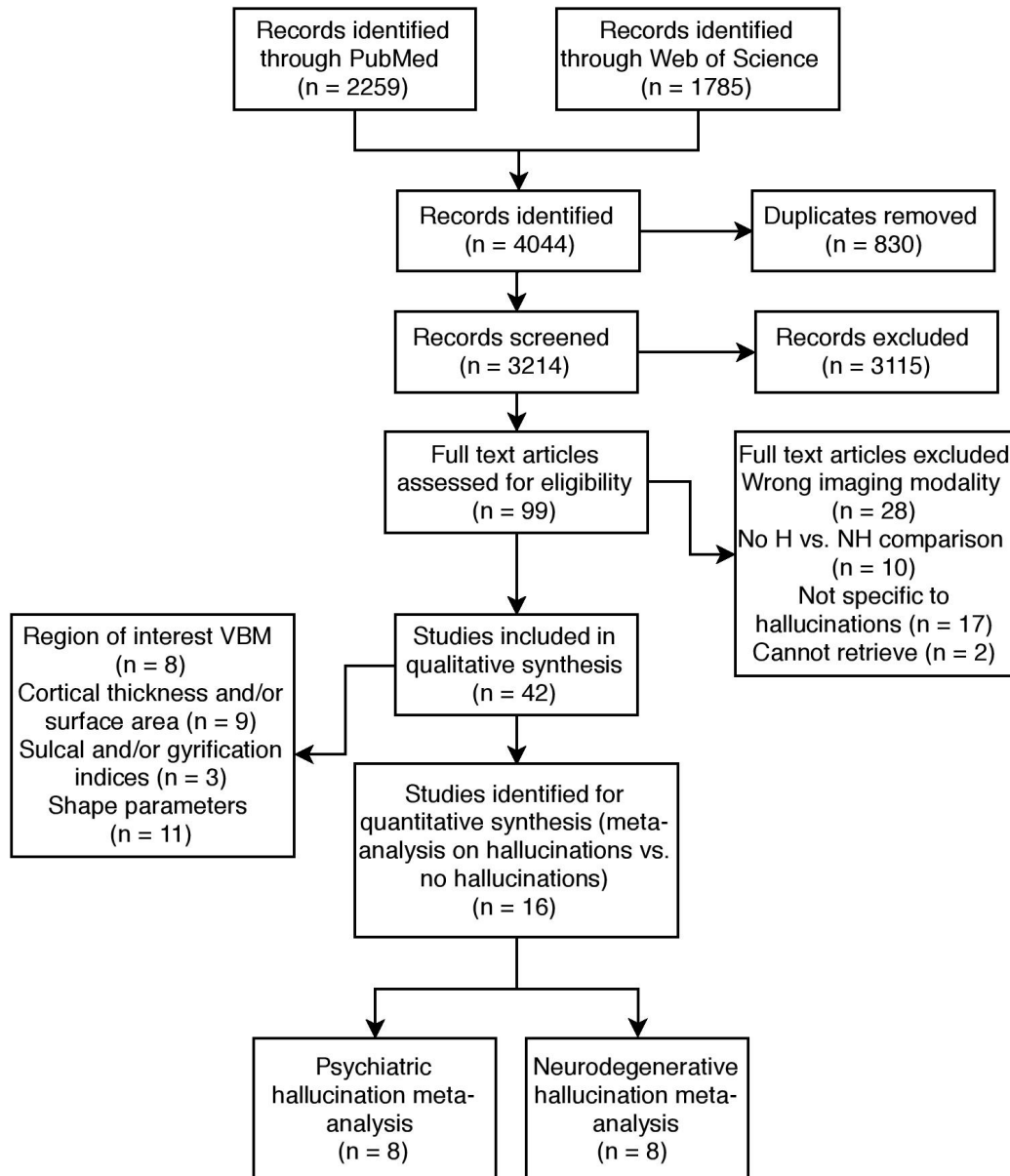
Figure 2.2 PRISMA flowchart for identification and selection of studies. Some studies performed analyses of
multiple structural features and are therefore represented more than once. Abbreviations: H: population with
hallucinations; NH: population without hallucination; VBM: voxel-based morphometry.

Table 2.1. Demographic and clinical characteristics of included studies.

Group	Study	Sample	N	Mean Age (SD)	M/F	Hallucination Assessment Scale (Timescale)	Modality
Psychiatric	Garrison et al., 2015	SCZ-H SCZ-NH	79 34	38.5 (9.8) 40.7 (9.8)	65/14 27/7	clinical interview (lifetime history)	mixed
	Gaser et al., 2004	SCZ-H SCZ-NH	29 56	36.2 (10.9) †	52/33 †	SAPS (variable up to weeks before/after scanning)	auditory
	Shapleske et al., 2002	SCZ-H SCZ-NH	41 31	35.5 (8.8) 32.0 (7.5)	41 31	SAPS (course of illness)	auditory
	van Swam et al., 2012 *a	SCZ-H SCZ-NH	10 10	40.9 (8.8) 36.3 (5.6)	5/5 7/3	PANSS, semi-structured interview (course of illness)	auditory
	van Tol et al., 2014	SCZ-H SCZ-NH	31 20	33.4 (12.5) 35.0 (9.7)	27/4 17/3	PANSS (previous week)	auditory
	Huang et al., 2015	FES-H FES-NH	18 18	22.6 (6.7) 22.7 (3.9)	10/8 9/9	PANSS, HAHRS (previous month)	auditory
	Smieskova et al., 2012 *b	FEP-H ARMS-LT-NH	16 13	25.1 (4.6) 24.6 (2.2)	12/4 8/5	BRPS (variable)	auditory
	Neves et al., 2016	BD-H BD-NH	9 12	37.7 (12.1) 39.9 (15.0)	3/6 6/6	MINI-Plus (lifetime history)	auditory or visual
Neurodegenerative	Goldman et al., 2014	PD-H PD-NH	25 25	74.8 (6.0) 75.4 (6.1)	17/8 18/7	MDS-UPDRS (at least previous month)	mixed
	Meppelink et al., 2011	PD-H PD-NH	11 13	Not reported	Not reported	NPI (previous month)	visual
	Pagonbarraga et al., 2014	PD-H PD-NH	15 27	64.1 (9) 66.3 (8)	Not reported	MDS-UPDRS (previous month)	passage and/or presence

	Ramirez-Ruiz et al., 2007	PD-H	18	Not reported	8/12	NPI Spanish version, semi-structured interview (previous year)	visual
		PD-NH	20		7/11		
	Watanabe et al., 2013	PD-H	13	66.6 (5.5)	7/6	UPDRS (not specified)	visual
		PD-NH	13	63.6 (10.7)	5/8		
	Shin et al., 2012	nPD-H	46	71.3 (5.9)	26/38	NPI (not specified)	visual
		nPD-NH	64	70.7 (5.7)	18/9		
	Lee et al., 2016 *c	AD-H	17	74.3 (7.3)	4/13	NPI Korean version (at least previous month)	auditory or visual
		AD-NH	25	72.4 (9.4)	6/19		
	Blanc et al., 2014	AD-H	39	76.0 (7.4)	20/19	NPI (previous month)	auditory or visual
		AD-NH	39	76.4 (7.2)	20/19		

Abbreviations: AD: Alzheimer's disease; PD: Parkinson's disease; SCZ: schizophrenia; FES: first episode schizophrenia; BD: bipolar disorder; nPD: Parkinson's disease without dementia; FEP: first episode psychosis; ARMS-LT: at risk mental state long-term; X-H: population X with hallucinations; X-NH: population X without hallucinations; NPI: Neuropsychiatric Inventory Questionnaire; MDS-UPDRS: Movement Disorder Society (MDS)-sponsored version of the Unified Parkinson's disease Rating Scale (UPDRS); PANSS: Positive and Negative Symptom Scale; HAHRS: Hoffman Auditory Hallucination Rating Scale; MINI-Plus; Mini International Neuropsychiatric Interview (MINI) Plus; SAPS: Scale for the Assessment of Positive Symptoms; BRPS: Brief Psychiatric Rating Scale. †Age and gender were not available for H and NH groups separately and are presented for the total sample of patients with schizophrenia.

Table 2.2. Imaging characteristics and key results of included studies.

Group	Study	Software, (Tesla), FWHM (mm)	Covariates	Statistical Threshold	Original stereotaxic space, n Foci	Main result
Psychiatric	Garrison et al., 2015	SPM8 (1.5), 8	TIV	p<0.001, uncorrected minimum cluster size=100 voxels	MNI, 2	H>NH: bilateral occipital lobe

Gaser et al., 2004	SPM99 (1.5), 8	SANS total score, SAPS total score without auditory hallucination sub-items, gender	p<0.001, uncorrected, k=100 voxels	Talairach, 4	H<NH: L transverse temporal (Heschl's) gyrus R middle/inferior frontal gyrus, L middle temporal gyrus, L paracingulate gyrus
Shapleske et al., 2002	AFNI (1.5), -4.2	age and handedness	absolute value of standard error <1.96	Talairach, 1	H<NH: L insular cortex
van Swam et al., 2012	Brain Voyager QX 1.9 (3), Not reported	none	p<0.05, cluster size >15 voxels, corrected for multiple comparisons (Bonferroni p < 0.0063)	MNI, 7	H>NH: L middle frontal gyrus, L posterior cingulate gyrus, L frontal insula, L para-hippocampal gyrus, L postcentral sulcus, R visual cortex H<NH: posterior inferior temporal sulcus, postcentral gyrus
van Tol et al., 2014	SPM8 (3), 8	age, sex	p<0.05 FWE-corrected (cluster level), voxel-wise threshold of p<0.005 uncorrected	MNI, 3	H<NH: L putamen
Huang et al., 2015	SPM8 (3), 8	age, gender, years of education	p<0.001, uncorrected	Talairach, 0	n.s.

	Smieskova et al., 2012	SPM8 (3), 8	age, gender and total GMV	p<0.001, uncorrected (cluster-forming threshold) p<0.05 FWE-corrected	MNI, 3	H<NH: L para-hippocampal gyrus H>NH: L superior frontal gyrus, L caudate
	Neves et al., 2016	SPM8 (1.5), 8	total GMV	p<0.05, whole-brain FWE-corrected	Not reported, 0	n.s.
Neurodegenerative	Goldman et al., 2014	SPM8 (1.5), 8	TIV	p<0.01, uncorrected, cluster extent threshold k=10	Talairach, 18	H<NH: bilateral cuneus, bilateral fusiform gyrus, bilateral inferior parietal lobule, bilateral precentral gyrus, bilateral middle occipital gyrus, R lingual gyrus, bilateral cingulate gyrus, L paracentral lobule
	Meppelink et al., 2011	SPM5 (3), 10	total GM	p<0.05, brain-volume corrected cluster-level	MNI, 0	n.s.
	Pagonbarraga et al., 2014	SPM5 (1.5), 12	age, gender and global GMV	p<0.001, uncorrected, cluster size=207 voxels (determined by 1000	MNI, 4	H<NH: R vermis, R precuneus H>NH: posterior lobe of cerebellum, L inf. frontal cortex

			Monte Carlo simulations)		
Ramirez-Ruiz et al., 2007	SPM2 (1.5), 12	TIV, MMSE, Hamilton and Hoehn and Yahr scores	p<0.05, corrected cluster p-level	Talairach, 3	H<NH: bilateral sup. parietal lobe, L lingual gyrus
Watanabe et al., 2013	SPM8 (3), 8	TIV, age, and sex	p<0.01, FWE corrected, cluster size > 50 voxels and z-scores ≥ 3.00	MNI, 15	H<NH: bilateral middle frontal gyrus, L cingulate gyrus, R inferior parietal lobule, bilateral cuneus, L fusiform gyrus, L posterior lobe, L inferior occipital gyrus, L inferior frontal gyrus, L declive, R lingual gyrus
Shin et al., 2012	SPM8 (3), 6	age, sex, PD duration, intracerebral volume, K-MMSE score	p<0.05, FWE corrected, uncorrected p<0.001 at the voxel level, minimum cluster size=100 voxels	Talairach, 5	H<NH: R inferior frontal gyrus, L thalamus, L uncus, L para-hippocampal gyrus
Lee et al., 2016	SPM8 (3), 8	age, gender, education, TIV, CDR score, NPI non-psychotic scores	p<0.001 uncorrected, extent threshold of contiguous 100 voxels (k>100)	MNI, 6	H<NH: R inferior parietal lobule, R lingual gyrus, L cuneus, R middle frontal gyrus, R superior occipital

					gyrus, R middle temporal gyrus
Blanc et al., 2014	SPM12b (1.5), 8	age, total amount of GM	p<0.001, uncorrected, minimum cluster size=25 voxels	MNI, 3	H<NH: R insula / inferior frontal gyrus, L superior frontal gyrus, bilateral lingual gyrus

Abbreviations: AD: Alzheimer's disease; PD: Parkinson's disease; SCZ: schizophrenia; FES: first episode schizophrenia; BD: bipolar disorder; nPD: Parkinson's disease without dementia; FEP: first episode psychosis; ARMS-LT: at risk mental state long-term; X-H: population X with hallucinations; X-NH: population X without hallucinations; NPI: Neuropsychiatric Inventory Questionnaire; MDS-UPDRS: Movement Disorder Society (MDS)-sponsored version of the Unified Parkinson's disease Rating Scale (UPDRS); PANSS: Positive and Negative Symptom Scale; HAHRS: Hoffman Auditory Hallucination Rating Scale; MINI-Plus; Mini International Neuropsychiatric Interview (MINI) Plus; SAPS: Scale for the Assessment of Positive Symptoms; BRPS: Brief Psychiatric Rating Scale; SANS: Scale for the Assessment of Negative Symptoms; FWE: family-wise error; TIV: total intracranial volume; GM: grey matter; GMV: grey matter volume; CDR: Clinical Dementia Rating scale; MMSE: Mini-Mental State Examination; K-MMSE: Korean version of MMSE; L: left; R: right; n.s.: non-significant

2.4.2 Grey matter correlates of hallucination status

In psychiatric patients with hallucinations, relative to those without, GM reductions were identified in the left insula, right inferior frontal gyrus (IFG), left anterior cingulate/paracingulate gyrus, and left middle temporal gyrus, while GM increases were observed in the bilateral fusiform gyrus (Table 2.3, Figure 2.3). Significant decreases in GM were apparent in six brain regions in patients with neurodegenerative disorders with hallucinations compared to those without: (1) left lingual gyrus; (2) right supramarginal gyrus / parietal operculum; (3) left fusiform gyrus; (4) left parahippocampal gyrus; (5) right thalamus; (6) right lateral occipital gyrus (Table 2.3, Figure 2.3). Individuals with psychiatric relative to neurodegenerative hallucinations showed decreased GM in the left insula and anterior cingulate/paracingulate gyrus, and greater GM in the right lingual gyrus, IFG, and supramarginal gyrus, left thalamus, fusiform gyrus, inferior occipital gyrus,

parahippocamapal and hippocampal gyri, and bilateral superior frontal gyrus (Table 2.4, Figure 2.3). There were no regions of GM alterations that were common to hallucination status between the psychiatric and neurodegenerative meta-analyses.
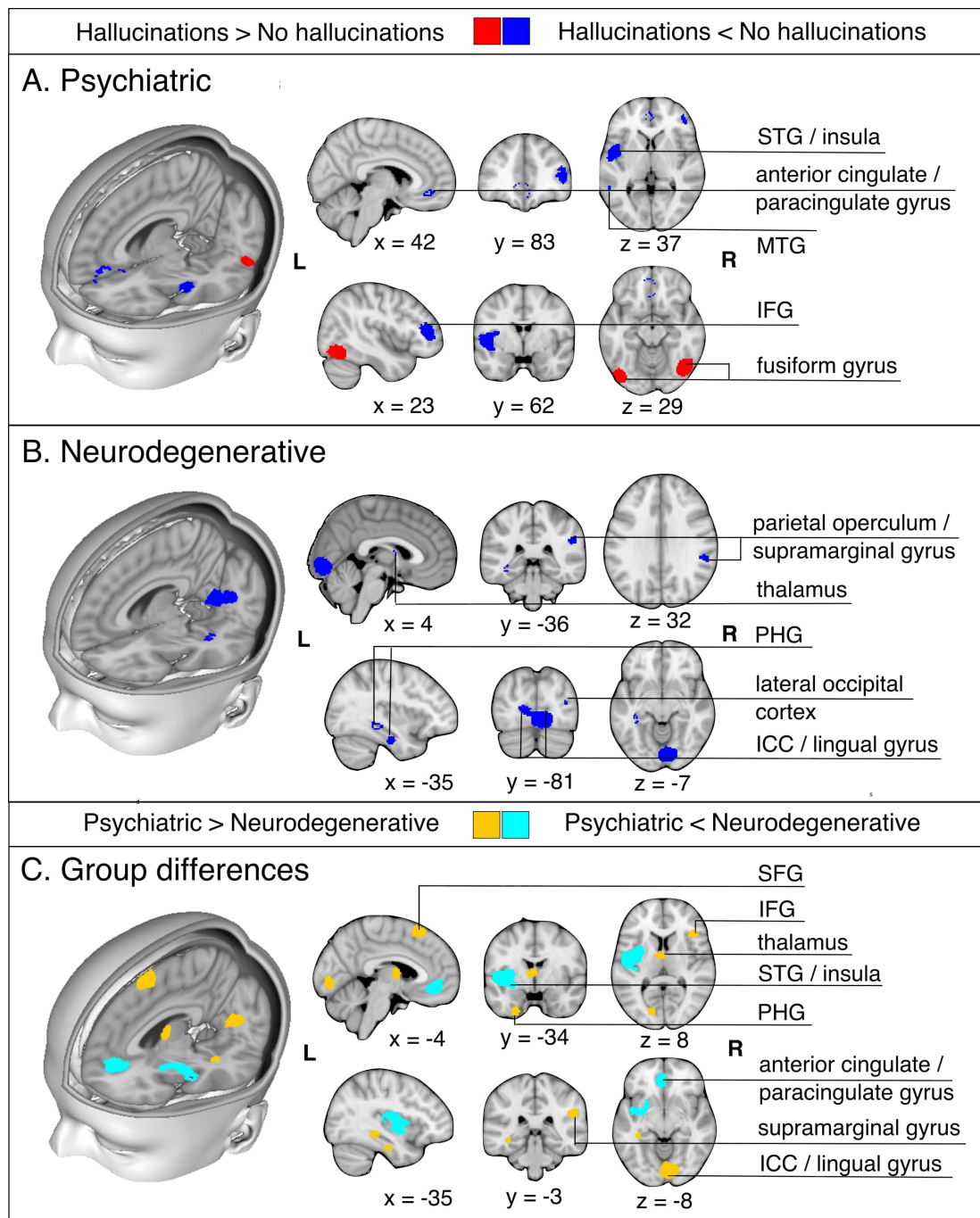
Figure 2.3. Meta-analysis results for individuals with hallucinations compared to those without hallucinations in psychiatric and in neurodegenerative disorders. A. For psychiatric disorders (A), the meta-analysis revealed grey

matter decreases in the left insula, right inferior frontal gyrus (pars triangularis) / frontal pole, left anterior
cingulate gyrus / paracingulate gyrus, left middle temporal gyrus, and grey matter increases in the bilateral
fusiform gyrus in patients with hallucinations relative to those without. B. For neurodegenerative disorders, the
meta-analysis revealed decreases in the left lingual gyrus / intracalcarine cortex, left fusiform gyrus, right
supramarginal gyrus, left parahippocampal gyrus, right thalamus, and right lateral occipital cortex. C. Formal
comparison between meta-analyses revealed reduced GM in the left insula and left anterior
cingulate/paracingulate gyrus for individuals with psychiatric relative to neurodegenerative hallucinations, while
those with neurodegenerative hallucinations exhibited less GM in the right lingual gyrus, IFG, and
supramarginal gyrus, left thalamus, fusiform gyrus, inferior occipital gyrus, parahippocamapal and hippocampal
gyri, and bilateral SFG compared to the neurodevelopmental hallucination group. Abbreviations: STG: superior
temporal gyrus; MTG: middle temporal gyrus; IFG: inferior frontal gyrus; PHG: parahippocampal gyrus; ICC:
intracalcarine cortex; SFG: superior frontal gyrus

Table 2.3. Regions of significant differences in grey matter between patients with hallucinations compared to
those without for psychiatric and neurodegenerative disorders.

Group	Contrast	Region	MNI coordinate of peak local maximum	Cluster size (# of voxels)	SDM Z-score	Uncorrected p-value	Jackknife sensitivity analysis*
Psychiatric	H<NH	L insula	-46, 2, -2	820	-1.885	0.000046	7/8
		R inferior frontal gyrus, pars triangularis / frontal pole	48, 36, 8	281	-1.464	0.000826	7/8
		L anterior cingulate gyrus / paracingulate gyrus	0, 36, -2	132	-1.259	0.00280	7/8
		L middle temporal gyrus	-58, -42, -2	30	-1.259	0.00280	7/8
	H>NH	R fusiform gyrus	44, -64, -18	574	1.455	0.000088	7/8

		L lateral occipital cortex / fusiform gyrus	-40, -82, -16	345	1.454	0.000098	7/8
Neurodegenerative	H<NH	L lingual gyrus / intracalcarine cortex	0, -86, -4	1275	-2.621	0.00001	8/8
		L fusiform gyrus / inferior temporal gyrus	-36, -18, -26	50	-1.860	0.00097	7/8
		R supramarginal gyrus / parietal operculum	54, -36, 30	75	-1.609	0.00348	6/8
		L parahippocampal gyrus	-38, -32, -10	42	-1.740	0.00186	7/8
		R thalamus	2, -2, 12	14	-1.637	0.00306	7/8
		R lateral occipital cortex	36, -80, 14	10	-1.511	0.00440	6/8

Abbreviations: H: Hallucinations; NH: No hallucinations; L: left; R: right. *The jackknife sensitivity analysis tests the reproducibility of significant brain regions by iteratively repeating the statistical analysis, but systematically excluding one study from each replication. Fractions show the number of study combinations in which the region was preserved out of the total number of dataset combinations.

Table 2.4. Regions of significant differences in grey matter between psychiatric and neurodegenerative hallucinations.

Contrast	Region	MNI coordinate of peak local maximum	Cluster size (# of voxels)	SDM Z-score	Uncorrected p-value
Psychiatric < Neurodegenerative	L insula	-42, -2, 2	1784	1.794	<0.0001
	L anterior cingulate gyrus / paracingulate gyrus	0, 44, -10	372	1.235	0.001115
Neurodegenerative < Psychiatric	R lingual gyrus	4, -84, -6	1080	-2.331	0.000021
	L superior frontal gyrus	-10, 26, 64	167	-1.403	0.001667

	R supramarginal gyrus	52, -34, 28	131	-1.365	0.002023
	L thalamus	-4, -4, 10	115	-1.516	0.000815
	L fusiform gyrus	-24, -2, -42	90	-1.494	0.001006
	R inferior frontal gyrus, pars triangularis	42, 24, 8	82	-1.444	0.001347
	L inferior occipital gyrus	-44, -78, -16	71	-1.482	0.001079
	L parahippocampal gyrus	-32, -18, -26	51	-1.450	0.001316
	R superior frontal gyrus	14, 36, -30	34	-1.515	0.000846
	L hippocampus	-36, -34, -8	33	-1.524	0.000769

2.4.3 Qualitative review of studies comparing individuals with hallucinations to those without using regional or non-voxelwise structural measures

28 studies employed a regional and/or non-voxelwise approach to evaluate structural MRI data with respect to hallucination status: seven studies performed VBM restricted to predefined ROIs, one performed source-based morphometry, nine explored cortical thickness (CT) and/or surface area, three investigated gyral/sulcal properties, and 11 assessed structure-specific shape parameters. Results are summarized in Tables 2.5–2.6. Overall, findings were heterogeneous, with few direct replications. In schizophrenia, the most consistent findings were reductions in CT in the vicinity of the left or right temporal gyrus for patients with hallucinations compared to those without, coincident with the reductions in GM in left MTG observed in the psychiatric meta-analysis (Figure 2.3). However, two studies reported increases in GM in temporal regions with hallucinations. Hallucinations in PD and DLB were characterized by distributed patterns of cortical thinning and related to hippocampal volume, though the direction of this association was mixed.

Table 2.5. Summary of systematic review from grey matter volume region of interest studies comparing individuals with and without hallucinations.

Group	Study	Sample (M/F)	Mean Age (SD)	Modality (Assessment)	Region(s) of interest	Analysis (Software)	Main result
Psychiatric	Garrison et al., 2015	79 (65/14) SCZ-H 34 (27/7) SCZ-NH	38.5 (9.8) 40.7 (9.8)	mixed (clinical interview)	medial prefrontal cortex (mPFC)	VBM (SPM12)	Gray matter volume H>NH: mPFC
	Cierpka et al., 2017	10 (6/4) SCZ-H 10 (8/2) SCZ-NH	36.5 (9.0) 32.1 (6.2)	auditory (BRPS, PANSS, PsyRatS)	cerebellum	VBM (SPM8)	Gray matter volume H<NH: R lobule VIIIa
	Kubera et al., 2014	10 (6/4) SCZ-H 10 (8/2) SCZ-NH	36.5 (9.0) 32.1 (6.2)	auditory (BRPS, PANSS, PsyRatS)	n/a	SBM (GIFT)	Gray matter volume SCZ-H<SCZ-NH: component consisting of MFG; IFG; STG; insula; IPL; rectal gyrus; transverse temporal gyrus; supramarginal gyrus; lingual gyrus; postcentral gyrus; fusiform gyrus; subcallosal gyrus; MTG;

						ITG; orbital gyrus
	Neves et al., 2016	9 (3/6) BD-H 12 (6/6) BD-NH	37.7 (12.1) 39.9 (15.0)	auditory or visual (MINI-Plus)	orbitofrontal cortex, ventral prefrontal areas, cingulate gyrus, fusiform gyrus, superior temporal sulcus, amygdala, insula, thalamus	VBM (SPM8)	Gray matter volume BD-H<BD-NH: R posterior insular cortex
	Stanfield et al., 2009	17 (n/a) BD-H 49 (n/a) BD-NH	36.4 (11.1) *	auditory (OPCRIT symptom checklist)	temporal lobe	VBM (SPM99)	Gray matter density BD-H<BD-NH: L middle temporal gyrus
Neurodegenerative	Janzen et al., 2012	13 (6/7) PD-H 13 (7/6) PDD-H 16 (9/7) PD-NH	66.0 (6.9) 67.7 (7.1) 64.3 (8.0)	visual (UPDRS)	pedunculopontine nucleus (PPN), thalamus	VBM (SPM8)	Gray matter volume PD-H+PDD-H< PD-NH: PPN, thalamus PD-H<PD-NH: PPN
	Sanchez-Castenada et al., 2010	6 (4/2) DLB-H 6 (4/2) DLB-NH 8 (6/2) PDD-H 7 (4/3) PDD-NH	70.2 (12.4) 71 (10.7) 75.3 (4.9) 70.6 (7.1)	visual (NPI)	frontal (BA 6, 8, 9, 10, 44, 45, and 47), occipital (BA 18,19), parietal (BA 7, 39, 40), and temporal (20) regions	VBM (SPM5)	Gray matter volume DLB-H<DLB-NH: R inferior frontal gyrus (BA 45) PDD-H<PDD-NH: L

						orbitofrontal lobe (BA 10)
	Colloby et al., 2017	41 (26/15) DLB-H 47 (33/14) AD-NH	78.6 (6.2) 79.0 (8.8)	visual (NPI)	substantia innomiata (SI)	VBM (SPM8)	Gray matter volume n.s.

Abbreviations: AD: Alzheimer's disease; PD: Parkinson's disease; PDD: Parkinson's disease with dementia; SCZ: schizophrenia; FES: first episode schizophrenia; BD: bipolar disorder; nPD: Parkinson's disease without dementia; FEP: first episode psychosis; ARMS-LT: at risk mental state long-term; DLB: dementia with Lewy bodies; X-H, X-NH: population X with and without hallucinations; NPI: Neuropsychiatric Inventory Questionnaire; MDS-UPDRS: Movement Disorder Society (MDS)-sponsored version of the Unified Parkinson's disease Rating Scale (UPDRS); PANSS: Positive and Negative Symptom Scale; HAHRS: Hoffman Auditory Hallucination Rating Scale; MINI-Plus; Mini International Neuropsychiatric Interview (MINI) Plus; SAPS: Scale for the Assessment of Positive Symptoms; BRPS: Brief Psychiatric Rating Scale; OPCRIT: Operational Criteria Checklist for Psychotic Illness and Affective Illness; MFG: medial frontal gyrus; IFG: inferior frontal gyrus; STG: superior temporal gyrus: IPL: inferior parietal lobule; MTG: middle temporal gyrus; ITG: inferior temporal gyrus; SBM: source-based morphometry; R: right; L: left. *H and NH groups combined.

Table 2.6. Summary of systematic review from non-voxelwise structural studies comparing individuals with and without hallucinations.

Measure (Group)	Study	Sample (M/F)	Mean Age (SD)	Modality (Assess-ment)	Analysis (Software)	Main result
Cortical thickness and/or surface area (Psychiatric)	Chen et al., 2015	18 (12/6) FES-H 31 (17/14) FES-NH	24.1 (6.3) 24.3 (5.9)	auditory (AHRS, SAPS/ SANS)	Whole-brain vertex-wise cortical thickness (FreeSurfer)	Cortical thickness FES-H<FES-NH: R Heschl's gyrus; Negative correlation with hallucination severity by AHRS: R HG

Cui et al., 2018	115 (52/63) SCZ-H 93 (47/36) SCZ-NH	26.4 (5.7) 27.3 (5.1)	auditory (PANSS, AHRS)	Whole-brain vertex-wise cortical thickness (FreeSurfer)	Cortical thickness SCZ-H<SCZ-NH: L middle temporal gyrus (MTG) Negative correlation with hallucination severity by PANSS P3, but not AHRS across all SCZ patients: L MTG
Morch-Johnsen et al., 2017	145 (82/63) SCZ-H 49 (33/16) SCZ-NH	31.1 (9.3) 30.9 (8.4)	auditory (PANSS)	ROI cortical thickness and surface area analysis of bilateral HG, planum temporale (PT) and superior temporal gyrus (STG) (FreeSurfer)	Cortical thickness SCZ-H<SCZ-NH: L HG Cortical surface area n.s.
Morch-Johnsen et al., 2018	49 (18/31) BD-H 108 (48/60) BD-NH	33.4 (12.0) 35.0 (11.4)	auditory (SCID)	Whole-brain vertex-wise and ROI cortical thickness (FreeSurfer)	Cortical thickness BD-H>BD-NH: L HG (ROI) and superior parietal lobule (whole-brain) Cortical surface area n.s.
Yun et al., 2016	27 (9/18) FEP-H 24 (12/12) FEP-NH	22.5 (5.0) 22.7 (5.1)	auditory (PANSS)	Support vector machine using cortical surface area and thickness measures	Optimal feature sets of individualized cortical structural covariance FEP-H vs. FEP-NH (83.6% accuracy): intraparietal sulcus,

					Broca's complex, anterior insula
					FEP-H vs. FEP-NH (82.3% accuracy): executive control network, Wernicke's module
	van Lutterveld et al., 2014	50 (19/31) NC-H 50 (19/31) NC-NH	40.8 (11.6) 40.5 (15.0)	auditory (modified LSHS)	Whole-brain vertex-wise cortical thickness (FreeSurfer)	Cortical thickness NC-H<NC-NH: L paracentral cortex, L pars orbitalis, R fusiform gyrus, R ITG, R insula
Cortical thickness and/or surface area (Neurodegenerative)	Ffytche et al., 2017	21 (15/6) PD-H 286 (192/94) PD-NH	64.43 (7.5) 61.97 (9.9)	visual (UPDRS)	Whole-brain vertex-wise cortical thickness (FreeSurfer)	Cortical thickness PD-H<PD-NH: R supramarginal gyrus, superior frontal cortex, lateral occipital cortex
	Delli Pizzi et al., 2014	18 (9/9) DLB-H 15 (7/8) AD-NH	75.5 (4.0) 75.6 (7.6)	visual (NPI)	Whole brain vertex-wise cortical thickness (FreeSurfer)	Cortical thickness DLB-H<AD-NH: R posterior regions (superior parietal gyrus, precuneus, cuneus, pericalcarine and lingual gyri) Negative correlation with hallucination severity by NPI hallucination item in DLB patients: R precuneus and superior parietal gyrus
	Delli Pizzi et al., 2016	19 (9/10) DLB-H	76.4 (4.4)	visual (NPI)	Between group differences in	Cortical thickness n.s.

		15 (6/9) AD-NH	76.5 (7.2)		cortical thickness of entorhinal, parahippocampal, and perirhinal structures (FreeSurfer)	
Sulci and gyrification measures (Psychiatric)	Garrison et al., 2015	79 (65/14) SCZ-H 34 (27/7) SCZ-NH	38.5 (9.8) 40.7 (9.8)	mixed (clinical interview)	ROI LGI of mPFC regions of interest (frontopolar, medial orbitofrontal, superior frontal and paracentral cortices) (FreeSurfer)	Local gyrification index SCZ-H<SCZ-NH: mPFC regions surrounding PCS (bilateral frontopolar, medial orbitofrontal, superior frontal and paracentral cortices)
	Kubera et al., 2018	10 (6/4) SCZ-H 10 (8/2) SCZ-NH	36.5 (9.0) 32.1 (6.2)	auditory (BRPS, PANSS, PsyRatS)	Whole-brain vertex-wise local gyrification index (FreeSurfer)	Local gyrification index SCZ-H<SCZ-NH: L Broca's area, R Broca's homologue, R superior middle frontal cortex SCZ-H>SCZ-NH: precuneus and superior parietal cortex Negative correlation between LGI and hallucination severity (BPRS total score): L Broca's area and R homologue, precuneus, superior parietal cortex

	Cachia et al., 2015	16 (9/7) SCZ-VH 17 (11/6) SCZ-NVH	30.4 (12.6) 30.5 (8.7)	visual (PANSS, SAPS)	Between group differences in global sulcal indices (BrainVISA)	Global sulcation index SCZ-H<SCZ-NH: R parietal cortex and L sylvian fissure
Shape parameters: volume, length, surface area, intensity (Psychiatric)	Rossell et al., 2001	42 (all M) SCZ-H 29 (all M) SCZ-NH	35.5 (9.0) 32.3 (7.4)	auditory (SAPS)	Between group differences in corpus callosum (divided into 4 sections: anterior, mid-anterior, mid-posterior, posterior), surface area and length	Corpus callosum surface area and length n.s.
	Shapleske et al., 2001	44 (all M) SCZ-H 30 (all M) SCZ-NH	35.5 (8.8) 32.0 (7.5)	auditory (SAPS)	Between group differences in Sylvian fissure length, planum temporale surface area and volume	Sylvian fissure length, planum temporale volume and surface area n.s.
	Hubl et al., 2010	13 (8/5) SCZ-H 13 (8/5) SCZ-NH	33 (8) 31 (9)	auditory (PANSS)	Between group differences in GMV of HG	Gray matter volume SCZ-H>SCZ-NH: R HG
	Garrison et al., 2015	79 (65/14) SCZ-H 34 (27/7) SCZ-NH	38.5 (9.8) 40.7 (9.8)	mixed (clinical interview)	Between group differences in length of paracingulate sulcus (PCS)	Length of paracingulate sulcus SCZ-H < SCZ-NH: L PCS
	Amad et al., 2014	16 (9/7) SCZ-A+VH 17 (11/6) SCZ-AH	30.4 (12.6) 30.5 (8.7)	visual (SAPS)	Between group differences in hippocampal volume	Mean hippocampal volume SCZ-A+VH>SCZ-AH Local hippocampal shape differences

					SCZ-A+VH>SCZ-AH: anterior and posterior end of CA1, subiculum
	Shin et al., 2005	17 (7/10) FEP-H 8 (2/6) FEP-NH	31.0 (5.0) 28.4 (4.8)	auditory (PANSS)	Between group differences in GM and WM volumes of frontal, parietal, temporal, occipital, cerebellum	Gray matter volume FEP-H>FEP-NH: frontal, parietal, and temporal lobes, ventricles White matter volume FEP-H>FEP-NH: temporal lobe
Shape parameters: volume, length, surface area, intensity (Neurodegenerative)	Ffytche et al., 2017	21 (15/6) PD-H 286 (192/94) PD-NH	64.43 (7.5) 61.97 (9.9)	visual (UPDRS)	Between group differences in subcortical GMV (FreeSurfer)	Subcortical grey matter volume PD-H<PD-NH: bilateral hippocampus, caudate, putamen
	Pereira et al., 2013	18 (6/12) PD-H 18 (6/12) PD-NH	73.7 (5.4) 73.8 (6.8)	visual (NPI)	Between group differences in hippocampal subfield volumes (fimbria, presubiculum, subiculum, CA1, CA2-3, CA4-DG, hippocampal fissure)	Hippocampal subfield volumes n.s.
	Yao et al., 2016	12 (10/2) PD-H 15 (10/5) PD-NH	70* 66*	visual (UPDRS)	Between group differences in hippocampal volume and vertex-wise analysis of	Hippocampal volume and shape n.s.

	Delli Pizzi et al., 2016	19 (9/10) DLB-H 15 (6/9) AD-NH	76.4 (4.4) 76.5 (7.2)	visual (NPI)	Between group differences in volumes of total hippocampi and hippocampal subfields (FreeSurfer)	Gray matter volume AD-NH<DLB-H: L total hippocampal volume, bilateral CA1, left CA2-3, CA4-DG and subiculum
					hippocampal shape	
	Lin et al., 2006	5 (3/2) AD-H 5 (3/2) AD-NH	73 (6) 73 (4)	visual (report from patient or caregiver)	Between group differences in white matter signal hyperintensities	Periventricular hyperintensity AD-H>AD-NH: occipital caps

Abbreviations: AD: Alzheimer's disease; PD: Parkinson's disease; PDD: Parkinson's disease with dementia; SCZ: schizophrenia; FES: first episode schizophrenia; BD: bipolar disorder; nPD: Parkinson's disease without dementia; FEP: first episode psychosis; ARMS-LT: at risk mental state long-term; DLB: dementia with Lewy bodies; X-H: population X with hallucinations; X-NH: population X without hallucinations; NPI: Neuropsychiatric Inventory Questionnaire; MDS-UPDRS: Movement Disorder Society (MDS)-sponsored version of the Unified Parkinson's disease Rating Scale (UPDRS); PANSS: Positive and Negative Symptom Scale; HAHRS: Hoffman Auditory Hallucination Rating Scale; MINI-Plus; Mini International Neuropsychiatric Interview (MINI) Plus; SAPS: Scale for the Assessment of Positive Symptoms; BRPS: Brief Psychiatric Rating Scale; OPCRIT: Operational Criteria Checklist for Psychotic Illness and Affective Illness; MFG: medial frontal gyrus; IFG: inferior frontal gyrus; STG: superior temporal gyrus: IPL: inferior parietal lobule; MTG: middle temporal gyrus; ITG: inferior temporal gyrus; SBM: source-based morphometry. LSHS: Launay and Slade Hallucination Scale (LSHS); R: right; L: left. *Median age.

2.5   Discussion

2.5.1 Distinct neuroanatomical signatures for hallucinations in neurodevelopmental and neurodegenerative disorders

Distinctive patterns of neuroanatomical alteration characterize hallucination status in patients with psychiatric and neurodegenerative diseases, with the former associated with fronto-

temporal deficits and the latter with medial temporal, thalamic and occipital deficits. These
results broadly align with prior meta-analyses investigating GM correlates of auditory verbal
hallucination (AVH) severity in schizophrenia, which found negative correlations between
AVH severity in schizophrenia and GMV within the bilateral superior temporal gyrus (STG),
bilateral Heschl's gyrus, and bilateral insula (Modinos et al., 2013; Palaniyappan et al., 2012;
Allen et al., 2008) and qualitative reviews on structural imaging studies of visual
hallucinations (VH) in neurodegenerative illnesses, which found GM atrophy associated with
VH in patients with PD in parietal, hippocampal, and occipito-temporal regions, primarily the
lingual and fusiform gyri (Pezzoli et al., 2017; Lenka et al., 2015). The distributed pattern of
structural changes seen in both hallucination signatures is suggestive of impairment in the
coordination of information flow. Indeed, AVH in schizophrenia have been associated with
increased functional activation in the STG, insula, anterior cingulate, and pre/post central
gyrus (Jardri et al., 2011; Kuhn et al., 2012), reduced resting connectivity between default
mode regions, disruptions to the salience network, and altered interactions between resting-
state networks (Alderson-Day et al., 2015; Palaniyappan and Liddle, 2012). Compared to
AVH, VH in schizophrenia have been associated with increased seed-based functional
connectivity between the amygdala and visual cortex (Ford et al., 2015), among the
hippocampus, medial prefrontal cortex, and caudate nuclei and white matter connectivity
between the hippocampus and visual areas (Amad et al., 2014), as well as decreased global
sulcation in the right hemisphere (Cachia et al., 2015). VH in PD have been associated with
increased functional activity in the lingual gyrus, cuneus, and fusiform gyrus (Zmigrod et al.,
2016), and hyperconnectivity in the default mode network (Yao et al., 2014). Cortical
thickness (CT) studies lend further support for divergent structural patterns, showing
localized decreases in CT in temporal regions in people with schizophrenia spectrum
disorders, and more widespread decreases in CT in dementia and PD.

I reviewed the brain structural abnormalities associated with hallucinations, yet how
changes to the brain's topological substrate translate to changes in an individual's
experiential landscape remain unknown. The findings are consistent with multiple models of
hallucinations (Figure 2.1). For instance, volume loss in temporal regions could reflect the

misattribution of inner speech to a non-self source (inner speech model), or relate to abnormalities in cortical feedback for predictive signal processing (predictive processing account), or could be the result (or cause) of heightened resting state activity in the auditory cortex (resting-state hypothesis), or a combination of some or all of these mechanisms. That substantial heterogeneity was observed in region of iterest VBM hypothesis-driven studies further emphasizes the limits of current theories.

These meta-analyses suggest that there are at least two broad biological categories of hallucination mechanisms: a neurodevelopmental psychiatric mechanism and a neurodegenerative mechanism. In support, structural signatures of hallucinations in the psychiatric meta-analysis overlap with comparisons of patients to healthy controls. For instance, a meta-analysis of GM changes in schizophrenia patients compared to healthy controls shows reductions in bilateral insula and anterior cingulate cortex (Glahn et al., 2008), coinciding with regions identified in the meta-analysis of hallucinations in neurodevelopmental psychiatric disorders, while thalamic, hippocampal, and occipital GM reductions in PD (Ffytche et al., 2017) partly coincide with the changes seen in neurodegenerative hallucinations. The relation between disorder-specific GM changes and hallucination category suggests that hallucinations share networks of brain regions with the pathologies of the disorder in which they are embedded.

2.5.2 Neurodevelopmental psychiatric hallucinations in schizophrenia spectrum and bipolar disorders

Knowledge of the structural correlates of hallucination types may help understand their cognitive phenotypes. For instance, hallucinations are linked to reality monitoring, the cognitive capacity to distinguish between self-generated and external sources of information (Simons et al., 2017). Impaired in schizophrenia, reality monitoring is associated with the structure and function of the anterior cingulate cortex (Simons et al., 2017; Buda et al., 2011). The cingulate gyrus is part of a network involving the inferior frontal gyrus, ventral striatum, auditory cortex, and right posterior temporal lobe, whose functional connectivity is related to the subjective extent to which a hallucination feels real (Raij et al., 2009). I propose that connectivity is key: together with the insula, the anterior cingulate constitutes a node of the

salience network, dysfunctions in which have been proposed as central to experiencing hallucinations (Palaniyappan and Liddle, 2012). Structural deficits in the insula in psychosis might also underpin atypical interactions between the DMN and salience network observed in hallucinations (Alderson-Day et al., 2015). The left STG and middle temporal gyrus were consistently implicated in the manifestation of AVH, emphasizing the importance of speech perception and processing in hallucinations in the psychosis spectrum.

2.5.3 Neurodegenerative hallucinations in Parkinson's and Alzheimer's disease

Abnormalities in the occipital cortex in neurodegenerative diseases suggest that deficits in sensory regions contribute to hallucinations of the associated sensory modality since visual hallucinations are more common in PD than in schizophrenia. Hallucinations in PD and AD were characterized by GM reduction in the thalamus and parahippocampal gyrus (PHG). The thalamus mediates information in the cortical hierarchies via corticothalamo-cortico circuits and contributes to working memory maintenance (Bolkan et al., 2017), while the PHG is implicated in processing contextual associations in the service of memory formation and generating expectations about spatial relations (Aminoff et al., 2013). Their involvement supports memory-related processes in hallucinations, though may equally relate to neurodegenerative pathologies. The anterior cingulate was implicated in hallucinations occurring in psychiatric disorders, but not neurodegenerative aetiology. As the anterior cingulate is involved in self-referential processing, this is consistent with the observation that psychotic hallucinations address the individual and vary across continental location and historical period (Laroi et al., 2014). Conversely, hallucinations in PD have a more passive quality and form historically stable categories of visual percepts (Diederich et al., 2009).

2.5.4 Hallucinations in non-clinical groups and non-dominant senses as targets for future research

The multimodality of hallucinations is under-documented and under-researched, with <2% of studies included in this review probing hallucinations beyond audition or vision. However, 30-50% of schizophrenia or PD patients report hallucinations in more than one modality (Ffytche et al., 2017): olfactory hallucinations are present in around 12% (Stevenson et al., 2011) and tactile sensations frequently co-occur with auditory hallucinations (66%; Woods et al., 2015). Despite the dimensionality of hallucinations, many questionnaires and theoretical models target unimodal accounts. Non-clinical individuals who hallucinate or hear voices are receiving increasing interest in scientific research, yet only one study in this review assessed a structural correlate (cortical thickness) of hallucinations in this population (van Lutterveld et al., 2014). Similarly, no studies investigated brain structure or function of hallucinations in borderline personality disorder, in spite of a high point prevalence of hallucinations of 43% (Niemantsverdiet et al., 2017). Although hallucinations are recognized to occur across diagnostic boundaries, the current scope of transdiagnostic research on hallucinations remains narrow.

The prevalence of auditory hallucinations in the general population varies across the lifespan with peaks in early life (<30 years) and between 50-59 years (Krakvik et al., 2015). Results from these meta-analyses predict that early onset of hallucinations will have a pattern of frontotemporal structural deficits similar to psychiatric disorders with neurodevelopmental origins, whilst later onset will show a neurodegenerative pattern of GM change in the occipital cortex, medial temporal lobe and thalamus. In any case, empirical neuroimaging and cognitive research in non-clinical groups and non-dominant modalities is necessary to extend the limits of current knowledge.

2.5.5 Limitations

As with all meta-analyses, statistical power is restricted by the size of the extant literature, both in terms of the number of studies meeting inclusion criteria and sample sizes of original studies, which in neuroimaging the experience of hallucinations remains immature. Despite

this, the overall sample size was comparable to other SDM meta-analyses (n=233 H, n=194 NH for psychiatric; n=128 H, n=162 NH for neurodegenerative) (Xu et al., 2016; Fusar-Poli, 2012). Neuroimaging meta-analyses are often subject to heterogeneity in methodology. I noted broadly uniform software parameters and spatial smoothing, but variation in covariates and statistical thresholds (Table 2.2). However, all meta-analyses employed the same threshold throughout the brain, limiting bias towards any *a priori* regions of interest and improving reliability of results. The psychiatric/neurodevelopmental and neurodegenerative meta-analyses illustrate cross-sectional neuroanatomical differences between patients with and without hallucinations. However, the prevalence of hallucinations increases with the duration of illness for PD, but generally decrease over time for schizoaffective disorder, schizophrenia, bipolar disorder, and depression, whilst the content may equally change over the trajectory of the disorder (Ffytche et al., 2017; Goghari and Harrow, 2016). Future analyses of longitudinal neuroimaging data may clarify illness category separation in the temporal evolution of hallucinations. The divergence in the meta-analytic findings for psychiatric and neurodegenerative disorders may be partly attributable to differences in modality, since hallucinations experienced in schizophrenia spectrum and bipolar psychosis were predominantly auditory, while those in PD and AD were mostly visual. However, the reported modalities are partly construed by the questionnaire used, which often assume a unimodal account or neglect to ask about multimodal experiences or differentiate between hallucination modalities. A quantitative and qualitative comparison of the phenomenological properties of hallucinations in schizophrenia and PD found that 55% of patients with schizophrenia had VH and 45% of patients with PD had AH, emphasizing that sensory modality is not a mutually exclusive class (Llorca et al., 2016). Moreover, hallucinations involving more than one modality were reported in approximately 80% of patients for schizophrenia and PD alike. Differences in hallucinations between disorders emerge in the frequency, duration, capacity of control, negative valence, and impact of hallucinations on patients, such that people with schizophrenia were more heavily affected by their hallucinations (Llorca et al., 2016). It is therefore unlikely that differences between the meta-analyses are due to modality alone, but capture a more complex picture of illness pathology, hallucination properties like content and affect, and mechanisms of onset or occurrence.

Finally, there was a significant difference in the ages of the participants in the two meta-analyses, although each meta-analysis had its own age-matched control group and thus the comparison between disorders did not capture differences due to aging.

2.5.6 Sound and Vision: A collaboration between service-users, artists and the public to explore the lived experience of hallucinations

These brain imaging meta-analyses suggest separate brain mechanisms for the experience of hallucinations in neurodevelopmental psychiatric disorders like schizophrenia, compared to hallucinations in neurodegenerative disorders such as Parkinson's disease. But what is it like to experience hallucinations? And is the experience of hallucinations the same for patients with different disorders?

The work in this chapter led me to develop a public engagement project entitled *Sound and Vision: A collaboration between service-users, artists and the public to explore the lived experience of hallucinations*, along with the support of my supervisor, John Suckling (REC: 20/LO/0420). Following informed consent, this project pairs local artists with participants who experience hallucinations to collaboratively create representative visual art. I engaged two groups of peoples who experienced hallucinations: n=5 young to middle-aged adults given a diagnosis of a psychotic disorder, primarily schizophrenia, and n=5 older adults with a neurodegenerative condition, primarily Parkinson's disease (PD). Participants were recruited from the Cambridgeshire and Peterborough Foundation NHS Trust Clozapine Clinic and the Cambridge Parkinson's Disease Research Clinic, respectively. Participants over 18 years of age were included if they were currently or had recently experienced hallucinations as one of the symptoms of their disorder, had the capacity to consent, and were able to read and understand English. Five local artists were employed through connections with a consultant psychiatrist and were each paired with two participants, one from each patient group, to balance artistic styles between groups. Eligible participants were identified by their responsible clinician and I contacted them to discuss their participation. The procedure includes two semi-structured discussions between participant, artist, and me: the first allowing participants to describe their experiences of hallucinations and the artist to ask questions, and a second 1–6 weeks later to present preliminary sketches and ideas, and to

discuss any modifications such that the participant feels it is an accurate representation of
their experience. An interview guide was developed based on advisory groups with people
with lived experience of hallucinations, as well as prior interview guides (Woods et al., 2015;
Mosimann et al., 2008). The interview guide was used, where necessary, to stimulate
discussion between artist and participant, where questions were flexible and led to an organic
conversation based on topics they wished to discuss. Discussions were audio recorded, where
consented, for further analysis. Artworks will be photographed and once the study is
complete, they will be displayed on-line and at science festivals with attendees encouraged to
complete online surveys to collect structured information on their perceptual and
hallucination-like experiences and life history. The resulting unique dataset will be the
foundation for exploration of the content of hallucinations across the general population. The
project is open to recruitment, and the full protocol can be found at ClinicalTrials.gov
Identifier: NCT04399096.

2.5.7 Conclusion

Hallucinations in clinical and non-clinical populations are diverse in content, modality,
frequency, and affect, among other dimensions. Though hallucinations have been explored
transdiagnostically at the level of phenomenology, little empirical work has made group
comparisons of brain structure related to hallucinations. I show that hallucinations in
psychiatric disorders have distinct neuroanatomical organization from the pattern observed in
neurodegenerative diseases, and in doing so hypothesise at least two structural substrates
associated with the hallucinatory experience. This categorical differentiation in the
neurobiology of hallucinations is important for optimizing or developing treatment strategies,
and makes specific predictions about other disorders, such as personality disorder, and the
onset of hallucinations in the general population. The structural networks involved in
hallucinations partly coincide with the respective case-control comparisons, and are thus
embedded within the broader neuroanatomical phenotype, emphasising the importance of
non-hallucinating patient control groups and age-matched healthy controls. Hallucinations are
experienced in a variety of mental health contexts and are important phenomena in probing

our perception of the external world, but theoretical work has not yet captured the diversity of hallucinations across modalities or diagnoses. By hypothesising at least two mechanisms for hallucinations, I suggest incorporating this plurality in future research.

Chapter 3   Alterations in cingulate and temporal lobe cortical folding associated with hallucinations in schizophrenia

3.1   Abstract

Hallucinations are percepts without origin in physical reality that occur in health and disease. Our first perceptions begin during gestation, making foetal brain development fundamental to how we experience a diverse world. Despite longstanding research on the brain structures supporting hallucinations and on perinatal contributions to the pathophysiology of schizophrenia, what links these two distinct lines of research remains unclear. Sulcal patterns derived from structural magnetic resonance (MR) images can provide a proxy in adulthood for early brain development. I studied two independent datasets of patients with schizophrenia who underwent clinical assessment and 3T MR imaging from the United Kingdom and Shanghai, China (n = 181 combined) and 63 healthy controls from Shanghai. Participants were stratified into those with (n = 79 UK; n = 22 Shanghai) and without (n = 43 UK; n = 37 Shanghai) hallucinations from the PANSS P3 scores for hallucinatory behaviour. I quantified the length, depth, and asymmetry indices of the paracingulate and superior temporal sulci (PCS, STS), which have previously been associated with hallucinations in schizophrenia, using BrainVISA software for sulcal segmentation, and developed a semi-automated method to measure the PCS, validated against the gold-standard manual approach. In both ethnic groups, I demonstrated a significantly shorter left PCS in patients with hallucinations compared to those without, and to healthy controls. Reduced PCS length and STS depth corresponded to focal deviations in their geometry. The discovery of

neurodevelopmental alterations contributing to hallucinations provides mechanistic insight into the pathological consequences of prenatal origins. This chapter addresses the questions:

- Cortical sulcation has been associated with hallucinations in schizophrenia. Does reduced left hemisphere paracingulate sulcus length replicate in two independent, ethnically-distinct datasets? Does a similar relationship exist between hallucinations and right hemisphere superior temporal sulcus depth? What is the role of cerebral asymmetries?
- Is an accessible manual segmentation protocol valid for enabling replicable measurements between different raters? Can this method be implemented with existing software packages to develop a new semi-automated method to measure the PCS?

3.2 Introduction

3.2.1 Development of cerebral sulci

The foetal brain undergoes remarkable development during gestation, transforming from a smooth surface at 22 weeks to a complexly folded topography characteristic of the adult brain. These indentations, or sulci, emerge in a specific temporal sequence *in utero*, with many primary convolutions forming in the second trimester, followed by secondary and tertiary sulci in the second to third trimesters (Figure 3.1) (Nishikuni and Ribas, 2013; Chi et al., 1977). The primary sulci, such as the cingulate sulcus or central sulcus, are under strong genetic control and maintain a relatively stable morphology across individuals, whereas the secondary and tertiary sulci, such as the paracingulate or mid-fusiform sulcus (Miller et al., 2021) are under weaker genetic control and greater in-womb environmental influence, and show greater inter-individual and inter-hemispheric variability, often displaying a prominent hemispheric asymmetry in the general population. While the complex cellular processes underlying cortical folding remain unclear (Borrell, 2018), sulcal patterns are functionally significant: their location can predict the location of cytoarchitectonic (Broadman) areas (Fischl et al., 2008), local sulcal morphology influences peak activity for large-scale

networks like the default mode network (DMN) (Lopez-Persem et al., 2019), and some tertiary sulci components have distinct myelin content profiles and functional network connectivity fingerprints (Miller et al., 2021). Sulcal architecture additionally has clinical significance and influences cognition. Deviations in cortical folding are associated with adulthood psychopathology and IQ, and the presence or absence of sulci contribute to cognitive control mechanisms (Papini et al., 2020; Tissier et al., 2018), suggesting that variations in prenatally established secondary/tertiary sulci may be markers for detecting neuropsychiatric disorders or predicting clinical and cognitive outcomes.
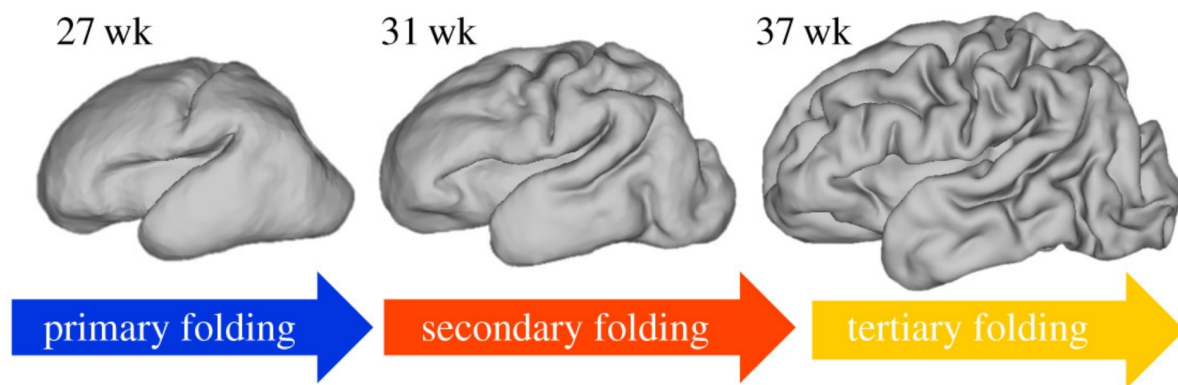
Figure 3.1. Gestational development of cerebral sulci. Adapted from Garcia et al., 2018.

3.2.2 Deviant cortical sulcation implicated in hallucinations in schizophrenia

A starting point: In 2015, an article by Garrison et al. evidenced that reduced length of the paracingulate sulcus was associated with a lifetime history of hallucinations in patients with schizophrenia compared to patients who had never experienced hallucinations and to healthy controls. In sum, a structural biomarker – a cortical fold in the medial prefrontal cortex, which is established in utero – was associated with a complex aspect of adulthood psychopathology: hallucinations. This finding suggests that the way we perceive the world in adult life is correlated with gestational brain development.

This article followed a rich sequalae of research characterizing the variation of paracingulate sulcus morphology and implicating its alterations in schizophrenia pathology.

The paracingulate sulcus (PCS) is a complex structure on the medial prefrontal cortical surface that lies dorsal to the cingulate sulcus. It was identified by Elliot Smith in 1907, but was not adequately characterized until 1996, when Thomas Paus conducted the first large-scale study (in N = 247 healthy volunteers) to describe cingulate sulcal patterns, their variability, and asymmetries between left and right hemispheres. The PCS forms between the 30–36 week of gestation in humans, although there remains disagreement whether it is a secondary or tertiary sulcus (Paus et al., 1996 consider it a tertiary sulcus, whereas more recent sources consider it a secondary sulcus, see Amiez et al., 2018). The PCS has long been considered to be specific to the human brain, but a recent comparative neuroimaging investigation has observed that the PCS is present in chimpanzee brains (Amiez et al., 2021). It is characterized by high inter-individual and inter-hemispheric variability, including fragmentation, intersection by other sulci, and even absence (Figure 3.2). The PCS shows a notable leftward asymmetry among the general population (i.e., more frequently present or prominent in the left hemisphere and more frequently absent in the right) (Amiez et al., 2018) that is not affected by sex, handedness, or race, although there are interactive effects of gender and handedness in the distribution of PCS patterns between hemispheres (Wei et al., 2017). Interestingly, the PCS leftward asymmetry is not present in chimpanzees, offering an avenue of insight to study human brain evolution (Amiez et al., 2021).
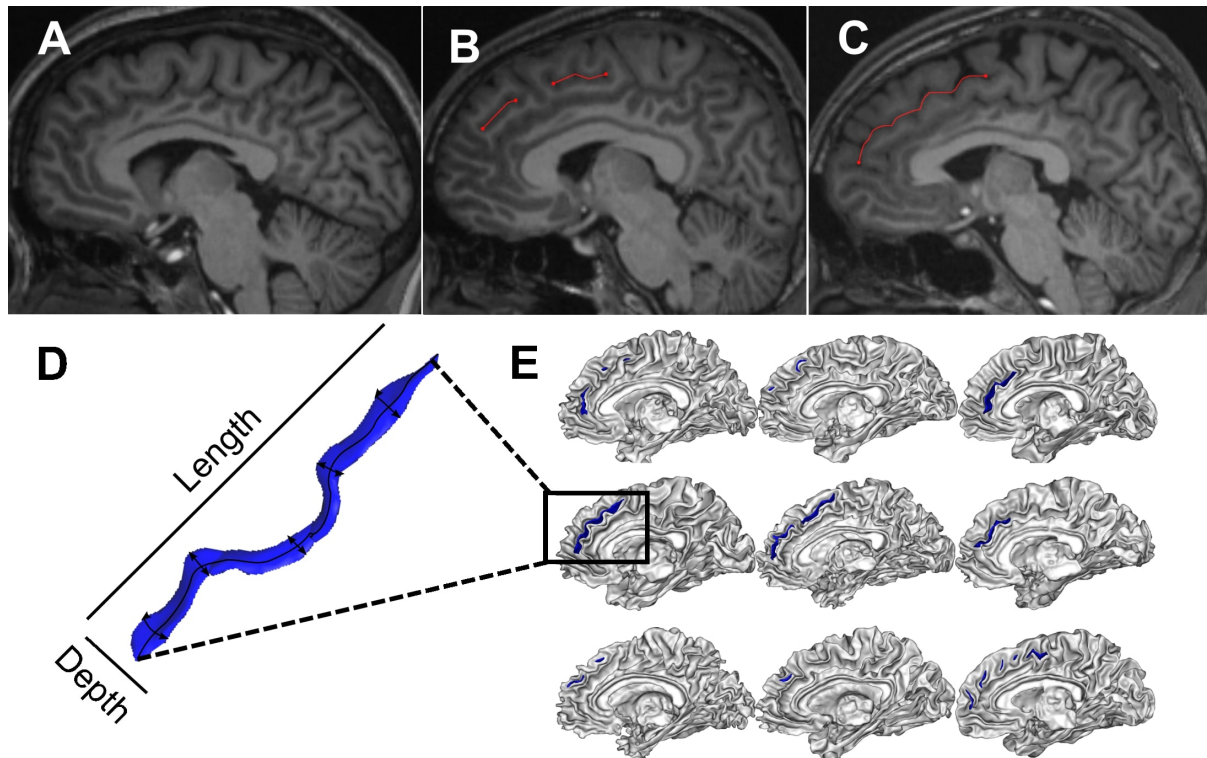
Figure 3.2. Variability in paracingulate sulcus (PCS) morphology. The PCS may be absent (A), fragmented by other sulci (B), or continuous (C). Sulci can be quantified through different shape measurements such as depth and length (D). Illustrative examples of PCS organization are shown in (E) for n = 9 participants.

The leftward asymmetry of the PCS is reduced in schizophrenia patients, such that the left hemisphere PCS is less prominent/present, making it nearly equally likely to appear in either hemisphere (Yücel et al., 2002; Clark et al., 2010; Le Provost et al., 2003). This reduction in asymmetry has functional consequences: PCS presence or absence influences the detection of anterior cingulate cortex activations in patients (Artiges et al., 2006) and reduced leftward PCS asymmetry is associated with worse spatial working memory performance across patients and controls (Fornito et al., 2006). It has previously been shown that the bilateral absence of the PCS is associated with impairments in reality monitoring in healthy individuals (Buda et al., 2011) and the association between reduced left hemisphere PCS length and hallucinations in schizophrenia has since been replicated (Garrison et al., 2018).

Sulcal contributions to hallucinations are not limited to the PCS. Localized deviations in the superior temporal sulcus (STS) in schizophrenia patients with auditory hallucinations

have been reported (Cachia et al., 2008; Plaze et al., 2011), as well as global decreases in cortical sulcation in patients with auditory and visual hallucinations compared to auditory alone (Cachia et al., 2015). Cingulate and temporal lobe folding overlap in their temporal emergence during sulcal ontogenesis at the foetal stage: the cingulate sulcus forms around 19–25 weeks of gestation, with its secondary branches and the PCS appearing around 30–36 weeks, and the STS forms between 23–29 weeks, with the right STS emerging one week prior to that on the left (Nishikuni and Ribas, 2013). The STS displays a robust rightward depth asymmetry at the base of Heschl's gyrus, regardless of language dominance and certain atypical conditions (Leroy et al., 2015), though this asymmetry has not been investigated in schizophrenia. Due to the stability of sulci patterns during brain maturation (Cachia et al., 2016), their topological variants in adulthood imply deviations in early brain development resulting in an intransient structural marker for a reality monitoring network (Subramaniam et al., 2012), and a risk factor for experiencing hallucinations. This aligns with the developmental risk model of schizophrenia, which integrates perinatal hazards and aberrant neurodevelopmental processes during gestation along with postnatal experiences like urban upbringing or childhood trauma into the disorder's pathogenesis (Murray et al., 2017).

3.2.3 Hemispheric lateralization in schizophrenia, language, and auditory hallucinations

Cerebral asymmetries are an axiom of human brain organization that are implicated in language development, handedness, and higher-order cognition functions. Atypical hemispheric asymmetries have been consistently reported in schizophrenia, such as reduced left hemisphere lateralization of planum temporale volumes and length of the lateral sulcus (Oertel et al., 2010; Sommer et al., 2001). Left-hemispheric language dominance is reduced in schizophrenia patients compared to healthy controls, and in patients that experience auditory hallucinations compared to those who do not (Ocklenburg et al., 2013). Certain asymmetries emerge perinatally, such as the earlier growth and greater depth of the right hemisphere STS compared to the left, which is related to speech perception and production (Leroy et al., 2015). As seen in Chapter 2, hallucinations in schizophrenia are associated with hemispheric structural abnormalities, such as reduced GM and CT in the left middle temporal

gyrus. Despite these observations, sulcal asymmetries have not been investigated in the context of hallucinations in schizophrenia.

3.2.4 Challenges to identifying morphologically variable sulci

Although primary sulci like the cingulate sulcus are relatively stable cortical landmarks across the population, secondary sulci, such as the PCS, exhibit substantial phenotypic complexity and interindividual and interhemispheric variability (Figure 3.2), hindering techniques for their accurate identification and measurement. Paus et al. (1996) proposed a qualitative 3-category classification of PCS as prominent, present, and absent that has been widely employed by structural MRI studies assessing the PCS. However, ambiguities in PCS patterns pose boundary definition problems that introduce subjectivity in this classification scheme (Leonard et al., 2009). Moreover, the PCS is undefined or conflated with other sulci in some classic neuroanatomical atlases (i.e., Ono et al., 1990), complicating its nomenclature and definition (Ten Donkelaar et al., 2018). Differences between measurement techniques, and even between experts using the same technique, may introduce discrepancies in sulcal measurements (Leonard et al., 2009). The current gold standard method for quantifying the length of the PCS remains manual segmentation, a method that has proven sensitive to differences in hallucination occurrence (Garrison et al., 2015; 2018), but that is unable to provide other biologically meaningful sulcal metrics, such as depth (Leroy et al., 2015), and has yet to be validated between experienced raters. Validating whether manual segmentation protocols contain sufficient anatomical detail for replication between raters is essential in advancing neuroimaging research related to the PCS. However, even with a detailed protocol, manual segmentation is a labour-intensive and time-consuming process that requires extensive training and regular inter-rater evaluations to obtain accurate, objective measurements. While automated methods show success in extracting detailed 3-dimensional sulcal curves and in identifying morphologically reliable primary and secondary sulci, such as the cingulate sulcus and STS (Mangin et al., 2004), the open challenge lies in labelling variable secondary/tertiary sulci like the PCS, which to date can only be completed with manual intervention. Accurate labelling of sulci is necessary to meaningfully determine the

functional significance of sulcal architecture diversity in health and disease, and automated methods are necessary to make large-scale studies more feasible.

3.2.5 Objectives

Chapter 2 characterized multiple brain mechanisms supporting the diversity of hallucinations, including fronto-temporal deficits associated with hallucination status in patients with a psychiatric disorder. This chapter focusses on the psychiatric structural pattern, considering the role of cingulate and temporal lobe sulcal topology, products of early neurodevelopment, in the experience of hallucinations associated with schizophrenia. I studied two ethnically independent structural MRI datasets of patients with schizophrenia (n = 181) and healthy controls (n = 63) to empirically test theoretical predictions linking hallucinations, cortical folding patterns, and cerebral asymmetries. To address these hypotheses, I first validate an open-access protocol on measuring the paracingulate sulcus. I then develop a semi-automated method by incorporating this protocol with a software package, BrainVISA, for automatically detecting, but not labelling, secondary/tertiary cortical folds. Semi-automated measurements of the PCS from two independent datasets directly replicated reduced left PCS length in schizophrenia patients with hallucinations compared to those without, showing ethnic invariance of a prenatally determined structural marker for hallucinations. Sulcal 3D-segmentations allowed visualization of their geometry, illustrating a focal displacement in curvature of the PCS and STS associated with hallucinations that is strikingly similar to the sulcal kink previously observed in the STS of patients with hallucinations. Extending reported structural asymmetry reductions in schizophrenia, I evaluate the relationship between sulcal asymmetries and hallucination status.

3.3   Methods

3.3.1 Participants, study design, and scanning acquisition

Two MRI datasets were re-purposed from independent studies of patients with recent-onset schizophrenia who underwent clinical assessment and 3T structural neuroimaging: (1) a

predominantly White British sample assessed at multiple sites in the UK (Deakin et al., 2018) and (2) a Han Chinese sample assessed in Shanghai, China (Li et al., 2018). (1) Participants in the UK dataset were recruited for a randomised, double blind, placebo-controlled trial evaluating the benefit of minocycline on negative symptoms of schizophrenia (BeneMin) in patients with a schizophrenia-spectrum disorder that had begun within the past 5 years (Deakin et al., 2018). The study was registered as an International Standard Randomised Controlled Trial, number ISRCTN49141214, and the EU Clinical Trials register (EudraCT) number 2010-022463-35I, and was approved by the North West Manchester NHS Research Ethics Committee (reference number 11/NW/0218). (2) Patients with schizophrenia were recruited from the Shanghai Mental Health Centre for a study to examine striatal brain activations during monetary and affective incentive processing (Li et al., 2018). Healthy age- and gender-matched controls were recruited through advertisements from local communities. The study was approved by Shanghai Mental Health Centre and the Institute of Psychology. Written, informed consent was obtained from all participants in each study (Table 3.1).

Table 3.1. Eligibility criteria for participants in UK multicentre and Shanghai studies.

	UK, multicentre	China, Shanghai
Inclusion criteria	• Meeting DSM-IV criteria for schizophrenia, schizophreniform, or schizoaffective psychosis as assessed by the research team • Within 5 years of first diagnosis • Male or female aged 16–35 years • IQ greater than 70 as assessed by the Wechsler Test of Adult Reading (WTAR) • Able to understand and give written informed consent • Participants were required to be taking stable antipsychotic treatment from a mental health-care team • Fluent in English	• Meeting DSM-IV criteria for schizophrenia using the Structured Clinical Interview for DSM-IV Axis I Disorders (SCID-I) • Male or female aged 16–50 years • Able to understand and give written informed consent

| Exclusion criteria | • Current diagnosis of substance misuse

• Current serious risk of suicide or violence

• Had a relevant current or past medical disorder or were pregnant or breastfeeding

• Used tetracycline antibiotics within 2 months of baseline visit or had a history of sensitivity or intolerance to an antibiotic

• Meeting MRI exclusion criteria as defined by local scanning centre | • Current co-morbid DSM-IV Axis I disorder

• History of other neurological, mental or substance disorder

• History of receiving electroconvulsive therapy in the past six months

• Meeting MRI exclusion criteria as defined by local scanning centre |

For both datasets, symptom severity was assessed using the Positive and Negative Symptom Scale (PANSS) and high-resolution T1-weighted structural images were acquired on a 3T MRI scanner (Table 3.2). The principal differences between the datasets were in their design. The UK study was a randomised, longitudinal trial with clinical measures taken over a 12-month period. Only the pre-randomised data were used in this chapter. The Shanghai dataset was cross-sectional and recruited healthy controls. Olanzapine equivalent doses were calculated based on daily-defined doses presented by the World Health Organization's Collaborative Centre for Drug Statistics Methodology (Leucht et al., 2016).

Table 3.2. Reproducibility and comparability of scanning sequences for UK multicentre and Shanghai studies.

	UK			China
	Manchester	Cambridge	Edinburgh	Shanghai
MRI scanner	Philips Achieva	Siemens Trim Trio	Siemens Verio	Siemens
Field strength (Tesla)	3 T	3 T	3 T	3 T
Head coil	8-channel	12-channel	12-channel	32-channel
TE T1 (ms)	3.1	2.98	2.98	3
FOV T1 (mm)	256	256	256	256
Flip angle (deg)	8	9	9	9
Image matrix	256 x 256	256 x 256	256 x 256	256 x 256
Voxel dimensions (mm^3)	1 x 1 x 1.2	1 x 1 x 1	1 x 1 x 1.2	1 x 1 x 1
Number of slices	170	176	160	176

From the six local neuroimaging centres involved in the UK study, three were excluded due to gender imbalances between groups (i.e., no female patients), leaving n = 85 patients scanned in Manchester, n = 24 in Cambridge, and n = 13 in Edinburgh for the comparison of brain morphology (Table 3.3). Chapter 5, which explores the resting-state functional MRI (rsfMRI) data from these subjects, additionally includes centres Birmingham and UCL, considering the reduced sample from lack of or poor quality rsfMRI data.

Table 3.3. Gender and age across scanning centres and hallucination status.

Centre	Manchester		Cambridge		Edinburgh		Birmingham		UCL		KCL	
Hallucination status	H+	H–	H+	H–	H+	H–	H+	H–	H+	H–	H+	H–
N	51	34	19	5	9	4	6	12	10	6	4	6
Sex (M/F)	36/15	23/11	13/6	4/1	5/4	3/1	5/1	12/--	7/3	6/--	4/--	4/2
Mean age (S.D.)	25.4 (4.6)	26.5 (6.2)	26.1 (6.4)	21.8 (5.5)	27.0 (5.9)	29.5 (3)	25.3 (5.1)	24.5 (4.6)	26.2 (3.7)	25.5 (6.7)	27.4 (3.4)	28 (5.7)

3.3.2 Hallucination grouping

Patients were grouped into those with (H+; n = 79 UK sample, n = 22 Shanghai sample) and without (H-; n = 43 UK sample, n = 37 Shanghai sample) hallucinations, defined by a score of > 2 (H+) and <= 2 (H-) on the PANSS P3 item for hallucinatory behaviour at the time of assessment, as has been used previously for assessing the underlying brain structure related to hallucination presence (van Tol et al., 2014; Escarti et al., 2019). Additionally, 63 healthy controls (HC) were recruited into the Shanghai study. The P3 hallucinatory behaviour item measures severity of hallucinations on a scale from 1 (absent) to 7 (extreme) in the week before clinical assessment. Although not a measure of lifetime history of hallucinations, the P3 score shows good convergent validity with other questionnaires assessing hallucination presence (Kim et al., 2010). The P3 score was additionally available for the UK dataset at 2, 4, 6, 9, and 12 months. The average P3 measured periodically over the 1-year period was

compared to P3 scores at randomization in attempt to closer serve as a proxy for lifetime hallucination history (see Table 3.4 in Results section 3.4.1).

3.3.3 Paracingulate sulcus manual tracing measurement

The length of the PCS was manually measured on both hemispheres of each MR images according to a previously described protocol (Garrison et al, 2015), with open access at www.repository.cam.ac.uk/handle/1810/264520. Briefly, individual images were imported into Multi-image Analysis GUI (Mango) medical imaging visualization software (v.4.0.1, http://ric.uthscsa.edu/mango/) and manually linearly aligned with 6 orthogonal degrees of freedom (DOF) to the plane of the anterior and posterior commissures (ACPC). A coordinate origin set to the anterior commissure along the ACPC line defined the quadrants for PCS measurement. Manual tracing was performed on a sagittal slice, +/-4 mm from the transverse medial line, according to the hemisphere being traced. The cingulate sulcus was first defined as the first major sulcus running dorsal to the corpus callosum in the anterior–posterior direction. The PCS was then identified, if present, as a salient sulcus, running parallel, horizontal and dorsal to the cingulate sulcus, and visible for >=3 sagittal slices measured from the medial (x=0) plane. The PCS was measured using the "trace line" function in Mango, starting at the point in the first quadrant (y>0, z>0) at which the sulcus runs in a posterior direction to its end point, which could fall outside the first quadrant if the sulcus is continuous. Where the PCS was discontinuous, additional segments were included if the interruption between segments was <20 mm and if they also began in the first quadrant.

3.3.4 Semi-automated sulcal segmentation for measurement of the paracingulate and superior temporal sulci

Sulcal patterns show potential as markers of psychopathology and interindividual variability in cortical surface morphology, but their widespread study is limited by manual characterization and tracing of their ambiguous anatomy. PCS morphology is highly variable and requires a set of rules to achieve accurate sulcus labelling. Here, I assess whether partially automating the measuring procedure is feasible and corresponds to manual measurements. In this semi-automated procedure, the tracing of all cortical sulci is

automated, producing a structural representation of sulci (termed a "cortical folds graph"), but the identification of which sulcus is the PCS is completed manually. Initial automatic sulcal segmentation was performed using BrainVISA version 4.5 software (http://brainvisa.info) with standard parameters. For comparability to manual tracing, T1-weighted images were first linearly aligned to the ACPC plane and brought into MNI152 template space using a 6 DOF alignment with FSL commands. Aligned images were imported into the BrainVISA's Morphologist 2015 pipeline (http://brainvisa.info/web/morphologist.html) to segment all cortical sulci. No non-linear spatial normalization was applied to MRIs to overcome potential bias that may result from the sulcus shape deformations induced by the non-linear warping process. Using standard parameters, images were corrected for spatial inhomogeneities, skull-stripped, segmented into grey matter (GM), white matter (WM), and cerebrospinal fluid (CSF), separated by hemisphere, and had their 3D surfaces reconstructed corresponding to the GM-WM and GM-CSF interface. Cortical folds were automatically detected based on the image intensity of the MRI, a stable and robust definition that is not affected by variations in cortical thickness or GM/WM contrast. BrainVISA can provide automatic reliable recognition of the majority of primary cortical sulci, and some secondary sulci, including the superior temporal sulcus (STS; Ochiai et al., 2004), using artificial neural networks trained on manually labelled sulcal graphs to learn statistical maps of sulci presence probabilities. However, these sulcal recognition methods are not reliable for labelling the PCS due to its high interindividual morphological variability. Therefore, the STS was automatically labelled with BrainVISA, while the PCS was manually identified from the segmented folds following the same definition outlined in the manual tracing protocol. The PCS was labelled by CPER and MA, supervised by CPER. Where the PCS was discontinuous, the "Compute Euclidian Distance" tool was used to measure the distance between segments; as in the manual protocol, additional segments were included if the interruption between segments was <20 mm. BrainVISA represents extracted sulci as graphs, with nodes of the sulci indicating locations where the sulcus curves or changes direction. The "Split Sulcus" tool was used to split a graphical representation of a sulcus into smaller fragments for cases when a representation included too many nodes and needed to be disconnected to smaller sections to accurately

identify the PCS. Once labelled through manual or automated identification, BrainVISA commands were used to automatically extract morphological measures from labelled sulci, such as length, depth, width, and surface area of the sulci. This offers an additional advantage over the fully manual method, which is only capable of measuring length. Native space summary measurements of sulcal length and mean depth were automatically computed for automatically labelled STS and manually labelled PCS. Sulcal length was measured as the geodesic length of the junction between a sulcus and the hull of the brain and mean depth relates to the average depth across all vertices that correspond to the bottom of a sulcus, with depth of a single vertex corresponding to the geodesic distance from the bottom of the sulcus to the brain hull (Figure 3.2) (Pizzagalli et al., 2020).

3.3.5 Reliability of manual and semi-automated protocols

To assess the reliability of the manual PCS measurement protocol, four independent raters were trained de novo based on the cited protocol, such that each participant scan from a subset of the T1 data (n = 122 MR images from the UK dataset) was evaluated by at least 2 raters. All raters used the same tracing program (Mango) and style (keypad). Prior to reliability testing, raters measured the PCS from 10 training scans previously labelled by JRG, who developed the protocol. Labelled training scans were reviewed by one of two experienced raters (JRG or CPER, trained by JRG, both with over 3 years of experience with brain MRI processing and segmentation and have each measured the PCS in >100 subject scans) and discrepancies were discussed and clarified. The consistency of PCS length measurements between raters was evaluated with the intraclass correlation coefficient (ICC), calculated in RStudio (v.1.0.136) using a two-way random analysis of variance model that measured absolute agreement (ICC (2,k)) (Shrout et al., 1979). The reliability of PCS identification from the manual and automated tracings was used as a proxy to determine whether the semi-automated method could be used in place of the fully manual method. The consistency between PCS length measurements derived from manual and semi-automated (BrainVISA) segmentations were compared with the ICC, analogous to the ICC calculations between raters for the manual method.

Manual tracings and automated tracings were both reliably characterized, with excellent absolute agreement between all raters (Right Hemisphere: ICC = 0.968; Left Hemisphere: ICC = 0.935; see Table 3.4 for 95% confidence intervals) and between manual and semi-automated methods (Right Hemisphere: ICC = 0.943; Left Hemisphere: ICC = 0.933; see Table 3.5 for 95% confidence intervals) (Shrout et al., 1979). Figure 3.3 illustrates the comparison of the manual and semi-automated methods for measuring the PCS. The most common reason for discrepancies between raters on the manual method were ambiguities in identifying the PCS when the cingulate sulcus was split, as opposed to continuous. The most common reasons for discrepancies between the manual and semi-automated method were that, on the one hand, the BrainVISA software occasionally does not identify small sulcal fragments that were identified by manual tracing, leading to underestimation of PCS length, and on the other, the software occasionally includes additional sulcal branches that are too small to split (using the Split Sulcus tool described above), leading to overestimation of PCS length. Considering the reliability of the semi-automated method, and for comparability to the STS measures, the PCS measurements computed from BrainVISA are used for all subsequent analyses. All available MR images (n = 166 for the UK dataset, including all six centres, and n = 122 for the Shanghai dataset) were processed using the BrainVISA Morphologist pipeline for semi-automated measurement of the PCS. The pipeline failed for N=7 MRI scans.

Table 3.4. Reliability of manual PCS measurement method.

	n observations	ICC	CI lower bound	CI upper bound
RH All	122	0.968	0.965	0.972
R1 vs. R2	30	0.971	0.962	0.977
R1 vs. R3	31	0.978	0.972	0.983
R1 vs. R4	15	0.964	0.949	0.975
R3 vs. R4	24	0.946	0.914	0.961
LH All	122	0.935	0.929	0.942
R1 vs. R2	30	0.959	0.947	0.968
R1 vs. R3	28	0.934	0.914	0.949

| R1 vs. R4 | 11 | 0.931 | 0.893 | 0.956 |
| R3 vs. R4 | 25 | 0.917 | 0.836 | 0.942 |

Intraclass correlation coefficients (ICC) assessing consistency of PCS length measurements between raters. The PCS was measured for N=122 T1 scans among N=4 raters trained de novo on the manual measurement protocol, such that each scan was traced by at least 2 raters. Confidence intervals (CI) are reported for each ICC.

Table 3.5. Reliability of semi-automated to manual sulcal measurement method. Intraclass correlation coefficients assessing of paracingulate sulcus length measurements between manual and semi-automated (BrainVISA) methods.

	n observations	ICC	CI lower bound	CI upper bound
RH Manual vs. Semi-automated	237	0.943	0.938	0.948
LH Manual vs. Semi-automated	237	0.933	0.922	0.941
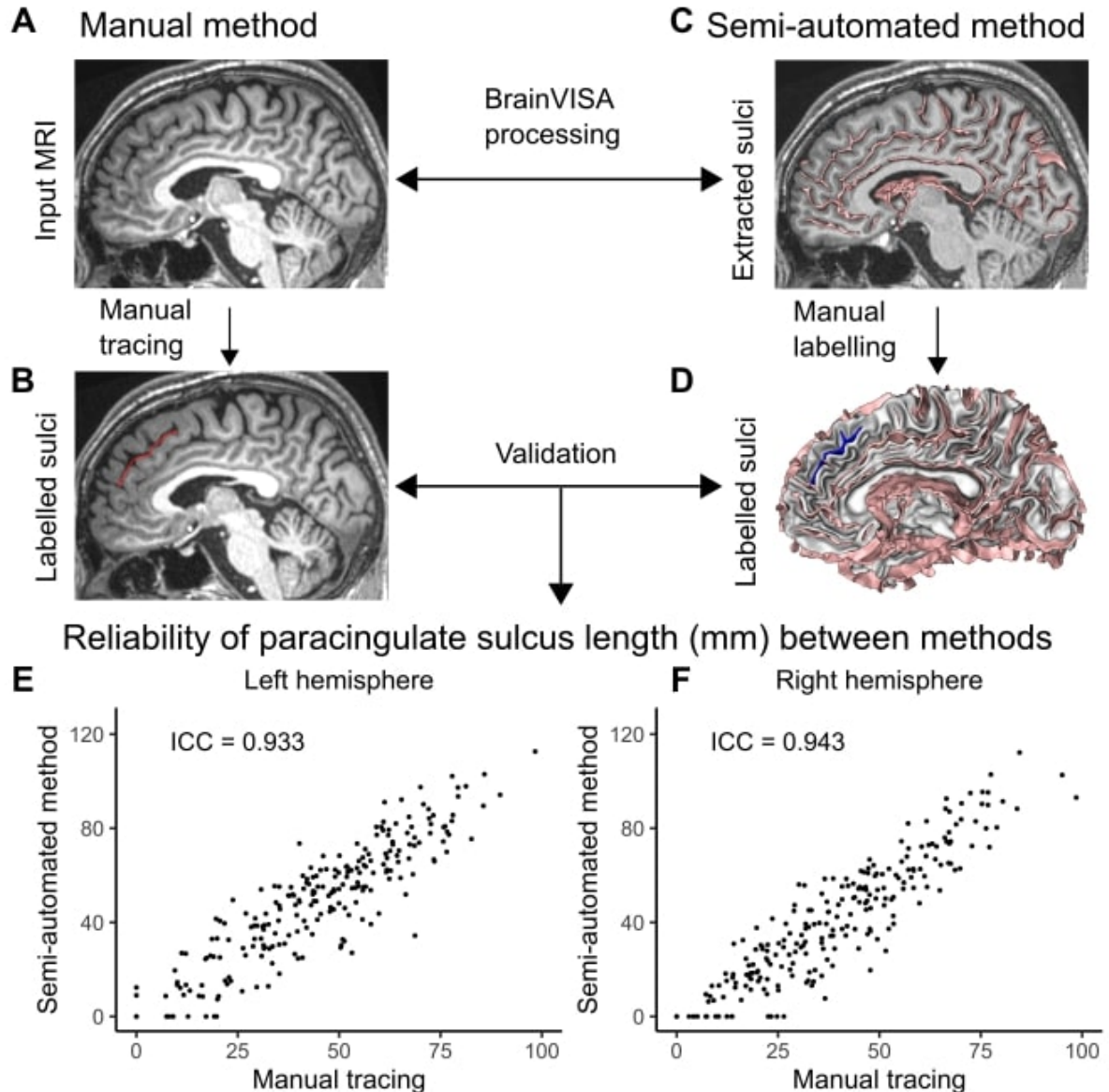
Figure 3.3. Validation of manual and semi-automated methods for paracingulate sulcus identification and length measurement. A–B. The PCS was manually traced from T1 images using Mango medical imaging visualization software. C. Semi-automated sulcal segmentation was performed using BrainVISA software. D. The PCS was manually identified from BrainVISA whole-brain sulcal graphs. E–F. The reliability of PCS lengths calculated from manual tracing and semi-automated BrainVISA processing were compared using the intraclass correlation coefficient (ICC). Right hemisphere (n=237): ICC=0.943 (0.938–0.948)); left hemisphere (n=237): ICC=0.933 (0.922–00.941). BrainVISA sulcal extractions failed for N=7 scans.

3.3.6 Creation of group-wise average sulcal maps for the paracingulate and superior temporal sulci

To visualize the average morphology of the sulci of interest in each group (H+, H-, HC), I created 3D maps of the PCS and STS in standard MNI152 stereotaxic space. First, graphical representations of the sulci were converted to 3D volumes using the BrainVISA 'Create Sulcus Label Volume' tool. For each image, the resultant volumetric PCS labels were overlaid on the bias-corrected input MRI using FSLeyes to visually inspect each label and ensure later comparability to the manual tracing. For each hemisphere of each group, I used FSL commands to merge the group sulcal labels. Since individual PCS labels were thin, spanning approximately 2 voxels in width, resultant sulcal maps were systematically smoothed by iteratively increasing sigma until an optimal level was reached via visual inspection at sigma=0.75. The UK and Shanghai datasets were merged to produce average sulcal maps since there were no significant between-sample differences in the morphological classification of the PCS (see Results sections 3.4.1) or in prior studies (Wei et al., 2017). The positional difference between group sulcal maps was quantified using fslmaths, representing the location of maximal difference between group-average sulcal maps. The average sulcal maps were visualized in FSLeyes for group comparisons of sulcal geometry.

3.3.7 Cortical atlas

To interrogate the locus of putative sulcal shifts, I used the Human Connectome Project multimodal parcellation version 1.0 (HCPMMP1.0), a surface-based anatomical atlas developed by Glasser et al. (2016), which decomposes the cortex into 180 anatomical regions per hemisphere. This parcellation was chosen for its finer-grained division of the medial prefrontal cortex in comparison to other atlases. 'fslstats', the FSL command line tool for calculating various values and statistics from MR image intensities, was used to determine the co-ordinates ($P_1 = x_1, y_1, z_1$) of maximum difference between the group-average sulcal map for patients with hallucinations (H+) subtracted from the group-average sulcal map for patients without hallucinations (H−). To map the location of group-wise sulcal displacement

to the nearest HCPMMP1.0 region, the distance between P1 and the centre of gravity of each HCPMMP1.0 parcel ($P_2=x_2,y_2,z_2$) was calculated using the formula:

$$d(P_1, P_2) = \sqrt{(x_2 - x_1)^2 + (y_2 - y_1)^2 + (z_2 - z_1)^2}$$

Annotation files for the HCPMMP1.0 matching the standard stereotaxic brain (i.e., fsaverage; FreeSurfer v 6.0) were downloaded from https://figshare.com/articles/HCP-MMP1_0_projected_on_fsaverage/3498446 and overlaid atop the fsaverage brain along with group-average sulcal maps for the PCS and STS. Cortical Explorer (http://corticalexplorer.com; Budd, 2017), an interactive web-based user interface for parsing the HCPMMP1.0 per-parcel data within a 3D scene, was used to visualize the different cortical areas.

3.3.8 Sulcal asymmetries related to hallucination status

As described earlier, the PCS has consistently been characterized to show a leftward asymmetry that is reduced in patients with schizophrenia. The STS displays a robust rightward depth asymmetry at the base of Heschl's gyrus, regardless of language dominance and certain atypical conditions (Leroy et al., 2015). This asymmetry has not been investigated in schizophrenia, though reductions in volume, gyrification, and cortical thickness have all been observed in the superior temporal gyrus, as reported in Chapter 2. Length and depth asymmetry indexes (AI) were computed for both PCS and STS: AI = 2*(R − L)/(R + L), for left (L) and right (R) measures, with a positive AI representing a longer or deeper sulci in the right hemisphere.

3.3.9 Statistical analyses

Demographic and clinical differences between groups by sample (UK H+, UK H-, Shanghai H+, Shanghai H-, Shanghai HC) were examined with one-way ANOVAs or chi-square tests for categorical data and t tests or Mann-Whitney U test for continuous variables, according to their distributions. Per hemisphere linear regression analyses for PCS length by group, controlling for potential effects of age, sex, scanning centre, and total intracranial volume

(TIV) were performed to address hypotheses concerning PCS and STS length and depth differences. This analysis was performed in each dataset separately and in both datasets combined. The datasets were merged for subsequent analyses considering the homogeneity between the UK and Shanghai samples and the ethnic invariance of sulcal morphology (Wei et al., 2017). Sulcal AIs were assessed within each group using one-sample t-tests and between groups (H+, H-, HC) using 1-way ANOVAs. Planned comparisons for group differences in PCS length, and PCS length and STS depth asymmetries in healthy controls, were evaluated at p<0.05. Exploratory analyses for PCS depth, STS length and depth, and asymmetry indices were corrected by FDR (FDR<0.05). Residual analysis plots were generated to assess the assumptions of linear regression.

3.4 Results

3.4.1 Multi-ethnic samples of schizophrenia patients with and without hallucinations, and healthy controls

Demographic and clinical differences between groups by sample (UK H+, UK H-, Shanghai H+, Shanghai H-, Shanghai HC) showed no significant group differences for gender, years of education, and olanzapine equivalent doses (Table 3.4). Post-hoc comparisons using Tukey HSD indicated no differences in mean age, but the 5-group 1-way ANOVA showed a significant main effect (F(4,236) = 2.44, p=0.048). Individuals from the UK and Shanghai samples did not differ in their group-respective hallucination symptom scores (PANSS P3). However, the datasets differed in the ratio of patients with hallucinations to those without, with 65% of patients experiencing hallucinations in the UK sample, similar to that previously reported (Jardri et al., 2011), but only 37% in the Shanghai sample. This could reflect recruitment differences between the two studies and/or cultural variation in the reporting or diagnosis of hallucinations (Luhrmann et al., 2015). All participants in the UK sample and 93% of patients in the Shanghai sample were on stable antipsychotic medication at the time of scanning. Dosing information required for olanzapine equivalent calculations was missing for n = 4 H+; n = 3 H- from the UK sample and n = 5 H+; n = 7 H- from the Shanghai sample.

Table 3.6. Characteristics of study participants.

	UK, multicentre		China, Shanghai			Test statistic, p-value
	H+	H-	H+	H-	HC	
Total n	79	43	22	37	63	n/a
Manchester, n	51	34				
Cambridge, n	19	5				
Edinburgh, n	9	4				
Male/Female (% Female)	54/25 (31.6)	30/13 (30.2)	15/7 (31.8)	21/16 (43.2)	36/27 (42.9)	$x^2(4) = 3.56$, p=0.47
Mean age (SD)	25.65 (5.21)	26.23 (5.96)	22.04 (6.00)	23.89 (5.21)	24.70 (7.35)	$F(4,236) = 2.44$, p=0.048
Years education (SD)	12.57 (1.95)	12.72 (2.07)	11.73 (2.62)	13.16 (2.78)	13.34 (2.49)	$F(4,189) = 2.19$, p=0.07
IQ (SD)	99.65 (11.11)	99.26 (12.22)	93.57 (18.82)	94.84 (18.90)	116.20 (15.02)	$F(4,231) = 19.19$, p<.001
PANSS positive (SD)	18.68 (4.47)	14.20 (3.81)	19.32 (5.56)	10.68 (3.29)	n/a	$F(3,156) = 34.53$, p<.001
PANSS positive minus P3 (SD)	14.70 (4.20)	12.94 (3.76)	15.14 (5.01)	9.65 (3.24)	n/a	$F(3,156) = 14.36$, p<.001
PANSS negative (SD)	15.70 (4.82)	18.51 (6.61)	21.77 (6.14)	15.54 (6.60)	n/a	$F(3,157) = 7.50$, p<.001
PANSS general (SD)	18.68 (4.46)	14.20 (3.81)	19.31 (5.56)	10.67 (3.29)	n/a	$F(3,156) = 34.53$, p<.001

PANSS P3 Hallucination (SD)	3.96 (0.97)	1.21 (0.47)	4.18 (1.01)	1.03 (0.16)	n/a	F(3,177) = 211.1, p<.001
PANSS P3 Hallucination year average (SD)	3.45 (0.98)	1.23 (0.34)	n/a	n/a	n/a	F(1,120) = 205.1, p<.001
PANSS P1 Delusion	3.57 (1.45)	2.35 (1.43)	3.18 (1.62)	2.24 (1.48)	n/a	F(3,177) = 10.09, p<.001
Total intracranial volume, cm³ (SD)	1428442 (211694)	1413090 (218906)	1548539 (132577)	1555657 (183254)	1544055 (152890)	F(4,239) = 10.09, p<.001
Olanzapine equivalent dose	10.76 (5.43)	10.78 (5.59)	13.97 (9.04)	10.26 (8.35)	n/a	F(3, 156) = 1.345, p=0.262

Abbreviations: H+: Hallucinations; H-: No hallucinations; HC: Healthy controls; PANSS: Positive and Negative Syndrome Scale.

3.4.2 Left paracingulate sulcus length is reduced in schizophrenia patients with hallucinations in ethnically independent samples

The length of the left hemisphere PCS calculated from structural MRI was reduced in schizophrenia patients with hallucinations compared to those without in both the UK (t(114)= 2.293, p=0.0237, β=0.197) and Shanghai (t(109)= 2.332, p=0.0215, β=0.280), samples separately, and combined (t(227)=3.264,p=0.0013, β=0.222), replicating previous work (Garrison et al., 2015; 2018). In the Shanghai sample, the left PCS was also shorter in patients with hallucinations compared to healthy controls (t(109)=2.716, p=0.0077, β=0.327). These tests survived correction for additional covariates that were not included in the final model (i.e., years of education, IQ, global gyrification, total cortical surface area, olanzapine equivalent dose, PANSS P1 Delusion score, and PANSS positive symptoms minus P3 Hallucination score). There were no significant effects in the right hemispheric PCS (t(227)= -0.306, p=0.760, β= -0.021), or in average PCS length (t(226)=1.801,p=0.0731, β=0.121).

The length of the right STS was reduced in patients with hallucinations compared to those without, but this reduction was not significant when controlling for age, sex, scanner site, and TIV (t(227)=1.240, q=0.349, β=0.090). Mean depth, however, was significantly reduced in the patients with hallucinations compared to HCs, controlling for covariates (t(227)=2.381, q=0.0465, β=0.209). The depth of the PCS was not significantly different between groups for either hemisphere. Left PCS length and right STS depth results are shown in Figure 3.4. Bilateral PCS and STS length and depth measurements are reported in Table 3.5 and visualized in Figure 3.5.
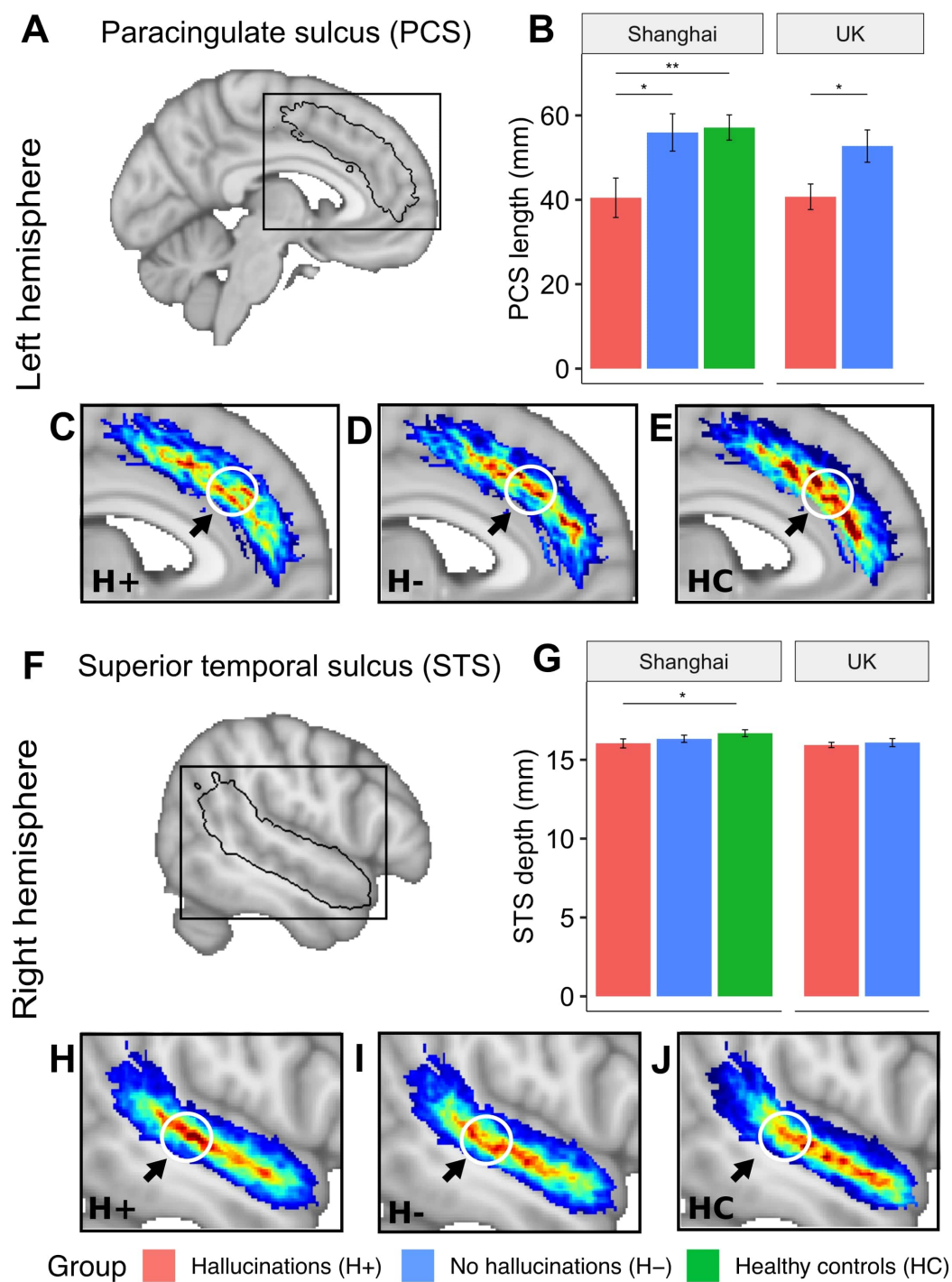
Figure 3.4. Local sulcal deviations associated with hallucinations. The length of the left PCS is significantly reduced in patients with hallucinations compared to those without and to HCs for both the Shanghai and UK multi-centre datasets (B). The mean depth of the right STS is significantly reduced in patients with hallucinations compared to HCs (G). Group-wise average sulcal maps after linear spatial normalization for (A) the left hemisphere paracingulate sulcus (PCS) (C-E) and (F) the right hemisphere superior temporal sulcus

(STS) (H–J) display local curvature shifts between patients with (H+; n = 101) and without hallucinations (H-; n = 80) and healthy controls (HC; n = 63). This displacement makes the sulcus more direct and less arched for the H+ group and explains the reduced length of the left PCS. A parallel sulcal shift is present in the right STS. Arrows pointing to white circles indicate the area of maximum difference between the average sulcal maps of participants with and without hallucinations, which occurs in HCPMMP1.0 area a32pr for the PCS and area STSdp for the STS. Average sulcal maps are linearly projected onto the MNI template. The colour bar represents the degree of overlap of sulci between participants in each group (H+, H-, HC), with red indicating higher overlap and thus the typical shape within group. Error bars denote the standard error of the mean. * p<0.05; ** p<0.01.

3.4.3 Reduced PCS length relates to a local displacement in curvature that emulates sulcal deviations in the STS

Although a shorter left PCS is a marker for hallucination status in patients with schizophrenia, the morphological features of the sulcus that lead to this observation have not previously been explored. The group-average sulcal maps illustrated focal displacement in the sulcal curvature such that the average PCS of H+ participants was straighter, yet broken, in comparison to the more arched and continuous PCS characteristic of H- and HC participants (Figure 3.4). In the right STS, a consistent pattern was observed, with less arching in schizophrenia patients with hallucinations compared to those without. The left PCS shift mapped to MNI coordinate x=-4, y=36, z=28, which was closest to HCPMMP1.0 parcel left hemisphere area 32 prime (a32pr), and the right STS shift mapped to MNI coordinate x=55, y=-28, z=0, which was closest to HCPMMP1.0 parcel right hemisphere dorsal posterior STS (STSdp). As both the anterior cingulate and STS show fine-grained gradients in functional organization (Palomero-Gallagher et al., 2019; Deen et al., 2015), the detailed subdivisions of the HCPMMP1.0 parcellation allowed me to interpret structural differences by their mapping to functional specializations. Results are shown in Figure 3.4.
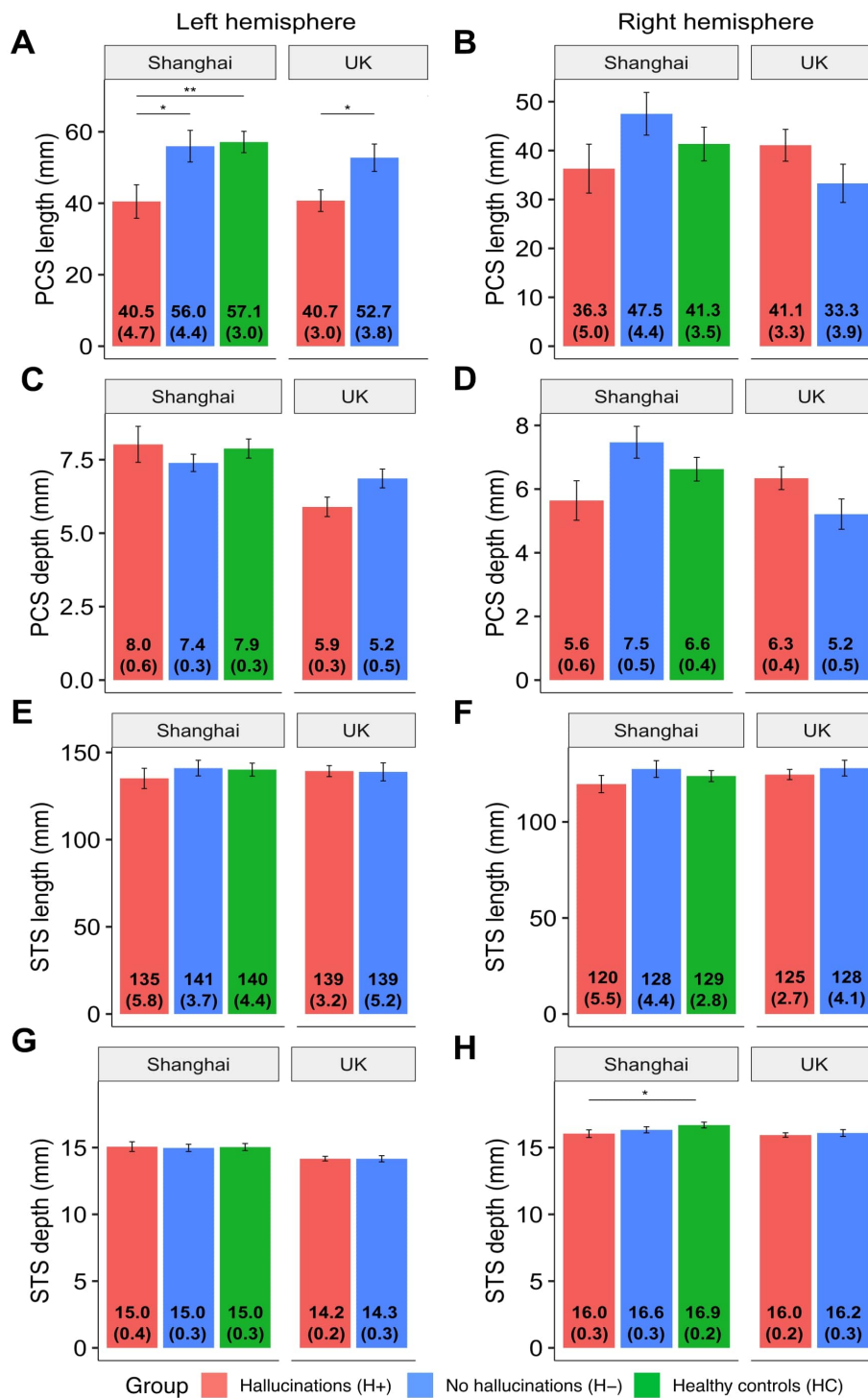
Figure 3.5. Bilateral sulcal measurements. Measurements are displayed by hemisphere (left, right), group (H+, H-, HC) and dataset (Shanghai, UK) for the paracingulate sulcus (PCS) (length: A–B; depth: C–D) and superior temporal sulcus (STS) (length: E–F; depth: G–H).

Table 3.7. Group-wise measurements of sulcal length, depth, and asymmetry indices for paracingulate and superior temporal sulci.

			H+ (N=101)	H- (N=80)	HC (N=63)	Test statistic, q-value
Paracingulate sulcus (PCS)	Length	L, mm (SE)	40.67 (2.58)	54.24 (2.89)	57.14 (2.99)	n/a
		R, mm (SE)	40.06 (2.77)	39.95 (3.01)	41.33 (3.45)	n/a
		AI, % (SE)	–3.92 (10.65)	–41.08 (10.04) †	–39.17 (10.54) †	F(2,229)=4.25, q=0.0404*
	Depth	L, mm (SE)	6.33 (0.302)	7.11 (0.220)	7.88 (0.326)	n/a
		R, mm (SE)	6.19 (0.311)	6.27 (0.365)	6.62 (0.372)	n/a
		AI, % (SE)	–4.13 (9.46)	–26.72 (8.06) †	–20.76 (8.83) †	F(2,227)=1.87, q=0.275
Superior temporal sulcus (STS)	Length	L, mm (SE)	138.41 (2.77)	139.88 (3.44)	140.15 (3.73)	n/a
		R, mm (SE)	123.63 (2.30)	127.79 (2.97)	123.85 (2.88)	n/a
		AI, % (SE)	–10.84 (2.67) †	–8.41 (3.30) †	–11.64 (3.50) †	F(2,234)=0.272, q=0.841
	Depth	L, mm (SE)	14.36 (0.160)	14.61 (0.190)	15.04 (0.267)	n/a
		R, mm (SE)	15.99 (0.146)	16.41 (0.186)	16.87 (0.233)	n/a
		AI, % (SE)	+10.93 (1.21) †	+11.69 (1.28) †	+11.76 (1.61) †	F(2,234)=0.129, q=0.879

Positive values represent longer or deeper sulci in the right hemisphere. UK and Shanghai samples were merged due to ethnic invariance on sulcal morphology. † FDR<0.05 for sulcal AI assessed within each group using 1-sample t-test. * FDR<0.05 for sulcal AI assessed between groups using 1-way ANOVA.

3.4.4 Sulcal asymmetries related to hallucination status

One-sample t-tests revealed that the STS was significantly deeper in the right hemisphere than the left, but longer in the left hemisphere than the right, within all groups (p<0.05). The PCS was significantly longer and deeper in the left hemisphere than the right for HCs and H- (FDR<0.05), but the AI was not significant for H+. A 3-group 1-way ANOVA showed a significant main effect of group on PCS length AI (F(2,229)=4.25, q=0.0404). Post hoc comparisons using Tukey HSD revealed that the PCS length AI of patients with hallucinations was significantly reduced compared to those without (p=0.0264), but was not significantly different between H+ and HC (p=0.0629), or between HC and H- (p=0.992). AI for PCS depth and STS depth and length were not significant between groups. Results are displayed in Figure 3.6 and Table 3.7.
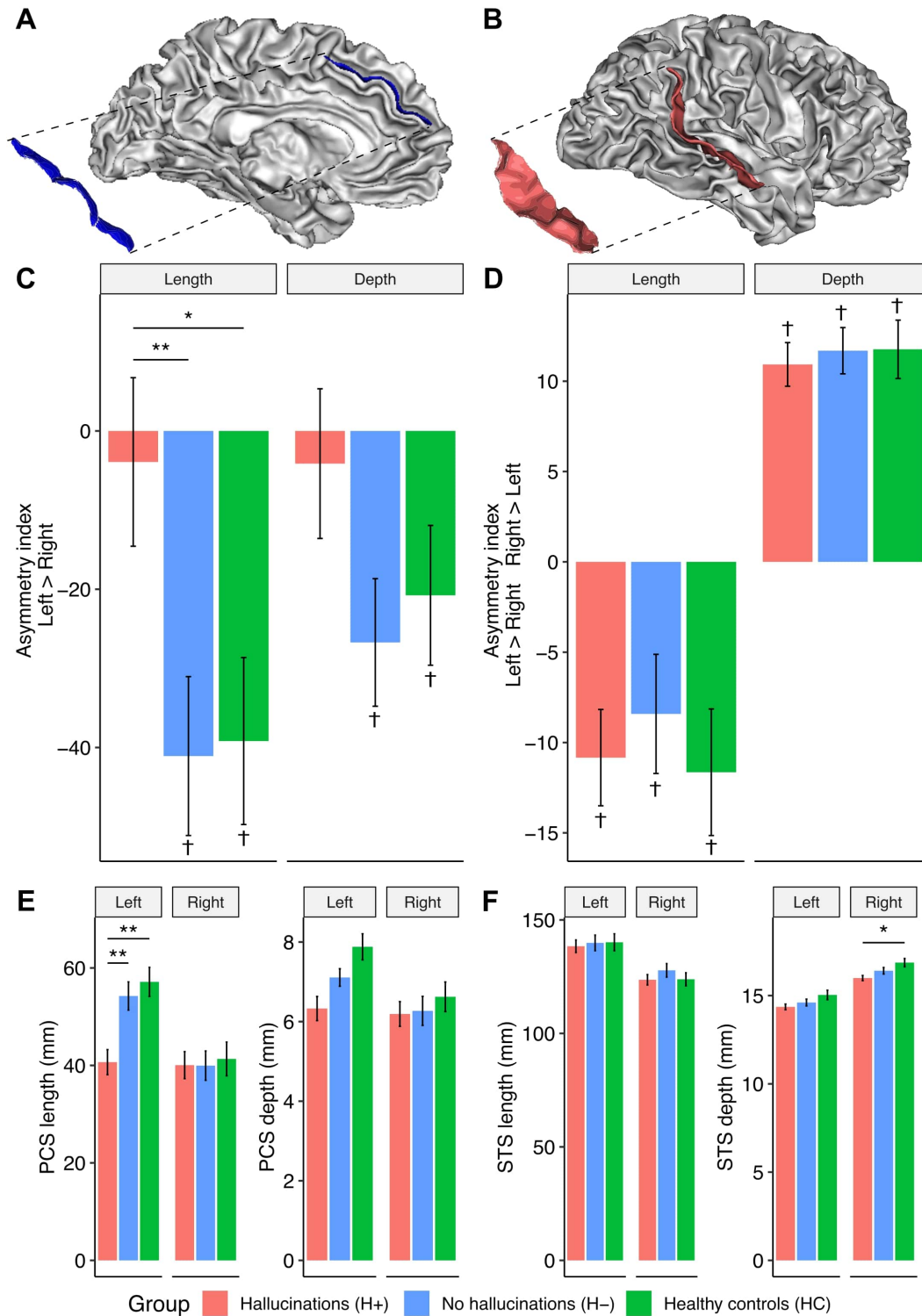
Figure 3.6. Asymmetry of length and depth measurements of the paracingulate and superior temporal sulci. 3D
representations of the left hemisphere paracingulate sulcus (PCS) (A) and right hemisphere superior temporal

sulcus (STS) (B). Asymmetry indices for the length and depth of the PCS (C) and STS (D). Positive values represent longer or deeper sulci in the right hemisphere compared to the left. Bilateral length and depth measurements for the PCS (E) and STS (F). Error bars denote standard error of the mean. Dagger indicates sulcal AI assessed within each group using 1-sample t-test. Asterisk indicates sulcal metrics assessed between groups using 1-way ANOVA for AI and linear regression for hemispheric PCS and STS length and depth measurements, controlling for age, sex, scanner site, and total intracranial volume. *p<0.05; **p<0.01.

3.5   Discussion

This chapter shows that specific alterations in the morphology of the paracingulate and superior temporal sulci are associated with hallucinations in schizophrenia. Bearing in mind that sulcal patterns are established during gestation and are fixed across the first decades of life, these results indicate a structural risk factor for hallucinations arising in early life that may interact with subsequent life experiences and culturally acquired expectations that are known to colour hallucination content.

3.5.1 Local sulcal deviations as markers for schizophrenia pathology

The association of reduced left PCS length with hallucinations replicated in two independent samples representing British and Han Chinese ethnicities. This is noteworthy considering that brain imaging research in schizophrenia has produced heterogeneous findings, in part due to varying sample characteristics (i.e., antipsychotic naïve vs. medicated, early episode vs. chronic schizophrenia), in part due to differences in scanning acquisition or processing method, although recent efforts to standardize methods across large-scale samples are beginning to clarify these inconsistencies (van Erp et al., 2018). BrainVISA provides a stable and robust sulcal surface definition that is not affected by variations in cortical thickness or grey matter/white matter contrast (Mangin et al., 2004) and can therefore be reliably extracted irrespective of the specific MRI scanner or acquisition sequence. Moreover, while certain sulci can widen and become shallower from early adulthood (20 years) to later life (82 years) (Kochunov et al., 2005), the pattern or arrangement of sulcal variants is relatively stable, at least from childhood (7 years) to adulthood (32 years) (Cachia et al., 2016), suggesting that sulcal patterns are minimally modified by life experience and may therefore

be more robust markers of schizophrenia pathology than other macrostructural features of the brain. For instance, the orbitofrontal cortex shows high interindividual variability in the sulcogyral pattern that has been classified into three types, the distribution of which is significantly different in the left hemisphere of schizophrenia patients than in healthy controls (Isomura et al., 2017). Moreover, schizophrenia patients have shallower superior temporal, right inferior frontal, and left calcarine sulci, with a deeper superior frontal sulcus predicting better cognitive scores (MacKinley et al., 2020), and morphometric similarity of sulcal width characterizes a subgroup of schizophrenia patients with extreme cognitive deficits (Janssen et al., 2021). Together with the results in this chapter, these findings indicate that sulcal topography may provide a robust structural trait marker for schizophrenia subgroups and symptoms, including hallucinations.

3.5.2 Mechanisms underlying sulcal geometry and asymmetry

Visualizing the group-average sulcal maps demonstrated that PCS length and STS depth differences corresponded to focal, geometric deviations. This observation is strikingly similar to the displacement of the sulcal junction between the right STS and its anterior branch in schizophrenia patients with hallucinations heard inside compared to outside the head (Plaze et al., 2011). Quantifying the differences between the group-average sulcal maps localized the maximum positional differences to subdivisions of the STS and PCS. Each of these areas show heterogeneous functional specialization: the STS supports a range of social processes regionally specialized across a posterior-to-anterior axis, from language to theory of mind, to voice and face recognition (Deen et al., 2015), while the anterior cingulate encompasses heterogeneous cytoarchitectonic, neurotransmitter receptors, and functional subdivisions that are associated with diverse cognitions of emotional reactivity, attention, fear, theory of mind, memory, and an individual's ability to evaluate and report current bodily sensations, thoughts, and experiences (Palomero-Gallagher et al., 2019). The sulcal kink of the STS identified here mapped to the dorsal posterior STSdp, a subdivision of the posterior STS, which is responsive to voice perception tasks and tasks engaging face and biological motion perception (Deen et al., 2015). The maximal difference between the average PCS

morphology of schizophrenia patients with and without hallucinations mapped onto the midcingulate area anterior 32 prime (a32pr), an area primarily functionally connected with other medial prefrontal regions, cingulate and insular regions (Baker et al., 2018). I hypothesize that sulcal patterns may be markers for relationships between cortical folding and intrinsic network functioning. These hypotheses will be explored in Chapters 4 and 5.

The association between local sulcal geometry and complex psychopathology in adulthood suggests that variations to the genetic, cellular, and environmental factors that govern cortical sulcation in the second to third trimesters of pregnancy influence the later development of specific psychotic symptoms. For instance, arcuate U-fiber systems may modulate the heritability of sulcal length and depth (Kochunov et al., 2012). A recent study using neurite orientation dispersion and density imaging, a novel multi-compartment diffusion MRI model of cortical microstructure, showed that neurite orientation dispersion (a measure of microstructural complexity of dendrites and axons) is leftward asymmetric in frontal areas and rightward asymmetric in early auditory areas in two independent samples of healthy adults (Schmitz et al., 2019). Microstructural properties may therefore contribute to the sulcal asymmetries observed here. Prior research on sulcal asymmetries have shown an absence of the typical leftward PCS asymmetry in schizophrenia patients (Yücel et al., 2002; Le Provost et al., 2003; Fornito et al., 2006; Leroy et al., 2015; Wei et al., 2017). The results in this chapter of reduced asymmetry index of PCS length in patients with hallucinations compared to those without and to healthy controls advance this research, showing specificity of reduced asymmetry to schizophrenia patients experiencing hallucinations. Considering the PCS length asymmetry indices were comparable between non-hallucinating schizophrenia patients and healthy controls, it is possible that previous reports of reduced PCS leftward asymmetry in schizophrenia were driven by patients with hallucinations. The rightward STS depth asymmetry was also lower in patients with hallucinations, with a significantly diminished mean depth of the right STS in patients with hallucinations compared to healthy controls, but not to patients without hallucinations. Reduced asymmetry indices in patients with hallucinations also supports empirical evidence that the reduction in structural and functional brain asymmetries in schizophrenia correlate with the severity of auditory hallucinations (Ocklenburg et al., 2015). Interestingly, certain genetic determinants of

schizophrenia also modulate brain asymmetries in the auditory system, and it has recently been shown that there are lateralized genetic influences on frontal and temporal sulci (Pizzagalli et al., 2020), suggesting that sulcal descriptors offer insight into brain lateralization processes that relate to hallucinations in schizophrenia.

3.5.3 Clinical implications

Hallucinations are a universal human experience, but are liable to local cultural variation. Whereas in Western countries voices are reported as commanding, violent and critical, and are attributed with diagnostic labels, in Eastern countries people are more likely to report rich relationships with their voices and ascribe positive meaning (Luhrmann et al., 2015). Reduced PCS length was associated with hallucinations in two ethnically distinct (British White vs. Han Chinese) groups of people with schizophrenia. The PCS is located on the anterior cingulate cortex, a key node of the salience network. As the salience network monitors the environment and directs attention, common anomalies to intrinsic networks *in utero* may interact with cultural expectations to influence how people attend to their environment, and experience hallucinations (see Luhrmann et al., 2015, for a description of "social kindling", a hypothesis that cultural expectations shape the voice hearing experience of people with a psychotic disorder). This finding has clinical relevance. Although culture scaffolds perception, there is also evidence that the way in which people focus their attention on their environment can be changed through cultural priming, a technique to manipulate a person's cultural value system (Nisbett and Masuda, 2003). For instance, cultural priming techniques to activate a collectivistic mindset is associated with changes in functional connectivity in the default mode network (Knyazev et al., 2018). Although the mosaic of sulcal features of the brain are intransient and not appropriate targets for therapy, cultural priming of Eastern values proffers a novel possibility for treatments to mitigate the distressing experience of hallucinations that is a common feature in Western cultures. At the very least, an individual's cultural background should be considered in diagnosis and treatment.

3.5.4 Towards automated tools and harmonization protocols for identifying the paracingulate sulcus

The semi-automated approach using BrainVISA showed excellent consistency (ICC>0.9; Shrout et al., 1979) with the manual method in measuring the length of the PCS. This method was beneficial compared to the manual method in its ability to provide additional morphology metrics, such as depth, and to generate 3D representations of the sulci, which showed group-wise average alterations in the shape of the sulci. However, this approach still relies on manual intervention in identifying the PCS, a process that is labour intensive and requires training. Novel approaches in deep learning show promise in detecting morphologically variable sulci to make this line of research tractable for large datasets. Moving forward, I hope to use the manual PCS labels created here as training data for automated algorithms. I have begun to do so with colleagues in the Computer Science Department (Yang et al., 2019), but further work is required to develop a more reliable algorithm, and to translate this to a tool that could be usable by other researchers without manual intervention. This work must progress in tandem with a standardized boundary definition and classification system for the PCS, which to date varies between research groups. The sulcal organization of the medial prefrontal cortex is complex, making it difficult to identify the PCS in ambiguous cases, such as when the cingulate sulcus is split. In an investigation of measurement technique across 200 MRI scans of healthy adults, Leonard et al. (2009) show that variation in boundary and sulcal definition influences measurements. Harmonized protocols across research groups have been successful in uniting research initiatives for other cortical structures, such as the hippocampal subfields (Wisse et al., 2017). Such harmonized segmentation efforts will be necessary for developing automated tools in identifying the PCS.

The deviations found in the PCS and STS raise the question of which other sulci serve as functional landmarks for psychopathology or clinical and cognitive outcomes. While BrainVISA can automatically detect around 30–40 morphologically reliable primary and secondary sulci (ICC 0.75–0.9 for reliability estimates; Pizzagalli et al., 2020), estimates predict >100 tertiary sulci per hemisphere (Miller et al., 2021). This observation, along with

the results in this chapter, emphasize the need to develop computational tools, along with harmonized neuroanatomical descriptions, to automatically identify variable secondary/tertiary sulci.

3.5.5 Limitations

The PANSS P3 measures current symptoms as opposed to lifetime history and does not distinguish between hallucination modality. The results could therefore be interpreted as a marker for treatment resistance, though the P3 score available for the UK dataset at 2, 4, 6, 9, and 12 months showed convergence with cross-sectional scores. The results may not be specific to auditory hallucinations, though these are the most common modality reported among schizophrenia patients. Future studies should employ more fine-grained assessments of hallucinations. I additionally controlled for PANSS P1 Delusion score, and PANSS positive symptoms minus P3 Hallucination score for the sulcal length/depth analyses, which were not significant, indicating that these findings are specific to hallucinations, as opposed to overall psychosis severity. Though the two datasets were reasonably matched for key demographic and clinical characteristics, limited information was available for duration of untreated illness. Considering the longitudinal stability of folding patterns, I would not expect the results to be influenced by duration of illness or medication. However, longitudinal studies characterizing quantitative features of sulci linking structural development from foetal to adult life periods will be important in establishing whether the sulcal deviations described here have predictive value for conversion to psychosis or stratification for clinical interventions. Though larger than many previous studies, the current samples are still relatively modest in size, and these findings require replication in larger samples.

3.5.6 Conclusion

The current chapter replicates and advances work on sulcal alterations related to hallucinations, demonstrating reduced length of the left hemisphere paracingulate sulcus in patients with hallucinations compared to those without and to health controls, and reduced depth of the right hemisphere superior temporal sulcus depth in patients with hallucinations

compared to health controls. The asymmetry index of PCS length was additionally reduced in patients with hallucinations. Visualization of sulci illustrated focal deviations in their geometry. A novel semi-automated method for measuring the PCS was consistent with a reliable manual segmentation protocol. These results suggest that hallucinations, a complex aspect of psychopathology in adulthood, are in part the reflection of intrauterine neurodevelopmental changes. Assessing brain development in the late foetal period and the interaction between sulcal architecture, functional connectivity, and behavioural experiences will generate greater knowledge of the mechanisms supporting hallucinations, and holds synergistic prospects of novel treatment strategies and preventive interventions for mitigating risk of future hallucinations.

Chapter 4   From folds to networks: Structural covariance of large-scale networks associated with hallucinations in schizophrenia

4.1   Abstract

Brain development occurs in a coordinated pattern. This synchronization of regional growth may be captured by structural covariance networks, which represent how interindividual differences in regional brain morphology covary with other brain regions across the population and reflect similar topography to resting-state networks. Chapter 3 illustrated how the geometry of specific sulci relate to hallucinations in schizophrenia. This chapter explores how focal sulcal deviations integrate with a whole-brain neurodevelopmental framework. I construct structural covariance networks of the local gyrification index according to the HCPMMP1.0 multimodal surface-based atlas (180 brain regions per hemisphere), organized by regional belonging to large-scale networks. Nonparametric permutation testing demonstrated increased gyrification covariance within and between the salience and auditory networks in schizophrenia patients with hallucinations compared to those without and to healthy controls. I compliment this work with whole-brain analyses of more commonly studied brain structural metrics: grey matter, cortical thickness, and local gyrification. These whole-brain analyses have the dual aim of reproducing the structural findings from Chapter 2 and investigating whether sulcal morphology alterations are accompanied by other brain structural alterations. This chapter addresses the questions:

- Sulcal patterns are products of early neurodevelopment. How do deviations in sulcal geometry of the PCS and STS relate to whole-brain neurodevelopmental coordination

of large-scale networks, specifically the salience and auditory networks, which have been implicated in hallucinations? Do other brain structural metrics characterize hallucinations?

4.2   Introduction

The brain develops in a coordinated pattern of growth, with certain brain regions showing shared growth trajectories (Aboud et al., 2019). This maturational coupling is not equal throughout the cortex: the higher association cortices show the strongest correlation with the rest of the cortex, while the primary sensory cortices show the lowest (Lerch et al., 2006). The medial frontal cortex, temporal and perisylvian language regions show the strongest coupling with mean cortical development (Raznahan et al., 2011). Sulcal development is equally driven by regionally distinct biological processes, such that different pairs of sulci will show differing similarity of their growth trajectory. For instance, the volumes of sulcal edges and the sulcal subarachnoid space increase with time (from 21–38 gestational weeks) for the left calcarine and parietooccipital sulci, while the Sylvian fissure shows a completely different pattern of growth, shrinking as bordering sulci grow (Mallela et al., 2020).

Indeed, different brain areas have distinct morphologies, but these morphologies are not independent of those in other brain areas. Brain regions show a high level of correlation of structural properties within the human population, and these patterns of interregional cortical associations are referred to as structural covariance (Alexander-Bloch et al., 2013; Aboud et al., 2019). Structural covariance can be explored using regions of interest (ROI) or using network-level approaches that determine the covariance between every pair-wise combination of brain regions for every subject in a given dataset or population. Practically, these estimates can be represented in a matrix composed of subjects (rows) by brain regions (columns), where the value for each brain region is some structural property, such as grey matter, cortical thickness, or local gyrification index (Figure 4.1). Computing the correlation between values in brain regions results in a structural covariance matrix, which represents group-level correlations.
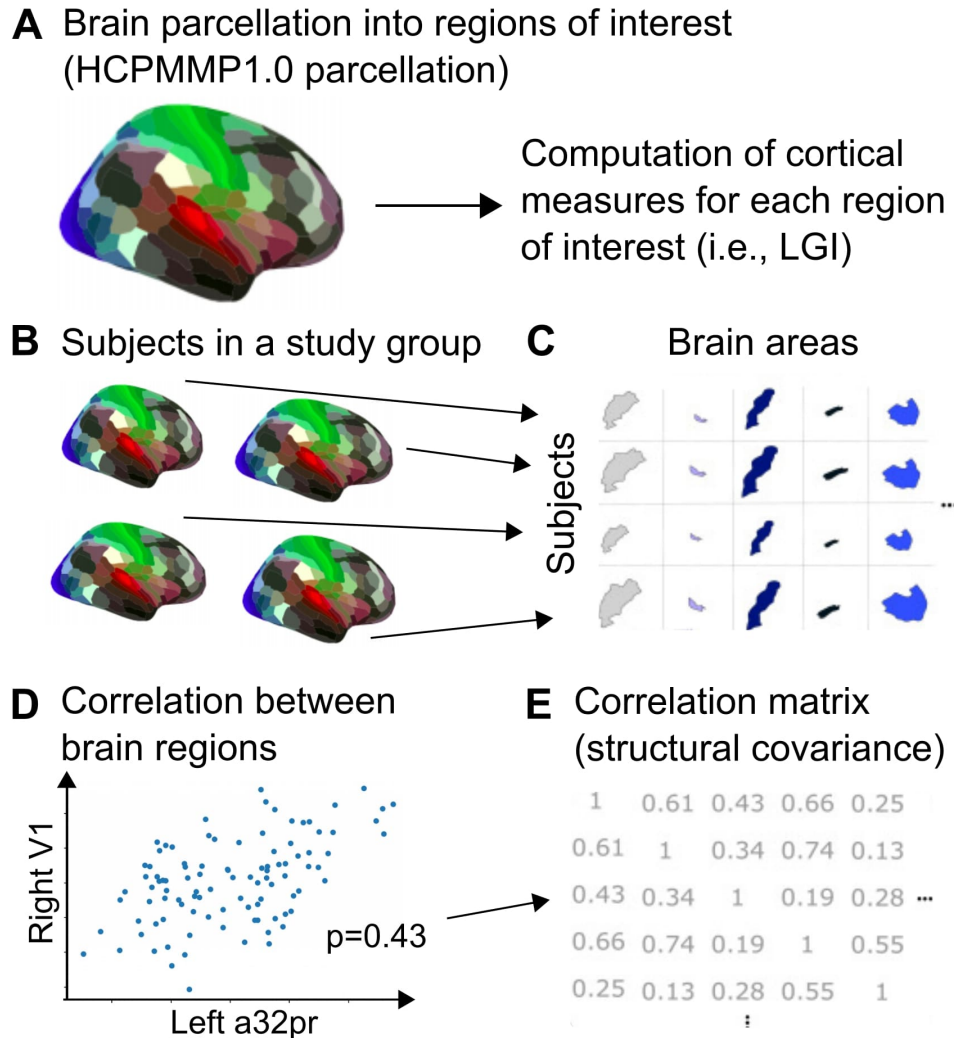
Figure 4.1. Illustration of structural covariance analysis. A. The brain is parcellated based on an atlas (i.e., HCPMMP1.0). B. A cortical measure of interest (i.e., LGI) is calculated for each brain region (C). This is done for multiple subjects in each study group (i.e., healthy controls). D. The correlation between brain regions is calculated across subjects. E. The matrix of all correlations is the structural covariance matrix. Adapted from Carmon et al., 2020.

Mounting evidence suggests that structural covariance networks reflect developmental coordination between brain regions, such that areas with highly correlated anatomical properties, like gyrification, result from similarities in maturational trajectories (Alexander-Bloch et al., 2013). What's more, structural covariance networks partially recapitulate the topography of resting-state functional connectivity networks, especially sensory, language,

and frontal networks (Zielinski et al., 2010), although they are not direct reflections of functional or structural connectivity (Alexander-Bloch et al., 2013). These structural networks are seen across the lifespan, but they show significant changes in different developmental or aging periods, with rapid maturation in early childhood (Geng et al., 2017), more stable connectivity in young adulthood, and reduced intra-network, but increased inter-network connectivity between the DMN–sensorimotor/visual network in older age (Chen et al., 2011). Although the cellular mechanisms that underlie patterns of cortical covariance remain poorly understood, neurodevelopmental events that influence structural covariance networks significantly affect postnatal outcomes and higher cognitions in adult life (Kim et al., 2020; Papini et al., 2020).

Patterns of correlated structural variation are altered in neurodevelopmental and psychiatric disease. Structural covariance networks of gyrification have shown increased segregation in the anterior insula and dorsolateral prefrontal cortex and reduced centrality of the cingulate cortex in schizophrenia patients compared to healthy controls (Palaniyappan et al., 2015) and properties of gyrification based connectomes predict transition to psychosis from at-risk mental state with a balanced accuracy of 81% (Das et al., 2018). Covariance networks of grey matter volume have demonstrated reduced salience and fronto-parietal control networks in schizophrenia patients compared to healthy controls (Spreng et al., 2019), and have demonstrated a positive association between frontal–temporal grey matter and auditory hallucination severity in schizophrenia (Modinos et al., 2009). These results suggest that structural covariance networks offer insights into the emergence of functional connectivity and index large-scale network integrity, specifically in relation to the pathophysiology of schizophrenia. Of the different intrinsic networks, I chose to focus on the salience and auditory networks based on previous accounts of their role in auditory hallucinations and in positive symptoms of psychosis more broadly (Mallikarjun et al., 2018; Alderson-Day et al., 2015; Palaniyappan and Liddle, 2012). Auditory hallucinations are the most frequent modality reported by schizophrenia patients and have been widely associated with speech and language regions in structural and functional MRI studies (i.e., middle/superior temporal gyri, Broca's area, and regions in the auditory network, which primarily process auditory information, including speech, language, tone, and pitch)

(Alderson-Day et al., 2015; 2016). The salience network engages the anterior cingulate and anterior insula to determine the origin and salience of internal and external stimuli and coordinates the transition between functional networks related to self- and task-processing. Growing evidence suggests that aberrant salience network activity in schizophrenia is instrumental in bringing about positive symptoms, namely hallucinations and delusions (Supekar et al., 2019).

Individual differences in cortical anatomy are characteristic of human brains, yet arbitrary interruptions and branching of cortical sulci renders sulcal morphology sufficiently distinct from variability in other brain morphology measures. A number of methods have been proposed for automated identification of sulci, but are generally limited to primary sulci or morphologically reliable secondary sulci. Extraction of secondary/tertiary sulci is unreliable due to variability in sulcal bifurcation, fragmentation, and absence, preventing the parcellation-based partitioning of sulci in the same way as other morphometric indices like cortical thickness or grey matter. Local gyrification index (LGI) is the ratio of the cortical area within sulcal folds to the cortical area visible on the outer surface that envelops the hemisphere (Schaer et al., 2008; 2012) (Figure 4.2). A higher LGI indicates a more involuted cortical surface and is reduced by having fewer and shorter sulci. Moreover, LGI has proven the most sensitive and effective index of cortical folding in distinguishing alterations in cortical folding, outperforming curvature-based measures in identifying preterm from term infants (Shimony et al., 2016).
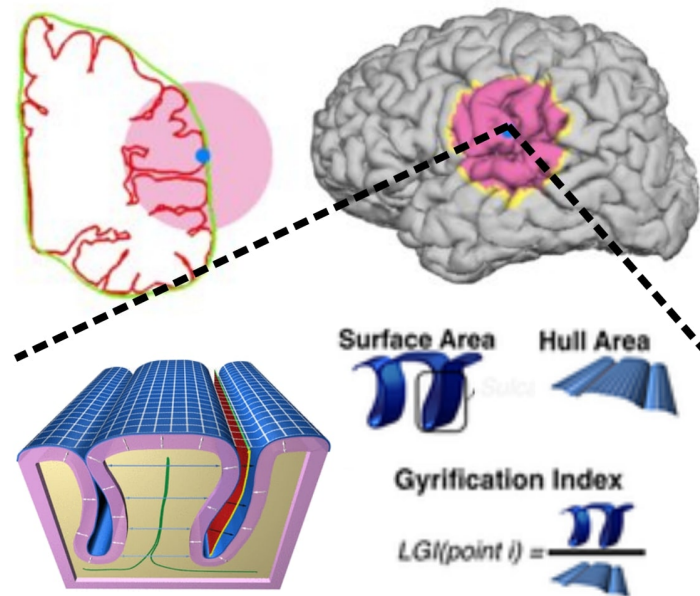
Figure 4.2. Illustration of local gyrification index (LGI). The LGI represents the amount of cortex buried within the sulcal folds and is calculated at each pial vertex as the ratio between pial surface area and the exposed cortical convex hull area. Adapted from Aleman-Gomez et al., 2013 and Matsuda and Ohi, 2018).

This chapter exploits the sensitivity of local gyrification-based structural covariance networks for reflecting brain maturation and resting-state networks. I hypothesized that deviations in frontal and temporal sulcal anatomy would reflect more general alterations in the topographical organization of large-scale networks; specifically, that patients with and without hallucinations would diverge in the inter-regional structural covariance of the salience and auditory networks. To succinctly estimate cortical topology over spatially extended resting-state networks and overcome unreliability in whole-brain sulcal extraction, the regional LGI was computed as a proxy for sulcal morphology. Additionally, I complement this work with whole-brain surfaced- and volume-based analyses of cortical thickness, LGI, and grey matter volume, with the dual aim of reproducing studies reviewed in Chapter 2 and exploring whether the sulcal deviations associated with hallucinations identified in Chapter 3 are accompanied by other brain structural alterations.

4.3   Methods

4.3.1 Image processing

4.3.1.1   Cortical surface reconstructions

Cortical thickness (CT) and local gyrification index (LGI) were calculated using the
FreeSurfer analysis package (v.6.0, http://surfer.nmr.mgh.harvard.edu/). Cortical surfaces
from each participant's T1-weighted MRI scan were automatically reconstructed using the
recon-all pipeline. The technical procedures have been detailed in previous publications
(Fischl and Dale, 2000; Fischl et al., 2001; 2002) and have been demonstrated to show good
test-retest reliability across scanner manufacturers and field strengths (Han et al., 2006).
Resultant cortical surfaces were visually inspected for quality and manually corrected in
Freeview, when appropriate, according to FreeSurfer user guidelines. Minor interventions
were required, typically around the temporal poles due to non-cortex material included in the
pial surface. There were no differences in the degree of manual intervention required between
groups. Images were then re-processed, incorporating the corrections to improve
reconstructed surface accuracy. CT was automatically generated from the FreeSurfer
processing pipeline and smoothed using a Gaussian kernel of FWHM of 10 mm. LGI was
calculated according to the method developed and described in detail by Schaer et al. (2008;
2012) and smoothed with a FWHM kernel of 5 mm. LGI calculations were visually assessed
for accuracy by overlaying LGI values over the cortical surface in TkSurfer.

4.3.1.2   Voxel-based morphometry

Structural MRI data were analysed with FSL-VBM version 5.0.10
(http://fsl.fmrib.ox.ac.uk/fsl), an optimized VBM protocol (Ashburner and Friston, 2000;
Good et al., 2001) carried out with FSL tools (Smith et al., 2004). First, all images were
visually inspected to ensure no gross morphological abnormalities and were reoriented to
match the orientation of the MNI152 template image. Quality of the structural data was

quantitatively assessed with FreeSurfer's Euler number, an index of the topological complexity of the reconstructed cortical surface and a reliable indicator of structural image quality (Rosen et al., 2018). A 5-group 1-way ANOVA revealed no significant differences in the Euler number for the left hemisphere $F(4,239)= 0.776$, $p=0.541$, nor the right $F(4,239)=1.402$, $p=0.234$. Structural images were brain-extracted with FSL Brain Extraction Tool (Popescu et al., 2012) and skull-stripped images were segmented into GM, WM, or CSF using FSL FAST. A study-specific template was created from n=45 subjects without hallucinations and a randomly selected subset of n=45 subjects with hallucinations, followed by non-linear registration to the ICBM-152 template, concatenation, and averaging of the resulting images. Images were smoothed using an isotropic Gaussian kernel with a sigma of 3.5 mm (FWHM $\cong$ 8 mm). To address the hypothesis of the GM changes in the paracingulate and medial prefrontal cortex regions, an 8 mm region of interest sphere was centred on coordinates sensitive to reality monitoring manipulations and hallucinations in schizophrenia (MNI x = -4, y = 57, z = 11), as has been done previously (Garrison et al., 2015).

4.3.2 Mapping sulci and intrinsic networks to a cortical atlas parcellation

4.3.2.1   Cortical atlas

The 360 region Human Connectome Project Multi-Modal Parcellation version 1.0 (HCPMMP1.0) is a surface-based population average atlas developed by Glasser et al. (2016), constructed from both functional and anatomical MRI data from 210 subjects in the HCP database. The input data for this atlas included task-based functional MRI, cortical thickness and T1w/T2w myelin maps, resting-state connectivity, resting-state-based visuotopic maps, and input from neuroanatomists, and the resultant parcellation was meticulously compared with extant neuroanatomical literature to identify 83 previously described cortical areas and 97 new areas, which were often subdivisions of existing areas. This atlas offers a fine-grained parcellation of the anterior cingulate and auditory cortices, which is advantageous considering the finding of anatomically specific sulcal alterations associated with hallucinations in these cortices (Chapter 3). Moreover, the parcellation was constructed using a surface-based approach, meaning that the cortex was modelled as a set of

2D vertices that respect sulcal and gyral features, which is important considering the
relevance of sulcal anatomy to hallucinations in schizophrenia.

4.3.2.2   Resting-state networks

Various approaches have used resting-state fMRI data to define resting-state networks. An
influential and commonly used functional connectivity atlas is the Yeo atlas, constructed
from functional and structural sequences from a group of 1000 young, healthy adults,
registered using surface-based algorithms (Yeo et al., 2011). Clustering was used to identify a
common set of 7 networks, as well as a more fine-grained 17 network parcellation. The 7
network parcellation includes commonly described intrinsic networks: the default mode
network (DMN), visual network, salience / ventral attention network, frontoparietal / central
executive network, dorsal attention network, limbic network, and somatosensory network. A
limitation of this 7 network parcellation is that it does not include an auditory / language
network, even though certain cortical regions have been identified as essential to auditory and
language processing. Considering the relevance of auditory regions to studying auditory
hallucinations in schizophrenia, an auditory network was defined in addition to the 7 Yeo
networks, to produce 8 resting-state networks. HCPMMP1.0 regions were mapped to one of 8
large-scale networks by calculating the surface overlap between each HCPMMP1.0 parcel
and each network. This mapping was constrained to be symmetric. Mapping calculations
were performed by Jakob Seidlitz and shared by Rafael Romero-Garcia. The auditory
network was defined by HCPMMP1.0 regions that corresponded to Early Auditory Cortex
and Auditory Association Cortex, described in the Neuroanatomical Supplementary Results
for Glasser et al. (2016), which included 13 regions. 8 additional regions from the Insular and
Frontal Opercular Cortex, Posterior Opercular Cortex, and Temporo-Parieto-Occipital
Junction were included in the auditory network based on their overlap with auditory and
language networks defined in the Cole-Anticevic Brain Network Parcellation (Ji et al., 2019)
and Gordon parcellation (Gordon et al., 2016). The Cole parcellation was constructed using a
clustering algorithm applied to resting-state data from 337 healthy volunteers from the HCP,
while the Gordon parcellation was developed from group-average resting-state functional

connectivity (rsFC) boundary maps of 120 healthy young adult subjects, which represent changes in rsFC patterns from one cortical location to another. Below lists the correspondence between HCPMMP1.0 areas and large-scale network:

Visual network: V1, MST, V6, V2,V3 V4, V8, V3A, V7, IPS1, FFC, V3B, LO1, LO2, PIT, MT, ProS, PHA1, PHA3, PH, DVT, V6A, VMV1, VMV3, PHA2, V4t, FST, V3CD, LO3,VMV2, VVC

Somatosensory network: 4, 3b, 5m, 5L, 24dd, 24dv, 1, 2, 3a, 6d, 6mp, 6v

Dorsal attention network: PEF, 7AL, 7Am, 7PL, 7PC, LIPv, VIP, MIP, IFJp, LIPd, 6a, PFt, AIP, TE2p, PHT, TPOJ2, TPOJ3, PGp, IP0

Salience network: FEF, 5mv, 23c, SCEF, 6ma, p24pr, 33pr, a24pr, p32pr, 6r, 46, 9-46d, 43, PFcm, PoI2, FOP4, MI, AVI, AAIC, FOP1, FOP3, FOP2, PFop, PF, PoI1, FOP5, a32pr

Limbic network: 10v, 10pp, 13l, OFC, EC, PeEc, TGd, TF, 25, pOFC, TGv, PI

Frontoparietal network: 55b, POS2, 7Pm, 8BM, 8C, 44, a47r, IFJa, IFSp, IFSa, p9-46v, a9-46v, a10p, 11l, i6-8, TE1p, IP2, IP1, PFm, p47r

Default mode network: RSC, SFL, PCV, 7m, POS1, 23d, v23ab, d23ab, 31pv, a24, d32, p32, 10r, 47m, 8Av, 8Ad, 9m, 8BL, 9p, 10d, 45, 47l, 9a, 47s, s6-8, Pir, PreS, H, TE1a, TE2a, PGi, PGs, 31pd, 31a, s32, p10p, TE1m, p24

Auditory network: A1, PSL, STV, OP4, OP1, OP2-3, 52, RI, TA2, STGa, PBelt, A5, STSda, STSdp, STSvp, TPOJ1, Ig, MBelt, LBelt, A4, STSva

4.3.3 Local gyrification index as a proxy for sulcal length and depth

The right and left hemisphere HCPMMP1.0 annotation files matching FreeSurfer's fsaverage were transformed to the individual cortical surface of each participant and the average LGI for each of the 360 parcellated brain regions (180 per hemisphere) included in the HCPMMP1.0 were extracted. The grand-average sulcal maps across all participants for the PCS and STS were thresholded at 25% of the image intensity, as previously for a similar

analysis (Jahn et al., 2016), and projected on to fsaverage space using FSL and FreeSurfer command tools. The HCPMMP1.0 regions that corresponded to the PCS and STS were determined by visualizing the HCPMMP1.0 labels atop the thresholded sulcal maps in fsaverage space in Freeview (Figure 4.3). Below lists the correspondence between HCPMMP1.0 areas and sulci:

Paracingulate sulcus: 24dd, 24dv, SCEF, p32pr, a32pr, d32, p32, 8BM, 9m

Superior temporal sulcus: STSdp, STSda, STSvp, STSva, A5, TPOJ1
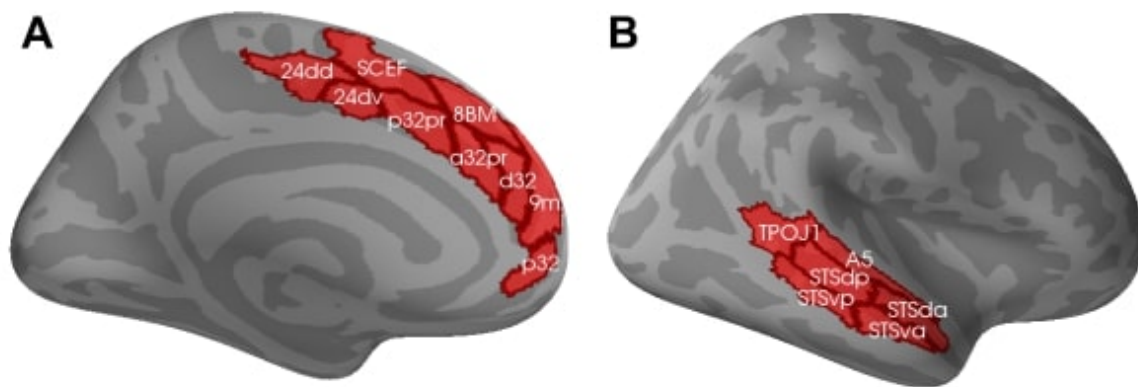
Figure 4.3. Correspondence between HCPMMP1.0 parcels and paracingulate and superior temporal sulci. A. Regions that overlap with the paracingulate sulcus (PCS) (24dd, 24dv, SCEF, p32pr, a32pr, d32, p32, 8BM, 9m). B. Regions that overlap with the superior temporal sulcus (STS) (STSdp, STSda, STSvp, STSva, A5, TPOJ1).

The average LGI in the HCPMMP1.0 parcels corresponding to the PCS and STS were respectively calculated for each hemisphere and correlated with the corresponding lengths and depths from BrainVISA (see Chapter 3, section 3.3.4). Pearson's correlations were used to test the relationship between sulcal length and depth and the respective average LGI in regions overlapping the PCS (HCPMMP1.0 areas: 24dd, 24dv, SCEF, p32pr, a32pr, d32, p32, 8BM, 9m) and STS (HCPMMP1.0 areas: STSdp, STSda, STSvp, STSva, A5, TPOJ1). The LGI across regions corresponding to the PCS and STS was significantly correlated to both left and right PCS and STS length and depth ($p<0.05$). For the PCS, average LGI was

significantly correlated with length (left: R=0.22, p<0.001; R=0.27, p<0.001) and depth (left: R=0.35, p<0.001; right: R=0.25, p<0.001); for the STS, average LGI was significantly correlated with length (left: R=0.15, p=0.019; right: R=0.21, p=0.0015) and depth (left: R=0.28, p<0.001; right: R=0.26, p<0.001). Correlations were small to modest, with the smallest correlation between STS LGI and left hemisphere STS length, and the strongest between PCS LGI and left hemisphere PCS depth (Figure 4.4).
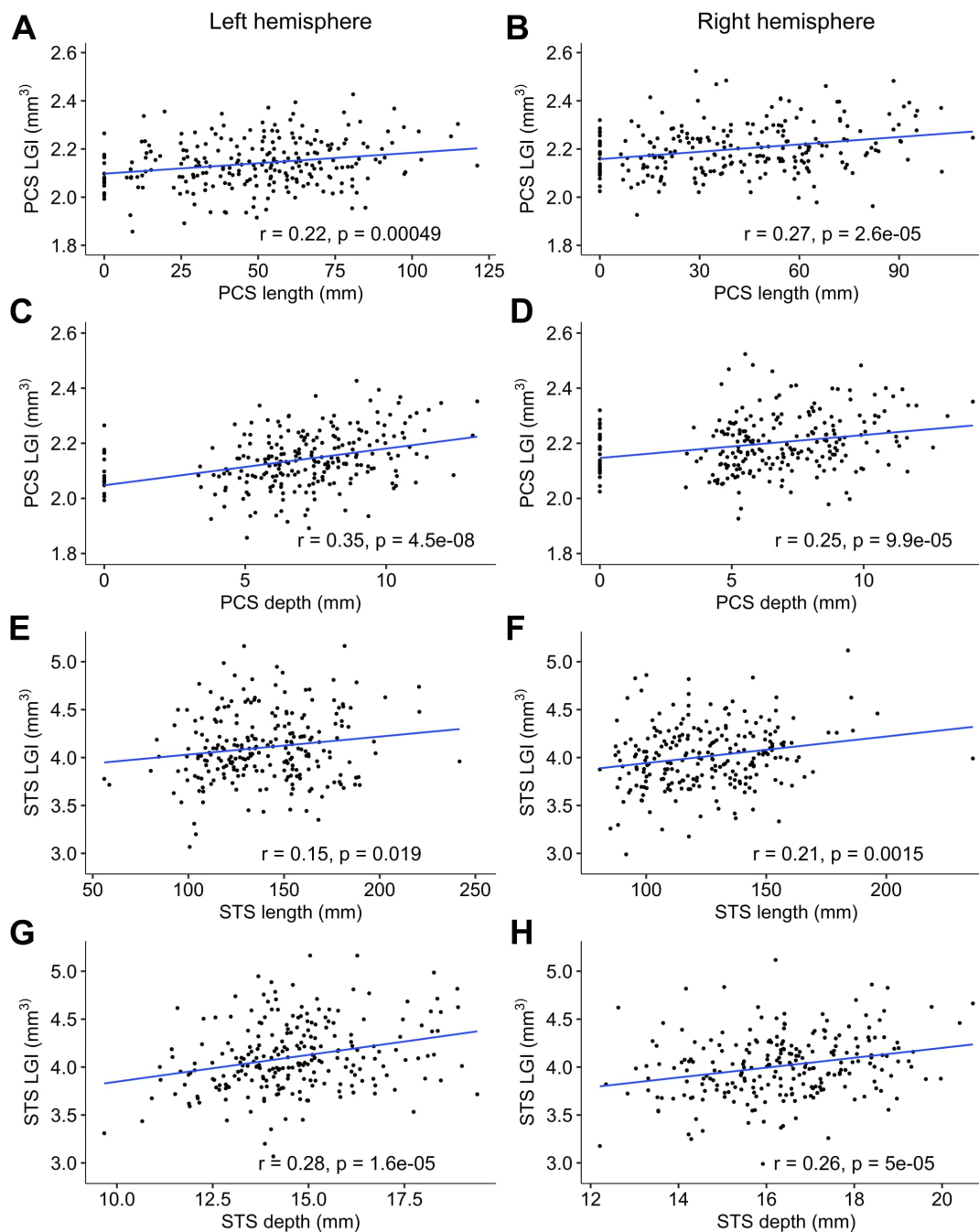
Figure 4.4. Correlation between sulcal LGI and sulcal length and depth. Average local gyrification index (LGI) in regions corresponding to the paracingulate (PCS; HCPMMP1.0 areas: 24dd, 24dv, SCEF, p32pr, a32pr, d32, p32, 8BM, 9m) and superior temporal sulci (STS; HCPMMP1.0 areas: STSdp, STSda, STSvp, STSva, A5,

TOPJ1) correlated against respective sulcal lengths (PCS: A–B, STS: E–F) and depths (PCS: C–D, STS: G–H)
calculated from BrainVISA sulcal extractions for the left and right hemispheres, respectively.

4.3.4 Structural covariance networks for local gyrification index between and within auditory and salience networks

Inter-regional structural covariance matrices of LGI were constructed for 360 parcellated brain regions (180 per hemisphere) according to the HCPMMP1.0 atlas for each group: H+ n = 101; H– n = 80; HC n = 63, adjusted for age, sex, scanning site, and total intracranial volume. Matrices were re-organized into eight well-established and replicable resting-state networks (section 4.3.2.2) and LGI values between regions located within the same network were averaged, resulting in an 8x8 matrix for each group of network-level LGI synchrony. Following the hypothesis that deviations in frontal and temporal sulcal anatomy would reflect alterations in large-scale topographical organization of salience and auditory networks, I evaluated the group differences in the inter-regional structural LGI covariance within and between the salience and auditory networks.

4.3.5 Lateralization of structural covariance networks for local gyrification index

While common resting state networks are often operationalized as symmetric across hemispheres, recent work has evidenced hemispheric asymmetry in resting-state functional connectivity (Raemaekers et al., 2018; Karolis et al., 2019), and this functional asymmetry may be reduced in schizophrenia patients (Agcaoglu et al., 2018). To investigate whether the lateralization of the sulcal length/depth findings were reflected in whole-brain intrinsic networks, the 8 resting-state networks were decomposed into their left and right hemisphere component brain regions. LGI values between regions located within the same network were averaged, resulting in a 16x16 matrix for each group.

4.3.6 Statistical analyses

To test the statistical significance between group-wise gyrification-based structural covariance networks, I performed nonparametric permutation testing with 5000 repetitions. For each iteration, the LGI parcellations of each participant were randomly assigned to one of three new groups with equivalent sample size to the original study groups (H+, H-, HC) and the between group difference in average correlation within and between the salience and auditory networks were re-computed to sample the null distributions against which the significance of the observed correlations was computed (Figure 4.5). This approach maintains the LGI values and covariates for each participant, but shuffles group assignment across individuals. The observed differences in means were evaluated against the obtained permutation distributions, and a two-tailed p-value was calculated based on its percentile position (<5%). Resultant p-values were corrected by FDR (FDR<0.05). I repeated this same analysis for the lateralized networks. Analyses were conducted in RStudio (v.1.0.136) and Matlab (v.2017b). To reproduce prior cortical morphology analyses related to hallucinations, I conducted whole-brain surfaced-based analyses of local gyrification index and cortical thickness within each sample separately, corrected for multiple comparisons across each hemisphere with Monte Carlo simulation (10 000 iterations) and a cluster-forming threshold of p<0.05. To reproduce prior work demonstrating increased grey matter within the medial prefrontal cortex (mPFC), I performed a VBM analysis in each sample separately. Nonparametric 2-sample t-tests were performed using FSL randomise with 5000 permutations and using threshold free cluster enhancement (TFCE) to identify clusters in which grey matter volume differed between groups at a statistical threshold of p<0.05 within the mPFC ROI. For both surface- and volume-based analyses, age and sex were included as confound regressors for the Shanghai data, and age, sex, and scanner for the UK data.

4.4   Results

4.4.1 Structural covariance networks for local gyrification index show increased gyral synchrony between auditory and salience networks

Having established convergent sulcal deviations in the PCS and STS, I sought to investigate their covariance in the context of resting-state networks to gain insights into their developmental coordination, and how they might enable or reflect the emergence of functional networks shown to contribute to the experience of hallucinations. Structural covariance matrices organized by established large-scale functional resting-state networks showed that mean (M) cross-correlation of the LGI for regions corresponding to the inter-salience–auditory networks was significantly greater for H+ compared to H– individuals ($M_{H+} = 0.501$, $M_{H-} = 0.355$, $M_{HC} = 0.375$, $q = 0.0084$) (Figure 4.5). The mean LGI cross-correlation was also significantly increased within (intra) each network (salience: $M_{H+} = 0.493$, $M_{H-} = 0.371$; $M_{HC} = 0.375$, $q = 0.0147$; auditory: $M_{H+} = 0.631$, $M_{H-} = 0.532$; $M_{HC} = 0.523$, $q = 0.0292$) after correcting for FDR < 0.05. It is typical in structural covariance testing to discard low values of correlations between parcellated regions, attributing them to noise. Results were stable across a range of thresholds, but the greatest difference was observed with no threshold, suggesting that weak correlations, large in number, are important contributors to inter-regional cortical synchronization.
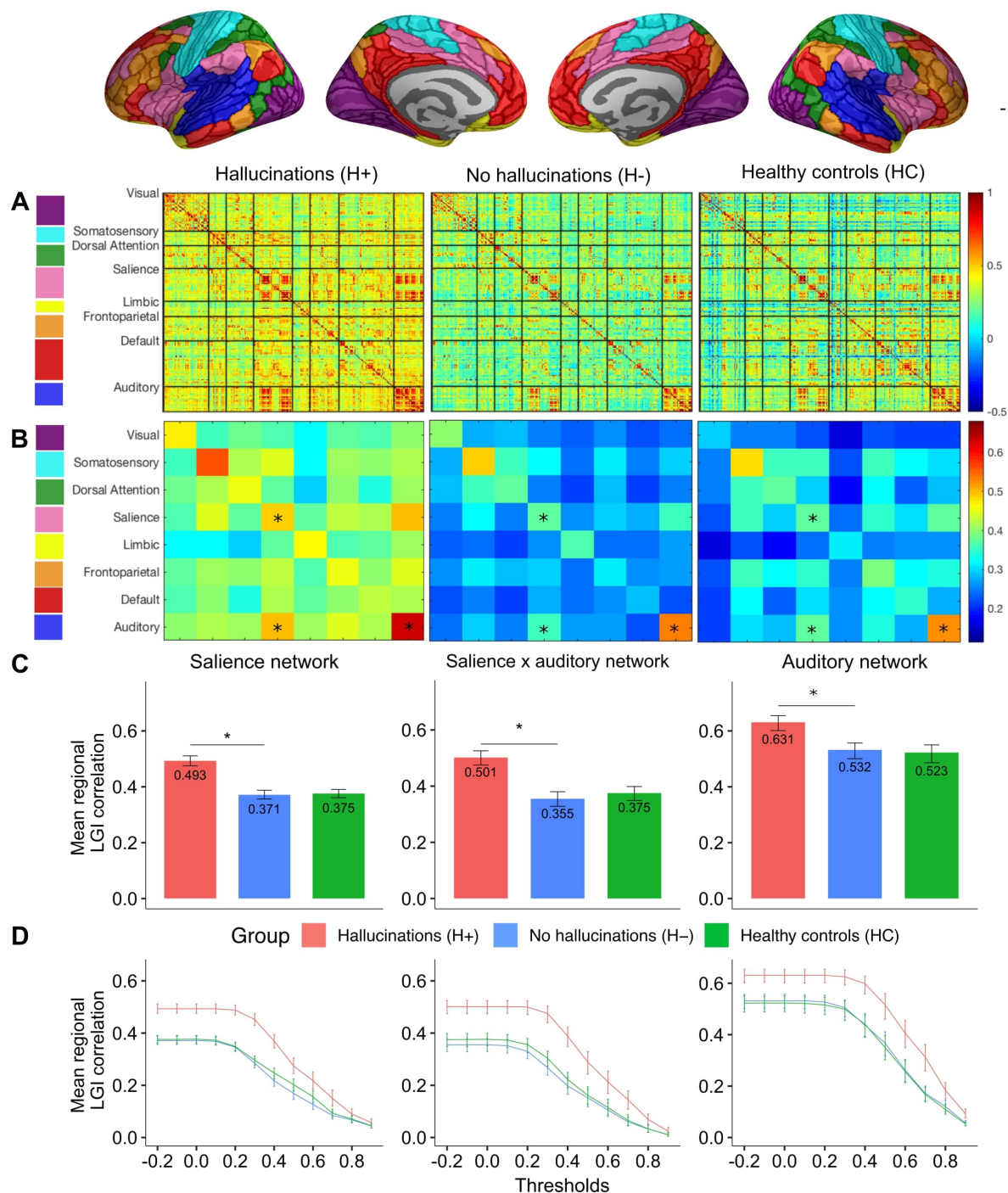
Figure 4.5. Stages in construction and analysis of gyrification-based correlation matrices. A. Local gyrification index (LGI) was computed for 360 parcellated brain regions (180 per hemisphere) according to the HCPMMP1.0 atlas and was used to construct interregional Pearson's correlation (360 x 360), adjusted for age, gender, scanning site, and total intracranial volume for each of the 3 study groups (H+, H-, HC). Matrices were

re-ordered according to 8 well-established and replicable resting-state networks. B. Each brain region was assigned a corresponding network and the LGI values between regions located within the same network were averaged, resulting in 8x8 group-wise matrices. C. Nonparametric permutation testing with 5000 resamplings was employed to test the significance of differences in patients with and without hallucinations in the mean LGI covariance within, and between, the salience and auditory networks. The observed differences in means were evaluated against the permutation null-distributions, and a two-tailed p-value calculated based on its percentile position (significance <5%). D. Mean regional LGI partial correlation within brain regions corresponding to the intra-salience, intra-auditory, and inter salience-auditory networks for correlation thresholds ranging from -0.2 to 1. Error bars represent the 95% bootstrap confidence intervals generated by resampling 5000 times with reassignment across participants within each group. * FDR < 0.05.

4.4.1.1 Lateralization of structural covariance

Decomposing networks by hemisphere showed that the mean LGI was significantly increased in patients with hallucinations compared to those without for the intra-hemispheric right salience network (R-R salience, q = 0.0120), the inter-hemisphere salience network (R-L salience, q = 0.0131), intra-left auditory network (L-L auditory, q = 0.0131), and between lateralized inter salience and auditory networks (L salience-L auditory, q = 0.0131; R salience-L auditory, q = 0.0131; R salience-R auditory, q = 0.004; L salience-R auditory, q = 0.0131).

4.4.1.2 Visualization of whole brain LGI correlations

To increase the level of spatial detail within focal and network-level sulcal and gyral alterations, I visualized the correlations between the LGI in left a32pr and right STSdp, the respective locations of the PCS and STS kinks, to all other parcels in the HCPMMP1.0 atlas (Figure 4.6). The group-wise illustrations suggest from visual assessment that the hallucination group had higher LGI connectivity of left a32pr to right temporal and insular cortices, as well as the left temporal pole, in comparison to the group without hallucinations and to healthy controls.
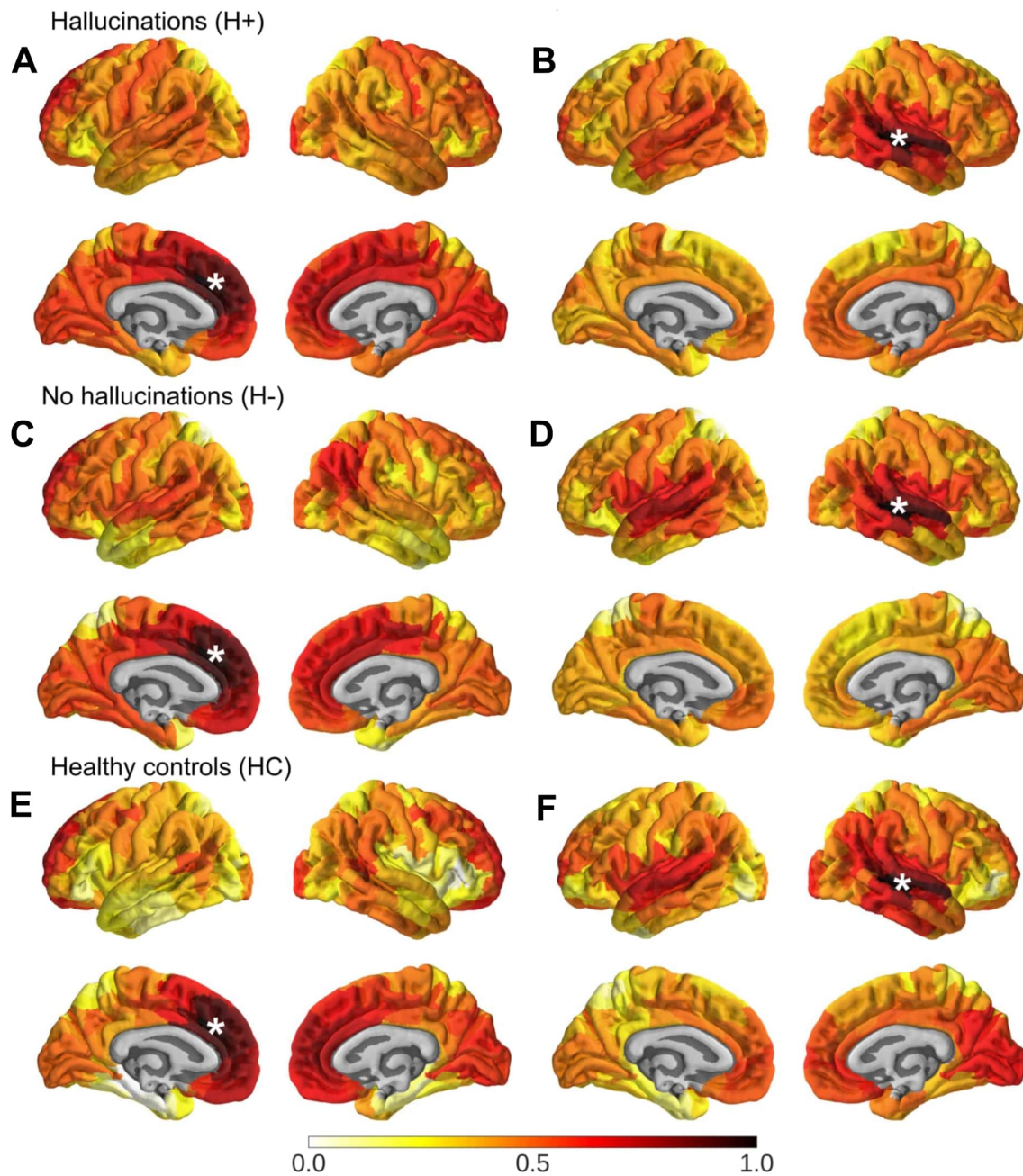
Figure 4.6. Whole-brain correlations for LGI from HCPMMP1.0 regions left a32pr and right STSdp. A white asterisk indicates the seed regions left a32pr and right STSdp, which were the loci of the sulcal displacements identified for the PCS and STS, respectively. A–F. Correlation between LGI in seed regions and all other 360 regions defined by the HCPMMP1.0 atlas for A–B. Hallucinations (H+; n = 101); C–D. No hallucinations (H-; n = 80); E–F. Healthy controls (HC; n = 63). The colour scale represents the correlation coefficient (Pearson's r)

of each regional LGI measure for the HCPMMP1.0 parcellation to the LGI in left a32pr (A, C, E) and right STSdp (B, D, F).

4.4.2 Whole-brain morphology analyses: local gyrification, cortical thickness, and grey matter

4.4.2.1 Surface-based local gyrification index and cortical thickness

Cortical statistical maps displayed decreased LGI in patients with hallucinations (H+) compared to those without (H–) in the rostral middle frontal cortex for the UK sample. Cortical thickness was increased for H+ in the left lingual gyrus for both datasets (UK and Shanghai), and increased in the left inferior parietal and bilateral precuneus for the UK dataset only. Compared to healthy controls, schizophrenia patients (H+ and H– combined) showed increased LGI in the left superior frontal cortex and reduced thickness in the left pars opercularis. Cortical surface representations were plotted using BrainsForPublication v0.2.1 (10.5281/zenodo.1069156) (Figure 4.7).

UK: Hallucinations (H+) vs No hallucinations (H-)

A   Local gyrification index

B   Cortical thickness

Shanghai: Hallucinations (H+) vs No hallucinations (H-)

C   Local gyrification index

D   Cortical thickness

All: Schizophrenia vs Healthy controls (HC)

E   Local gyrification index

F   Cortical thickness
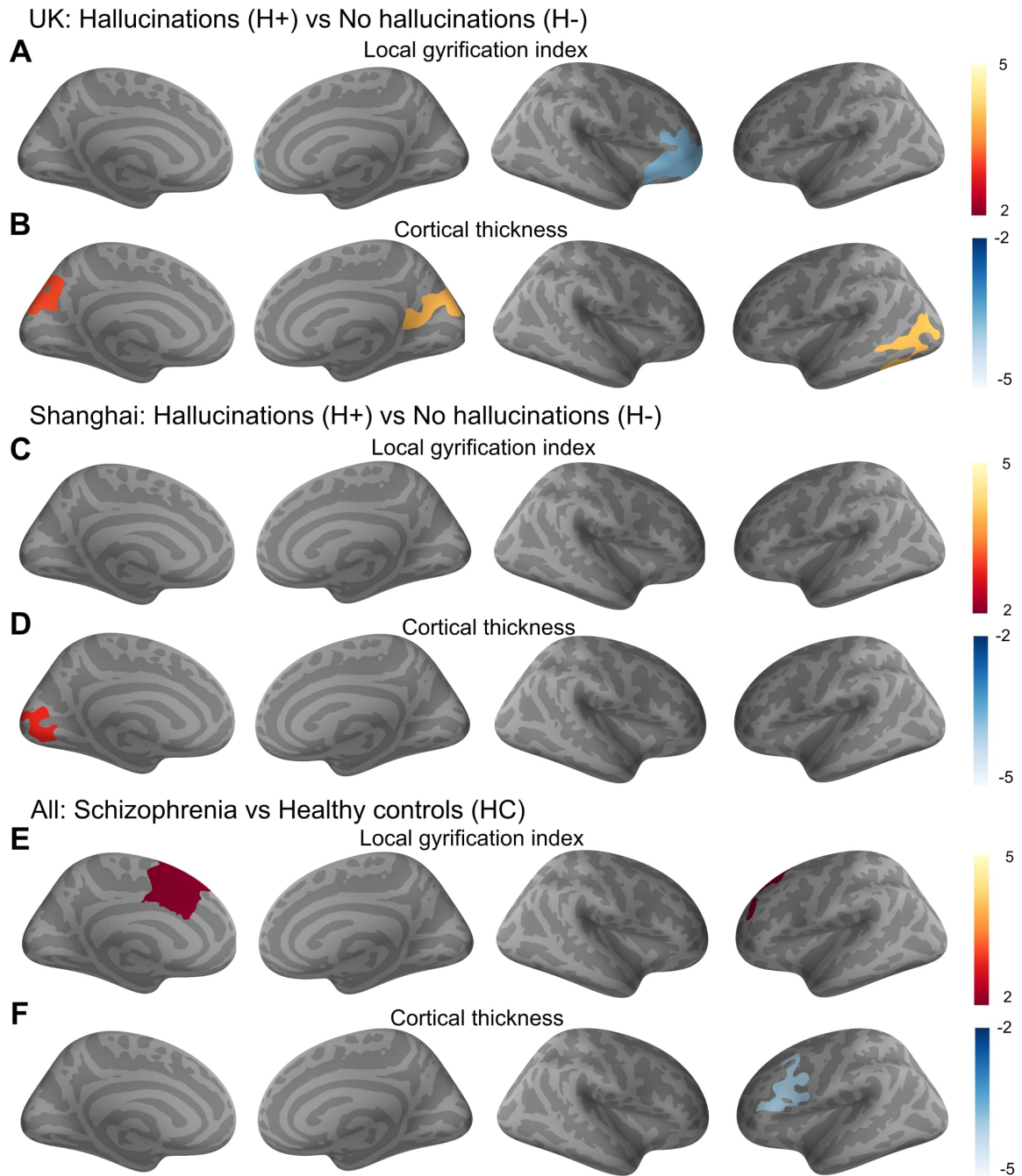
Figure 4.7. Clusters showing significant difference in LGI and cortical thickness between schizophrenia patients with and without hallucinations. A–B. UK dataset, C–D Shanghai dataset, E–F, schizophrenia patients (H+ and H- combined) compared to healthy controls for the Shanghai dataset. All results were corrected for multiple comparisons using Monte Carlo simulation with 10 000 iterations with a cluster-forming threshold of p<0.05

and corrected for multiple comparisons across each hemisphere. The colour bar shows the logarithmic scale of p values (–log10).

4.4.2.2   Voxel-based morphometry

The VBM analysis showed that for the UK dataset, GM volume was significantly greater in schizophrenia patients with hallucinations compared to those without in the mFPC ROI (MNI: x = 0, y = 56, z = 4, cluster size = 149, t-value = 7.87, TFCE-corrected p-value = 0.0012), as has been found previously (Garrison et al., 2015). GM volume in the mPFC ROI was not significantly different between patients with and without hallucinations for the Shanghai dataset (TFCE-corrected p-value = 0.322).

4.5   Discussion

This chapter demonstrates increased LGI covariance within and between regions relating to salience and auditory networks. Although LGI decreases dramatically from childhood to adolescence, and decreases more gradually across adulthood, it chiefly reflects cortical folding, suggesting that perinatal alterations to developing structural networks are related to experiencing hallucinations in adulthood. Since the salience and auditory networks are supported by the anterior cingulate and insula, and temporal regions, respectively, these results converge with prior research demonstrating differences in local folding patterns in cingulate and temporal regions in schizophrenia (Cachia et al., 2008; 2015; Garrison et al., 2015; 2018; MacKinley et al., 2020) and integrates these spatially localized differences in support of hypotheses of aberrant fronto-temporal, salience, and auditory network connectivity underpinning the experience of hallucinations in schizophrenia (Mallikarjun et al., 2018; Simons et al., 2017; Palaniyappan and Liddle, 2012; Shergill et al., 2000). Moreover, the hemisphere-specific network results suggest that hallucination status has a lateralized association to the coordination of local gyrification within and between salience and auditory intrinsic networks.

4.5.1 Mechanisms for increased gyrification covariance

What is the mechanism by which reduced morphological congruity between auditory and cingulate cortices develops, and could it represent a structural presage of later-life hallucinations? The challenge in interpreting structural covariance networks lies in an incomplete understanding of their cellular, genetic, and experience-dependent plasticity underpinnings. Although the biological interpretation of structural covariance networks is incomplete, recent work shows that genetic influences contribute to patterns of covariance in neuroanatomy. By calculating local correlations of cortical thickness, Alexander-Bloch et al. (2020) have shown that the cortical pattern of shared genetic influences on cortical thickness relates to sulcal and gyral organization, especially in primary somatomotor, superior temporal/insular, and cingulate areas, with high variability when traversing sulcal or gyral boundaries, but more homogenous local correlations within an area demarcated by sulci or gyri. The average local correlations are lower in sulci than in gyri, indicating that the genetic influences on cortical thickness colocalize with sulcal and gyral architecture. This shows an indirect link between genetic influence and gyrification covariance matrices and suggests that genetic constraints on cortical folding processes are detectable in the thickness of the resultant matured cortex. In support of this, biomechanical models have demonstrated a relationship between cortical folding and thickness, with wider folds expected for increased average cortical thickness (Bayly et al., 2013).

Studies on the microstructural basis of sulcal macrostructure suggest that neuronal density changes, dendritic arborisation, synaptic pruning, and organization of axonal connections, individually or together, drive gyrification. In rhesus monkeys, anterograde and retrograde tracing techniques have shown that despite regional heterogeneity in their projections, the medial prefrontal cortices are unified by bidirectional connections with the superior temporal cortex and neighbouring auditory association cortices (Barbas et al., 1999). One of such connections, the arcuate fasciculus, shows left-lateralized reduced mean and radial diffusivity in children reporting psychotic experiences compared to those without (Dooley et al., 2020), suggesting that developmental changes to fronto-temporal association

tracts may underpin the increased gyral synchrony between salience and auditory regions observed here. Advances in diffusion imaging of neonates will help clarify the development of white matter (WM) tracts and their relationship to cortical folding. For instance, WM connectivity weighted by fractional anisotropy (measuring the directional profile of water diffusion in each voxel) and neurite density index (indexing the fraction of tissue that includes axons or dendrites) positively correlates with age across 25–45 weeks gestation, but this maturation varies by brain region, with intra-frontal, frontal to cingulate, frontal to caudate and inter-hemispheric connections developing more slowly (Batalle et al., 2017).

I hypothesize that auditory hallucinations in schizophrenia patients and the accompanying patterns of brain structure are due to differences in maturational coupling between temporal and cingulate regions. The evidence accumulating regarding prenatal inflammatory exposure (Allswede and Cannon, 2018), maternal stress, obstetric complications (Pugliese et al., 2019), and expression of schizophrenia risk genes in foetal life as factors conferring vulnerability to schizophrenia would be of major relevance to how the intrauterine environment contributes to the variations in cortical folding that impact postnatal pathology. I speculate that auditory hallucinations in schizophrenia may relate to alterations to the maturational trajectories in temporal and cingulate regions, and thus their structural covariance. Mechanistic predictions follow, including the role of genes involved in driving the maturational trajectories of cortical patterning (Alexander-Bloch et al., 2020) and the impact of events that disrupt foetal neurodevelopment (Nosarti et al., 2012; Batalle et al., 2017). Longitudinal studies following prenatal cohorts until adult life will be required to establish such predictions.

4.5.2 Partial replication of surface-based and grey matter alterations in hallucinations and schizophrenia

I partially replicate findings of surface-based morphometry and grey matter volume alterations associated with hallucinations in schizophrenia, showing reduced CT in the left lingual gyrus in patients with hallucinations in both datasets, and additionally for the UK sample only: increased thickness in the left inferior parietal and bilateral precuneus, reduced gyrification in the middle frontal cortex, and increased grey matter in the medial prefrontal

cortex. Many of these alterations were observed in Chapter 2, with previous reports of reduced LGI in the middle frontal cortex (Kubera et al., 2018) and increased GM in the medial prefrontal cortex (Garrison et al., 2015) in schizophrenia patients with hallucinations compared to those without, as well as increased thickness in the parietal cortex in bipolar disorder patients with hallucinations (Mørch-Johnsen et al., 2018). However, the replication of increased lingual gyrus thickness is novel. Although primarily considered a visual region, the lingual gyrus has equally been implicated in language function (i.e., processing pseudowords and real words; Xiao et al., 2005). Reduced thickness in the lingual gyrus has also been reported for hallucinations in dementia with Lewy bodies (Delli Pizzi et al., 2014), perhaps suggesting that these samples had visual hallucinations, although this is speculative in the absence of detailed hallucination assessment. The larger size of the UK sample compared to the Shanghai might explain the difference in the number of significant regions, but confirmation is required through replication in independent samples. Recent initiatives like ENIGMA (Enhancing Neuro Imaging Genetics through Meta-Analysis) are making progress on this front, but have not yet been applied to hallucinations in specific. A recent ENIGMA report comparing 4474 schizophrenia patients to 5098 controls found reduced thickness in the left pars opercularis of the inferior frontal gyrus, as demonstrated here, although more widespread alterations were also documented in the report (van Erp et al., 2018).

While these (non-sulcal) structural patterns were not wholly consistent between UK and Shanghai datasets, grey matter and cortical thickness are more subject to plastic changes as a function of aging, learning, experience, and medication, suggesting that sulcal topology and its covariance presents a more robust and specific indicator of hallucinations, and pinpoints that foetal brain features may influence the way in which people experience their environment. The interaction between early neurodevelopment and experiential diversity may help explain, for instance, why trauma plays a major role in some hallucinations, but a minor or no role in others (Luhrmann et al., 2019).

4.5.3 Limitations

While structural covariance networks have been widely used to study brain regional relationships across groups of subjects, a recent study assessing the reliability and comparability of structural covariance networks has shown that there are significant differences in structural covariance networks due to site effects in two datasets of healthy age- and sex- matched adults (n = 86 each), and when comparing between scan and re-scan sessions for the same individuals (Carmon et al., 2020). This study did not assess LGI, but showed that surface area and volume are more reliable than cortical thickness for covariance networks, and suggested that a large number of subjects were needed for accurate networks, depending on the parcellation (i.e., >30 subjects for the Desikan-Killiany parcellation with 68 regions bilaterally). The covariance matrices calculated in this chapter used well over the recommendation (H+ n = 101; H– n = 80; HC n = 63), and controlled for scanning site, though replication of this analysis in larger samples will be important to establish its validity. Another limitation of covariance networks is that they are calculated at a group level, obscuring subject-level information. New techniques, such as morphometric similarity mapping, estimate the inter-regional correlation between multiple MRI metrics (i.e., GM volume, surface area, cortical thickness, mean curvature, or diffusion-weighted imaging measures of white matter connectivity) within an individual, producing morphometric similarity networks (MSN), which have been shown to capture individual differences in cognition (Seidlitz et al., 2018). Similarly, the recently developed person-based similarity index (PBSI) is based on the concept of morphometric similarity, but additionally indexes the degree of similarity of an individual's MSN to the other individuals in a group across cortical regions. The PBSI of sulcal width (PBSI-SW) has highlighted a subgroup of schizophrenia patients with extreme deficits in estimated IQ and lower cortical sulcation at follow-up compared to other patients and to healthy controls (Janssen et al., 2021).

The local gyrification index was used as a proxy for sulcal length and depth. Although the LGI in brain parcellations corresponding to the PCS and STS significantly correlated with the length and depth of these sulci, the correlations were small to moderate, indicating that there are differences in the measurement types (LGI vs. sulcal metrics). However, creating

whole-brain "sulcal covariance networks" in the same way that LGI covariance matrices were calculated would require measuring all cortical sulci. Available software can reliably detect around 30–40 morphologically stable sulci per hemisphere (Pizzagalli et al., 2020), but there are many other more variable sulci that cannot be automatically measured without manual intervention. Since large numbers of subjects are required for reliable structural covariance matrices, an approach using "sulcal covariance networks" will not be feasible until all sulci can be accurately detected with fully automated methods.

Finally, VBM, the method used here for voxel-wise comparisons of grey matter volume, is sensitive to scanner or MR sequence differences. For this reason, a multi-centre reproducibility protocol was developed to standardize MRI acquisition across sites and manufacturers for the UK sample (Deakin et al., 2018; Lisiecka et al., 2015), and whole-brain analyses of cortical gyrification, thickness, and grey matter volume were conducted within UK and Shanghai samples separately, to scanner/sequence confounds.

4.5.4 Conclusion

In sum, this chapter demonstrates that the specific sulcal deviations observed in Chapter 3 are elements of global alterations in inter-regional correlations of cortical folding. The covariance of the local gyrification index in regions corresponding to the salience and auditory networks was increased in schizophrenia patients with hallucinations compared to those without. As local gyrification index partly reflects neurodevelopmental processes, these results suggest that deviations within and between developing salience and auditory networks may be a risk factor for the manifestation of hallucinations related to schizophrenia in adulthood. The partial replication between datasets of structural changes in grey matter, cortical thickness, and local gyrification indicates that other regional macrostructure is involved in this risk, but is a less robust correlate of hallucination occurrence.

Chapter 5   Resting-state functional connectivity patterns associated with hallucinations in schizophrenia and cingulate lobe folding

5.1   Abstract

The auditory hallucinations that commonly occur in schizophrenia have been proposed to arise from alterations in the brain's intrinsic functional connectivity; specifically, abnormal interactions between the resting-state activity of the auditory and medial anterior cingulate cortices (ACC). The ACC encompasses distinct subdivisions based on cytoarchitectural and functional connectivity profiles whose organization is influenced by the sulcal pattern on the medial wall. Chapter 3 demonstrated that the length of the paracingulate sulcus (on the medial ACC) is a robust trait marker for hallucinations. Considering the evidence linking resting-state activity to hallucinations, and that local sulcal morphology influences functional organization, this chapter investigates resting-state activity in relation to hallucinations and PCS morphology. I analyse resting-state functional MRI (rsfMRI) data from the 203 people with a schizophrenia diagnosis and 63 healthy controls (HC) from the same independent datasets used in Chapters 3 and 4 (United Kingdom and Shanghai), grouped into those with (H+) and without (H–) hallucinations (UK: n=93 H+, n=51 H–; Shanghai: n=22 H+, n=37 H–, n=63 HC). Using seed-based connectivity extracted from a region along the left PCS, I assess whether PCS morphology is associated with connectivity related to hallucination status. Considering the role of global network topology shown in Chapter 4, I evaluated the mean functional connectivity within and between salience and auditory networks and assess graph theory derived measures of global functional topology. The results show a significant interaction between left PCS length and hallucination status on connectivity, but the spatial

pattern of connectivity does not reproduce between UK and Shanghai datasets. There were no group differences between H+ and H– for any resting-state measure, indicating that resting-state activity is not a trait marker for hallucinations. However, rsfMRI was significantly different between schizophrenia patients (H+ and H– combined) compared to HC, supporting the notion of schizophrenia as a disorder of functional dysconnectivity. This chapter addresses the questions:

- Does a structural marker (sulcal morphology) for hallucinations correlate with connectivity?
- Is resting-state connectivity alone a trait marker for hallucinations?

5.2   Introduction

The experience of auditory hallucinations or hearing voices prevails in people with a diagnosis of schizophrenia. Since hallucinations arise in the absence of an external stimulus, it is plausible that their origin relates to alterations in the brain's intrinsic functional organization. Some researchers have described this as the "resting-state hypothesis" for auditory hallucinations, postulating that voices are generated by abnormally elevated resting-state activity in the auditory cortex and abnormal modulation of the auditory cortex by anterior cortical midline regions at rest, resulting in inner mental phenomena being falsely perceived by the brain as external (Northoff and Qin, 2011; Hunter et al., 2006). Correspondingly, the increased resting interactions of cortical regions predicts reduced neural responsiveness to external auditory stimuli, which has been reported by a multi-centre study demonstrating less activation to probe tones in left primary auditory cortex (BA41) in schizophrenia patients with current hallucinations compared to those without (Ford et al., 2009). Resting-state hypotheses are supported by bilateral anatomical connections between medial prefrontal and superior temporal cortices in primates (Barbas et al., 1999) and resting-state functional connectivity in humans (Margulies et al, 2007), as well as increased activity in speech-sensitive areas (left superior temporal gyrus and medial transverse temporal gyrus) during silence in healthy adults (Hunter et al., 2006). Chapter 3 demonstrated alterations to

local sulcal morphology within these connected regions (medial anterior cingulate and auditory cortices). Specifically, left hemisphere paracingulate sulcus (PCS) length was reduced in schizophrenia patients with hallucinations (H+) compared to those without (H–) and to healthy controls (HC), and right hemisphere superior temporal sulcus (STS) depth was reduced in H+ compared to HC. Additionally, Chapter 4 showed that the correlation of the local gyrification index within anatomical regions corresponding to salience and auditory networks was increased in H+ compared to H–. However, the functional consequences of deviations in local and network-level cortical folding, and their relationship to hallucinations, remains to be clarified.

If present, the PCS runs along the medial wall of the anterior cingulate cortex (ACC), and the STS separates the middle and superior temporal gyri. Both areas encompass distinct cytoarchitectonic and functional subdivisions that subserve complex cognition: the ACC is involved in inhibitory control, guiding attention, and error detection, while the STS is implicated in social perception, language, and theory of mind, organized along a posterior-to-anterior axis. Sulcal patterns form in gestation and may act as structural constraints on emerging functional networks (Le Guen et al., 2018). The PCS and STS display human-specific asymmetries in the general population and sulcal interruptions that contribute to inter-individual variability in sulcal organization. This variability is especially characteristic of the PCS, which emerges later in gestation than the STS, and is less morphologically stable between individuals and between hemispheres within a given individual. Variation in PCS morphology is relevant for structure-function relationships. The presence or absence of the PCS determines the location of cytoarchitectonic areas in the cingulate cortex, in particular area 32' (Vogt et al., 1995), and PCS presence/absence influences the location of feedback-related functional activity during a trial-and-error learning task in humans (Amiez et al., 2013). In people with a diagnosis of schizophrenia, the presence or absence of the PCS influences functional activation patterns in the ACC during cognitive interference tasks (Heckers et al., 2004; Artiges et al., 2006). In support, PCS presence/absence explains 14% of the variance of inhibitory control efficiency (Stroop interference task) in children and young adults (Tissier et al., 2018). The relationships between ACC sulcal pattern variability and microstructure, function, and cognition holds for other tertiary sulci in the prefrontal cortex as

well. For instance, the presence/absence of the inferior rostral sulcus in the ventromedial

prefrontal cortex influences the location and strength of peak default mode network activity

(Lopez-Persem et al., 2019), and the three components of the posterior middle frontal sulcus

in the lateral prefrontal cortex have distinct resting-state functional connectivity profiles,

myelin content, and functional task activations (Miller et al., 2021). Based on the evidence

that sulcal morphology influences functional connectivity, I hypothesize that variations in

ACC folding may contribute to functional differences between patients with and without

hallucinations.

Resting-state activity can be characterized through several approaches. Seed-based

analyses quantify the correlation in connectivity across time between a brain region of

interest (seed) to other cortical regions or networks, while independent component analyses

identify regions whose activity tends to correlate at rest, without requiring an a priori

hypothesis. Graph theoretical approaches represent the brain as a graph or network, with

brain regions acting as nodes, and functional or structural connections acting as edges, and

calculate attributes at local (nodal) and global (network) scales to assess the topological

patterns of the graph. Commonly measured attributes include characteristic path length (an

index of the efficiency of information transmission), clustering coefficient (the degree to

which a network segregates into distinct clusters), global efficiency (the ability of parallel

information transmission over the network), and local efficiency (a measure of efficiency of

information transfer within neighbouring nodes). Graph theory provides a powerful tool to

characterize large-scale functional and structural brain network topology that may be altered

in psychopathology, particularly for schizophrenia, which is considered a disorder of brain

network organization, such that it arises from a dysfunctional integration of information

between distributed brain regions (Rubinov and Bullmore, 2013). Regarding hallucinations in

schizophrenia and non-clinical voice hearers, there is preliminary evidence for altered rest

activity in left hemisphere temporal auditory/language regions and abnormal interactions

between resting-state networks, particularly the DMN, salience network, central executive

network, and sensory (auditory and visual) networks, but current evidence ultimately paints a

mixed picture of hyper- and dys-connectivity involving different pathways, such that "few if

any findings have directly replicated across studies" (see Alderson-Day et al., 2015; 2016 for recent reviews on rsfMRI and auditory hallucinations). Inconsistencies in findings might be due to differences in study design, scanning acquisition parameters, analysis methods, hallucination assessment (lifetime history vs. current), lack of a non-hallucinating patient control group, and small samples (20–30 per group). Larger samples have recently been studied (>30 per group), reporting no significant differences in resting-state functional connectivity between schizophrenia spectrum patients with hallucinations to those without (Hare et al., 2018; Zhu et al., 2016). However, greater auditory hallucination severity is associated with the strength of functional connectivity between the superior temporal gyrus and salience network (Hare et al., 2018), and greater connectivity between left auditory association cortex (seed) to left planum temporale, planum operculum, and superior marginal gyrus (Okuneye et al., 2020). Network-based statistics have shown that schizophrenia patients with hallucinations show intrinsic connectivity alterations primarily between fronto-insula/cingulate regions, with the highest number of altered connections in the left middle cingulate gyrus node (Schutte et al., 2021). Only one study has used graph theoretical approaches to assess resting-state functional network topology related to hallucination presence/absence in schizophrenia (Zhu et al., 2016), finding no significant differences in any network property associated with hallucination status. However, in comparison to healthy controls, both patient groups (H+ and H–) showed significantly reduced clustering coefficient, characteristic path length, global and local efficiency of functional networks. The sensitivity of graph theoretical approaches in capturing network topology changes in schizophrenia and psychosis (Kambeitz et al., 2016), but scant application to hallucinations in specific, motivates studies characterizing network topology in hallucinations in schizophrenia. Research incorporating direct replications in independent clinical samples is needed to clarify whether resting-state connectivity acts as a trait marker for hallucinations.

This chapter provides a more direct link between the abnormal development of sulcus morphology and hallucinations by studying resting-state functional connectivity. I explore whether function reflects structure by asking two questions: (1) Does a structural marker (sulcal morphology) for hallucinations correlate with connectivity? (2) Is resting-state connectivity alone a trait marker for hallucinations? I analyse the resting-state data that was

acquired at the time of the T1 structural scans for the multi-centre UK and Shanghai datasets described in Chapters 3 and 4, grouped into schizophrenia patients with and without hallucinations (UK: n = 93 H+, n = 51 H–; Shanghai: n = 22 H+, n = 37 H–) and n = 63 HC for the Shanghai dataset. Using seed-based connectivity extracted from area 32 prime along the left PCS, I hypothesize that connectivity will differ between patients with and without hallucinations and will be associated with PCS morphology (length). Following salience and auditory structural (gyrification) network alterations observed in Chapter 4, I compare the mean functional connectivity within and between auditory and salience networks between H+ and H–. I replicate graph theoretical approaches related to hallucinations in two independent samples. To confirm the stability of functional networks, I perform a test-retest reliability analysis for patients from the UK study assessed at one-year follow-up. I compliment these analyses with case-control differences in schizophrenia patients (H+ and H– combined) and healthy controls to reproduce prior work and discern whether connectivity patterns related to hallucinations are distinct from schizophrenia pathology.

5.3   Methods

5.3.1 Participants, study design, and scanning acquisition

This chapter uses MRI data from the same two datasets described in Chapter 3 (section 3.3.1). To recall, they were (1) a predominantly White British sample assessed at multiple sites in the UK and (2) a Han Chinese sample assessed in Shanghai, China. While the Shanghai study was cross-sectional, the UK multicentre study was longitudinal, with MR imaging performed at baseline and one-year follow-up. For both studies, whole-brain rsfMRI data were acquired following the structural scan. Functional acquisition details are summarized in Table 5.1 and refer to Chapter 3, section 3.3.1 for structural MR acquisition details.

Chapter 3 studied MR images from three (out of six) UK neuroimaging centres with the largest sample sizes due to gender imbalances between hallucination (H+) and no

hallucination (H–) groups in the remaining centres (i.e., there are no female H– patients from site 4 – Birmingham or site 5 – University College London (UCL)), resulting in n = 79 H+ and n = 43 H–. In this chapter there are two differences in the UK sample. First, I additionally analysed one-year follow-up data to assess the test-retest reliability of functional networks. During this year, subjects were assigned to placebo or minocycline arms; however, minocycline was shown to have no effect on psychotic symptoms or brain function (Deakin et al., 2018), indicating that it is unlikely to influence the test-retest reliability analysis. Moreover, the placebo and minocycline arms were balanced in H+ and H– groups (Table 5.2). Second, due to missing rsfMRI data for some subjects or exclusion due to processing errors, poor data quality (high fraction bad frames), or effects of motion, I include two additional centres (Birmingham and UCL) to increase the sample size. Of the subjects described in Chapters 3–4, n = 3 H+ and n = 4 H– did not have rsfMRI data, and the data for a further n = 5 H+ and n = 5 H– was excluded due to effects of motion or poor quality. The reduction in sample size was exacerbated at follow-up: n = 51 H+ and n = 18 H– participants dropped out or converted between H+ and H– groups from baseline to the one-year follow-up, and n = 2 H+ and n = 6 H– had poor quality functional data at follow-up. Without adding subjects from additional sites, this would result in n = 26 H+ and n = 19 H– at follow-up.

At baseline, Birmingham (site 4) contributed T1 MRI and rsfMRI data for n = 6 H+ and n = 10 H– subjects and UCL (site 5) contributed data for n = 10 H+ and n = 6 H–. At follow-up, Birmingham (site 4) contributed sMRI and rsfMRI data for n = 3 H+ and n = 7 H– subjects and UCL (site 5) contributed data for n = 1 H+ and n = 5 H–. Site 6, King's College London (KCL) was not included because there was only good quality structural and functional data for n = 2 patients (1 H+, 1 H-), which might introduce more variance than it would benefit the sample size. Considering that this sample differs slightly from that presented in Chapters 3–4, I replicate the paracingulate sulcus length linear regression analyses to confirm that the same relationship between structure-hallucination holds for this expanded dataset.

Table 5.1. Reproducibility and comparability of scanning sequences for UK multicentre and Shanghai studies.

	UK					China
Centre	Manchester	Cambridge	Edinburgh	Birmingham	UCL	Shanghai
MRI scanner	Philips Achieva	Siemens Trim Trio	Siemens Verio	Philips Archieva	Siemens Trim Trio	Siemens
Field strength (Tesla)	3T	3T	3T	3T	3T	3T
Head coil	8-channel	12-channel	12-channel	8-channel	12-channel	32-channel
TR EPI (ms)	2000	2000	2000	2000	2000	2600
TE EPI (ms)	30	30	26	30	30	30
Voxel dimensions (mm^3)	3 x 3 x 4.5	3 x 3 x 4.5	3.4 x 3.4 x 4	3 x 3 x 4.5	3 x 3 x 4.5	3.3 x 3.3 x 4
Number of volumes	512	512	512	512	512	176
EPI time (min)	17	17	17	17	17	8
FOV (mm)	192	192	220	192	192	210

5.3.2 Imaging pre-processing

Data were pre-processed using the speedypp.py tool (v2.0) distributed by Wavelet Despike software, a wavelet-based method for removing motion artefacts (www.brainwavelet.org), as described by (Patel et al., 2014). The first 10 volumes of each functional dataset were excluded to eliminate non-equilibrium magnetization effects. For each subject, the anatomical image was first skull-stripped and non-linearly transformed to the MNI152 template using AFNI 3dWarp. The images were then slice-time corrected and zero padded to expand the size of the image matrix in the phase-encoded direction. Matrices for non-linear warping to MNI standard space, registration to the first volume after equilibration, and co-registering to the skull-stripped anatomical were combined to create and apply a single warp field for

functional data. Spatial blurring (with 5-mm full width at half maximum Gaussian kernel) and whole-brain intensity normalisation (to median = 1000) were applied. Wavelet despiking was applied to model and correct for head motion artefacts. Temporal bandpass filtering (0.01–0.01 Hz) was performed to reduce the effects of low-frequency drifts and high-frequency physiological noises. The downsampled anatomical scan was segmented to obtain CSF and WM signals, which were used to regress 12 motion correction parameters and their first temporal derivatives, and cerebrospinal fluid (CSF) signal. Recommended default parameters were used at each processing stage. Labels from the HCPMMP1.0 parcellation (180 labels per hemisphere) in FreeSurfer's fsaverage space were mapped to the subject's segmentation volume (NIFTI file). 16 subcortical structures (8 per hemisphere) were concatenated to the parcellation. The parcellation was co-registered to the functional image using ANTS 3dresample and FSL flirt command line utilities (convert_xfm). The FSL command fslmeants was used to extract the mean time series of all the voxels included in each of the 360 cortical and 16 subcortical regions. 20 cortical ROIs were discarded (10 bilateral regions: 10pp, OFC, H, 25, s32, pOFC,TGv, 10, EC, TE1) because they showed no coverage (0 voxels across the fMRI time series) in at least one participant, resulting in a total of 340 cortical and 16 subcortical retained regions. Wavelet correlation analysis using maximal overlap discrete wavelet transform, a time-frequency transformation, was applied to decompose each regional time series into four frequency ranges for each dataset: UK: 0.125–0.25 (scale 1), 0.0625–0.125 (scale 2), 0.03125–0.0625 (scale 3), 0.015625–0.03125 (scale 4); Shanghai: 0.09615–0.19231 (scale 1), 0.04807–0.09615 (scale 2), 0.02404–0.04807 (scale 3), 0.01202–0.02404 (scale 4). Frequency bands were calculated following the formulas for the lower limit $(1/(2^{[n+1]} * TR))$ and higher limit $(1/(2^n * TR))$ of each scale, where UK TR=2 and Shanghai TR=2.6. Wavelet scale 2 and 3 were combined, which represent functionally relevant signals in the frequency range of 0.03125-0.125 for the UK sample and 0.02404-0.09615 for the Shanghai sample. This was done to maximize the overlap in frequency range between datasets and to align with previous reports assessing resting-state functional connectivity in psychosis (Gohel et al., 2018) and large-scale network development (Váša et al., 2020).

5.3.3 Quality control

Visual quality control to confirm alignment and quality was performed by overlaying the surface parcellation atop the volumetric one in Freeview, and overlaying the pre-processed time series, structural MRI, and CSF mask in FSLeyes. Framewise displacement (FD) (sum of absolute derivatives of 6 motion parameters) and mean DVARS (frame-to-frame root mean square variance in percent signal change across all brain voxels) were computed to quantify motion for each subject. Data driven thresholds (75th percentile + 1.5 times the Inter Quartile Range) for mean FD and mean DVARS were used to exclude participants with high motion. Within each dataset, there were no significant group differences in FD (UK baseline: $F(1,144)=1.42$, $p=0.235$, UK follow-up: $F(1,62)=2.415$, $p=0.125$, Shanghai: $F(2,119)=0.842$, $p=0.433$) or DVARS (UK baseline: $F(1,144)=0.05$, $p=0.824$, UK follow-up: $F(1,62)=0.128$, $p=0.642$; Shanghai: $F(2,119)=0.156$, $p=0.856$), indicating that head motion did not unequally affect a particular group.

5.3.4 Construction of seed-based maps and functional networks

Area 32 prime (a32pr) from the HCPMMP1.0 parcellation (i.e., the 360-region 'Glasser parcellation') (Glasser et al., 2016) is the anterior subdivision of area 32' originally described by Vogt (1995), located on the middle third of the cingulate cortex. a32pr is involved in cognitive control, attentional processing, detecting errors to influence internal models, and is associated with fear activation (van Heukelum et al., 2020; Vogt, 2009; Hoffstaedter et al., 2014). Left hemisphere a32pr (La32pr, Figure 5.1) was selected as the region of interest (ROI) or seed, based on the results in Chapter 3 illustrating that this was the location of a shift in paracingulate sulcus morphology between schizophrenia patients with and without hallucinations. First, pre-processed data was transformed from subject to MNI space through three steps using AFNI tools: (1) a linear transformation from pre-processed rsfMRI to structural MRI (native) space; (2) a non-linear transformation from structural MRI to MNI152; (3) applying this transform to the native space rsfMRI data, producing data in standard (MNI152) space. For each subject, the Pearson correlation was computed between

the mean time series of La32pr and all other voxels, which were then transformed into Fisher's Z-score for group analyses. Functional network connectivity was estimated by computing the Pearson correlation between time-series of each possible pair of regions, resulting in a frequency-specific 356 x 356 undirected connectivity graph based on a total of 126736 correlation coefficients. The resulting correlation coefficients R_{ij} between signal from regions i and j form the weight of the edges connecting (i, j). Negative correlations were excluded from the following analyses by setting them to zero, but thresholding was not applied, resulting in weighted, undirected connectivity matrices.
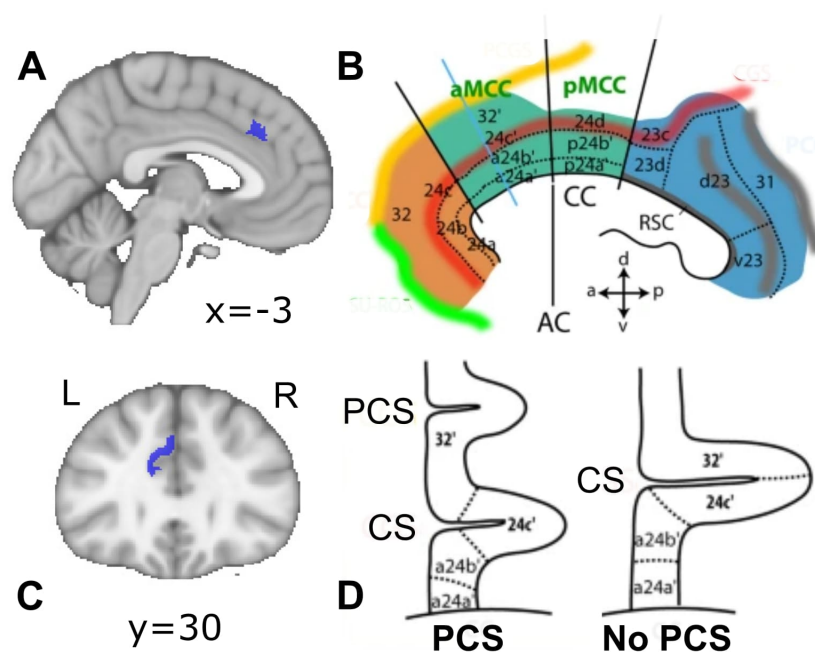
Figure 5.1. Area 32 prime, region of interest for seed-based connectivity. A. Area 32 prime (a32pr) from the 360-region HCPMMP1.0 parcellation by Glasser et al. (2016), left hemisphere sagittal view and coronal view (C). B. Cytoarchitectural parcellation of anterior cingulate cortex. a32pr lies in the anterior midcingulate cortex in region 32'. D. The presence/absence of the PCS influences the location of cytoarchitectonic areas. B and D are adapted from Amiez et al. (2021).

5.3.5 Functional connectivity within and between large-scale networks

To evaluate mean resting-state functional connectivity within and between large-scale networks, connectivity matrices were re-organized by the regional belonging of HCPMMP1.0 areas to one of 9 large-scale networks: visual, somatosensory, default mode, salience, dorsal

attention, limbic, auditory, frontoparietal, subcortical. The correspondences between HCPMMP1.0 region and network are given in Chapter 4, section 4.3.2.2, with an additional subcortical network composed of bilateral: Thalamus-Proper, caudate, putamen, pallidum, hippocampus, amygdala, accumbens-area, ventralDC. The results in Chapter 4 demonstrated increased gyrification covariance within and between salience and auditory networks, and work by others have implicated salience and auditory structural and functional networks in the occurrence of hallucinations (Mallikarjun, et al., 2018; Palaniyappan et al., 2011; Okuneye et al., 2020). I therefore calculated the mean resting-state functional connectivity (rsFC) within and between auditory and salience networks. Given the laterality of the findings in Chapter 3–4, I additionally calculated mean rsFC within left and right salience and auditory networks, and between left-left salience-auditory, left-right salience-auditory, right-right salience-auditory and right-left salience-auditory networks.

5.3.6 Graph theory analysis

To investigate the topological properties of brain networks, I calculated graph theory network parameters: path length, clustering coefficient, global efficiency, and local efficiency from the undirected and weighted matrices using the Brain Connectivity Tool Box (BCT) (Version 2019-03-03; https://sites.google.com/site/bctnet/) implemented in Matlab 2020b. These metrics were selected to reproduce prior analysis assessing graph theoretical properties related to hallucinations (Zhu et al., 2016), and since these measures have been commonly investigated in schizophrenia pathology more generally (Lynall et al., 2010). These same 4 parameters were calculated globally (for the whole graph), and within the auditory and salience networks. I additionally evaluated the degree and strength of the PCS and STS nodes since I hypothesized these structural nodes identified in Chapter 3 would have functional implications. Characteristic path length is calculated as the average shortest path length across all nodal connections in the graph. It indexes the efficiency of information transmission. Clustering coefficient is determined by estimating the number of triangles around a node and represents the degree to which a network segregates into distinct clusters. It is often used as a measure of local connectivity, whereas path length is thought to reflect

more global connectivity. Global efficiency measures the ability of parallel information transmission over the network. Local efficiency characterizes the efficiency of information transfer within neighbouring nodes. It is inversely related to shortest path length. Degree is defined as the number of links connected to a given node and reflects the centrality of a node and strength as the sum of the weights of all links between a given node and all other nodes in the graph.

5.3.7 Test-retest reliability of network topology in the UK dataset

While large-scale functional networks have been detected across populations and scanners, the long-term inter-session reliability of topological measures extracted from rsfMRI data remains in question (Braun et al., 2012). Moreover, few, if any, neuroimaging studies have characterized functional patterns related to hallucinations in a longitudinal context. One-year follow-up structural and functional MRI data was available for subjects in the UK dataset since the aim of study (BeneMin; Deakin et al., 2018) was to evaluate the benefit of minocycline on negative symptoms of schizophrenia. Chapters 3 and 4 analysed the baseline scans before randomization to minocycline or placebo to preclude an effect of minocycline and to compare to the Shanghai cross-sectional study. Here, I characterized the functional networks of patients at one-year follow-up to assess the reliability of functional networks characterizing hallucinations.

5.3.8 Statistical analyses

Two-sample t-tests were used to compare patients with (H+) and without (H–) in a group-level analyses of seed-based connectivity maps, including left hemisphere PCS length as a covariate. This analysis tested for a main effect of group (hallucination status), a main effect of PCS length, and a group by PCS interaction. Tests were performed in the UK and Shanghai datasets separately. For the Shanghai sample, t-tests were additionally used to compare healthy controls (HC) vs. schizophrenia patients (H+ and H– combined). Tests were evaluated using FSL randomise nonparametric permutation-testing tool, with 5000 permutations, using threshold-free cluster enhanced (TFCE) and a family-wise error (FWE) corrected cluster significance threshold of $p < 0.05$ to control for multiple (spatial)

comparisons. The location of each cluster was determined by mapping MNI coordinates to the corresponding AAL region using the RStudio package 'label4MRI' (https://github.com/yunshiuan/label4MRI) and to the corresponding HCPMMP1.0 region using the regional centre of gravity coordinates from the Glasser et al., 2016 Supplemental file: "Supplementary Neuroanatomical Results For A Multi-modal Parcellation of Human Cerebral Cortex".

For each functional network connectivity and graph theoretic measure, a linear mixed model was applied to assess group differences (H+ vs. H- for UK; H+ vs. H- vs. HC for Shanghai). These metrics were: mean connectivity within and between salience and auditory networks (bilaterally and for left and right hemisphere separately), mean connectivity between nodes corresponding to the paracingulate and superior temporal sulci, degree and strength of the PCS and STS nodes, and global and local efficiency, clustering coefficient, and path length for the whole-brain graph, as well as for the salience and auditory networks individually. Functional connectivity and graph theory analyses were conducted in RStudio version 4.0.3 and were corrected by FDR (FDR < 0.05). For all analyses, age, sex, and mean framewise displacement were included as covariates. Scanning site was additionally included as a covariate for the UK multi-centre dataset.

5.4   Results

5.4.1 Participants

From baseline to one-year follow-up, 53 patients from the UK study dropped out, 17 converted from hallucinating to no longer experiencing hallucinations, or vice versa, 5 had missing data, and 8 were excluded due to motion, resulting in 61 that remained in their original H+ or H– groups (see Figure 5.2 for illustration of patient flow). There were no differences between H+ and H- in terms of the fraction of participants on minocycline or placebo arms ($\chi^2(1)=0.542$, p=0.461), suggesting no impact on the test-retest reliability analysis. A linear regression model controlling for age, sex, scanning centre, and total

intracranial volume, as in Chapter 3, showed that left hemisphere PCS length was significantly reduced in patients with hallucinations compared to those without (t(147)=2.137, p=0.0343, β=0.169; F(8,147)=3.09, p=0.00299). There were no significant group effects for right hemispheric PCS length (t(146)=-1.060, p=0.291, β=0.081). No data from the participants recruited in Shanghai were excluded. Participant characteristics are summarized in Table 5.2.

Table 5.2. Characteristics of study participants.

	UK				Shanghai		
	Baseline		Follow-up				
	H+	H–	H+	H–	H+	H–	HC
Total N	93	51	30	31	22	37	63
Manchester, n	51	26	18	15			
Cambridge, n	18	5	4	2			
Edinburgh, n	8	4	4	2			
Birmingham, n	6	10	3	7			
UCL, n	10	6	1	5			
Male/Female (% Female)	64/29 (31%)	41/10 (20%)	22/8 (27%)	26/5 (16%)	15/7 (32%)	21/16 (43%)	36/27 (43%)
Mean age (SD)	25.76 (5.04)	26.10 (6.04)	29.23 (4.83)	27.44 (5.83)	21.95 (5.88)	23.89 (5.21)	24.70 (7.35)
Years education (SD)	12.50 (1.90)	12.85 (1.97)	12.57 (1.50)	12.95 (1.88)	11.73 (2.62)	13.16 (2.78)	13.34 (2.49)
IQ (SD)	99.41 (11.55)	100.04 (11.92)	98.62 (13.07)	102.87 (11.87)	93.57 (18.82)	94.84 (18.90)	116.20 (15.02)
PANSS positive (SD)	18.41 (4.54)	13.55 (3.44)	15.45 (4.02)	10.91 (3.37)	19.32 (5.56)	10.68 (3.29)	n/a
PANSS positive minus P3 (SD)	14.34 (4.17)	12.21 (3.44)	11.90 (3.88)	9.91 (3.37)	15.14 (5.01)	9.65 (3.24)	n/a

PANSS negative (SD)	16.31 (5.00)	17.71 (6.67)	15.29 (4.82)	13.03 (5.50)	21.77 (6.14)	15.54 (6.60)	n/a
PANSS P3 Hallucination (SD)	4.05 (1.01)	1.29 (0.57)	3.55 (0.68)	1.00 (0.00)	4.18 (1.01)	1.03 (0.16)	n/a
PANSS P1 Delusion (SD)	3.42 (1.60)	2.37 (1.41)	2.84 (1.46)	1.82 (1.36)	3.18 (1.62)	2.24 (1.48)	n/a
Total intracranial volume, cm^3 (SD)	1437803 (195095)	1467599 (195904)	1405704 (198789)	1483416 (170981)	1548539 (132577)	1555656 (183253)	1544055 (152890)
Olanzapine equivalent dose (SD)	10.46 (5.72)	9.91 (5.44)	12.98 (6.15)	9.27 (5.94)	13.97 (9.04)	10.26 (8.36)	n/a
Minocycline/Placebo (% Placebo)	45/47* (51%)	29/22 (43%)	13/17 (57%)	15/16 (52%)	n/a	n/a	n/a
Left hemisphere PCS length, mm (SE)	41.55 (2.79)	52.28 (3.42)	n/a	n/a	40.48 (4.68)	55.96 (4.43)	57.13 (2.99)
Right hemisphere PCS length, mm (SE)	36.96 (2.78)	36.56 (3.58)	n/a	n/a	36.30 (5.00)	47.51 (4.37)	41.33 (3.45)

*Information on allocation (minocycline/placebo) was not available for N=1 subject (H+).
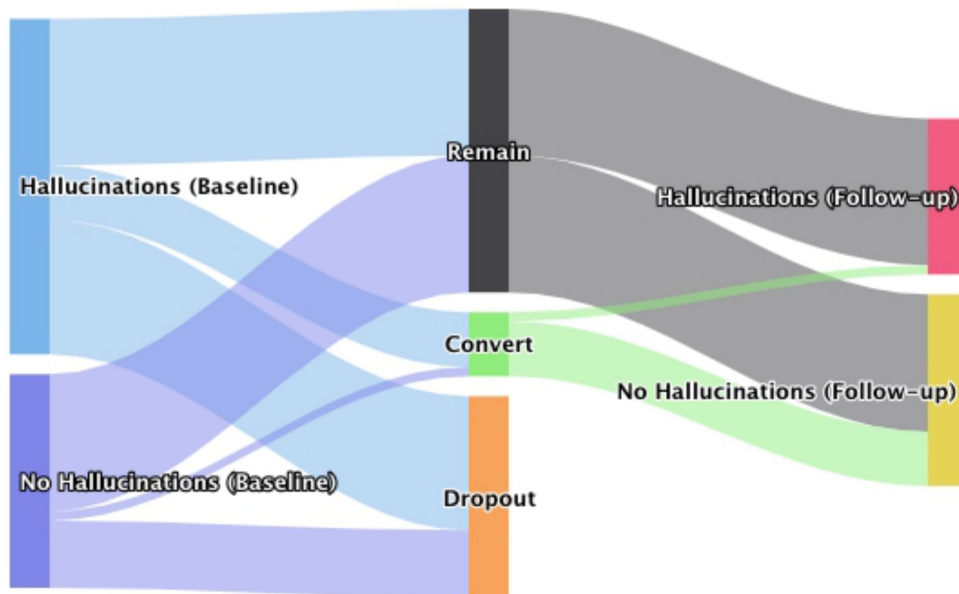
Figure 5.2. Sankey diagram illustrating patient flow between baseline and one-year follow-up for UK study. Width of lines represents number of subjects.

5.4.2 Seed-based connectivity interaction between hallucination status and left hemisphere paracingulate sulcus length

For the UK dataset, there was a significant interaction between hallucination status and left hemisphere paracingulate sulcus length, such that patients with hallucinations (H+) showed a negative correlation between left a32pr seeded connectivity and left PCS length, while patients without hallucinations (H–) demonstrated a positive correlation. For the Shanghai dataset, there was a significant interaction between hallucination status and left hemisphere paracingulate sulcus length in the same cross-over pattern as for the UK dataset, however, it was not significant when controlling for covariates (age, sex, mean framewise displacement, FD) due to a significant effect of mean FD. There was no main effect of group (H+ vs. H–) or PCS length for either dataset. The location of significant clusters for the UK and Shanghai datasets are described in Table 5.3 and visualized in Figure 5.3.
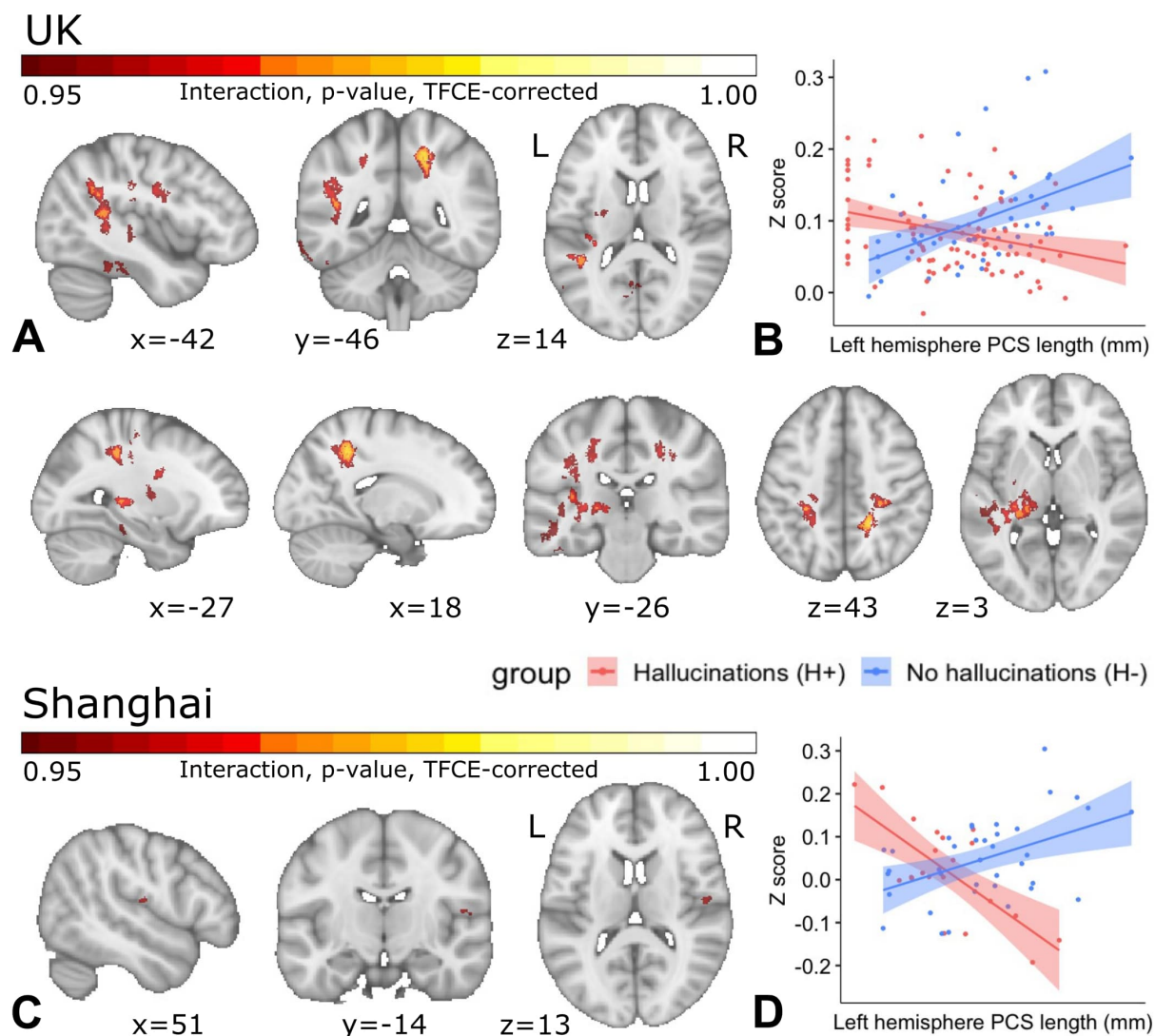
Figure 5.3. Interaction between hallucination status and left paracingulate sulcus length for resting-state connectivity seeded from left hemisphere region a32pr. Clusters showing a significant interaction (p < 0.05 FWE corrected) are overlaid onto the MNI152 standard brain. Images are in neurological orientation (i.e., left hemisphere on left side of image). Scatter plots display Z-values of clusters displaying a significant interaction between hallucination status and PCS length, such that patients with hallucinations show a negative correlation between PCS length and resting-state connectivity, while patients without hallucinations show a positive correlation. Results for the UK dataset are displayed in A–B, and for the Shanghai dataset in C–D. Error bands represents standard error.

Table 5.3. Clusters showing significant interaction between hallucination status and left hemisphere paracingulate sulcus length. UK dataset (top) and Shanghai dataset (bottom).

Dataset	MNI coordinates of peak voxel (x, y, z)	Number of voxels	T-value of peak coordinate	Location of cluster from AAL atlas (HCPMMP 1.0 atlas)
UK	-27, -36, 43	8053	5.25	Left postcentral gyrus (AIP_L)
	-42, -46, 14	6946	4.94	Left middle temporal gyrus (TE2p_L)
	18, -46, 44	3320	5.48	Right precuneus (31pd_R)
	-4, -63, 15	995	4.21	Left superior frontal gyrus, medial (v23ab_L)
	-29, -31, -23	136	4.4	Left fusiform gyrus (PHA3_L)
	-49, -20, 19	133	3.77	Left rolandic operculum (PFcm_L)
	-12, -38, 24	123	3.87	Left posterior cingulate gyrus (31pv_L)
	44, 15, -17	86	5.06	Right Temporal pole: superior temporal gyrus (STGa_R)
	-20, -45, -35	63	3.78	Left Cerebellum Lobule IX
	-23, -31, 23	51	3.58	Left caudate
Shanghai	51, -14, 13	32	5.07	Right rolandic operculum (OP4_R, PBelt_R)

5.4.3 Seed-based connectivity is reduced in schizophrenia patients relative to healthy controls and correlated with paracingulate sulcus length

Schizophrenia patients showed reduced connectivity seeded from left a32pr compared to healthy controls in the Shanghai dataset, primarily in subcortical regions (thalamus and caudate), cerebellum, left posterior cingulate gyrus, anterior cingulate/paracingulate gyri, and right insula and auditory cortex (see Table 5.4 for locations of significant clusters and Figure 5.4 for a visualization). Z-values within this cluster were not significant between patients with and without hallucinations. A post-hoc analysis demonstrated that Z-values were

significantly correlated with left hemisphere paracingulate sulcus length by linear correlation (r=0.29 [0.11–0.45], p=0.0016) and in a model controlling for group (F(3,112) = 21.49, p<0.001, R²=0.37; PCS length (β=0.23, p=0.0036)).
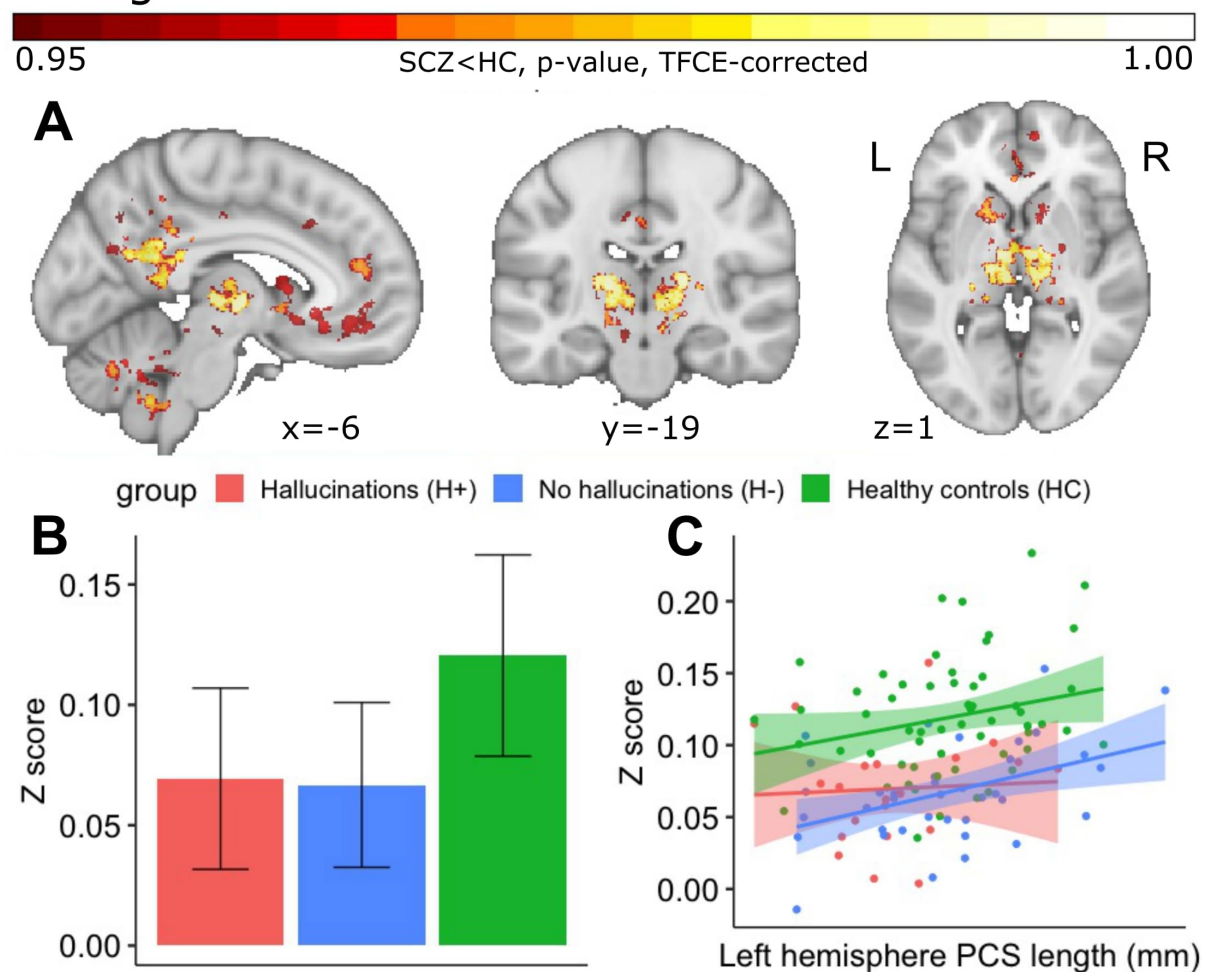
Figure 5.4. Group differences in resting-state functional connectivity seeded from left hemisphere region a32pr. A. Significant decrease of resting-state functional connectivity in schizophrenia patients compared to healthy controls (Shanghai dataset only), p < 0.05 FWE corrected, overlaid onto the MNI152 standard brain. B. Z-values of clusters displaying a significant difference between schizophrenia patients and healthy controls. Error bars represent standard deviation. C. Group-wise correlation between Z-values of significant clusters and left hemisphere paracingulate sulcus length. Error band represents standard error.

Table 5.4. Clusters showing significant reductions in schizophrenia patients compared to healthy controls for the Shanghai dataset.

MNI coordinates of peak voxel (x, y, z)	Number of voxels	T-value of peak coordinate	Location of cluster from AAL atlas (HCP MMP 1.0 atlas)
18, -21, 11	8467	6.29	Right thalamus
19, -50, -39	7825	5.49	Right cerebellum 8
-3, -36, 22	7136	4.91	Left posterior cingulate gyrus (RSC_L)
-16, 15, 7	3428	5	Left caudate
5, 40, 6	3326	4.51	Right Anterior cingulate and paracingulate gyri (a24_R)
11, 11, -2	2181	4.16	Right caudate
40, 3, 13	602	4.27	Right insula (FOP2_R)
6, -43, -23	592	4.59	Vermis Lobule I, II
16, -75, -38	266	4.07	Right cerebellum Crus II
30, -34, 20	230	4.1	Right Heschl gyrus (RI_R)
43, 1, -16	137	4.67	Right Superior temporal gyrus (PI_R)
-25, 50, -28	118	4.11	Left Superior frontal gyrus, orbital part (VVC_L)
-8, 23, 36	117	3.48	Median cingulate and paracingulate gyri (p32pr_L, a24pr_L)
-11, -61, 45	114	3.83	Left precuneus (7m_L)
16, -58, 25	108	4.07	Left cuneus (POS_R)
-3, -23, -12	105	3.45	Left Cerebellum Lobule IV, V

5.4.4 Network connectivity and graph theoretical measures are not related to hallucination status, but are altered in patient groups relative to healthy controls

Within auditory network connectivity, between auditory and salience network connectivity, global efficiency, local efficiency, clustering coefficient, and strength of the superior temporal sulcus node were significantly reduced in schizophrenia patients with (H+) and without (H–) hallucinations relative to healthy controls (HC) in the Shanghai dataset. Path length was significantly increased in both patient groups relative to HC. The connectivity between paracingulate and superior temporal sulci nodes and the degree of the STS was significantly reduced in the H– group relative to HC, but not in the H+ group. There were no significant differences between patients with and without hallucinations within the Shanghai or UK dataset. Auditory network clustering coefficient, global efficiency, and local efficiency were significantly reduced in both patient groups relative to HC, and path length was significantly increased. Between left auditory–right salience and left auditory–left salience mean resting-state connectivity was significantly lower in H+ and H- relative to HC (FDR-corrected $p<0.05$). Results are presented in Figures 5.5–5.6.

5.4.5 No significant differences between baseline and one-year follow-up network topology

There were no significant differences between baseline and one-year follow-up graph theoretical or mean resting-state network measures in H+ or H– for the UK study. Results are shown in Figures 5.5–5.6.
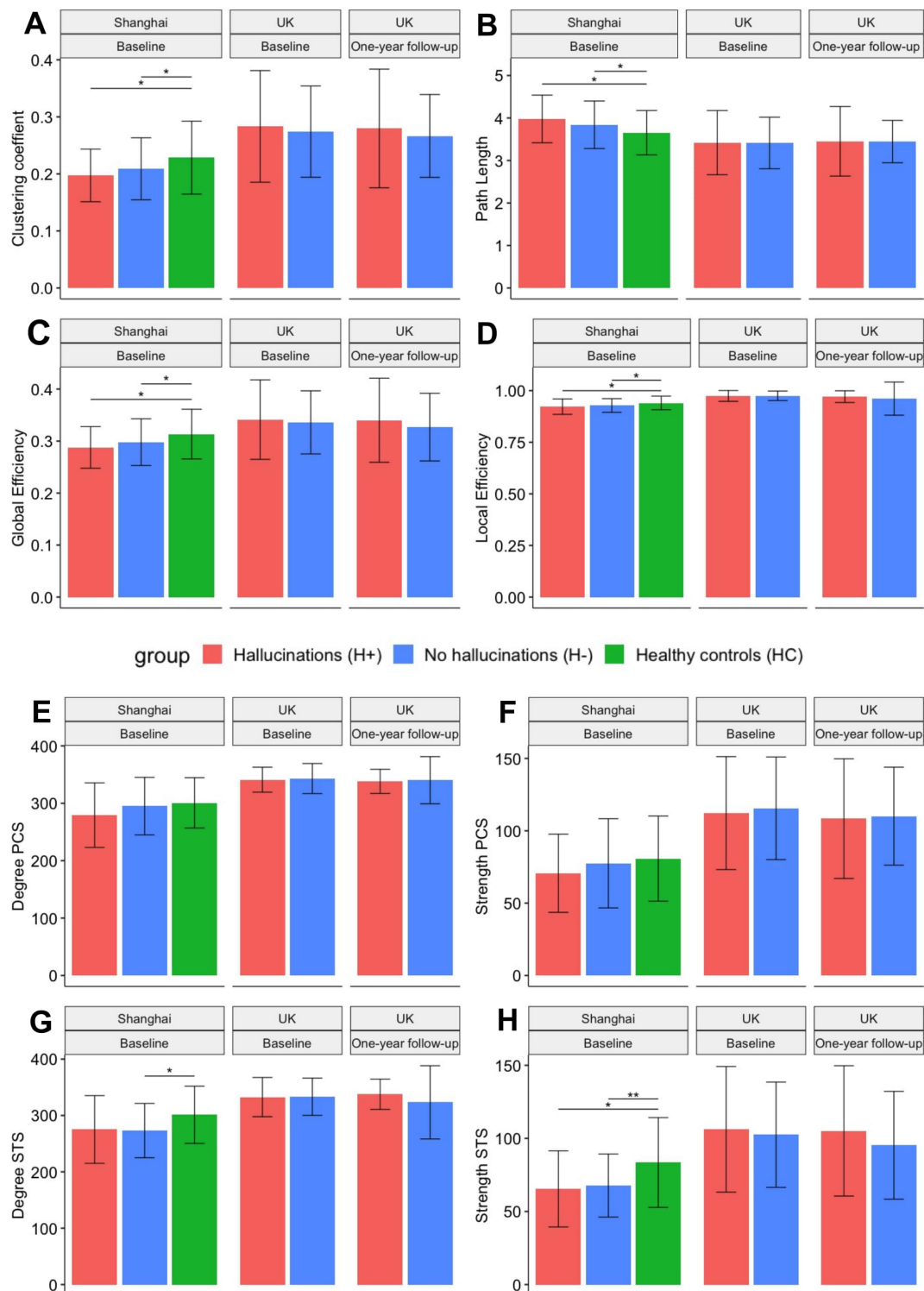
Figure 5.5. Graph theoretical measures of weighted functional network connectivity across groups. Clustering coefficient (A), path length (B), global efficiency (C) and local efficiency (D), degree and strength of the paracingulate sulcus (E, F) and superior temporal sulcus (G, H) nodes are plotted across groups for the Shanghai

and UK datasets at baseline and one-year follow-up (UK dataset only). Error bars represent standard deviation.
*p<0.05, **p<0.01, FDR-corrected.
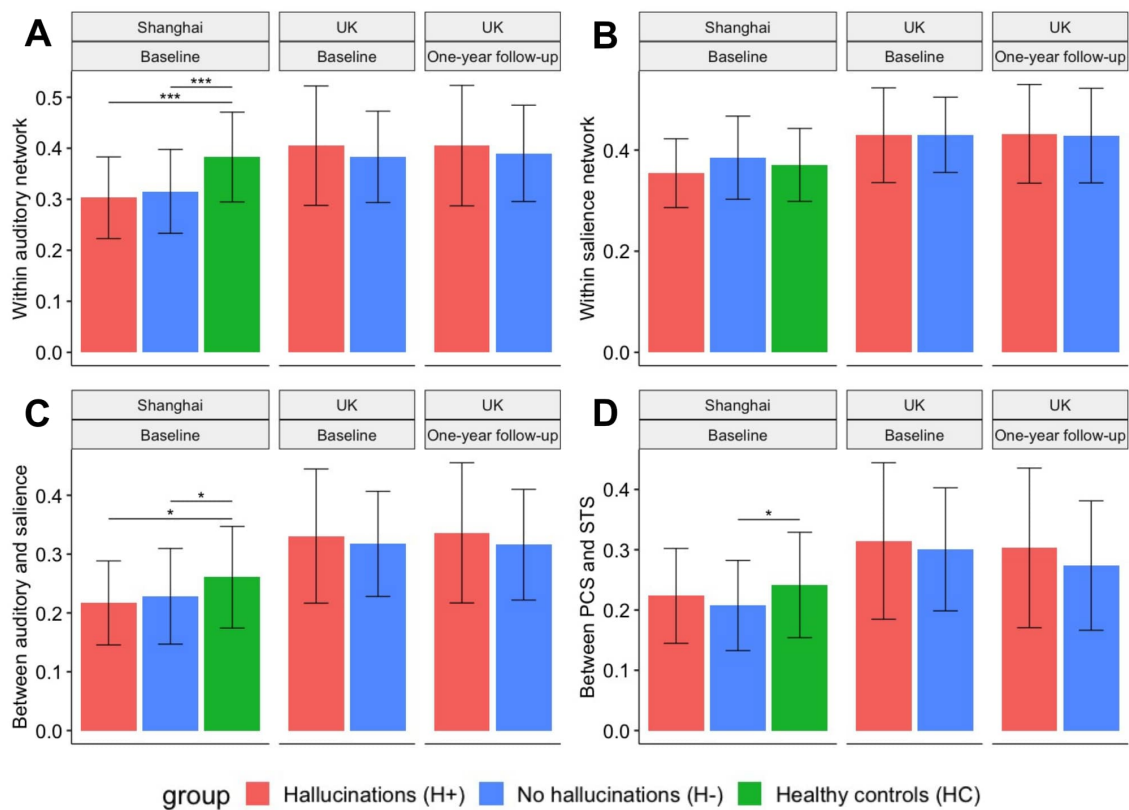
Figure 5.6. Mean resting-state functional connectivity within and between salience and auditory networks and between paracingulate and superior temporal sulcus nodes across groups. Mean connectivity within the auditory network (A), salience network (B), between auditory and salience networks (C), and between paracingulate and superior temporal sulcus nodes (D) are plotted across groups for the Shanghai and UK datasets at baseline and one-year follow-up (UK dataset only). Error bars represent standard deviation. *p<0.05, **p<0.01, FDR-corrected.

5.5 Discussion

The main goals of this chapter were to investigate the functional correlates of variations in paracingulate sulcus morphology, a structural marker of hallucinations in schizophrenia, and to test the hypothesis that resting-state connectivity is a trait marker of hallucinations. These analyses were motivated by the work in Chapters 3–4 demonstrating focal and network-level

alterations in sulcal and gyral architecture related to hallucinations. The results indicate that left hemisphere paracingulate sulcus length interacts with the pattern of resting-state connectivity associated with hallucination presence. Resting-state connectivity alone is not a trait marker of hallucinations, but is a robust marker of schizophrenia, with both patient groups (hallucinations and no hallucinations) exhibiting reduced functional connectivity and network topology compared in healthy controls. These results offer insights into the interaction between schizophrenia pathology, sulcal architecture, and functional connectivity.

5.5.1 Variation in paracingulate sulcus morphology is associated with functional differences related to hallucinations

First, there was a significant interaction between PCS length and hallucination status on connectivity seeded from the area 32 prime in the anterior midcingulate cortex, suggesting that variations in anterior cingulate folding patterns contribute to functional differences between patients with and without hallucinations. This aligns with previous reports that the presence or absence of the PCS influences the location of fMRI activation during cognitive interference tasks in schizophrenia patients. Artiges et al. (2006) showed that activation of the midcingulate anterior cortex was dependent on group (schizophrenia, healthy control) and PCS pattern (present, absent), such that patients without a PCS showed reduced activation, while Heckers et al. (2004) showed that dorsal ACC activation patterns differed according to PCS morphology, but not according to diagnosis. More recent work has shown that the location of midcingulate cortex feedback-related activity in a trial-and-error learning task in humans strongly relates to local sulcal morphology, such that feedback-related activity peaks in the PCS when the PCS is present, but in the cingulate sulcus when the PCS is absent (Amiez et al., 2013). Another study found a direct relationship between the gyrification index in the prefrontal cortex and functional connectivity within subjects at high genetic risk for schizophrenia, showing a positive association between prefrontal gyrification and measures of lateral-medial prefrontal connectivity, but a negative relationship to prefrontal-thalamic connectivity (Dauvermann et al., 2012). Which mechanisms explain why local cortical folding influences functional connectivity? Amiez et al. (2013) suggest that spatial differences in functional activation arise because PCS morphology alters the location of

surrounding cytoarchitectonic areas, and each area has distinct functional properties. For instance, when the PCS is absent, the cingulate sulcus is bounded by area 24c' and area 32', but when the PCS is present, area 24c' lies on both banks of the cingulate sulcus, and area 32' is in the PCS (Figure 5.1). Dauvermann et al. (2012) hypothesize that increased prefrontal gyrification reflects increased short range prefrontal connectivity and reduced long range connectivity. Extending this, Voorhies et al. (2021) propose that deeper tertiary sulci reflect reduced short-range white matter fibers, which in turn, increase the neural signalling efficiency that influences functional connectivity and cognition. The patterns of resting-connectivity associated with the interaction of hallucination status and PCS length differed between the UK and Shanghai datasets, indicating that the relationship between connectivity, sulcal morphology, and hallucinations is not clear-cut. However, the datasets differed in sample size and in proportion of patients with/without hallucinations. The partial replication indicates that sulcal length relates to connectivity and that this structure-function relationship may have a role in the pathophysiology of hallucinations in schizophrenia. A similar relationship has been observed for developmental dyscalculia in Turner's syndrome, wherein the right intraparietal sulcus shows reduced depth and abnormal shape and abnormal functional activation during an fMRI arithmetic task (Molko et al., 2003), suggesting that sulcal-functional relationships are not unique to schizophrenia pathology, but may constitute an axiom of neurodevelopmental disorders or traits.

5.5.2　Schizophrenia is associated with reduced seed-based connectivity and alterations in functional network topology

Second, regardless of hallucination status, schizophrenia patients showed significantly reduced seed-based connectivity compared to healthy controls in: bilateral subcortical regions (thalamus, caudate), bilateral cerebellum, posterior cingulate gyrus, precuneus, bilateral anterior cingulate gyrus (including paracingulate gyrus), right insula and superior temporal regions, and left precuneus, as well as reduced connectivity within the auditory network and between auditory and salience networks. These findings align with recent meta-analyses and high-powered studies comparing resting-state connectivity between schizophrenia patients to

healthy controls, which have demonstrated reduced resting-state connectivity within the medial prefrontal cortex (including anterior cingulate cortex), insula, left precuneus and posterior cingulate gyrus, right cerebellum, right superior temporal gyrus, and subcortical regions (thalamus, putamen, caudate) (Li et al., 2019; Dong et al., 2018; Mwansisya et al., 2017), and decreased functional network connectivity between the salience network (composed of the ACC and insula) and superior temporal gyrus (Hare et al., 2018) and between prefrontal to subcortical networks (Giraldo-Chica and Woodward, 2017). Moreover, both patient groups (H+ and H−) showed increased path length and decreases in global and local efficiency, clustering coefficient, and degree and strength of the superior temporal sulcus node, in comparison to healthy controls. This directly replicates work by Zhu et al. (2016), in which the authors found reduced clustering coefficient, global and local efficiency, and increased path length in schizophrenia patient groups (H+ and H−) relative to healthy controls, but no difference between patient groups (H+ vs. H−). It also supports a meta-analysis of graph theory analyses of rsfMRI studies in patients with schizophrenia, which reported a significant reduction in clustering coefficient and local efficiency for schizophrenia patients in comparison to healthy controls (Kambeitz et al., 2016). That these findings reproduce prior work gives confidence to the methods used and supports proposals that schizophrenia is a disorder of brain network dysconnectivity.

5.5.3 Resting-state connectivity does not differentiate schizophrenia patients with and without hallucinations

Third, there were no significant differences in seed-based connectivity or functional network measures between patients with and without hallucinations, suggesting that resting-state connectivity alone is not a trait marker for hallucinations. This is consistent with previous work finding no significant changes in functional network connectivity between schizophrenia patients with hallucinations to those without (Hare et al., 2018) and reproduces findings from a graph-based analysis showing no differences in global metrics of functional networks between schizophrenia patients with and without AVH (Zhu et al., 2016). Although some studies have found altered resting-state functional connectivity in patients with hallucinations, these were limited to small sample sizes of <=20 per group (Alonso-Solis et

al., 2015; Rolland et al., 2015) or 20–30 per group (Shinn et al., 2013; Huang et al., 2018).
Studies that did not include a non-hallucinating patient control group found alterations in
functional connectivity between patients with H+ compared to HC, particularly within
frontal, fronto-temporal, fronto-insular, limbic, and occipital regions (Sommer et al., 2012a;
Schutte et al., 2021). However, these findings cannot disentangle the effects of schizophrenia
pathology, which is largely considered a disorder of widespread connectivity alterations.
Rather than a marker of susceptibility to hallucinate, rsfMRI may instead directly reflect the
brain activity associated with the hallucinatory experiences; that is, rsfMRI may be a state
marker for hallucinations. This proposal is supported by significant associations between
hallucination severity and functional connectivity and by meta-analyses of state studies of
hallucinations, which compare brain activity while an individual is hallucinating compared to
periods when they are not, using a within-subject design. Such meta-analyses have indicated
consistent activation in the postcentral gyrus, inferior frontal gyrus, insula,
hippocampus/parahippocampal region, superior and middle temporal gyri, subcortical and
cerebellar regions during hallucinations in schizophrenia spectrum disorders (including some
non-clinical studies and some PET studies) (Zmigrod et al., 2016; Jardri et al., 2011; Kompus
et al., 2011).

5.5.4 Trait and state markers of hallucinations

Although the results do not provide support for a resting-state hypothesis of auditory
hallucinations, the resting-state signal may still offer insights into the neural basis of
hallucinations. This study used static functional connectivity (FC), a method that models
brain connectivity as a constant state through the scanning acquisition period and produces a
single average correlation of the mean time-series of brain regions. The spontaneous and
fluctuating nature of hallucinations may be better represented with dynamic FC, a method
that exposes the time-varying connectivity that changes across the duration of the scan.
Recent studies using dynamic functional connective showed that schizophrenia patients with
auditory hallucinations show significantly lower connectivity strength between left
hemisphere speech and auditory areas compared to controls in one of five most common

transient dynamic FC states, but no significant differences between groups in static FC (Zhang et al., 2018). Using dynamic causal modelling of rsfMRI while patients experienced hallucinations, Lefebvre et al. (2016) showed that the salience network controls the interaction between the central executive and default mode networks across all stages of the hallucinatory experience. In addition, disease-related alterations in brain function are sensitive to different frequency bands (Gohel et al., 2018; Lynall et al., 2010). While this chapter used frequency bands of 0.03125-0.125 for the UK sample and 0.02404-0.09615 for the Shanghai dataset, it is possible that connectivity differences related to hallucinations exist in different frequency ranges since differences between psychosis patients and healthy controls in resting-state BOLD signal power is frequency band-dependent (Gohel et al., 2018). Although this chapter used rsfMRI, other measures of brain function may be stronger indicators of trait (risk factor or susceptibility to hallucinations). For instance: functional activity during speech-based or auditory tasks (Kuhn et al., 2012; Kompus et al., 2011; Ford et al., 2009); amplitude reductions in mismatch negativity, an EEG-derived event-related potential elicited by a discriminable change in auditory stimulation (Francis et al., 2020; Fisher et al., 2014); reductions in beta and alpha activity of resting EEG (Arora et al., 2021), decreased anterior cingulate cortex and increased left superior temporal gyrus glutamate+glutamine levels (Hjelmervik et al., 2019); and increased activity in medial prefrontal cortex, as measured by near infrared spectroscopy (Yanagi et al., 2020). Such trait markers may be clinically useful for developing strong *a priori* strategies for fMRI-neurofeedback target localization (Fovet et al., 2016), or predicting vulnerability to psychosis (Wang et al., 2018) or whether individuals with schizophrenia will be difficult to treat (Palaniyappan et al., 2016).

5.5.5 Limitations

Several limitations should be considered in interpreting these findings. First, there are important differences between the UK and Shanghai datasets, namely, the UK dataset lacked a healthy control group and represents a longitudinal, multicentre study, while the Shanghai dataset was cross-sectional and acquired from a single centre. Despite this, both samples were similar in key demographic and clinical characteristics, such as age, sex distribution, and

hallucination PANSS P3 scores. Although larger than many previous neuroimaging studies of hallucinations, the samples were nonetheless modest in size. Identifying trait markers of symptoms likely requires large-scale population studies, on the order of hundreds to thousands of subjects. To focus on the hypotheses extending from Chapter 3, the functional connectivity analysis was seeded from left a32pr. However, future work could investigate the connectivity of multiple seeds along the PCS, since subregions of the cingulate gyrus have differing connectivity patterns in schizophrenia (Wang et al., 2015), or seeded from other structurally relevant regions, such as the superior temporal sulcus, whose variability is implicated in hallucinations. The UK dataset presented here includes patients from two additional scanning sites (Birmingham and UCL) to that described in Chapters 3–4. The reason for this is that poor rsfMRI imaging quality reduced the sample size. In Chapters 3–4, the largest 3 centres of the 6 multi-centre UK study were used to minimize the bias in gender for patients with and without hallucinations. In this Chapter, n = 32 subjects (at baseline) were included from two additional sites, to resolve the trade-off between small sample size and imbalanced covariates. Notably, there were no female patients not experiencing hallucinations from the additional centres. There is an interactive effect of sex and handedness on PCS morphology, but no effect of sex on the leftward lateralization of the PCS (Wei et al., 2017), and sex was not a significant covariate in the linear regression model of PCS length here (t(147)=-0.811, p=0.419, β=0.093). PCS length was not measured for the UK dataset one-year follow-up. Until a fully automated method is developed, this work is time intensive and requires interrater reliability checks with an independent rater, who was not available at the time of this analysis. Although I hypothesize that PCS length will be stable at one-year follow-up, no study has evaluated whether medication or illness chronicity is capable of influencing sulcal properties. This would be interesting to evaluate in future work, for which I offer predictions in Chapter 6 (section 6.3.2). Finally, the seed-based analysis was conducted at a group level, using an averaged image analysis approach. However, neuroimaging practices of smoothing and averaging often obscure subject-level variation in anatomy, especially the organization of secondary or tertiary sulci like the PCS. Since voxel-wise analyses are difficult without averaging, I used an average seed corresponding to the MNI template, but modelled individual variation by including PCS

length. Future investigations and interpretations of structure-functional relationship function in schizophrenia research need to take better account of local variation in sulcal morphology (for an example, see Miller et al., 2021).

5.5.6 Conclusion

In summary, this chapter reports the association of interindividual variation in PCS morphology to a seed-based resting-state functional connectivity group-analysis of hallucination presence/absence in schizophrenia patients, suggesting that local variation in anterior cingulate folding correlates with connectivity seeded from this region at rest and may have a role in the pathophysiology of hallucinations. Seed-based connectivity and functional network topology were not associated with hallucination status, indicating that intrinsic connectivity is not a trait marker for hallucinations, but were robustly associated with a diagnosis of schizophrenia in comparison to healthy controls, supporting theories of schizophrenia as a functional dysconnectivity syndrome. The establishment of clear anatomo-functional links between sulcal pattern variability and functional organization is important to understanding the mechanistic aetiology of neurodevelopmental disorders like schizophrenia.

Chapter 6 General discussion

6.1 Summary

The goal of this thesis has been to advance our understanding of the anatomical and functional correlates of hallucinations, primarily in schizophrenia, following hypotheses of neurodevelopmental origins of hallucinations. I achieved this through first comparing the grey matter organization of hallucinations in neurodegenerative diseases (Parkinson's and Alzheimer's) to neurodevelopmental disorders (schizophrenia spectrum and bipolar disorder), demonstrating distinct neuroanatomical patterns associated with hallucinations. Focusing on the neurodevelopmental pattern, I replicate in two independent MRI datasets of schizophrenia patients and healthy controls that paracingulate sulcus length is reduced in patients with hallucinations, and show PCS asymmetry reductions and superior temporal sulcus depth reductions, embedded in a framework of increased cortical folding synchrony between salience and auditory networks. Resting-state functional connectivity was not directly correlated with hallucinations, but was associated with an interaction between paracingulate sulcus length and hallucination status. Together, these results suggest that hallucinations are in part the reflection of intrauterine neurodevelopmental changes. Defining the perinatal brain changes that are sensitive to subsequent life experiences offers empirical opportunities to test aetiological models of schizophrenia and provides new understanding of the consequences of cortical folding variation for large-scale functional networks.

6.2   Mechanistic insight from neurodevelopmental brain structural risk factors for hallucinations

6.2.1 Local and network level deviations in sulcal and gyral architecture

The most robust anatomical feature related to hallucinations in schizophrenia was reduced left hemisphere paracingulate sulcus length (in comparison to no hallucinations), whose group average maximum sulcal positional difference localized to left area 32 prime (La32pr), and to a lesser extent, reduced right hemisphere superior temporal sulcus depth (in comparison to healthy controls), which localized to its dorsal posterior subdivision (RSTSdp). The specificity of these findings is striking. La32pr and RSTSdp are novel subregions proposed by Glasser et al. (2016), but roughly correspond to the more widely studied area 32', located on the middle third of the cingulate cortex (Vogt et al., 2009), and the right posterior STS (rpSTS), respectively. Area 32' is involved in cognitive control, attentional processing, detecting errors to influence internal models, and is associated with fear activation (van Heukelum et al., 2020; Vogt, 2009; Hoffstaedter et al., 2014), while the rpSTS is involved in language processing, perceiving social interactions, and has been proposed to play a special role in detecting whether auditory feedback from speech production matches higher level expectations of self-generated speech (i.e., beliefs about what your speech should sound like) (Cheng et al., 2018; Isik et al., 2017; Yamamoto et al., 2019). Anterograde and retrograde tracing techniques have shown that medial prefrontal and temporal auditory association areas are anatomically connected in primates (Barbas et al., 1999) and more recent work using *in vivo* probabilistic fiber tractography with diffusion tensor imaging in humans has shown that the rpSTS is anatomically connected to the median cingulate and paracingulate gyri (Cheng et al., 2018). Moreover, area 32' and rpSTS are functionally connected in humans. In a study that mapped the resting-state functional connectivity of 16 seeds along the anterior cingulate, the authors found that the seed most closely located to left a32pr (identified in their paper as left superior seed 4, MNI coordinates $x = -5$, $y = 25$, $z = 36$) was positively correlated with dorsolateral prefrontal cortices, the

inferior parietal lobule, including Wernicke's area, and portions of the inferior temporal and medial temporal lobes (hippocampus and amygdala), and negatively predicted activity within the superior temporal gyrus and auditory cortex (Margulies et al., 2007). These studies indicate that the focal sulcal alterations observed, which form *in utero*, may be capable of influencing the development of structural and functional connections.

While I found specific structural differences, I also observed more widespread changes: increased gyrification covariance in regions corresponding to auditory and salience (structural) networks, and local changes in other structural metrics: increased cortical thickness in patients with hallucinations (H+) for the left lingual gyrus (for both datasets), increased thickness in H+ for left inferior parietal and bilateral precuneus, reduced gyrification in H+ in the rostral middle frontal cortex, and increased grey matter in H+ in the medial prefrontal cortex for the UK dataset. Because the UK dataset was larger than the Shanghai dataset, it is difficult to discern whether the greater number of significantly altered regions in the UK dataset was due to sample size differences or other features. Replication in larger samples is needed for confirmation. Specific alterations in sulcal patterns are likely not unique to hallucinations in schizophrenia, but linked to other neurodevelopmental disorders too. For instance, the caudal branches of the posterior STS are longer in individuals with autism compared to controls and their length correlates with performance on social cognition tasks (Hotier et al., 2017). The orbitofrontal sulcogyral pattern is altered in schizophrenia spectrum disorders, bipolar disorder, autism, and attention-deficit/hyperactivity disorder, suggesting it may be a transdiagnostic marker of socially impairing neurodevelopmental conditions (Nakamura et al., 2020).

6.2.2 The formation and function of sulcal patterns

A key insight of this thesis is that sulcal morphology and gyrification covariance are associated with hallucinations in adulthood (from Chapters 3 and 4). That sulcal and gyral architecture are products of brain development in the second to third trimesters of gestation raises a number of questions: (1) How do sulci develop? (2) What is their function in mediating brain structural and functional organization? (3) What factors can alter the cortical

folding process? I discuss these questions to explore possible mechanisms underlying the findings in this thesis.

(1) How do sulci develop? The complex geometry of the brain's prenatally determined convolutions is indispensable for higher cognitions and postnatal outcomes, but the mechanisms underlying cortical folding remain poorly understood. Theories describing cortical folding have proposed the driving force of gyrification to be axonal tension, radial intercalation of neurons into different cortical layers, and tangential expansion of the cortex due to local variations in cytoarchitecture (Ronan and Fletcher, 2016; Borell, 2018). One hypothesis is that a local abundance of basal radial glia cells in the outer subventricular zone leads to a fanning out of fibers and neurons, producing a gyrus-like structure (Jiang et al., 2021). These developmental processes may be initiated by gradients in gene expression that exist in different cortical layers (Miller et al., 2014). This genetic protomap is also hypothesized to support the spatial and temporal invariance of sulcal pits, the deepest points in primary sulci that are the first to appear in brain development. Recent work demonstrates there is a specific period of pit emergence for different cortical regions (Yun et al., 2020). The time-locked regional development of cortical sulci can give clues to which developmental processes may be affected (i.e., gliogenesis, axonogenesis, and myelinogenesis, which are correlated with cortical folding development). For instance, neurite orientation dispersion increases until 38 weeks and correlates with cortical curvature (Batalle et al., 2017). Resting-state modularity, local efficiency, normalized clustering coefficient, and the small world index decrease with increasing gestational age across sulcal development (19–40 weeks) (De Asis-Cruz et al., 2021). Asymmetrical growth in sulci is detected from 20–23 weeks gestation and is thought to be determined by asymmetries in the expression of genes such as LIM-domain-only 4 (LMO4) (Sun and Hevner, 2014). Mapping spatial and temporal brain developmental processes will offer insight into normal and abnormal cortical maturation.

(2) What is their function in mediating brain structural and functional organization? It is not yet understood how large-scale networks emerge, but foetal resting-state networks show efficient and economic small-world topology and modular organization by second

trimester, and overlap with adult brain networks, indicating that key properties of functional architecture are present before birth (Turk et al., 2019). Gyri and sulci have different properties in microstructure and connectivity that may contribute to developing axonal wiring and functional patterns. Somata and arbors of pyramidal neurons are stretched in gyri, but compressed in sulci, producing different lengths of apical segments with different types of action potentials. Compared to sulci, gyri have higher cortical thickness and neuron number in the deep lamina, less diverse temporal patterns, lower frequency fMRI signals, higher clustering coefficient and global efficiency, and stronger small-worldness (Jiang et al., 2021). Mathematical neural network models of information transmission in the brain support a hypothesis that sulci (modelled as cuts on an otherwise smooth surface) increase the efficiency of information transmission between two points on the surface (Heyden and Ortiz, 2019). Empirical studies show that long-range white matter connections between distant gyro-gyral regions is stronger than gyro-sulcal or sulco-sulcal connections. Information is exchanged between neighbouring gyri and gyri-sulci through short-range white matter fibers, called U-shaped fibers, which course along sulci (Jiang et al., 2021). The spatial organization of white matter tracts are important during brain maturation (Batalle et al., 2017) and the white matter structure of the arcuate fasciculus (connecting the inferior frontal gyrus to temporal lobe) has been implicated in hallucinations (Psomiades et al., 2016).

My inspection of average sulcal maps in Chapter 3 illustrated that not only are straightforward metrics like length and depth of a sulcus functionally significant, but sulcal shape is too, with the PCS more broken, and the STS less kinked, in patients with hallucinations compared to those without and to healthy controls. I suggest that new measures to quantify sulci, such as branching frequency, curvature, or number of fragments, will be useful in understanding the consequences of cortical folding. In support of this, a novel cortical measure reflecting the local shape within a sulcal or gyral region, including widening or deepening and branching (the shape complexity index, SCI), captures infant brain development from 6 to 24 months, revealing increased SCI with age and sexual dimorphisms in the insula, middle cingulate, parieto-occipital sulcal and Broca's regions (Kim et al., 2016).

(3) What factors can alter the cortical folding process? While primary sulci show high heritability (Pizzagalli et al., 2020), the presence/absence of the PCS is weakly influenced by

genetic factors, but strongly influenced by environmental factors, with 66% of the variance in PCS presence/absence in the left or right hemisphere in monozygotic and dizygotic twin pairs explained by unique environment (Amiez et al., 2018). In a cohort of 119 healthy pregnant women with foetal MRI performed at two time points between 24 and 40 weeks gestation, elevated maternal stress and anxiety were associated with increased local gyrification index in the frontal and temporal lobe, as well as global LGI (Wu et al., 2020). In a similar study of 144 healthy pregnant women, lower maternal socioeconomic status, education and occupation level, were associated with increased LGI in the frontal, temporal, parietal, and occipital lobes, as well as increased sulcal depth, except for the frontal lobe (Lu et al., 2021). These studies demonstrate that modifiable environmental factors outside the womb can influence foetal cortical folding development, and align with prior work showing that maternal daily life stress during pregnancy is associated with increased risk for schizophrenia spectrum disorders in male offspring (Fineberg et al., 2016).

6.2.3 Revisiting the transdiagnostic approach

A key insight from Chapter 2 is that there were distinct grey matter correlates for hallucinations between schizophrenia spectrum vs. Parkinson's. The findings in Chapters 3–4 of a sulcal network associated with hallucinations raises questions concerning their nosology and relevance to other diagnoses. Do paracingulate and superior temporal sulci deviations selectively present in schizophrenia patients who develop hallucinations, or do they confer vulnerability to aberrant perceptions in other disorders, both with strong neurodevelopmental influences (i.e., bipolar disorder) and neurodegenerative causes (i.e., Parkinson's disease)? Early onset and psychotic subtypes of bipolar disorder have been associated with local sulcation in the right prefrontal dorsolateral region and left superior parietal cortex, respectively (Sarrazin et al., 2018). Sulcal architecture is established during foetal life, but its influence on cognition endures from birth into senescence: sulcal widening with age is associated with poorer cognitive performance in the elderly (Liu et al., 2011). Though no study has investigated the relationship between specific sulcal morphology and hallucinations in clinical conditions other than schizophrenia, it is possible that the sulcal risk factor

identified here may apply to hallucinations in other neurodevelopmental or neurodegenerative conditions. What about in the general population? In a sample of 50 individuals who experienced death of a spouse in the past year, 82% experienced bereavement hallucinations (speaking to, hearing, or being touched by the deceased) or illusions (feeling the presence of the deceased) in the month after the loss, and nearly one third continued to experience hallucinations one year later (Grimby et al., 1993). Is there a brain structural pattern that could predispose who will hallucinate following bereavement, or other traumatic events?

Are sulcal anomalies modality-specific or general risk factors for hallucinations (Fernyhough, 2019)? Two studies comparing schizophrenia patients experiencing auditory and visual hallucinations to auditory alone show reduced right hemisphere global sulcation (Cachia et al., 2015) and incomplete hippocampal inversion (Cachia et al., 2020) in those with auditory and visual hallucinations, demonstrating a link between visual hallucinations and neurodevelopmental mechanisms. It would be interesting to assess whether visual hallucinations are associated with increased structural covariance between visual and salience networks.

6.2.4 No support for resting-state activity as a trait marker of hallucinations

A key insight from Chapter 5 was that resting-state connectivity, assessed using seed-based and network-level approaches, was not associated with hallucinations, without considering individual PCS length measurements. In contrast, when PCS length was included, both UK and Shanghai datasets showed a significant cross-over interaction between hallucination status and PCS length on connectivity, though the affected regions did not replicate between datasets. The weak relationship between resting-state functional connectivity (rsFC) and hallucinations contrasts that of sulcal morphology and hallucinations. The longstanding hypothesis that elevated resting activity in the auditory cortex and abnormal interactions between midline anterior cortex structures predispose an individual to experience auditory hallucinations drew initial evidence from early fMRI and electrophysiological studies during hallucinations or auditory tasks. Since this proposal, some studies have shown differences in rsFC between patients with and without hallucinations, though these have had small samples

size (n<20–30 per group) and have used heterogenous methodology, with no direct replications. More recent higher-powered studies (n>200 subjects total) have shown associations between hallucination severity and rsFC, but no significant differences between patients with and without hallucinations. Although rsFC is likely a state marker for hallucinations (Zmigrod et al., 2016), there is little evidence to support that it is a trait marker. In contrast, rsFC appears to be a clear trait marker in distinguishing schizophrenia patients from healthy controls. Although it is challenging to capture hallucinations in the scanner, technological advances in wearable non-invasive imaging devices, like functional near-infrared spectroscopy, may be suitable in capturing spontaneous activity related to hallucinations in larger, real-world samples (Yanagi et al., 2020).

Although I did not observe regional or network resting-state alteration in trait hallucinations, it is possible that differences occur at a finer-grained level. 7 Tesla fMRI allows acquisition of high resolution and high signal-to-noise ratio data to investigate how the fMRI signal varies according to cortical layer, which house different populations of neurons that support different computations. Layer specific projections between medial prefrontal and auditory cortices have been demonstrated in primates, with medial prefrontal cortices sending primarily feedback projections terminating in the upper layers of auditory cortices, which are enriched in GABAergic receptors, and receiving predominantly feedback projections originating from deep layers (5–6) of temporal polar cortices (Barbas et al., 1999). Resting-state functional interactions between medial prefrontal and auditory cortices may occur between layer specific feedforward and feedback projections that cannot be distinguished with the 3 Tesla resolution of data presented here.

6.3   Clinical and theoretical implications

6.3.1 Clinical implications

The robust link between hallucinations and local and network-level sulcal topology raises the question of whether the prenatally formed sulcal pattern offers predictive value for identifying individuals who might develop hallucinations or who will show treatment

resistance. Retrospective analyses of clinical trials highlight the potential of gyrification-based covariance networks in this goal: graph theory-based properties of gyrification covariance networks in first episode psychosis differentiate groups who will and will not respond to treatment over the subsequent 4 years (Ajnakina et al., 2021). Likelihood of remission after 17 months of antipsychotic medication treatment for psychosis is related to alterations in gyrification-based covariance networks, particularly at the edges between the left lingual and medial orbitofrontal cortex and left pars orbitalis to left rostral anterior cingulate cortex (Dazzan et al., 2021). Finally, connectome properties of gyrification-based covariance networks are associated with transition to psychosis in individuals at high clinical risk (Das et al., 2018). These studies suggest that global alterations in gyrification covariance are related to treatment outcome, but local measures may also play a role (Sampedro et al., 2021). Although PCS length alone should not at this stage be considered a biomarker for hallucinations or their treatment, the integration of sulcal or local gyrification MRI measurers with other clinical, demographic, genetic, or peripheral blood measures may be useful in deep learning algorithms aimed to develop clinical decision aid tools.

Localizing the macrostructural and functional properties related to hallucination presence/absence has important consequences for treatment options. A specific example is repetitive transcranial magnetic stimulation (rTMS), a procedure used to reduce auditory hallucination frequency and severity in schizophrenia, which involves pulsing brief repetitive pulses of electrical current through an electromagnetic coil place against the scalp to stimulate a specific brain region. This treatment shows moderate efficacy and no major safety concerns, though it is recommended by NICE guidelines to only be used in a research context until the quantity and quality of research for this treatment improves (Li et al., 2020; NICE, 2020). A number of parameters including frequency of stimulation and anatomical site contribute to the outcome of rTMS, and so anatomical heterogeneity is a possible source for the ambiguity of efficacy in therapeutic trials. Individuals with cortical folding deviations may reflect a subgroup of patients that is more resistant or responsive to treatment. Understanding the neurobiology of hallucinations may help guide the choice of which treatment will be tolerable and effective for a given individual.

The sulcal morphology findings are clinically important beyond hallucinations in schizophrenia. Individuals born very preterm show widespread deviations in gyrification that contribute to neurodevelopmental psychopathology and reduced adult IQ (Hedderich et al., 2019; Papini et al., 2020). Psychiatric conditions with neurodevelopmental origins, such as schizophrenia and autism spectrum disorders, are associated with atypical sulcal patterns (Nakamura et al., 2020). Although the mosaic of sulcal features of the brain are determined early in life and are not modifiable targets for therapy, understanding how sulcation influences connectivity and cognition to alter risk for psychopathology is potentially modifiable; for instance, the development of stress reduction interventions in at-risk pregnant women during the second to third trimester.

6.3.2 Theoretical implications

The findings in this thesis support a neurodevelopmental theory of schizophrenia, more recently extended to hallucinations, describing deviations in intrauterine brain development, reflected in gyrification and sulcation in the adult brain, as contributors to the pathophysiology of hallucinations in schizophrenia (Cachia et al., 2015; 2020). They equally support the involvement of the salience and auditory networks, consistent with theories of salience network dysconnectivity in schizophrenia and psychotic experiences (Palaniyappan and Liddle, 2012), and with models including the role of language circuits and inner speech (Ćurčić-Blake et al., 2017). Resting-state connectivity was not associated with hallucination presence/absence, but it is possible that fronto-temporal structural connectivity modulates the neural activity that is shown to be altered during hallucinations.

Current theories of hallucinations in psychosis include those that propose perception is instantiated in a cortical hierarchy, mediated by feedforward and feedback processes that have layer-specific targets (Corlett et al., 2019). Recently, layer-specific dynamics of neuronal activity by optogenetic stimulation have been shown to induce visual hallucinations in mice (Marshel et al., 2019). That sulcal organization influences laminar gradations (Wagstyl et al., 2018) links the findings in this thesis to predictive processing accounts of perception and hallucinations. I speculate that the increased cortical folding covariance between and within salience and auditory networks reported here could be a source, for

instance, of the development of prior expectations with overly strong influence on perceptual inferences, or shifts in the weighting of external and internal information, such as inner speech. Another mechanistic avenue relates these results to neurochemical mechanisms of hallucinations. Cortical folding contributes to the specification of the cytoarchitecture of different cortical regions (Wagstyl et al., 2018), and cytoarchitecture relates to the distribution of neurotransmitter receptor binding sites and local concentrations of neurotransmitters and modulators. Indeed, subdivisions of the cingulate cortex (anterior cingulate, midcingulate, posterior cingulate, and retrosplenial cortices) have different neurotransmitter receptor organizations, for instance the anterior cingulate has highest AMPA, kainate, α2, 5-HT1A, and D1, but lowest GABA-A densities, while the midcingulate cortex has lowest AMPA, kainate, α2, and D1 densities (Palomero-Gallagher et al., 2008). As discussed earlier, variations in paracingulate sulcus pattern influence the location of these subdivisions. These observations are relevant considering recent research linking dopamine release capacity and D2 receptor density to the severity of hallucinations in schizophrenia (Cassidy et al., 2018) and theories on the role of excitatory and inhibitory neurotransmitters in hallucinations (Jardri et al., 2016). This thesis does not provide direct support for these theories, but observes possible mechanistic links.

As described in Chapters 1–2, the theoretical landscape of hallucinations lacks reconciliation (Curcic-Blake et al., 2017). Future work should integrate different levels of explanation and attempt to address the sensory plurality of hallucinations and the different distributions of modalities between disorders (i.e., why auditory hallucinations are more prevalent in schizophrenia, but visual hallucinations predominate in Parkinson's).

6.4   Strengths and limitations

A strength of this thesis is that it has been hypothesis driven and motivated by relevant literature. I began with an intriguing link between hallucinations and brain structure (paracingulate sulcus length). Situating this finding within the literature, I hypothesized that there might be common structural correlates of hallucinations across disorders, but find distinct grey matter organizations in psychiatric versus neurodegenerative conditions. I

hypothesized that the association between PCS length and hallucination status would replicate, and that a similar relationship would exist for the STS. Considering the involvement of salience and auditory networks, and the sensitivity of gyrification-based covariance networks to schizophrenia and psychosis, I hypothesized alterations associated with hallucinations. Hypothesizing a link between structure and function, I investigate the resting-state functional correlates of local sulcal morphology and hallucination status, but find a weak link (partial replication of an interaction effect, but no main effects). I conduct identical image processing and statistical analyses in two independent samples to assess the replicability of these findings. I extend these replications in novel ways.

Although the sample size was larger than or similar to previous studies in neuroimaging hallucination research, it is still modest in comparison to the magnitude of MR data in current multi-site cohort studies (>1000 per group) that are becoming more widely available. Neither study (UK; Deakin et al., 2018; Shanghai; Li et al., 2018) was designed to assess the neurobiological basis of hallucinations, therefore there was not detailed information about the hallucinatory experiences (i.e., modality, lifetime history, frequency). Grouping patients based on lifetime history of hallucinations would have been preferable to current hallucinations, assessed by the PANSS; however, since patients were in early stages of illness, it is possible that current and lifetime history correlate more strongly than in chronic illness, when hallucinations may have remitted for some individuals. Finally, my interpretations that the sulcal deviations associated with hallucinations represent alterations in neurodevelopment rests on the assumption that sulcal patterns measured from MR images in adulthood are accurate indices of perinatal brain development. There is evidence that the position and spatial variance of sulcal pits are similar between those in foetal and adult brains (Yun et al., 2020), and that sulcal patterns in the anterior cingulate cortex are stable from childhood to adulthood (Cachia et al., 2016), indicating that sulcal morphology from adult MRI reflects *in utero* cortical folding. However, sulci can widen with age in regionally specific relationships (Jin et al., 2018), and plastic changes to surrounding grey matter and cortical thickness may have subtle influences on sulcal parameters. Future work should characterize whether other lifestyle factors, like medication or illness chronicity, impact cortical sulci.

6.5   Ongoing projects, predictions, and recommendations for future research

6.5.1 Ongoing projects

1. **Sound and Vision: A collaboration between service-users, artists, and the public to explore the lived experience of hallucinations**

As discussed in Chapter 2 (section 2.5.6), I have developed a public engagement project using collaborative arts-based methods to explore the lived experience of hallucinations in schizophrenia spectrum and Parkinson's disease. To date, 7 participants (4 with a diagnosis of Parkinson's and 3 with a diagnosis of schizophrenia) have participated in both interviews with an artist. Preliminary sketches by one artist resulting from collaborative discussions with service-users with lived experience of hallucinations are illustrated in Figure 6.1. A central component of this study is that artworks will be displayed on a publicly available website that will encourage viewers to complete on-line surveys collecting structured information on their perceptual and hallucination-like experiences and life history, amassing a unique dataset that will be the origin for exploration of the content of hallucinations. Following the hypothesis from Chapter 2 that there are at least two, and likely many more, mechanisms involved in the experience of hallucinations, an artistic account of the content of hallucinations will allow one to ask whether content can discriminate the underlying mechanisms, and whether hallucinations experienced in non-clinical populations are similar or different from those of patients with psychiatric or neurological diseases. Moreover, integrating participatory methods like arts-based research into hallucination research can enhance dialogue between participants and researchers and provide an enduring resource to catalyse conversations with the public and non-specialist audiences about hallucinations.

Figure 6.1. Artworks illustrating the lived experience of hallucinations. The preliminary artwork on the left represents a lived experience of visual hallucinations and sensed presence in Parkinson's disease. That on the right represents a lived experience of auditory hallucinations in schizophrenia. The artworks were produced by Dr Fiona Blake, whose further artwork can be found at: https://www.fionablake.art/

2. **Developing computational tools for automated labelling of the paracingulate sulcus**

Chapter 3 validated an existing manual method for detecting the PCS and applied it to neuroimaging software to develop a semi-automated method for segmenting the PCS. Despite this advancement in leading to more objective classifications of the PCS, the requirement of user-input still remains a barrier in characterising the PCS in large datasets. Using the semi-automated PCS tracings produced from the UK and Shanghai datasets, I have supplied collaborators in the Computer Science Department with training data for the development of a fully automated deep learning method to characterise the PCS (Yang et al., 2019). A fully automated method for detecting this variable sulcus will enable study of how inter-individual variations in secondary/tertiary sulcal morphology holds meaningful associations with micro and macrostructure, resting-state functional connectivity, and cognitive operations. Future

work by computer scientists is required to develop a more reliable algorithm, and to translate this to a tool that is useable by other researchers without manual intervention.

6.5.2 Predictions

1. **Across the lifespan in healthy individuals, adolescents and young adults who report hallucination experiences will show grey matter patterns associated with hallucinations similar to the psychiatric meta-analysis (Chapter 2), while healthy older adults will show patterns more similar to the neurodegenerative meta-analysis.**

Based on the meta-analyses in Chapter 2, I hypothesize that grey matter organizations associated with hallucination experiences in the healthy population will vary with age. I predict that hallucinatory experiences in adolescence and younger adulthood (<30 years) associated with patterns similar to the frontotemporal structural alterations in psychiatric disorders with neurodevelopmental origins, whilst later onset hallucinations (>50 years) will show a neurodegenerative pattern of grey matter change in the occipital cortex and thalamus.

2. **Hallucinations in psychiatric disorders with neurodevelopmental origins will associate with similar deviations in cortical sulcation to those in schizophrenia.**

Hallucinations are reported by 34% of people with bipolar disorder (Shinn et al., 2012), which is linked to alterations in early brain development, particularly for early-onset and psychotic subtypes (Sarrazin et al., 2018; Kloiber et al., 2020). One study assessing PCS presence/absence in bipolar disorder found that participants with bipolar I disorder (n = 54) were significantly less likely to show a PCS bilaterally compared to healthy controls (n = 116) (Fornito et al., 2007). I predict that PCS length will be reduced in bipolar disorder patients. Other sulci may also be implicated.

3. **Reduced paracingulate sulcus length will be associated with treatment resistant hallucinations.**

Prior work has shown reduced local folding in the bilateral superior temporal sulcus, Broca's region and homologue, and superior frontal cortex, in schizophrenia patients with treatment

resistant auditory hallucinations (Cachia et al., 2008; Kubera et al., 2018). In Chapter 3, olanzapine equivalent doses were not a significant covariate in a linear model of PCS length and hallucination status, but having treatment resistant hallucinations does not entail that an individual will have a higher dosage; indeed, as patients were taking medication and still experiencing hallucinations (assessed by PANSS P3), they may have been treatment resistant. Early identification of treatment resistance would allow for earlier clozapine use, the only evidence-based antipsychotic for treatment resistant schizophrenia (Kane et al., 2019).

4. **Paracingulate sulcus (PCS) length will not correlate with duration of illness or medication dosage, though PCS width will increase with age more progressively than in healthy controls.**

Considering the stability of anterior cingulate cortex sulcal patterns (Cachia et al., 2016), I hypothesize that PCS length will not correlate with duration of illness or medication dosage in schizophrenia. However, sulci widen with age, and I predict based on recent work that PCS width will increase more progressively in schizophrenia patients with hallucinations (Janssen et al., 2021).

5. **Visual hallucinations in schizophrenia will show increased local gyrification covariance within and between the visual and salience networks.**

Chapter 4 demonstrated increased gyrification covariance between regions corresponding to within and between salience and auditory networks. I therefore predict that schizophrenia patients with visual hallucinations or multimodal visual and auditory hallucinations will show increased gyrification covariance within and between salience and visual networks compared to those without hallucinations or to those with unimodal auditory hallucinations.

6. **Hallucinations in schizophrenia will be associated to other markers of early brain development that relate to cortical folding, such as myelin content.**

Variations in local sulcal morphology affect microstructural profiles of myelin content across cortical depth. Two recent studies show that tertiary sulci in the prefrontal cortex have higher myelin content in the deep cortical layers compared to neighbouring gyri (Miller et al., 2021) and first-episode schizophrenia patients show depth- and region-dependent alterations in

myelin (Wei et al., 2020). I hypothesize that the sulcal deviations in Chapter 3 will be associated with microstructural changes in depth-dependent myelin.

7. Paracingulate sulcus length will not be influenced by genetic factors, but will be associated with in-womb environmental factors.

Length is the least heritable sulcal measurement (compared to mean depth, width, and surface area), and PCS presence/absence is weakly influenced by genetic factors, but more strongly influenced by the in-womb environment (Pizzagalli et al., 2020; Amiez et al., 2018). I therefore predict that PCS length will not be correlated with gene expression or polygenic risk scores for schizophrenia, but will be associated with factors such as maternal stress or infection. However, the gyrification covariance within and between the salience and auditory networks may be related to genetic factors considering that patterns of structural similarity in schizophrenia patients spatially overlap with patterns of gene expression (Morgan et al., 2019), and that cortical thickness covariance has a genetic basis (Alexander-Bloch et al., 2020).

6.5.3 Recommendations for future research

1. Development and use of comprehensive assessment tools for hallucinations

Chapter 2 reported a range of questionnaires used to assess hallucination status, which varied in the time frame bounding the hallucination, from within the current week (i.e., PANSS) to lifetime history (i.e., AHRS), and none conducted follow-up assessments for whether patients later developed hallucinations. Critically, few instruments evaluating hallucination presence distinguish between auditory and visual hallucinations or whether hallucinations occur at all in other modalities, such as tactile or olfactory. Even fewer assess specific phenomenological characteristics of hallucinations, which is potentially confounding as experiential differences may map to different neural substrates (Plaze et al., 2011). Understanding the neurobiology supporting the content of hallucinations may help in personalizing treatment strategies; as an example, hallucination content is related to cognitive profile in PD (Ffytche et al., 2017; Naasan et al., 2021). I recommend a more granular evaluation of hallucination modality,

phenomenological properties, and lifetime and current history, including possible remission of hallucinations from antipsychotic medication.

2. Large sample sizes and replication

It is increasingly clear that understanding the links between brain and behaviour in psychiatric illness requires large sample sizes, both because the disorders and symptoms are highly heterogenous, and because the brain and human behaviour are complex systems, comprising multiple levels of spatial and temporal granularity that interact in non-linear feedback loops. Each level, or factor, often only contributes a small effect. This is especially true for genetic variants, and also for case-control neuroanatomical profiles; for instance, the largest regional effect size of cortical thickness and surface area comparing 4474 people with schizophrenia to 5098 healthy controls was Cohen's d=0.284 (0.197–0.37) when controlling for global mean cortical thickness (van Erp et al., 2018). Although large samples are often hindered by limited resources and/or novel techniques/therapies, more direct replication is needed in parallel to deeper characterization of the neurobiology of hallucinations. This recommendation is not unique to hallucination research, but applies to many subfields of Psychiatry, Neuroscience, and related disciplines. Large-scale multi-site collaborations like ENIGMA and UK Biobank pave this route.

3. Longitudinal studies

Hallucinations can be transient symptoms in the short-term, but their longitudinal course is relatively unknown. A study assessing the longitudinal course of hallucinations in psychotic and mood disorders showed that while 80% of schizophrenia patients had hallucinations at their baseline assessment (mean age of 23.1), 40–45% had frequent or persistent hallucinations at a 20-year follow-up (Goghari et al., 2013). In those whose hallucinations cease, is there plastic re-organization of the covariance of salience and auditory networks? Is sulcal morphology indicative of those whose hallucinations will persist in the long term? Longitudinal studies assessing whether local and network-level sulcation are associated with treatment response or resistance will be important to answer these questions.

Moreover, recent advances in foetal brain imaging (Dubois et al., 2021), coupled with cohort studies following from birth to early adulthood, will be fundamental to mapping the developmental trajectory of cortical folds to understand how the emergence of sulci relate to functional connectome development and postnatal cognition and psychopathology. Examples of these initiatives include the Adolescent Brain Cognitive Development (ABCD) study, a multi-site U.S. study following around 11,875 children age 9–10 for the subsequent 10 years, collecting neuroimaging, cognitive, behavioural, environmental and mental health outcomes (Karcher et al., 2020) and the Developing Human Connectome Project (dHCP), a UK based Open Science project collecting functional MRI data from around 337 infants born 37–44.5 weeks postmenstrual age (Eyre et al., 2021). These present exciting opportunities to test hypotheses related to cortical folding, structure-function network maturation, and cognitive and mental health outcomes.

4. Clarity of tertiary sulci developmental timeline, nomenclature, and labelling

Primary sulci have been reasonably well-characterized in their temporal emergence in gestation and can be automatically identified and labelled. However, the more variable tertiary and some secondary sulci are more ambiguous. Some are absent from classical neuroanatomical atlases; the PCS, for instance, is not mentioned in Ono's nomenclature in his atlas of the cerebral sulci (1990). For others, different names have been used for the same structure, or the same name for different structures. One reason for the absence of some tertiary sulci is that classic dissection methods failed to differentiate shallow surface indentations of sulci from those produced by veins and arteries (Miller et al., 2021). Historical ambiguity of their definition has prevented accurate characterization of when these sulci develop. There is need for a standard of reference for the more variable secondary and tertiary sulci to assess normal foetal sulcation and to characterize abnormalities that may predispose to later illness.

6.6   Conclusions

Hallucinations are a transdiagnostic experience, but prevail in schizophrenia. There is longstanding evidence that schizophrenia pathology has roots in neurodevelopmental deviations during *in utero* life, and more recent evidence that this holds for hallucinations in specific. Neuroimaging research has demonstrated structural and functional alterations in the relevant matured neural systems, particularly localized in frontal and temporal lobes for auditory hallucinations in schizophrenia. However, the neurobiological basis for hallucinations, and its link to early brain development, remains unclear. This thesis targets this gap. I investigate how the anatomical and functional organization of the brain supports hallucinations, chiefly in schizophrenia, through a comparative approach to hallucinations in Parkinson's disease, and through analysis of two independent MRI datasets of schizophrenia patients with and without hallucinations to quantify cingulate and temporal lobe sulcal morphology, grey matter, cortical thickness, local gyrification, structural (gyrification) covariance of auditory and salience networks, and resting-state functional MRI connectivity. I find that hallucinations in schizophrenia show a distinct neuroanatomical organization that is characterized by deviations to local sulcal morphology and more widespread relationships between cortical folding in brain regions corresponding to auditory and salience networks, while resting-state is not directly associated with hallucinations. In doing so, this thesis provides evidence that sulcal topology in the adult brain, a product of neurodevelopment, presents a vulnerability to develop hallucinations, thus linking foetal cortical folding to adulthood psychopathology and supporting neurodevelopmental theories and hypotheses for hallucinations in schizophrenia. These observations offer an interesting window to understanding normal perception, the boundaries between self and other, and the processes underlying how we construct our consciously experienced reality.

References

Aboud KS, Huo Y, Kang H, Ealey A, Resnick SM, Landman BA, Cutting LE (2019) Structural covariance across the lifespan: Brain development and aging through the lens of inter-network relationships. Hum Brain Mapp 40:125-136.

Agcaoglu O, Miller R, Damaraju E, Rashid B, Bustillo J, Cetin MS, Van Erp TGM, McEwen S, Preda A, Ford JM, Lim KO, Manoach DS, Mathalon DH, Potkin SG, Calhoun VD (2018) Decreased hemispheric connectivity and decreased intra- and inter-hemisphere asymmetry of resting state functional network connectivity in schizophrenia. Brain Imaging Behav 12:615-630.

Ajnakina O, Das T, Lally J, Di Forti M, Pariante CM, Marques TR, Mondelli V, David AS, Murray RM, Palaniyappan L, Dazzan P (2021) Structural Covariance of Cortical Gyrification at Illness Onset in Treatment Resistance: A Longitudinal Study of First-Episode Psychoses. Schizophr Bull.

Albajes-Eizagirre A, Radua J (2018) What do results from coordinate-based meta-analyses tell us? Neuroimage 176:550-553.

Alderson-Day B, Fernyhough C (2015) Inner Speech: Development, Cognitive Functions, Phenomenology, and Neurobiology. Psychol Bull 141:931-965.

Alderson-Day B, McCarthy-Jones S, Fernyhough C (2015) Hearing voices in the resting brain: A review of intrinsic functional connectivity research on auditory verbal hallucinations. Neurosci Biobehav Rev 55:78-87.

Alderson-Day B, Diederen K, Fernyhough C, Ford JM, Horga G, Margulies DS, McCarthy-Jones S, Northoff G, Shine JM, Turner J, van de Ven V, van Lutterveld R, Waters F, Jardri R (2016) Auditory Hallucinations and the Brain's Resting-State Networks: Findings and Methodological Observations. Schizophr Bull 42:1110-1123.

Aleman-Gomez Y, Janssen J, Schnack H, Balaban E, Pina-Camacho L, Alfaro-Almagro F, Castro-Fornieles J, Otero S, Baeza I, Moreno D, Bargallo N, Parellada M, Arango C,

Desco M (2013) The human cerebral cortex flattens during adolescence. J Neurosci 33:15004-15010.

Alexander-Bloch A, Giedd JN, Bullmore E (2013) Imaging structural co-variance between human brain regions. Nat Rev Neurosci 14:322-336.

Alexander-Bloch AF et al. (2020) Imaging local genetic influences on cortical folding. Proc Natl Acad Sci U S A 117:7430-7436.

Allen P, Laroi F, McGuire PK, Aleman A (2008) The hallucinating brain: a review of structural and functional neuroimaging studies of hallucinations. Neurosci Biobehav Rev 32:175-191.

Allswede DM, Cannon TD (2018) Prenatal inflammation and risk for schizophrenia: A role for immune proteins in neurodevelopment. Dev Psychopathol 30:1157-1178.

Alonso-Solis A, Vives-Gilabert Y, Grasa E, Portella MJ, Rabella M, Sauras RB, Roldan A, Nunez-Marin F, Gomez-Anson B, Perez V, Alvarez E, Corripio I (2015) Resting-state functional connectivity alterations in the default network of schizophrenia patients with persistent auditory verbal hallucinations. Schizophr Res 161:261-268.

Amad A, Cachia A, Gorwood P, Pins D, Delmaire C, Rolland B, Mondino M, Thomas P, Jardri R (2014) The multimodal connectivity of the hippocampal complex in auditory and visual hallucinations. Molecular psychiatry 19:184-191.

American Psychiatric Association., American Psychiatric Association. DSM-5 Task Force. (2013) Diagnostic and statistical manual of mental disorders : DSM-5, 5th Edition. Washington, D.C.: American Psychiatric Association.

Amiez C, Wilson CRE, Procyk E (2018) Variations of cingulate sulcal organization and link with cognitive performance. Sci Rep 8:13988.

Amiez C, Neveu R, Warrot D, Petrides M, Knoblauch K, Procyk E (2013) The location of feedback-related activity in the midcingulate cortex is predicted by local morphology. J Neurosci 33:2217-2228.

Amiez C, Sallet J, Novek J, Hadj-Bouziane F, Giacometti C, Andersson J, Hopkins WD, Petrides M (2021) Chimpanzee histology and functional brain imaging show that the paracingulate sulcus is not human-specific. Commun Biol 4:54.

Aminoff EM, Kveraga K, Bar M (2013) The role of the parahippocampal cortex in cognition. Trends Cogn Sci 17:379-390.

Arora M, Knott VJ, Labelle A, Fisher DJ (2021) Alterations of Resting EEG in Hallucinating and Nonhallucinating Schizophrenia Patients. Clin EEG Neurosci 52:159-167.

Artiges E, Martelli C, Naccache L, Bartres-Faz D, Leprovost JB, Viard A, Paillere-Martinot ML, Dehaene S, Martinot JL (2006) Paracingulate sulcus morphology and fMRI activation detection in schizophrenia patients. Schizophr Res 82:143-151.

Ashburner J, Friston KJ (2000) Voxel-based morphometry--the methods. Neuroimage 11:805-821.

Baker CM, Burks JD, Briggs RG, Milton CK, Conner AK, Glenn CA, Sali G, McCoy TM, Battiste JD, O'Donoghue DL, Sughrue ME (2018) A Connectomic Atlas of the Human Cerebrum-Chapter 6: The Temporal Lobe. Oper Neurosurg (Hagerstown) 15:S245-S294.

Ballard C, Kales HC, Lyketsos C, Aarsland D, Creese B, Mills R, Williams H, Sweet RA (2020) Psychosis in Alzheimer's Disease. Curr Neurol Neurosci Rep 20:57.

Barbas H, Ghashghaei H, Dombrowski SM, Rempel-Clower NL (1999) Medial prefrontal cortices are unified by common connections with superior temporal cortices and distinguished by input from memory-related areas in the rhesus monkey. J Comp Neurol 410:343-367.

Batalle D, Hughes EJ, Zhang H, Tournier JD, Tusor N, Aljabar P, Wali L, Alexander DC, Hajnal JV, Nosarti C, Edwards AD, Counsell SJ (2017) Early development of structural networks and the impact of prematurity on brain connectivity. Neuroimage 149:379-392.

Bauer SM, Schanda H, Karakula H, Olajossy-Hilkesberger L, Rudaleviciene P, Okribelashvili N, Chaudhry HR, Idemudia SE, Gscheider S, Ritter K, Stompe T (2011) Culture and the prevalence of hallucinations in schizophrenia. Compr Psychiatry 52:319-325.

Baumeister D, Sedgwick O, Howes O, Peters E (2017) Auditory verbal hallucinations and continuum models of psychosis: A systematic review of the healthy voice-hearer literature. Clin Psychol Rev 51:125-141.

Bayly PV, Okamoto RJ, Xu G, Shi Y, Taber LA (2013) A cortical folding model incorporating stress-dependent growth explains gyral wavelengths and stress patterns in the developing brain. Phys Biol 10:016005.

Berrios GE (1996) The history of mental symptoms : descriptive psychopathology since the nineteenth century. Cambridge England ; New York, NY, USA: Cambridge University Press.

Blanc F, Noblet V, Philippi N, Cretin B, Foucher J, Armspach JP, Rousseau F, Alzheimer's Disease Neuroimaging I (2014) Right anterior insula: core region of hallucinations in cognitive neurodegenerative diseases. PLoS One 9:e114774.

Blom JD (2010) A dictionary of hallucinations. New York: Springer.

Boes AD, Prasad S, Liu H, Liu Q, Pascual-Leone A, Caviness VS, Jr., Fox MD (2015) Network localization of neurological symptoms from focal brain lesions. Brain 138:3061-3075.

Bolkan SS, Stujenske JM, Parnaudeau S, Spellman TJ, Rauffenbart C, Abbas AI, Harris AZ, Gordon JA, Kellendonk C (2017) Thalamic projections sustain prefrontal activity during working memory maintenance. Nat Neurosci 20:987-996.

Borrell V (2018) How Cells Fold the Cerebral Cortex. J Neurosci 38:776-783.

Braun CM, Dumont M, Duval J, Hamel-Hebert I, Godbout L (2003) Brain modules of hallucination: an analysis of multiple patients with brain lesions. J Psychiatry Neurosci 28:432-449.

Braun U, Plichta MM, Esslinger C, Sauer C, Haddad L, Grimm O, Mier D, Mohnke S, Heinz A, Erk S, Walter H, Seiferth N, Kirsch P, Meyer-Lindenberg A (2012) Test-retest reliability of resting-state connectivity network characteristics using fMRI and graph theoretical measures. Neuroimage 59:1404-1412.

Buda M, Fornito A, Bergstrom ZM, Simons JS (2011) A specific brain structural basis for individual differences in reality monitoring. J Neurosci 31:14308-14313.

Budd S (2017) The Cortical Explorer: A web-based user-interface for exploration of brain data. In. London: Imperial College of Science, Technology and Medicine.

Cachia A, Amad A, Brunelin J, Krebs MO, Plaze M, Thomas P, Jardri R (2015) Deviations in cortex sulcation associated with visual hallucinations in schizophrenia. Molecular psychiatry 20:1101-1107.

Cachia A, Cury C, Brunelin J, Plaze M, Delmaire C, Oppenheim C, Medjkane F, Thomas P, Jardri R (2020) Deviations in early hippocampus development contribute to visual hallucinations in schizophrenia. Transl Psychiatry 10:102.

Cachia A, Borst G, Tissier C, Fisher C, Plaze M, Gay O, Riviere D, Gogtay N, Giedd J, Mangin JF, Houde O, Raznahan A (2016) Longitudinal stability of the folding pattern of the anterior cingulate cortex during development. Dev Cogn Neurosci 19:122-127.

Cachia A, Paillere-Martinot ML, Galinowski A, Januel D, de Beaurepaire R, Bellivier F, Artiges E, Andoh J, Bartres-Faz D, Duchesnay E, Riviere D, Plaze M, Mangin JF, Martinot JL (2008) Cortical folding abnormalities in schizophrenia patients with resistant auditory hallucinations. Neuroimage 39:927-935.

Carmon J, Heege J, Necus JH, Owen TW, Pipa G, Kaiser M, Taylor PN, Wang Y (2020) Reliability and comparability of human brain structural covariance networks. Neuroimage 220:117104.

Carter R, Ffytche DH (2015) On visual hallucinations and cortical networks: a trans-diagnostic review. J Neurol 262:1780-1790.

Cassidy CM, Balsam PD, Weinstein JJ, Rosengard RJ, Slifstein M, Daw ND, Abi-Dargham A, Horga G (2018) A Perceptual Inference Mechanism for Hallucinations Linked to Striatal Dopamine. Curr Biol 28:503-514 e504.

Chen X, Liang S, Pu W, Song Y, Mwansisya TE, Yang Q, Liu H, Liu Z, Shan B, Xue Z (2015) Reduced cortical thickness in right Heschl's gyrus associated with auditory verbal hallucinations severity in first-episode schizophrenia. BMC Psychiatry 15:152.

Chen ZJ, He Y, Rosa-Neto P, Gong G, Evans AC (2011) Age-related alterations in the modular organization of structural cortical network by using cortical thickness from MRI. Neuroimage 56:235-245.

Cheng C, Fan LZ, Xia XL, Eickhoff SB, Li H, Li HF, Chen J, Jiang TZ (2018) Rostro-caudal organization of the human posterior superior temporal sulcus revealed by connectivity profiles. Human Brain Mapping 39:5112-5125.

Chi JG, Dooling EC, Gilles FH (1977) Left-right asymmetries of the temporal speech areas of the human fetus. Arch Neurol 34:346-348.

Cierpka M, Wolf ND, Kubera KM, Schmitgen MM, Vasic N, Frasch K, Wolf RC (2017) Cerebellar Contributions to Persistent Auditory Verbal Hallucinations in Patients with Schizophrenia. Cerebellum 16:964-972.

Clark GM, Mackay CE, Davidson ME, Iversen SD, Collinson SL, James AC, Roberts N, Crow TJ (2010) Paracingulate sulcus asymmetry; sex difference, correlation with

semantic fluency and change over time in adolescent onset psychosis. Psychiatry Res 184:10-15.

Collerton D, Perry E, McKeith I (2005) Why people see things that are not there: a novel Perception and Attention Deficit model for recurrent complex visual hallucinations. Behav Brain Sci 28:737-757; discussion 757-794.

Colloby SJ, Elder GJ, Rabee R, O'Brien JT, Taylor JP (2017) Structural grey matter changes in the substantia innominata in Alzheimer's disease and dementia with Lewy bodies: a DARTEL-VBM study. Int J Geriatr Psychiatry 32:615-623.

Corlett PR, Horga G, Fletcher PC, Alderson-Day B, Schmack K, Powers AR, 3rd (2019) Hallucinations and Strong Priors. Trends Cogn Sci 23:114-127.

Craig TK, Rus-Calafell M, Ward T, Leff JP, Huckvale M, Howarth E, Emsley R, Garety PA (2018) AVATAR therapy for auditory verbal hallucinations in people with psychosis: a single-blind, randomised controlled trial. Lancet Psychiatry 5:31-40.

Cui Y, Liu B, Song M, Lipnicki DM, Li J, Xie S, Chen Y, Li P, Lu L, Lv L, Wang H, Yan H, Yan J, Zhang H, Zhang D, Jiang T (2018) Auditory verbal hallucinations are related to cortical thinning in the left middle temporal gyrus of patients with schizophrenia. Psychol Med 48:115-122.

Curcic-Blake B, Ford JM, Hubl D, Orlov ND, Sommer IE, Waters F, Allen P, Jardri R, Woodruff PW, David O, Mulert C, Woodward TS, Aleman A (2017) Interaction of language, auditory and memory brain networks in auditory verbal hallucinations. Prog Neurobiol 148:1-20.

Das T, Borgwardt S, Hauke DJ, Harrisberger F, Lang UE, Riecher-Rossler A, Palaniyappan L, Schmidt A (2018) Disorganized Gyrification Network Properties During the Transition to Psychosis. JAMA Psychiatry 75:613-622.

Dauvermann MR, Mukherjee P, Moorhead WT, Stanfield AC, Fusar-Poli P, Lawrie SM, Whalley HC (2012) Relationship between gyrification and functional connectivity of the prefrontal cortex in subjects at high genetic risk of schizophrenia. Curr Pharm Des 18:434-442.

Dazzan P et al. (2021) Symptom Remission and Brain Cortical Networks at First Clinical Presentation of Psychosis: The OPTiMiSE Study. Schizophr Bull 47:444-455.

De Asis-Cruz J, Andersen N, Kapse K, Khrisnamurthy D, Quistorff J, Lopez C, Vezina G, Limperopoulos C (2021) Global Network Organization of the Fetal Functional Connectome. Cereb Cortex 31:3034-3046.

Deakin B et al. (2018) The benefit of minocycline on negative symptoms of schizophrenia in patients with recent-onset psychosis (BeneMin): a randomised, double-blind, placebo-controlled trial. Lancet Psychiatry 5:885-894.

Dean K, Murray RM (2005) Environmental risk factors for psychosis. Dialogues Clin Neurosci 7:69-80.

Deen B, Koldewyn K, Kanwisher N, Saxe R (2015) Functional Organization of Social Perception and Cognition in the Superior Temporal Sulcus. Cereb Cortex 25:4596-4609.

Delli Pizzi S, Franciotti R, Bubbico G, Thomas A, Onofrj M, Bonanni L (2016) Atrophy of hippocampal subfields and adjacent extrahippocampal structures in dementia with Lewy bodies and Alzheimer's disease. Neurobiol Aging 40:103-109.

Delli Pizzi S, Franciotti R, Tartaro A, Caulo M, Thomas A, Onofrj M, Bonanni L (2014) Structural alteration of the dorsal visual network in DLB patients with visual hallucinations: a cortical thickness MRI study. PLoS One 9:e86624.

Di Biase MA, Zhang F, Lyall A, Kubicki M, Mandl RCW, Sommer IE, Pasternak O (2020) Neuroimaging auditory verbal hallucinations in schizophrenia patient and healthy populations. Psychol Med 50:403-412.

Diederich NJ, Fenelon G, Stebbins G, Goetz CG (2009) Hallucinations in Parkinson disease. Nat Rev Neurol 5:331-342.

Dietz AG, Goldman SA, Nedergaard M (2020) Glial cells in schizophrenia: a unified hypothesis. Lancet Psychiatry 7:272-281.

Dong D, Wang Y, Chang X, Luo C, Yao D (2018) Dysfunction of Large-Scale Brain Networks in Schizophrenia: A Meta-analysis of Resting-State Functional Connectivity. Schizophr Bull 44:168-181.

Dooley N, O'Hanlon E, Healy C, Adair A, McCandless C, Coppinger D, Kelleher I, Clarke M, Leemans A, Frodl T, Cannon M (2020) Psychotic experiences in childhood are associated with increased structural integrity of the left arcuate fasciculus - A population-based case-control study. Schizophr Res 215:378-384.

Dubois J, Alison M, Counsell SJ, Hertz-Pannier L, Huppi PS, Benders M (2021) MRI of the Neonatal Brain: A Review of Methodological Challenges and Neuroscientific Advances. J Magn Reson Imaging 53:1318-1343.

Dudek A, Krzystanek M, Krysta K, Gorna A (2019) Evolution of Religious Topics in Schizophrenia in 80 Years Period. Psychiatr Danub 31:524-529.

Dudley R, Aynsworth C, Cheetham R, McCarthy-Jones S, Collerton D (2018) Prevalence and characteristics of multi-modal hallucinations in people with psychosis who experience visual hallucinations. Psychiatry Res 269:25-30.

Eickhoff SB, Laird AR, Grefkes C, Wang LE, Zilles K, Fox PT (2009) Coordinate-based activation likelihood estimation meta-analysis of neuroimaging data: a random-effects approach based on empirical estimates of spatial uncertainty. Hum Brain Mapp 30:2907-2926.

Escarti MJ et al. (2019) Auditory hallucinations in first-episode psychosis: A voxel-based morphometry study. Schizophrenia Research 209:148-155.

Esquirol JEtD, Hunt EK (1845) Mental maladies. A treatise on insanity. Philadelphia,: Lea and Blanchard.

Eversfield CL, Orton LD (2019) Auditory and visual hallucination prevalence in Parkinson's disease and dementia with Lewy bodies: a systematic review and meta-analysis. Psychol Med 49:2342-2353.

Eyre M et al. (2021) The Developing Human Connectome Project: typical and disrupted perinatal functional connectivity. Brain.

Fernyhough C (2019) Modality-general and modality-specific processes in hallucinations. Psychol Med:1-7.

Ffytche DH, Creese B, Politis M, Chaudhuri KR, Weintraub D, Ballard C, Aarsland D (2017) The psychosis spectrum in Parkinson disease. Nat Rev Neurol 13:81-95.

Fineberg AM, Ellman LM, Schaefer CA, Maxwell SD, Shen L, Chaudhury NH, Cook AL, Bresnahan MA, Susser ES, Brown AS (2016) Fetal exposure to maternal stress and risk for schizophrenia spectrum disorders among offspring: Differential influences of fetal sex. Psychiatry Res 236:91-97.

Fischl B, Dale AM (2000) Measuring the thickness of the human cerebral cortex from magnetic resonance images. Proc Natl Acad Sci U S A 97:11050-11055.

Fischl B, Liu A, Dale AM (2001) Automated manifold surgery: constructing geometrically accurate and topologically correct models of the human cerebral cortex. IEEE Trans Med Imaging 20:70-80.

Fischl B, Rajendran N, Busa E, Augustinack J, Hinds O, Yeo BT, Mohlberg H, Amunts K, Zilles K (2008) Cortical folding patterns and predicting cytoarchitecture. Cereb Cortex 18:1973-1980.

Fischl B, Salat DH, Busa E, Albert M, Dieterich M, Haselgrove C, van der Kouwe A, Killiany R, Kennedy D, Klaveness S, Montillo A, Makris N, Rosen B, Dale AM (2002) Whole brain segmentation: automated labeling of neuroanatomical structures in the human brain. Neuron 33:341-355.

Fisher DJ, Smith DM, Labelle A, Knott VJ (2014) Attenuation of mismatch negativity (MMN) and novelty P300 in schizophrenia patients with auditory hallucinations experiencing acute exacerbation of illness. Biol Psychol 100:43-49.

Ford JM, Palzes VA, Roach BJ, Potkin SG, van Erp TG, Turner JA, Mueller BA, Calhoun VD, Voyvodic J, Belger A, Bustillo J, Vaidya JG, Preda A, McEwen SC, Functional Imaging Biomedical Informatics Research N, Mathalon DH (2015) Visual hallucinations are associated with hyperconnectivity between the amygdala and visual cortex in people with a diagnosis of schizophrenia. Schizophr Bull 41:223-232.

Ford JM et al. (2009) Tuning in to the voices: a multisite FMRI study of auditory hallucinations. Schizophr Bull 35:58-66.

Fornito A, Yucel M, Wood SJ, Proffitt T, McGorry PD, Velakoulis D, Pantelis C (2006) Morphology of the paracingulate sulcus and executive cognition in schizophrenia. Schizophr Res 88:192-197.

Fornito A, Malhi GS, Lagopoulos J, Ivanovski B, Wood SJ, Velakoulis D, Saling MM, McGorry PD, Pantelis C, Yucel M (2007) In vivo evidence for early neurodevelopmental anomaly of the anterior cingulate cortex in bipolar disorder. Acta Psychiatr Scand 116:467-472.

Fovet T, Orlov N, Dyck M, Allen P, Mathiak K, Jardri R (2016) Translating Neurocognitive Models of Auditory-Verbal Hallucinations into Therapy: Using Real-time fMRI-Neurofeedback to Treat Voices. Front Psychiatry 7:103.

Francis AM, Knott VJ, Labelle A, Fisher DJ (2020) Interaction of Background Noise and
Auditory Hallucinations on Phonemic Mismatch Negativity (MMN) and P3a
Processing in Schizophrenia. Front Psychiatry 11:540738.

Fusar-Poli P (2012) Voxel-wise meta-analysis of fMRI studies in patients at clinical high risk
for psychosis. J Psychiatry Neurosci 37:106-112.

Garrison JR, Fernyhough C, McCarthy-Jones S, Simons JS, Sommer IEC (2018)
Paracingulate Sulcus Morphology and Hallucinations in Clinical and Nonclinical
Groups. Schizophr Bull.

Garrison JR, Fernyhough C, McCarthy-Jones S, Haggard M, Australian Schizophrenia
Research B, Simons JS (2015) Paracingulate sulcus morphology is associated with
hallucinations in the human brain. Nat Commun 6:8956.

Gaser C, Nenadic I, Volz HP, Buchel C, Sauer H (2004) Neuroanatomy of "hearing voices":
a frontotemporal brain structural abnormality associated with auditory hallucinations
in schizophrenia. Cereb Cortex 14:91-96.

Geekie J, Read J (2009) Making sense of madness : contesting the meaning of schizophrenia.
London New York: Routledge.

Geng X, Li G, Lu Z, Gao W, Wang L, Shen D, Zhu H, Gilmore JH (2017) Structural and
Maturational Covariance in Early Childhood Brain Development. Cereb Cortex
27:1795-1807.

Gharehgazlou A, Freitas C, Ameis SH, Taylor MJ, Lerch JP, Radua J, Anagnostou E (2021)
Cortical Gyrification Morphology in Individuals with ASD and ADHD across the
Lifespan: A Systematic Review and Meta-Analysis. Cereb Cortex 31:2653-2669.

Giraldo-Chica M, Woodward ND (2017) Review of thalamocortical resting-state fMRI
studies in schizophrenia. Schizophr Res 180:58-63.

Glahn DC, Laird AR, Ellison-Wright I, Thelen SM, Robinson JL, Lancaster JL, Bullmore E,
Fox PT (2008) Meta-analysis of gray matter anomalies in schizophrenia: application
of anatomic likelihood estimation and network analysis. Biol Psychiatry 64:774-781.

Glasser MF, Coalson TS, Robinson EC, Hacker CD, Harwell J, Yacoub E, Ugurbil K,
Andersson J, Beckmann CF, Jenkinson M, Smith SM, Van Essen DC (2016) A multi-
modal parcellation of human cerebral cortex. Nature 536:171-178.

Goghari VM, Harrow M (2016) Twenty year multi-follow-up of different types of hallucinations in schizophrenia, schizoaffective disorder, bipolar disorder, and depression. Schizophr Res 176:371-377.

Goghari VM, Harrow M, Grossman LS, Rosen C (2013) A 20-year multi-follow-up of hallucinations in schizophrenia, other psychotic, and mood disorders. Psychol Med 43:1151-1160.

Gohel S, Gallego JA, Robinson DG, DeRosse P, Biswal B, Szeszko PR (2018) Frequency specific resting state functional abnormalities in psychosis. Hum Brain Mapp 39:4509-4518.

Goldman JG, Stebbins GT, Dinh V, Bernard B, Merkitch D, deToledo-Morrell L, Goetz CG (2014) Visuoperceptive region atrophy independent of cognitive status in patients with Parkinson's disease with hallucinations. Brain 137:849-859.

Good CD, Johnsrude IS, Ashburner J, Henson RN, Friston KJ, Frackowiak RS (2001) A voxel-based morphometric study of ageing in 465 normal adult human brains. Neuroimage 14:21-36.

Gordon EM, Laumann TO, Adeyemo B, Huckins JF, Kelley WM, Petersen SE (2016) Generation and Evaluation of a Cortical Area Parcellation from Resting-State Correlations. Cereb Cortex 26:288-303.

Grimby A (1993) Bereavement among elderly people: grief reactions, post-bereavement hallucinations and quality of life. Acta Psychiatr Scand 87:72-80.

Han X, Jovicich J, Salat D, van der Kouwe A, Quinn B, Czanner S, Busa E, Pacheco J, Albert M, Killiany R, Maguire P, Rosas D, Makris N, Dale A, Dickerson B, Fischl B (2006) Reliability of MRI-derived measurements of human cerebral cortical thickness: the effects of field strength, scanner upgrade and manufacturer. Neuroimage 32:180-194.

Hare SM, Law AS, Ford JM, Mathalon DH, Ahmadi A, Damaraju E, Bustillo J, Belger A, Lee HJ, Mueller BA, Lim KO, Brown GG, Preda A, van Erp TGM, Potkin SG, Calhoun VD, Turner JA (2018) Disrupted network cross talk, hippocampal dysfunction and hallucinations in schizophrenia. Schizophr Res 199:226-234.

Heckers S, Weiss AP, Deckersbach T, Goff DC, Morecraft RJ, Bush G (2004) Anterior cingulate cortex activation during cognitive interference in schizophrenia. Am J Psychiatry 161:707-715.

Hedderich DM, Bauml JG, Berndt MT, Menegaux A, Scheef L, Daamen M, Zimmer C, Bartmann P, Boecker H, Wolke D, Gaser C, Sorg C (2019) Aberrant gyrification contributes to the link between gestational age and adult IQ after premature birth. Brain 142:1255-1269.

Heyden S, Ortiz M (2019) Functional optimality of the sulcus pattern of the human brain. Math Med Biol 36:207-221.

Hjelmervik H, Craven AR, Sinceviciute I, Johnsen E, Kompus K, Bless JJ, Kroken RA, Loberg EM, Ersland L, Gruner R, Hugdahl K (2019) Intra-Regional Glu-GABA vs Inter-Regional Glu-Glu Imbalance: A 1H-MRS Study of the Neurochemistry of Auditory Verbal Hallucinations in Schizophrenia. Schizophr Bull.

Hoffman RE, Wu K, Pittman B, Cahill JD, Hawkins KA, Fernandez T, Hannestad J (2013) Transcranial magnetic stimulation of Wernicke's and Right homologous sites to curtail "voices": a randomized trial. Biol Psychiatry 73:1008-1014.

Hoffstaedter F, Grefkes C, Caspers S, Roski C, Palomero-Gallagher N, Laird AR, Fox PT, Eickhoff SB (2014) The role of anterior midcingulate cortex in cognitive motor control: evidence from functional connectivity analyses. Hum Brain Mapp 35:2741-2753.

Horga G, Abi-Dargham A (2019) An integrative framework for perceptual disturbances in psychosis. Nat Rev Neurosci 20:763-778.

Hotier S, Leroy F, Boisgontier J, Laidi C, Mangin JF, Delorme R, Bolognani F, Czech C, Bouquet C, Toledano E, Bouvard M, Petit J, Mishchenko M, d'Albis MA, Gras D, Gaman A, Scheid I, Leboyer M, Zalla T, Houenou J (2017) Social cognition in autism is associated with the neurodevelopment of the posterior superior temporal sulcus. Acta Psychiatr Scand 136:517-525.

Huang P, Cui LB, Li X, Lu ZL, Zhu X, Xi Y, Wang H, Li B, Hou F, Miao D, Yin H (2018) Identifying first-episode drug naive patients with schizophrenia with or without auditory verbal hallucinations using whole-brain functional connectivity: A pattern analysis study. Neuroimage Clin 19:351-359.

Huang P, Xi Y, Lu ZL, Chen Y, Li X, Li W, Zhu X, Cui LB, Tan Q, Liu W, Li C, Miao D, Yin H (2015) Decreased bilateral thalamic gray matter volume in first-episode

schizophrenia with prominent hallucinatory symptoms: A volumetric MRI study. Sci Rep 5:14505.

Hubl D, Dougoud-Chauvin V, Zeller M, Federspiel A, Boesch C, Strik W, Dierks T, Koenig T (2010) Structural analysis of Heschl's gyrus in schizophrenia patients with auditory hallucinations. Neuropsychobiology 61:1-9.

Hugdahl K (2009) "Hearing voices": auditory hallucinations as failure of top-down control of bottom-up perceptual processes. Scand J Psychol 50:553-560.

Hunter MD, Eickhoff SB, Miller TW, Farrow TF, Wilkinson ID, Woodruff PW (2006) Neural activity in speech-sensitive auditory cortex during silence. Proc Natl Acad Sci U S A 103:189-194.

Isik L, Koldewyn K, Beeler D, Kanwisher N (2017) Perceiving social interactions in the posterior superior temporal sulcus. P Natl Acad Sci USA 114:E9145-E9152.

Isomura S, Hashimoto R, Nakamura M, Hirano Y, Yamashita F, Jimbo S, Yamamori H, Fujimoto M, Yasuda Y, Mears RP, Onitsuka T (2017) Altered sulcogyral patterns of orbitofrontal cortex in a large cohort of patients with schizophrenia. NPJ Schizophr 3:3.

Janssen J, Diaz-Caneja CM, Alloza C, Schippers A, de Hoyos L, Santonja J, Gordaliza PM, Buimer EEL, van Haren NEM, Cahn W, Arango C, Kahn RS, Hulshoff Pol HE, Schnack HG (2021) Dissimilarity in Sulcal Width Patterns in the Cortex can be Used to Identify Patients With Schizophrenia With Extreme Deficits in Cognitive Performance. Schizophr Bull 47:552-561.

Janzen J, van 't Ent D, Lemstra AW, Berendse HW, Barkhof F, Foncke EM (2012) The pedunculopontine nucleus is related to visual hallucinations in Parkinson's disease: preliminary results of a voxel-based morphometry study. J Neurol 259:147-154.

Jardri R, Pouchet A, Pins D, Thomas P (2011) Cortical activations during auditory verbal hallucinations in schizophrenia: a coordinate-based meta-analysis. Am J Psychiatry 168:73-81.

Jardri R, Hugdahl K, Hughes M, Brunelin J, Waters F, Alderson-Day B, Smailes D, Sterzer P, Corlett PR, Leptourgos P, Debbane M, Cachia A, Deneve S (2016) Are Hallucinations Due to an Imbalance Between Excitatory and Inhibitory Influences on the Brain? Schizophr Bull 42:1124-1134.

Ji JL, Spronk M, Kulkarni K, Repovs G, Anticevic A, Cole MW (2019) Mapping the human brain's cortical-subcortical functional network organization. Neuroimage 185:35-57.

Jiang X, Zhang T, Zhang S, Kendrick KM, Liu T (2021) Fundamental functional differences between gyri and sulci: implications for brain function, cognition, and behavior. Psychoradiology 1:23-41.

Jin K, Zhang T, Shaw M, Sachdev P, Cherbuin N (2018) Relationship Between Sulcal Characteristics and Brain Aging. Front Aging Neurosci 10:339.

Johns LC, Kompus K, Connell M, Humpston C, Lincoln TM, Longden E, Preti A, Alderson-Day B, Badcock JC, Cella M, Fernyhough C, McCarthy-Jones S, Peters E, Raballo A, Scott J, Siddi S, Sommer IE, Laroi F (2014) Auditory verbal hallucinations in persons with and without a need for care. Schizophr Bull 40 Suppl 4:S255-264.

Jones SR (2010) Do we need multiple models of auditory verbal hallucinations? Examining the phenomenological fit of cognitive and neurological models. Schizophr Bull 36:566-575.

Kambeitz J, Kambeitz-Ilankovic L, Cabral C, Dwyer DB, Calhoun VD, van den Heuvel MP, Falkai P, Koutsouleris N, Malchow B (2016) Aberrant Functional Whole-Brain Network Architecture in Patients With Schizophrenia: A Meta-analysis. Schizophr Bull 42 Suppl 1:S13-21.

Kamp KS, Steffen EM, Alderson-Day B, Allen P, Austad A, Hayes J, Laroi F, Ratcliffe M, Sabucedo P (2020) Sensory and Quasi-Sensory Experiences of the Deceased in Bereavement: An Interdisciplinary and Integrative Review. Schizophr Bull 46:1367-1381.

Kane JM, Agid O, Baldwin ML, Howes O, Lindenmayer JP, Marder S, Olfson M, Potkin SG, Correll CU (2019) Clinical Guidance on the Identification and Management of Treatment-Resistant Schizophrenia. J Clin Psychiatry 80.

Karcher NR, Loewy RL, Savill M, Avenevoli S, Huber RS, Simon TJ, Leckliter IN, Sher KJ, Barch DM (2020) Replication of Associations With Psychotic-Like Experiences in Middle Childhood From the Adolescent Brain Cognitive Development (ABCD) Study. Schizophr Bull Open 1:sgaa009.

Karolis VR, Corbetta M, Thiebaut de Schotten M (2019) The architecture of functional lateralisation and its relationship to callosal connectivity in the human brain. Nat Commun 10:1417.

Kim SH, Jung HY, Hwang SS, Chang JS, Kim Y, Ahn YM, Kim YS (2010) The usefulness of a self-report questionnaire measuring auditory verbal hallucinations. Prog Neuropsychopharmacol Biol Psychiatry 34:968-973.

Kim SH, Lyu I, Fonov VS, Vachet C, Hazlett HC, Smith RG, Piven J, Dager SR, McKinstry RC, Pruett JR, Jr., Evans AC, Collins DL, Botteron KN, Schultz RT, Gerig G, Styner MA, Network I (2016) Development of cortical shape in the human brain from 6 to 24months of age via a novel measure of shape complexity. Neuroimage 135:163-176.

Kim SY, Liu M, Hong SJ, Toga AW, Barkovich AJ, Xu D, Kim H (2020) Disruption and Compensation of Sulcation-based Covariance Networks in Neonatal Brain Growth after Perinatal Injury. Cereb Cortex 30:6238-6253.

King DJ, Hodgekins J, Chouinard PA, Chouinard VA, Sperandio I (2017) A review of abnormalities in the perception of visual illusions in schizophrenia. Psychon Bull Rev 24:734-751.

Kjelby E, Sinkeviciute I, Gjestad R, Kroken RA, Loberg EM, Jorgensen HA, Hugdahl K, Johnsen E (2015) Suicidality in schizophrenia spectrum disorders: the relationship to hallucinations and persecutory delusions. Eur Psychiatry 30:830-836.

Kloiber S, Rosenblat JD, Husain MI, Ortiz A, Berk M, Quevedo J, Vieta E, Maes M, Birmaher B, Soares JC, Carvalho AF (2020) Neurodevelopmental pathways in bipolar disorder. Neurosci Biobehav Rev 112:213-226.

Knyazev GG, Merkulova EA, Savostyanov AN, Bocharov AV, Saprigyn AE (2018) Effect of Cultural Priming on Social Behavior and EEG Correlates of Self-Processing. Front Behav Neurosci 12:236.

Kochunov P, Rogers W, Mangin JF, Lancaster J (2012) A library of cortical morphology analysis tools to study development, aging and genetics of cerebral cortex. Neuroinformatics 10:81-96.

Kochunov P, Mangin JF, Coyle T, Lancaster J, Thompson P, Riviere D, Cointepas Y, Regis J, Schlosser A, Royall DR, Zilles K, Mazziotta J, Toga A, Fox PT (2005) Age-related morphology trends of cortical sulci. Hum Brain Mapp 26:210-220.

Kompus K, Westerhausen R, Hugdahl K (2011) The "paradoxical" engagement of the primary auditory cortex in patients with auditory verbal hallucinations: a meta-analysis of functional neuroimaging studies. Neuropsychologia 49:3361-3369.

Kong L, Herold CJ, Zollner F, Salat DH, Lasser MM, Schmid LA, Fellhauer I, Thomann PA, Essig M, Schad LR, Erickson KI, Schroder J (2015) Comparison of grey matter volume and thickness for analysing cortical changes in chronic schizophrenia: a matter of surface area, grey/white matter intensity contrast, and curvature. Psychiatry Res 231:176-183.

Krakvik B, Laroi F, Kalhovde AM, Hugdahl K, Kompus K, Salvesen O, Stiles TC, Vedul-Kjelsas E (2015) Prevalence of auditory verbal hallucinations in a general population: A group comparison study. Scand J Psychol 56:508-515.

Kubera KM, Sambataro F, Vasic N, Wolf ND, Frasch K, Hirjak D, Thomann PA, Wolf RC (2014) Source-based morphometry of gray matter volume in patients with schizophrenia who have persistent auditory verbal hallucinations. Prog Neuropsychopharmacol Biol Psychiatry 50:102-109.

Kubera KM, Thomann PA, Hirjak D, Barth A, Sambataro F, Vasic N, Wolf ND, Frasch K, Wolf RC (2018) Cortical folding abnormalities in patients with schizophrenia who have persistent auditory verbal hallucinations. Eur Neuropsychopharmacol 28:297-306.

Kuhn S, Gallinat J (2012) Quantitative meta-analysis on state and trait aspects of auditory verbal hallucinations in schizophrenia. Schizophr Bull 38:779-786.

Laroi F, Luhrmann TM, Bell V, Christian WA, Jr., Deshpande S, Fernyhough C, Jenkins J, Woods A (2014) Culture and hallucinations: overview and future directions. Schizophr Bull 40 Suppl 4:S213-220.

Le Guen Y, Leroy F, Auzias G, Riviere D, Grigis A, Mangin JF, Coulon O, Dehaene-Lambertz G, Frouin V (2018) The chaotic morphology of the left superior temporal sulcus is genetically constrained. Neuroimage 174:297-307.

Le Provost JB, Bartres-Faz D, Paillere-Martinot ML, Artiges E, Pappata S, Recasens C, Perez-Gomez M, Bernardo M, Baeza I, Bayle F, Martinot JL (2003) Paracingulate sulcus morphology in men with early-onset schizophrenia. Br J Psychiatry 182:228-232.

Lee YM, Chung YI, Park JM, Lee BD, Moon E, Jeong HJ, Kim JH, Kim HJ, Mun CW, Kim TH, Kim YH, Kim EJ (2016) Decreased gray matter volume is associated with the subtypes of psychotic symptoms in patients with antipsychotic-naive mild or moderate Alzheimer's disease: A voxel-based morphometry study. Psychiatry Res Neuroimaging 249:45-51.

Lefebvre S, Demeulemeester M, Leroy A, Delmaire C, Lopes R, Pins D, Thomas P, Jardri R (2016) Network dynamics during the different stages of hallucinations in schizophrenia. Hum Brain Mapp 37:2571-2586.

Lenka A, Jhunjhunwala KR, Saini J, Pal PK (2015) Structural and functional neuroimaging in patients with Parkinson's disease and visual hallucinations: A critical review. Parkinsonism Relat Disord 21:683-691.

Leonard CM, Towler S, Welcome S, Chiarello C (2009) Paracingulate asymmetry in anterior and midcingulate cortex: sex differences and the effect of measurement technique. Brain Struct Funct 213:553-569.

Lerch JP, Worsley K, Shaw WP, Greenstein DK, Lenroot RK, Giedd J, Evans AC (2006) Mapping anatomical correlations across cerebral cortex (MACACC) using cortical thickness from MRI. Neuroimage 31:993-1003.

Lerch JP, van der Kouwe AJ, Raznahan A, Paus T, Johansen-Berg H, Miller KL, Smith SM, Fischl B, Sotiropoulos SN (2017) Studying neuroanatomy using MRI. Nat Neurosci 20:314-326.

Leroux E, Delcroix N, Dollfus S (2017) Abnormalities of language pathways in schizophrenia patients with and without a lifetime history of auditory verbal hallucinations: A DTI-based tractography study. World J Biol Psychiatry 18:528-538.

Leroy F et al. (2015) New human-specific brain landmark: the depth asymmetry of superior temporal sulcus. Proc Natl Acad Sci U S A 112:1208-1213.

Leucht S, Samara M, Heres S, Davis JM (2016) Dose Equivalents for Antipsychotic Drugs: The DDD Method. Schizophr Bull 42 Suppl 1:S90-94.

Li J, Cao X, Liu S, Li X, Xu Y (2020) Efficacy of repetitive transcranial magnetic stimulation on auditory hallucinations in schizophrenia: A meta-analysis. Psychiatry Res 290:113141.

Li S, Hu N, Zhang W, Tao B, Dai J, Gong Y, Tan Y, Cai D, Lui S (2019) Dysconnectivity of Multiple Brain Networks in Schizophrenia: A Meta-Analysis of Resting-State Functional Connectivity. Front Psychiatry 10:482.

Li Z, Yan C, Lv QY, Yi ZH, Zhang JY, Wang JH, Lui SSY, Xu YF, Cheung EFC, Gur RE, Gur RC, Chan RCK (2018) Striatal dysfunction in patients with schizophrenia and their unaffected first-degree relatives. Schizophr Res 195:215-221.

Lim A, Hoek HW, Deen ML, Blom JD, Investigators G (2016) Prevalence and classification of hallucinations in multiple sensory modalities in schizophrenia spectrum disorders. Schizophr Res 176:493-499.

Lin SH, Yu CY, Pai MC (2006) The occipital white matter lesions in Alzheimer's disease patients with visual hallucinations. Clin Imaging 30:388-393.

Lisiecka DM, Suckling J, Barnes TR, Chaudhry IB, Dazzan P, Husain N, Jones PB, Joyce EM, Lawrie SM, Upthegrove R, Deakin B (2015) The benefit of minocycline on negative symptoms in early-phase psychosis in addition to standard care - extent and mechanism (BeneMin): study protocol for a randomised controlled trial. Trials 16:71.

Liu T, Wen W, Zhu W, Kochan NA, Trollor JN, Reppermund S, Jin JS, Luo S, Brodaty H, Sachdev PS (2011) The relationship between cortical sulcal variability and cognitive performance in the elderly. Neuroimage 56:865-873.

Lizano P, Lutz O, Ling G, Padmanabhan J, Tandon N, Sweeney J, Tamminga C, Pearlson G, Ruano G, Kocherla M, Windemuth A, Clementz B, Gershon E, Keshavan M (2018) VEGFA GENE variation influences hallucinations and frontotemporal morphology in psychotic disorders: a B-SNIP study. Transl Psychiatry 8:215.

Llorca PM, Pereira B, Jardri R, Chereau-Boudet I, Brousse G, Misdrahi D, Fenelon G, Tronche AM, Schwan R, Lancon C, Marques A, Ulla M, Derost P, Debilly B, Durif F, de Chazeron I (2016) Hallucinations in schizophrenia and Parkinson's disease: an analysis of sensory modalities involved and the repercussion on patients. Sci Rep 6:38152.

Logothetis NK (2003) The underpinnings of the BOLD functional magnetic resonance imaging signal. J Neurosci 23:3963-3971.

Logothetis NK (2008) What we can do and what we cannot do with fMRI. Nature 453:869-878.

Lopez-Persem A, Verhagen L, Amiez C, Petrides M, Sallet J (2019) The Human Ventromedial Prefrontal Cortex: Sulcal Morphology and Its Influence on Functional Organization. J Neurosci 39:3627-3639.

Lu YC, Kapse K, Andersen N, Quistorff J, Lopez C, Fry A, Cheng JH, Andescavage N, Wu Y, Espinosa K, Vezina G, du Plessis A, Limperopoulos C (2021) Association Between Socioeconomic Status and In Utero Fetal Brain Development. Jama Network Open 4.

Luhrmann TM, Padmavati R, Tharoor H, Osei A (2015) Differences in voice-hearing experiences of people with psychosis in the U.S.A., India and Ghana: interview-based study. Br J Psychiatry 206:41-44.

Luhrmann TM, Alderson-Day B, Bell V, Bless JJ, Corlett P, Hugdahl K, Jones N, Laroi F, Moseley P, Padmavati R, Peters E, Powers AR, Waters F (2019) Beyond Trauma: A Multiple Pathways Approach to Auditory Hallucinations in Clinical and Nonclinical Populations. Schizophr Bull 45:S24-S31.

Lynall ME, Bassett DS, Kerwin R, McKenna PJ, Kitzbichler M, Muller U, Bullmore E (2010) Functional connectivity and brain networks in schizophrenia. J Neurosci 30:9477-9487.

MacKinley ML, Sabesan P, Palaniyappan L (2020) Deviant cortical sulcation related to schizophrenia and cognitive deficits in the second trimester. Transl Neurosci 11:236-240.

Maijer K, Begemann MJH, Palmen S, Leucht S, Sommer IEC (2018) Auditory hallucinations across the lifespan: a systematic review and meta-analysis. Psychol Med 48:879-888.

Mallela AN, Deng H, Bush A, Goldschmidt E (2020) Different Principles Govern Different Scales of Brain Folding. Cereb Cortex 30:4938-4948.

Mallikarjun PK, Lalousis PA, Dunne TF, Heinze K, Reniers RL, Broome MR, Farmah B, Oyebode F, Wood SJ, Upthegrove R (2018) Aberrant salience network functional connectivity in auditory verbal hallucinations: a first episode psychosis sample. Transl Psychiatry 8:69.

Mangin JF, Riviere D, Cachia A, Duchesnay E, Cointepas Y, Papadopoulos-Orfanos D, Scifo P, Ochiai T, Brunelle F, Regis J (2004) A framework to study the cortical folding patterns. Neuroimage 23 Suppl 1:S129-138.

Margulies DS, Kelly AM, Uddin LQ, Biswal BB, Castellanos FX, Milham MP (2007) Mapping the functional connectivity of anterior cingulate cortex. Neuroimage 37:579-588.

Marshel JH, Kim YS, Machado TA, Quirin S, Benson B, Kadmon J, Raja C, Chibukhchyan A, Ramakrishnan C, Inoue M, Shane JC, McKnight DJ, Yoshizawa S, Kato HE, Ganguli S, Deisseroth K (2019) Cortical layer-specific critical dynamics triggering perception. Science 365.

Matsuda Y, Ohi K (2018) Cortical gyrification in schizophrenia: current perspectives. Neuropsychiatr Dis Treat 14:1861-1869.

McCarthy-Jones S, Trauer T, Mackinnon A, Sims E, Thomas N, Copolov DL (2014) A new phenomenological survey of auditory hallucinations: evidence for subtypes and implications for theory and practice. Schizophr Bull 40:231-235.

McGrath JJ et al. (2015) Psychotic Experiences in the General Population: A Cross-National Analysis Based on 31,261 Respondents From 18 Countries. JAMA Psychiatry 72:697-705.

Mellerio C, Lapointe MN, Roca P, Charron S, Legrand L, Meder JF, Oppenheim C, Cachia A (2016) Identification of Reliable Sulcal Patterns of the Human Rolandic Region. Front Hum Neurosci 10:410.

Meppelink AM, de Jong BM, Teune LK, van Laar T (2011) Regional cortical grey matter loss in Parkinson's disease without dementia is independent from visual hallucinations. Mov Disord 26:142-147.

Miller JA, D'Esposito M, Weiner KS (2021a) Using Tertiary Sulci to Map the "Cognitive Globe" of Prefrontal Cortex. J Cogn Neurosci:1-18.

Miller JA, Voorhies WI, Lurie DJ, D'Esposito M, Weiner KS (2021b) Overlooked Tertiary Sulci Serve as a Meso-Scale Link between Microstructural and Functional Properties of Human Lateral Prefrontal Cortex. J Neurosci 41:2229-2244.

Miller JA et al. (2014) Transcriptional landscape of the prenatal human brain. Nature 508:199-206.

Modinos G, Vercammen A, Mechelli A, Knegtering H, McGuire PK, Aleman A (2009) Structural covariance in the hallucinating brain: a voxel-based morphometry study. Journal of psychiatry & neuroscience : JPN 34:465-469.

Modinos G, Costafreda SG, van Tol MJ, McGuire PK, Aleman A, Allen P (2013) Neuroanatomy of auditory verbal hallucinations in schizophrenia: a quantitative meta-analysis of voxel-based morphometry studies. Cortex 49:1046-1055.

Moher D, Liberati A, Tetzlaff J, Altman DG, Group P (2009) Preferred reporting items for systematic reviews and meta-analyses: the PRISMA statement. BMJ 339:b2535.

Molko N, Cachia A, Riviere D, Mangin JF, Bruandet M, Le Bihan D, Cohen L, Dehaene S (2003) Functional and structural alterations of the intraparietal sulcus in a developmental dyscalculia of genetic origin. Neuron 40:847-858.

Moncrieff J, Middleton H (2015) Schizophrenia: a critical psychiatry perspective. Curr Opin Psychiatry 28:264-268.

Montagnese M, Leptourgos P, Fernyhough C, Waters F, Laroi F, Jardri R, McCarthy-Jones S, Thomas N, Dudley R, Taylor JP, Collerton D, Urwyler P (2021) A Review of Multimodal Hallucinations: Categorization, Assessment, Theoretical Perspectives, and Clinical Recommendations. Schizophr Bull 47:237-248.

Morch-Johnsen L, Nerland S, Jorgensen KN, Osnes K, Hartberg CB, Andreassen OA, Melle I, Nesvag R, Agartz I (2018) Cortical thickness abnormalities in bipolar disorder patients with a lifetime history of auditory hallucinations. Bipolar Disord 20:647-657.

Morch-Johnsen L, Nesvag R, Jorgensen KN, Lange EH, Hartberg CB, Haukvik UK, Kompus K, Westerhausen R, Osnes K, Andreassen OA, Melle I, Hugdahl K, Agartz I (2017) Auditory Cortex Characteristics in Schizophrenia: Associations With Auditory Hallucinations. Schizophr Bull 43:75-83.

Morgan SE, Seidlitz J, Whitaker KJ, Romero-Garcia R, Clifton NE, Scarpazza C, van Amelsvoort T, Marcelis M, van Os J, Donohoe G, Mothersill D, Corvin A, Pocklington A, Raznahan A, McGuire P, Vertes PE, Bullmore ET (2019) Cortical patterning of abnormal morphometric similarity in psychosis is associated with brain expression of schizophrenia-related genes. Proc Natl Acad Sci U S A 116:9604-9609.

Mosimann UP, Collerton D, Dudley R, Meyer TD, Graham G, Dean JL, Bearn D, Killen A, Dickinson L, Clarke MP, McKeith IG (2008) A semi-structured interview to assess visual hallucinations in older people. Int J Geriatr Psychiatry 23:712-718.

Muller AJ, Shine JM, Halliday GM, Lewis SJ (2014) Visual hallucinations in Parkinson's disease: theoretical models. Mov Disord 29:1591-1598.

Muller VI, Cieslik EC, Laird AR, Fox PT, Radua J, Mataix-Cols D, Tench CR, Yarkoni T, Nichols TE, Turkeltaub PE, Wager TD, Eickhoff SB (2018) Ten simple rules for neuroimaging meta-analysis. Neurosci Biobehav Rev 84:151-161.

Murray RM, Bhavsar V, Tripoli G, Howes O (2017) 30 Years on: How the Neurodevelopmental Hypothesis of Schizophrenia Morphed Into the Developmental Risk Factor Model of Psychosis. Schizophr Bull 43:1190-1196.

Mwansisya TE, Hu A, Li Y, Chen X, Wu G, Huang X, Lv D, Li Z, Liu C, Xue Z, Feng J, Liu Z (2017) Task and resting-state fMRI studies in first-episode schizophrenia: A systematic review. Schizophr Res 189:9-18.

Naasan G, Shdo SM, Rodriguez EM, Spina S, Grinberg L, Lopez L, Karydas A, Seeley WW, Miller BL, Rankin KP (2021) Psychosis in neurodegenerative disease: differential patterns of hallucination and delusion symptoms. Brain.

Nakamura M, Nestor PG, Shenton ME (2020) Orbitofrontal Sulcogyral Pattern as a Transdiagnostic Trait Marker of Early Neurodevelopment in the Social Brain. Clinical Eeg and Neuroscience 51:275-284.

Nayani TH, David AS (1996) The auditory hallucination: a phenomenological survey. Psychol Med 26:177-189.

Nenadic I, Smesny S, Schlosser RG, Sauer H, Gaser C (2010) Auditory hallucinations and brain structure in schizophrenia: voxel-based morphometric study. Br J Psychiatry 196:412-413.

Neves Mde C, Duarte DG, Albuquerque MR, Nicolato R, Neves FS, Souza-Duran FL, Busatto G, Correa H (2016) Neural correlates of hallucinations in bipolar disorder. Braz J Psychiatry 38:1-5.

NICE (2020) Transcranial mangetic stimulaltion for auditory hallucinations. In.

Niemantsverdriet MBA, Slotema CW, Blom JD, Franken IH, Hoek HW, Sommer IEC, van der Gaag M (2017) Hallucinations in borderline personality disorder: Prevalence, characteristics and associations with comorbid symptoms and disorders. Sci Rep 7:13920.

Nisbett RE, Masuda T (2003) Culture and point of view. Proc Natl Acad Sci U S A 100:11163-11170.

Nishikuni K, Ribas GC (2013) Study of fetal and postnatal morphological development of the brain sulci. J Neurosurg Pediatr 11:1-11.

Northoff G, Qin P (2011) How can the brain's resting state activity generate hallucinations? A 'resting state hypothesis' of auditory verbal hallucinations. Schizophr Res 127:202-214.

Nosarti C, Reichenberg A, Murray RM, Cnattingius S, Lambe MP, Yin L, MacCabe J, Rifkin L, Hultman CM (2012) Preterm birth and psychiatric disorders in young adult life. Arch Gen Psychiatry 69:E1-8.

O'Neill A, Mechelli A, Bhattacharyya S (2019) Dysconnectivity of Large-Scale Functional Networks in Early Psychosis: A Meta-analysis. Schizophr Bull 45:579-590.

Ochiai T, Grimault S, Scavarda D, Roch G, Hori T, Riviere D, Mangin JF, Regis J (2004) Sulcal pattern and morphology of the superior temporal sulcus. Neuroimage 22:706-719.

Ocklenburg S, Westerhausen R, Hirnstein M, Hugdahl K (2013) Auditory hallucinations and reduced language lateralization in schizophrenia: a meta-analysis of dichotic listening studies. J Int Neuropsychol Soc 19:410-418.

Ocklenburg S, Gunturkun O, Hugdahl K, Hirnstein M (2015) Laterality and mental disorders in the postgenomic age--A closer look at schizophrenia and language lateralization. Neurosci Biobehav Rev 59:100-110.

Oertel V, Knochel C, Rotarska-Jagiela A, Schonmeyer R, Lindner M, van de Ven V, Haenschel C, Uhlhaas P, Maurer K, Linden DE (2010) Reduced laterality as a trait marker of schizophrenia--evidence from structural and functional neuroimaging. J Neurosci 30:2289-2299.

Okuneye VT, Meda S, Pearlson GD, Clementz BA, Keshavan MS, Tamminga CA, Ivleva E, Sweeney JA, Gershon ES, Keedy SK (2020) Resting state auditory-language cortex connectivity is associated with hallucinations in clinical and biological subtypes of psychotic disorders. Neuroimage Clin 27:102358.

Ono M, Kubik, S. & Abernathey, C.D (1990) Atlas of the Cerebral Sulci. Stuttgart; New York, NY: Thieme.

Onofrj M, Taylor JP, Monaco D, Franciotti R, Anzellotti F, Bonanni L, Onofrj V, Thomas A (2013) Visual hallucinations in PD and Lewy body dementias: old and new hypotheses. Behav Neurol 27:479-493.

Pagonabarraga J, Soriano-Mas C, Llebaria G, Lopez-Sola M, Pujol J, Kulisevsky J (2014) Neural correlates of minor hallucinations in non-demented patients with Parkinson's disease. Parkinsonism Relat Disord 20:290-296.

Palaniyappan L, Liddle PF (2012) Does the salience network play a cardinal role in psychosis? An emerging hypothesis of insular dysfunction. J Psychiatry Neurosci 37:17-27.

Palaniyappan L, Balain V, Radua J, Liddle PF (2012) Structural correlates of auditory hallucinations in schizophrenia: a meta-analysis. Schizophr Res 137:169-173.

Palaniyappan L, Mallikarjun P, Joseph V, White TP, Liddle PF (2011) Reality distortion is related to the structure of the salience network in schizophrenia. Psychol Med 41:1701-1708.

Palaniyappan L, Park B, Balain V, Dangi R, Liddle P (2015) Abnormalities in structural covariance of cortical gyrification in schizophrenia. Brain Struct Funct 220:2059-2071.

Palaniyappan L, Marques TR, Taylor H, Mondelli V, Reinders A, Bonaccorso S, Giordano A, DiForti M, Simmons A, David AS, Pariante CM, Murray RM, Dazzan P (2016) Globally Efficient Brain Organization and Treatment Response in Psychosis: A Connectomic Study of Gyrification. Schizophr Bull 42:1446-1456.

Palomero-Gallagher N, Mohlberg H, Zilles K, Vogt B (2008) Cytology and receptor architecture of human anterior cingulate cortex. J Comp Neurol 508:906-926.

Palomero-Gallagher N, Hoffstaedter F, Mohlberg H, Eickhoff SB, Amunts K, Zilles K (2019) Human Pregenual Anterior Cingulate Cortex: Structural, Functional, and Connectional Heterogeneity. Cereb Cortex 29:2552-2574.

Papini C, Palaniyappan L, Kroll J, Froudist-Walsh S, Murray RM, Nosarti C (2020) Altered Cortical Gyrification in Adults Who Were Born Very Preterm and Its Associations With Cognition and Mental Health. Biological Psychiatry: Cognitive Neuroscience and Neuroimaging 5:640-650.

Patel AX, Kundu P, Rubinov M, Jones PS, Vertes PE, Ersche KD, Suckling J, Bullmore ET (2014) A wavelet method for modeling and despiking motion artifacts from resting-state fMRI time series. Neuroimage 95:287-304.

Paus T, Tomaiuolo F, Otaky N, MacDonald D, Petrides M, Atlas J, Morris R, Evans AC (1996) Human cingulate and paracingulate sulci: pattern, variability, asymmetry, and probabilistic map. Cereb Cortex 6:207-214.

Pereira JB, Junque C, Bartres-Faz D, Ramirez-Ruiz B, Marti MJ, Tolosa E (2013) Regional vulnerability of hippocampal subfields and memory deficits in Parkinson's disease. Hippocampus 23:720-728.

Pezzoli S, Cagnin A, Bandmann O, Venneri A (2017) Structural and Functional Neuroimaging of Visual Hallucinations in Lewy Body Disease: A Systematic Literature Review. Brain Sci 7.

Pezzoli S, Emsell L, Yip SW, Dima D, Giannakopoulos P, Zarei M, Tognin S, Arnone D, James A, Haller S, Frangou S, Goodwin GM, McDonald C, Kempton MJ (2018) Meta-analysis of regional white matter volume in bipolar disorder with replication in an independent sample using coordinates, T-maps, and individual MRI data. Neurosci Biobehav Rev 84:162-170.

Pizzagalli F, Auzias G, Yang Q, Mathias SR, Faskowitz J, Boyd JD, Amini A, Riviere D, McMahon KL, de Zubicaray GI, Martin NG, Mangin JF, Glahn DC, Blangero J, Wright MJ, Thompson PM, Kochunov P, Jahanshad N (2020) The reliability and heritability of cortical folds and their genetic correlations across hemispheres. Commun Biol 3:510.

Plaze M, Paillere-Martinot ML, Penttila J, Januel D, de Beaurepaire R, Bellivier F, Andoh J, Galinowski A, Gallarda T, Artiges E, Olie JP, Mangin JF, Martinot JL, Cachia A (2011) "Where do auditory hallucinations come from?"--a brain morphometry study of schizophrenia patients with inner or outer space hallucinations. Schizophr Bull 37:212-221.

Popescu V, Battaglini M, Hoogstrate WS, Verfaillie SC, Sluimer IC, van Schijndel RA, van Dijk BW, Cover KS, Knol DL, Jenkinson M, Barkhof F, de Stefano N, Vrenken H, Group MS (2012) Optimizing parameter choice for FSL-Brain Extraction Tool (BET) on 3D T1 images in multiple sclerosis. Neuroimage 61:1484-1494.

Powers AR, Mathys C, Corlett PR (2017) Pavlovian conditioning-induced hallucinations result from overweighting of perceptual priors. Science 357:596-600.

Psomiades M, Fonteneau C, Mondino M, Luck D, Haesebaert F, Suaud-Chagny MF, Brunelin J (2016) Integrity of the arcuate fasciculus in patients with schizophrenia with auditory verbal hallucinations: A DTI-tractography study. Neuroimage Clin 12:970-975.

Pugliese V, Bruni A, Carbone EA, Calabro G, Cerminara G, Sampogna G, Luciano M, Steardo L, Jr., Fiorillo A, Garcia CS, De Fazio P (2019) Maternal stress, prenatal medical illnesses and obstetric complications: Risk factors for schizophrenia spectrum disorder, bipolar disorder and major depressive disorder. Psychiatry Res 271:23-30.

Radua J, Romeo M, Mataix-Cols D, Fusar-Poli P (2013) A general approach for combining voxel-based meta-analyses conducted in different neuroimaging modalities. Curr Med Chem 20:462-466.

Radua J, Rubia K, Canales-Rodriguez EJ, Pomarol-Clotet E, Fusar-Poli P, Mataix-Cols D (2014) Anisotropic kernels for coordinate-based meta-analyses of neuroimaging studies. Front Psychiatry 5:13.

Radua J, Mataix-Cols D, Phillips ML, El-Hage W, Kronhaus DM, Cardoner N, Surguladze S (2012) A new meta-analytic method for neuroimaging studies that combines reported peak coordinates and statistical parametric maps. Eur Psychiatry 27:605-611.

Raemaekers M, Schellekens W, Petridou N, Ramsey NF (2018) Knowing left from right: asymmetric functional connectivity during resting state. Brain Struct Funct 223:1909-1922.

Raij TT, Valkonen-Korhonen M, Holi M, Therman S, Lehtonen J, Hari R (2009) Reality of auditory verbal hallucinations. Brain 132:2994-3001.

Ramirez-Ruiz B, Marti MJ, Tolosa E, Gimenez M, Bargallo N, Valldeoriola F, Junque C (2007) Cerebral atrophy in Parkinson's disease patients with visual hallucinations. Eur J Neurol 14:750-756.

Raznahan A, Lerch JP, Lee N, Greenstein D, Wallace GL, Stockman M, Clasen L, Shaw PW, Giedd JN (2011) Patterns of coordinated anatomical change in human cortical development: a longitudinal neuroimaging study of maturational coupling. Neuron 72:873-884.

Rolland B, Jardri R, Amad A, Thomas P, Cottencin O, Bordet R (2014) Pharmacology of hallucinations: several mechanisms for one single symptom? Biomed Res Int 2014:307106.

Rolland B, Amad A, Poulet E, Bordet R, Vignaud A, Bation R, Delmaire C, Thomas P, Cottencin O, Jardri R (2015) Resting-state functional connectivity of the nucleus accumbens in auditory and visual hallucinations in schizophrenia. Schizophr Bull 41:291-299.

Rosen AFG, Roalf DR, Ruparel K, Blake J, Seelaus K, Villa LP, Ciric R, Cook PA, Davatzikos C, Elliott MA, Garcia de La Garza A, Gennatas ED, Quarmley M, Schmitt JE, Shinohara RT, Tisdall MD, Craddock RC, Gur RE, Gur RC, Satterthwaite TD (2018) Quantitative assessment of structural image quality. Neuroimage 169:407-418.

Rossell SL, Shapleske J, Fukuda R, Woodruff PW, Simmons A, David AS (2001) Corpus callosum area and functioning in schizophrenic patients with auditory--verbal hallucinations. Schizophr Res 50:9-17.

Rubinov M, Bullmore E (2013) Schizophrenia and abnormal brain network hubs. Dialogues Clin Neurosci 15:339-349.

Sampedro F, Roldan A, Alonso-Solis A, Grasa E, Portella MJ, Aguilar EJ, Nunez-Marin F, Gomez-Anson B, Corripio I (2021) Grey matter microstructural alterations in schizophrenia patients with treatment-resistant auditory verbal hallucinations. J Psychiatr Res 138:130-138.

Sanchez-Castaneda C, Rene R, Ramirez-Ruiz B, Campdelacreu J, Gascon J, Falcon C, Calopa M, Jauma S, Juncadella M, Junque C (2010) Frontal and associative visual areas related to visual hallucinations in dementia with Lewy bodies and Parkinson's disease with dementia. Mov Disord 25:615-622.

Sarrazin S, Cachia A, Hozer F, McDonald C, Emsell L, Cannon DM, Wessa M, Linke J, Versace A, Hamdani N, D'Albis MA, Delavest M, Phillips ML, Brambilla P, Bellani M, Polosan M, Favre P, Leboyer M, Mangin JF, Houenou J (2018) Neurodevelopmental subtypes of bipolar disorder are related to cortical folding patterns: An international multicenter study. Bipolar Disord 20:721-732.

Schaer M, Cuadra MB, Tamarit L, Lazeyras F, Eliez S, Thiran JP (2008) A surface-based approach to quantify local cortical gyrification. IEEE Trans Med Imaging 27:161-170.

Schaer M, Cuadra MB, Schmansky N, Fischl B, Thiran JP, Eliez S (2012) How to measure cortical folding from MR images: a step-by-step tutorial to compute local gyrification index. J Vis Exp:e3417.

Schmitz J, Fraenz C, Schluter C, Friedrich P, Jung RE, Gunturkun O, Genc E, Ocklenburg S (2019) Hemispheric asymmetries in cortical gray matter microstructure identified by neurite orientation dispersion and density imaging. Neuroimage 189:667-675.

Schutte MJL, Bohlken MM, Collin G, Abramovic L, Boks MPM, Cahn W, Dauwan M, van Dellen E, van Haren NEM, Hugdahl K, Koops S, Mandl RCW, Sommer IEC (2021) Functional connectome differences in individuals with hallucinations across the psychosis continuum. Sci Rep 11:1108.

Segall JM, Turner JA, van Erp TG, White T, Bockholt HJ, Gollub RL, Ho BC, Magnotta V, Jung RE, McCarley RW, Schulz SC, Lauriello J, Clark VP, Voyvodic JT, Diaz MT, Calhoun VD (2009) Voxel-based morphometric multisite collaborative study on schizophrenia. Schizophr Bull 35:82-95.

Seidlitz J, Vasa F, Shinn M, Romero-Garcia R, Whitaker KJ, Vertes PE, Wagstyl K, Kirkpatrick Reardon P, Clasen L, Liu S, Messinger A, Leopold DA, Fonagy P, Dolan RJ, Jones PB, Goodyer IM, Consortium N, Raznahan A, Bullmore ET (2018) Morphometric Similarity Networks Detect Microscale Cortical Organization and Predict Inter-Individual Cognitive Variation. Neuron 97:231-247 e237.

Shapleske J, Rossell SL, Simmons A, David AS, Woodruff PW (2001) Are auditory hallucinations the consequence of abnormal cerebral lateralization? A morphometric MRI study of the sylvian fissure and planum temporale. Biol Psychiatry 49:685-693.

Shapleske J, Rossell SL, Chitnis XA, Suckling J, Simmons A, Bullmore ET, Woodruff PW, David AS (2002) A computational morphometric MRI study of schizophrenia: effects of hallucinations. Cereb Cortex 12:1331-1341.

Shergill SS, Brammer MJ, Williams SC, Murray RM, McGuire PK (2000) Mapping auditory hallucinations in schizophrenia using functional magnetic resonance imaging. Arch Gen Psychiatry 57:1033-1038.

Shimony JS, Smyser CD, Wideman G, Alexopoulos D, Hill J, Harwell J, Dierker D, Van Essen DC, Inder TE, Neil JJ (2016) Comparison of cortical folding measures for evaluation of developing human brain. Neuroimage 125:780-790.

Shin S, Lee JE, Hong JY, Sunwoo MK, Sohn YH, Lee PH (2012) Neuroanatomical substrates of visual hallucinations in patients with non-demented Parkinson's disease. J Neurol Neurosurg Psychiatry 83:1155-1161.

Shin SE, Lee JS, Kang MH, Kim CE, Bae JN, Jung G (2005) Segmented volumes of cerebrum and cerebellum in first episode schizophrenia with auditory hallucinations. Psychiatry Res 138:33-42.

Shinn AK, Baker JT, Cohen BM, Ongur D (2013) Functional connectivity of left Heschl's gyrus in vulnerability to auditory hallucinations in schizophrenia. Schizophr Res 143:260-268.

Shinn AK, Pfaff D, Young S, Lewandowski KE, Cohen BM, Ongur D (2012) Auditory hallucinations in a cross-diagnostic sample of psychotic disorder patients: a descriptive, cross-sectional study. Compr Psychiatry 53:718-726.

Shrout PE, Fleiss JL (1979) Intraclass correlations: uses in assessing rater reliability. Psychol Bull 86:420-428.

Simons JS, Garrison JR, Johnson MK (2017) Brain Mechanisms of Reality Monitoring. Trends Cogn Sci 21:462-473.

Smieskova R, Fusar-Poli P, Aston J, Simon A, Bendfeldt K, Lenz C, Stieglitz RD, McGuire P, Riecher-Rossler A, Borgwardt SJ (2012) Insular volume abnormalities associated with different transition probabilities to psychosis. Psychol Med 42:1613-1625.

Smith GE (1907) A New Topographical Survey of the Human Cerebral Cortex, being an Account of the Distribution of the Anatomically Distinct Cortical Areas and their Relationship to the Cerebral Sulci. J Anat Physiol 41:237-254.

Smith SM, Jenkinson M, Woolrich MW, Beckmann CF, Behrens TE, Johansen-Berg H, Bannister PR, De Luca M, Drobnjak I, Flitney DE, Niazy RK, Saunders J, Vickers J, Zhang Y, De Stefano N, Brady JM, Matthews PM (2004) Advances in functional and structural MR image analysis and implementation as FSL. Neuroimage 23 Suppl 1:S208-219.

Soares-Weiser K, Maayan N, Bergman H, Davenport C, Kirkham AJ, Grabowski S, Adams CE (2015) First rank symptoms for schizophrenia. Cochrane Database Syst Rev 1:CD010653.

Sommer I, Ramsey N, Kahn R, Aleman A, Bouma A (2001) Handedness, language lateralisation and anatomical asymmetry in schizophrenia: meta-analysis. Br J Psychiatry 178:344-351.

Sommer IE, Clos M, Meijering AL, Diederen KM, Eickhoff SB (2012a) Resting state functional connectivity in patients with chronic hallucinations. PLoS One 7:e43516.

Sommer IE, Slotema CW, Daskalakis ZJ, Derks EM, Blom JD, van der Gaag M (2012b) The treatment of hallucinations in schizophrenia spectrum disorders. Schizophr Bull 38:704-714.

Spreng RN, DuPre E, Ji JL, Yang G, Diehl C, Murray JD, Pearlson GD, Anticevic A (2019) Structural Covariance Reveals Alterations in Control and Salience Network Integrity in Chronic Schizophrenia. Cereb Cortex.

Stanfield AC, Moorhead TW, Job DE, McKirdy J, Sussmann JE, Hall J, Giles S, Johnstone EC, Lawrie SM, McIntosh AM (2009) Structural abnormalities of ventrolateral and orbitofrontal cortex in patients with familial bipolar disorder. Bipolar Disord 11:135-144.

Stevenson RJ, Langdon R, McGuire J (2011) Olfactory hallucinations in schizophrenia and schizoaffective disorder: a phenomenological survey. Psychiatry Res 185:321-327.

Storsve AB, Fjell AM, Tamnes CK, Westlye LT, Overbye K, Aasland HW, Walhovd KB (2014) Differential longitudinal changes in cortical thickness, surface area and volume across the adult life span: regions of accelerating and decelerating change. J Neurosci 34:8488-8498.

Subramaniam K, Luks TL, Fisher M, Simpson GV, Nagarajan S, Vinogradov S (2012) Computerized cognitive training restores neural activity within the reality monitoring network in schizophrenia. Neuron 73:842-853.

Sun T, Hevner RF (2014) Growth and folding of the mammalian cerebral cortex: from molecules to malformations. Nat Rev Neurosci 15:217-232.

Supekar K, Cai W, Krishnadas R, Palaniyappan L, Menon V (2019) Dysregulated Brain Dynamics in a Triple-Network Saliency Model of Schizophrenia and Its Relation to Psychosis. Biol Psychiatry 85:60-69.

Telles-Correia D, Moreira AL, Goncalves JS (2015) Hallucinations and related concepts-their conceptual background. Front Psychol 6:991.

Ten Donkelaar HJ, Tzourio-Mazoyer N, Mai JK (2018) Toward a Common Terminology for the Gyri and Sulci of the Human Cerebral Cortex. Front Neuroanat 12:93.

Tissier C, Linzarini A, Allaire-Duquette G, Mevel K, Poirel N, Dollfus S, Etard O, Orliac F, Peyrin C, Charron S, Raznahan A, Houde O, Borst G, Cachia A (2018) Sulcal Polymorphisms of the IFC and ACC Contribute to Inhibitory Control Variability in Children and Adults. eNeuro 5.

Turk E, van den Heuvel MI, Benders MJ, de Heus R, Franx A, Manning JH, Hect JL, Hernandez-Andrade E, Hassan SS, Romero R, Kahn RS, Thomason ME, van den Heuvel MP (2019) Functional Connectome of the Fetal Brain. J Neurosci 39:9716-9724.

van Erp TGM et al. (2018) Cortical Brain Abnormalities in 4474 Individuals With Schizophrenia and 5098 Control Subjects via the Enhancing Neuro Imaging Genetics Through Meta Analysis (ENIGMA) Consortium. Biol Psychiatry 84:644-654.

van Heukelum S, Mars RB, Guthrie M, Buitelaar JK, Beckmann CF, Tiesinga PHE, Vogt BA, Glennon JC, Havenith MN (2020) Where is Cingulate Cortex? A Cross-Species View. Trends Neurosci 43:285-299.

van Lutterveld R, van den Heuvel MP, Diederen KM, de Weijer AD, Begemann MJ, Brouwer RM, Daalman K, Blom JD, Kahn RS, Sommer IE (2014) Cortical thickness in individuals with non-clinical and clinical psychotic symptoms. Brain 137:2664-2669.

van Os J, Reininghaus U (2016) Psychosis as a transdiagnostic and extended phenotype in the general population. World Psychiatry 15:118-124.

van Swam C, Federspiel A, Hubl D, Wiest R, Boesch C, Vermathen P, Kreis R, Strik W, Dierks T (2012) Possible dysregulation of cortical plasticity in auditory verbal hallucinations-A cortical thickness study in schizophrenia. J Psychiatr Res 46:1015-1023.

van Tol MJ, van der Meer L, Bruggeman R, Modinos G, Knegtering H, Aleman A (2014) Voxel-based gray and white matter morphometry correlates of hallucinations in schizophrenia: The superior temporal gyrus does not stand alone. Neuroimage Clin 4:249-257.

Vasa F, Romero-Garcia R, Kitzbichler MG, Seidlitz J, Whitaker KJ, Vaghi MM, Kundu P, Patel AX, Fonagy P, Dolan RJ, Jones PB, Goodyer IM, Consortium N, Vertes PE, Bullmore ET (2020) Conservative and disruptive modes of adolescent change in human brain functional connectivity. Proc Natl Acad Sci U S A 117:3248-3253.

Vogt BA (2009) Cingulate neurobiology and disease. Oxford ; New York: Oxford University Press.

Vogt BA, Nimchinsky EA, Vogt LJ, Hof PR (1995) Human cingulate cortex: surface features, flat maps, and cytoarchitecture. J Comp Neurol 359:490-506.

Voorhies WI, Miller JA, Yao JK, Bunge SA, Weiner KS (2021) Cognitive insights from evolutionarily new brain structures in prefrontal cortex. bioRxiv:2020.2011.2007.372805.

Wagstyl K, Lepage C, Bludau S, Zilles K, Fletcher PC, Amunts K, Evans AC (2018) Mapping Cortical Laminar Structure in the 3D BigBrain. Cereb Cortex 28:2551-2562.

Wang C, Lee J, Ho NF, Lim JKW, Poh JS, Rekhi G, Krishnan R, Keefe RSE, Adcock RA, Wood SJ, Fornito A, Chee MWL, Zhou J (2018) Large-Scale Network Topology Reveals Heterogeneity in Individuals With at Risk Mental State for Psychosis: Findings From the Longitudinal Youth-at-Risk Study. Cereb Cortex 28:4234-4243.

Wang D, Zhou Y, Zhuo C, Qin W, Zhu J, Liu H, Xu L, Yu C (2015) Altered functional connectivity of the cingulate subregions in schizophrenia. Transl Psychiatry 5:e575.

Watanabe H, Senda J, Kato S, Ito M, Atsuta N, Hara K, Tsuboi T, Katsuno M, Nakamura T, Hirayama M, Adachi H, Naganawa S, Sobue G (2013) Cortical and subcortical brain atrophy in Parkinson's disease with visual hallucination. Mov Disord 28:1732-1736.

Waters F, Fernyhough C (2017) Hallucinations: A Systematic Review of Points of Similarity and Difference Across Diagnostic Classes. Schizophr Bull 43:32-43.

Waters F, Woods A, Fernyhough C (2014) Report on the 2nd International Consortium on Hallucination Research: evolving directions and top-10 "hot spots" in hallucination research. Schizophr Bull 40:24-27.

Waters F, Blom JD, Dang-Vu TT, Cheyne AJ, Alderson-Day B, Woodruff P, Collerton D (2016) What Is the Link Between Hallucinations, Dreams, and Hypnagogic-Hypnopompic Experiences? Schizophrenia bulletin 42:1098-1109.

Waters FA, Badcock JC, Michie PT, Maybery MT (2006) Auditory hallucinations in schizophrenia: intrusive thoughts and forgotten memories. Cogn Neuropsychiatry 11:65-83.

Wei W, Zhang Y, Li Y, Meng Y, Li M, Wang Q, Deng W, Ma X, Palaniyappan L, Zhang N, Li T (2020) Depth-dependent abnormal cortical myelination in first-episode treatment-naive schizophrenia. Hum Brain Mapp 41:2782-2793.

Wei X, Yin Y, Rong M, Zhang J, Wang L, Wu Y, Cai Q, Yu C, Wang J, Jiang T (2017) Paracingulate Sulcus Asymmetry in the Human Brain: Effects of Sex, Handedness, and Race. Sci Rep 7:42033.

Weinberger DR (2017) Future of Days Past: Neurodevelopment and Schizophrenia. Schizophr Bull 43:1164-1168.

Winkler AM, Kochunov P, Blangero J, Almasy L, Zilles K, Fox PT, Duggirala R, Glahn DC (2010) Cortical thickness or grey matter volume? The importance of selecting the phenotype for imaging genetics studies. Neuroimage 53:1135-1146.

Wisse LEM et al. (2017) A harmonized segmentation protocol for hippocampal and parahippocampal subregions: Why do we need one and what are the key goals? Hippocampus 27:3-11.

Woods A (2013) The voice-hearer. J Ment Health 22:263-270.

Woods A, Jones N, Alderson-Day B, Callard F, Fernyhough C (2015) Experiences of hearing voices: analysis of a novel phenomenological survey. Lancet Psychiatry 2:323-331.

Woods A, Jones N, Bernini M, Callard F, Alderson-Day B, Badcock JC, Bell V, Cook CC, Csordas T, Humpston C, Krueger J, Laroi F, McCarthy-Jones S, Moseley P, Powell H, Raballo A, Smailes D, Fernyhough C (2014) Interdisciplinary approaches to the phenomenology of auditory verbal hallucinations. Schizophr Bull 40 Suppl 4:S246-254.

Wu Y, Lu YC, Jacobs M, Pradhan S, Kapse K, Zhao L, Niforatos-Andescavage N, Vezina G, du Plessis AJ, Limperopoulos C (2020) Association of Prenatal Maternal Psychological Distress With Fetal Brain Growth, Metabolism, and Cortical Maturation. JAMA Netw Open 3:e1919940.

Xiao ZW, Zhang JX, Wang XY, Wu RH, Hu XP, Weng XC, Tan LH (2005) Differential activity in left inferior frontal gyrus for pseudowords and real words: An event-related fMRI study on auditory lexical decision. Human Brain Mapping 25:212-221.

Xu Y, Yang J, Hu X, Shang H (2016) Voxel-based meta-analysis of gray matter volume reductions associated with cognitive impairment in Parkinson's disease. J Neurol 263:1178-1187.

Yamamoto AK, Parker Jones O, Hope TMH, Prejawa S, Oberhuber M, Ludersdorfer P, Yousry TA, Green DW, Price CJ (2019) A special role for the right posterior superior temporal sulcus during speech production. Neuroimage 203:116184.

Yanagi M, Hosomi F, Kawakubo Y, Tsuchiya A, Ozaki S, Shirakawa O (2020) A decrease in spontaneous activity in medial prefrontal cortex is associated with sustained hallucinations in chronic schizophrenia: An NIRS study. Sci Rep 10:9569.

Yang J, Wang D, Rollins C, Leming M, Liò P, Suckling J, Murray G, Garrison J, Cachia A (2019) Volumetric Segmentation and Characterisation of the Paracingulate Sulcus on MRI Scans. bioRxiv:859496.

Yao N, Cheung C, Pang S, Shek-kwan Chang R, Lau KK, Suckling J, Yu K, Ka-Fung Mak H, Chua SE, Ho SL, McAlonan GM (2016) Multimodal MRI of the hippocampus in Parkinson's disease with visual hallucinations. Brain Struct Funct 221:287-300.

Yao N, Shek-Kwan Chang R, Cheung C, Pang S, Lau KK, Suckling J, Rowe JB, Yu K, Ka-Fung Mak H, Chua SE, Ho SL, McAlonan GM (2014) The default mode network is disrupted in Parkinson's disease with visual hallucinations. Hum Brain Mapp 35:5658-5666.

Yeo BT, Krienen FM, Sepulcre J, Sabuncu MR, Lashkari D, Hollinshead M, Roffman JL, Smoller JW, Zollei L, Polimeni JR, Fischl B, Liu H, Buckner RL (2011) The organization of the human cerebral cortex estimated by intrinsic functional connectivity. J Neurophysiol 106:1125-1165.

Yucel M, Stuart GW, Maruff P, Velakoulis D, Crowe SF, Savage G, Pantelis C (2001) Hemispheric and gender-related differences in the gross morphology of the anterior cingulate/paracingulate cortex in normal volunteers: an MRI morphometric study. Cereb Cortex 11:17-25.

Yucel M, Stuart GW, Maruff P, Wood SJ, Savage GR, Smith DJ, Crowe SF, Copolov DL, Velakoulis D, Pantelis C (2002) Paracingulate morphologic differences in males with established schizophrenia: a magnetic resonance imaging morphometric study. Biol Psychiatry 52:15-23.

Yun HJ, Vasung L, Tarui T, Rollins CK, Ortinau CM, Grant PE, Im K (2020) Temporal Patterns of Emergence and Spatial Distribution of Sulcal Pits During Fetal Life. Cereb Cortex 30:4257-4268.

Yun JY, Kim SN, Lee TY, Chon MW, Kwon JS (2016) Individualized covariance profile of cortical morphology for auditory hallucinations in first-episode psychosis. Hum Brain Mapp 37:1051-1065.

Zhang H, Li L, Wu M, Chen Z, Hu X, Chen Y, Zhu H, Jia Z, Gong Q (2016) Brain gray matter alterations in first episodes of depression: A meta-analysis of whole-brain studies. Neurosci Biobehav Rev 60:43-50.

Zhang W, Li S, Wang X, Gong Y, Yao L, Xiao Y, Liu J, Keedy SK, Gong Q, Sweeney JA, Lui S (2018) Abnormal dynamic functional connectivity between speech and auditory areas in schizophrenia patients with auditory hallucinations. Neuroimage Clin 19:918-924.

Zhu J, Wang C, Liu F, Qin W, Li J, Zhuo C (2016) Alterations of Functional and Structural Networks in Schizophrenia Patients with Auditory Verbal Hallucinations. Front Hum Neurosci 10:114.

Zielinski BA, Gennatas ED, Zhou J, Seeley WW (2010) Network-level structural covariance in the developing brain. Proc Natl Acad Sci U S A 107:18191-18196.

Zmigrod L, Garrison JR, Carr J, Simons JS (2016) The neural mechanisms of hallucinations: A quantitative meta-analysis of neuroimaging studies. Neurosci Biobehav Rev 69:113-123.